TECHNICAL UNIVERSITY OF MOLDOVA

JOURNAL OF ENGINEERING SCIENCE

Technical and applied scientific publication founded on 9 February 1995
Alternative title: Meridian ingineresc

2022
Vol. XXIX (2)

ISSN 2587-3474
eISSN 2587-3482

TECHNICAL UNIVERSITY OF MOLDOVA (PUBLISHING HOUSE)
„TEHNICA UTM" (PRINTING HOUSE)

According to the Decision of the NAQAER No. 19 from 06.12.2019, JES is classified as B+ journal

Main subjects areas of the Journal of Engineering Science:

A. Industrial Engineering

- Mechanical Engineering and Technologies
- Applied Engineering Sciences and Management
- Materials Science and New Technologies
- Electrical Engineering and Power Electronics
- Energy systems
- Light Industry, New Technologies and Design
- Industrial and Applied Mathematics
- Vehicle and Transport Engineering

B. Electronics and Computer Science

- Electronics and Communication
- Microelectronics and Nanotechnologies
- Biomedical Engineering
- Computers and Information Technology
- Automation

C. Architecture, Civil and Environmental Engineering

- Architecture, Urbanism and Cadaster
- Civil Engineering and Management
- Energy Efficiency and New Building Materials
- Environmental Engineering

D. Food Engineering

- Food Technologies and Food Processes
- Food Industry and Management
- Biotechnologies, Food Chemistry and Food Safety
- Equipment for Food Industries

The structure of the journal corresponds to the classification of scientific publications: ***Engineering, Multidisciplinary*.**

How to publish a paper:

1. Send the manuscript and information about the author to the **Editorial Board address:** jes@meridian.utm.md
2. Manuscripts are accepted only in English, by e-mail, in template file (www.jes.utm.md)
3. After a review, you will be notified of the editorial board's decision.
4. After the Journal has been published, we will send it to you immediately by mail.

Editor-in-Chief
Dr. hab. prof. univ. Viorel BOSTAN
Technical University of Moldova
viorel.bostan@adm.utm.md

Editorial Board

Responsible Editor
Dr. hab. Rodica STURZA
Editorial Board address: jes@meridian.utm.md

Editorial Production:
Dr. hab. Aliona Ghendov-Moșanu
Dr. Nicolae Trifan
Dr. Țurcan Iuliu
Dr. Svetlana Caterinciuc
Dr. Rodica Cujba

CONTENT

CONȚINUT

Journal of Engineering Science *Vol. XXIX, no. 2 (2022), pp. 8 - 17*
Fascicle *Industrial Engineering* *ISSN 2587-3474*
Topic *Mechanical Engineering and Technologies* *eISSN 2587-3482*

https://doi.org/10.52326/jes.utm.2022.29(2).01
UDC 621.833:621.89

THEORETICAL AND EXPERIMENTAL MODELLING OF THE TRIBOLOGICAL BEHAVIOUR ASPECTS OF CONTACT ELEMENTS IN THE PRECESSIONAL GEARING (PG)

Ion Bostan, ORCID ID: 0000-0001-9217-999x,
Petru Stoicev*, ORCID ID: 0000-0003-0405-1879,
Gheorghe Poștaru, ORCID ID: 0000-0003-2019-0975,
Maxim Vaculenco, ORCID ID: 0000-0003-2032-4750,
Alexandru Buga, ORCID ID: 0000-0002-4342-0502,
Mihail Kulev, ORCID ID: 0000-0002-9190-3007,
Andrei Poștaru, ORCID ID: 0000-0003-2413-2641,
Andrei Platon, ORCID ID: 0000-0001-8326-0147

Technical University of Moldova, 168 Ștefan cel Mare Blvd., MD-2004, Chisinau, Moldova
*Correspondence author: Petru Stoicev, *petru.stoicev@imi.utm.md*

Received: 02. 24. 2022
Accepted: 04. 22. 2022

Abstract. This paper deals with the theoretical-experimental model of the tribological behavior of the contact elements in precessional gears (PG) in the functions of conjugate profiles of linear velocities "*convex-concave*" or "*convex-convex*" for the corresponding geometric parameters (ρ_{k_i}, r, $\rho_{k_i} - r$) and the values of the kinematic force parameters (V_{E_1}, V_{E_2}, V_{a_i}) for each concrete position of the k_i points. The calculation of the constructive-functional and kinematic parameters of the "*roller-shoe*" and "*roller-roller*" elements of the tribocouple were adjusted for the experimental verification tests on the SMT-1 installation and adapted to the specific test conditions of the tribocouples with *conformal* contact of gear teeth made of plastics, which will be subjected to *sliding friction* and *rolling* processes of the concrete tribocouple elements.

Keywords: *precessional transmission, precessional gearing, contact load, tribomodel, sliding (rolling) friction, experimental modeling of the precessional gearing, tribological parameters, friction coefficient and force, power loss, mechanical efficiency.*

Rezumat. În lucrare este prezentat modelul teoretico-experimental al aspectelor de comportare tribologică a elementelor de contact în angrenaje precesionale (PG). În funcție de vitezele liniare ale profilelor conjugate „convex-concave" sau „convex-convexe", s-au dezvoltat parametrii (ρ_{k_i}, r, $\rho_{k_i} - r$) pentru geometria corespunzătoare și valorile parametrilor forței cinematice (V_{E_1}, V_{E_2}, V_{a_i}) pentru fiecare poziție concretă a punctelor k_i. Calculul parametrilor constructiv-funcționali și cinematici ai elementelor tribocuplului *„rolă-sabot"* și *„rolă-rolă"* au fost ajustați pentru încercările experimentale de verificare pe instalația SMT-1,

adaptată la condițiile specifice de încercare a tribocuplurilor cu contact *conform* dinţilor roţilor din material plastic şi care vor fi supuse la *frecare de alunecare* şi *de rulare* a elementelor tribocuplului concret.

Cuvinte cheie: *transmisie precesională, angrenaj precesional, sarcină de contact, tribomodel, frecare de alunecare (rulare), modelare experimentală a angrenajului precesional, parametri tribologici, coeficient și forță de frecare, pierderi de putere, eficiență mecanică*.

1. Introduction

According to previous research, it is known that *unlike* classical gears [1-7], in Precessional Transmission (PT) [8-17] the profile of the teeth of the central gear is variable - a fact, which *leads* to the variation of the contact geometry of the teeth in the same gear, changing from one shape to another: from convex-concave - at the foot of the central gear tooth, to convex-rectilinear - towards the middle of the tooth and, convex-convex - towards the tip of the tooth.

The manner and limits of variation of the profile of the central wheel depend on the configuration of the fundamental parameters of the precessional gearing Z, r, δ and θ by which the reference front tooth meshing up to 100% is possible to ensure. *This type of gearing represents* a sliding rolling tribocouple with a specific tribological structure and behaviour, characterized by:

1. *Specific construction features of triboelements* (variable shape of the profile of the central wheel tooth; small difference between the radii of curvature of the conjugated surfaces);
2. *High degree of contact multiplicity*;
3. *Variation of contact shape* („*convex-concave*", „*convex-rectilinear*" and „*convex-convex*") for different teeth that are simultaneously in the gear;
4. *Relative spherospatial motion* of surfaces in the contact area;
5. *Variation in large limits of the peripheral linear velocities* of the surfaces of the satellite teeth and the central wheel in the contact area during a precession cycle;
6. *Variable relative sliding velocity* of the conjugated surfaces *for the teeth that are simultaneously in contact*;
7. *Approximately uniform load distribution of the conjugated teeth contact* (on the „convex-concave" portion, where the *angle of engagement* achieves values with small deviations from a constant value).

Due to the complexity and specificity of the given tribosystem, set out in points 1-7 listed above, a fundamental study of the tribological behaviour of the Precessional gearing *is difficult to conduct*. For this reason *we resort to* modelling on simple (standardized) tribosystems, *where tribological processes* similar *to tribological processes occurring in the contact area of the precessional planetary gear can be realized*. In order to meet this requirement, tribomodelling is carried out on the concrete case of the gear under investigation.

The evolution of friction force (coefficient), power (energy) losses and triboelement wear intensity for the couple of concrete material of the wheels and under contact load conditions similar to the working conditions of the precessional gear are followed by the research.

2. Methodological proposals for experimental investigations of tribocontacts in the Precessional Gearing

The experimental modeling of the precessional gearing is proposed to be carried out on the basis of the tribosystematization proposed by Professor **Ion Crudu** [16], performed on a generalized tribomodel and shown in Figure 1.

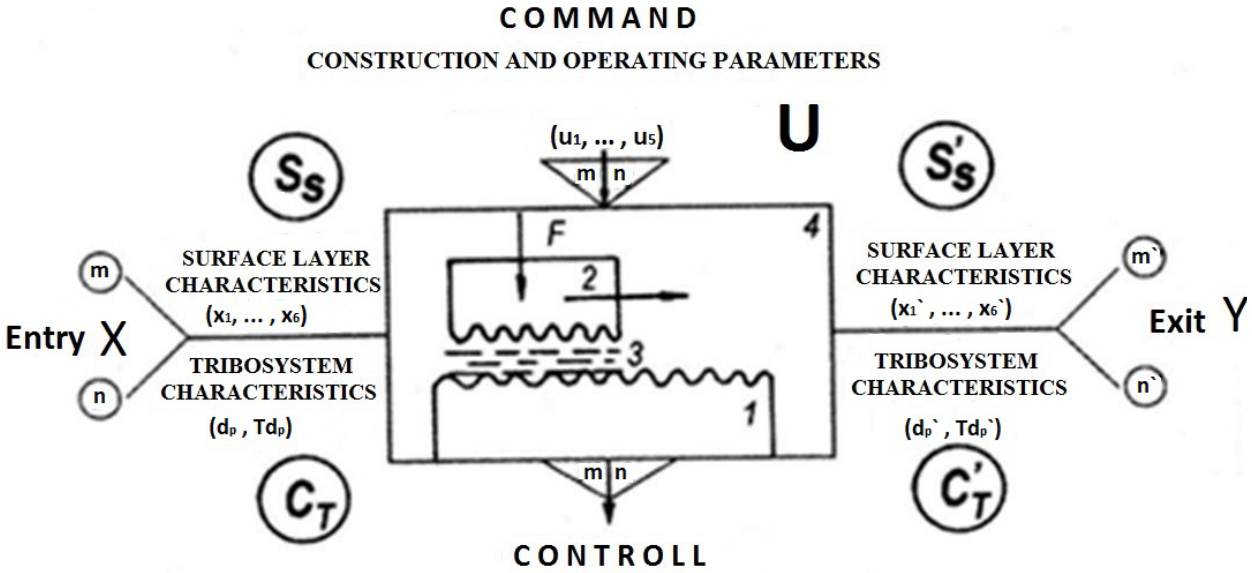

Figure 1. General structure of the physical tribomodel for the experimental recording of input and output data: 1-fixed triboelement; 2-mobile triboelement: 3-interposing medium; 4-working medium [16].

From a functional point of view, *the structure of the tribomodel is characterized by the following groups of parameters*:

1. X_i , Y_i – *input, output;*
2. U – *command;*
3. C – *control*

of which; m – *measurable sizes* and n – *immeasurable sizes*.

The basic *characteristics* are established for each of these size groups:

a. *Input - output sizes* $X_i \rightarrow Y_i$ *:*

a_1. ***Tribostate characteristics*** (S_{s0}, S_{s1}). These characteristics change over time and determine the behavior of the tribomodel over the test period. They are measurable *sequentially* - at the beginning and end of test sequence periods, or *singularly* - during a single run period. This category includes the following indicators:

X_1 - surface *roughness* in the contact zone (R_{Z0}, R_{Z1});

X_2 – *macrohardness* (HB_0, HB_1), (HRC_0, HRC_1) or *microhardness* of contact surfaces $(H_{\mu 0}, H_{\mu 1})$;

X_3 – *stress state* (σ_0, σ_1);

X_4 – *chemical composition of the surface layers, resulting from the influence of the environment and working conditions* (X_{40}, X_{41});

X_5 – *material structure* (metallurgical) (X_{50}, X_{51})

X_6 – *purity* (X_{60}, X_{61})

a_2. ***Tribomodel parameters*** (C_{T0}, C_{T1}). Defines the test duration, specific to each type of tribo-model and tribosystem.

b. *Command sizes* (U). Comprising two groups, with values, which are set at the beginning of the experimental tests:

b_1**. Tribo-model construction** $(\mathrm{U_c})$.

u_1 – *shape of the contact* (on flat surface, or cylindrical; *on line with different curvatures in the profile section*; point-shaped);

u_2 – *geometrical dimensions in the contact area*;

u_3 – *triboelement materials (material couples under test).*

b_2. *Test parameters*:

u_4 – *contact loading* (F_n) *and distribution on the triboform*;

u_5 – *relative velocity (sliding, rolling and combinations)*;

u_6 – *presence and type of lubricant*;

u_7 – *ambient temperature in the test chamber* (Θ);

u_8 – *environmental conditions (humidity).*

Control measurements (C), allow for the assessment of *wear level and other parameters by direct measurements*:

c_1 – *amount of material removed (worn)*;

c_2 – *evolution of the friction moment*;

c_3 – *temperature evolution in the contact area*;

c_4 – *evolution of vibration level, etc.*

As a result, based on the real precessional gearing, the main characteristics of the tribomodel are established for a group of sizes. Finally, the values of these quantities are sought from the condition of ensuring the similarity of tribological processes in the contact of the tribomodel and the precessional gear.

For experimental research the tribomodel was made on an installation of 2070 SMT-1 model manufactured according to GRSI RF: 7717-80 (Figure 2) [17].

The kinematic scheme of the 2070 SMT-1 installation is shown in fig.3 The SMT-1 machine (installation) can operate according to closed or open contour force schemes according to 3 kinematic schemes: the revolutions from the electric motor 19 - via belt wheel 1 and toothed belt transmission 5 - are transmitted simultaneously to the upper sample 13 via the belt wheel 6 and to the bottom sample 14 via the belt wheel 3.

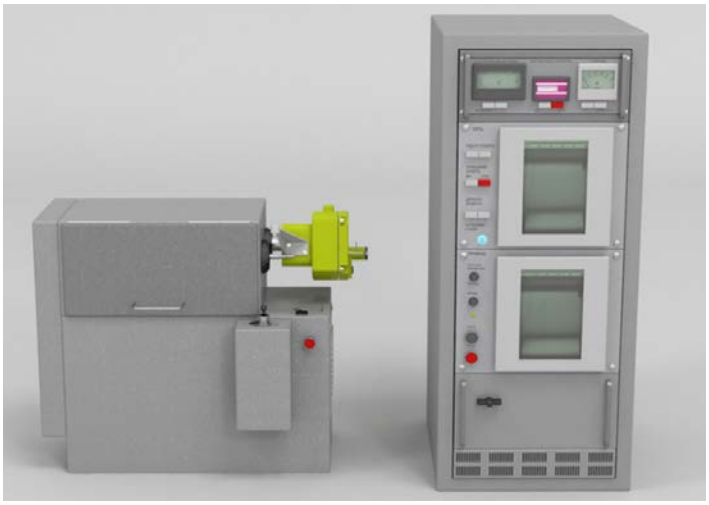

Figure 2. General view of the SMT-1 installation [17].

The sample 13 is installed on the shaft 12 of the folding trolley where the gear wheels 10 and 11 are located inside.

The folding trolley is balanced by means of the spring mechanism 8. An elastic sensor 7 is installed on the bottom sample shaft to record the friction moment through a non-contacting collector, from which signals are recorded on a recording board.

The loading (stressing) of the samples is carried out by means of the spring mechanism 16. The amount (magnitude) of the applied normal force is adjusted by turning the lever 15, and the transmission of the indications to the recording board is made via the flexible connection from the resistor 17.

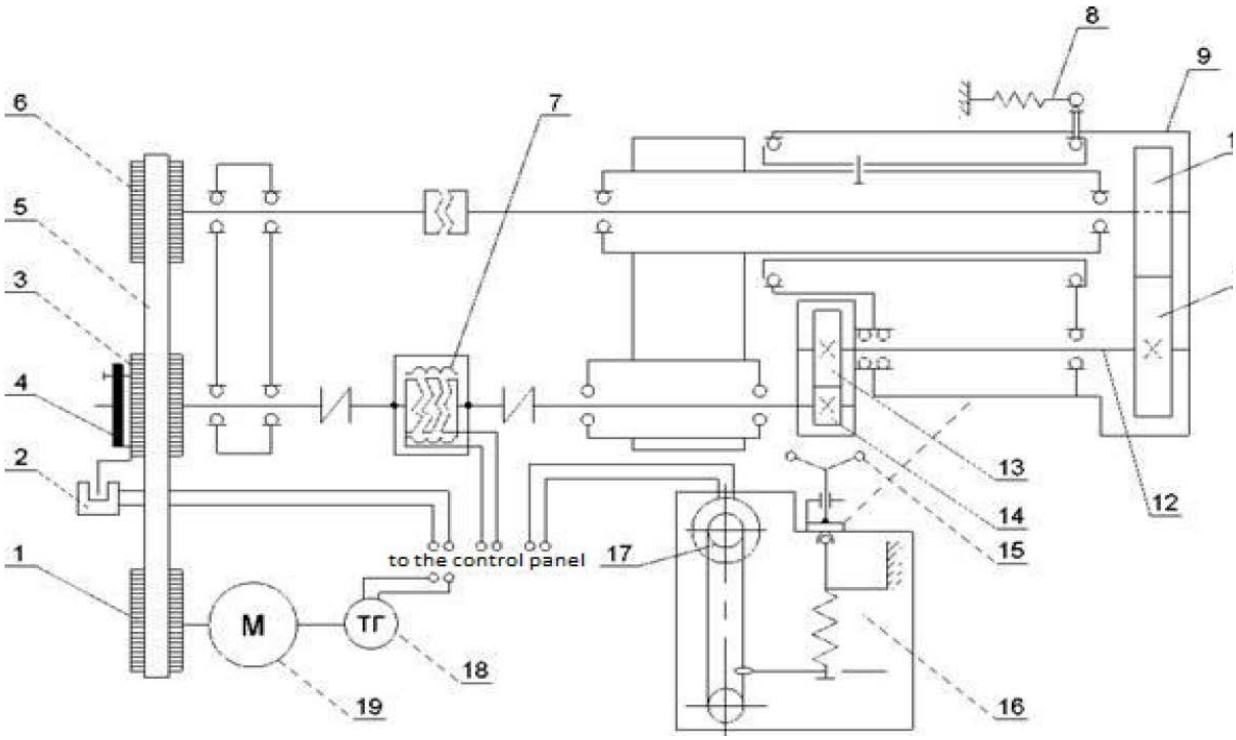

Figure 3. Kinematic scheme of the SMT-1 installation, adapted for experimental testing of the PG (with sliding or rolling motion of the rollers) [17].

The number of revolutions per minute of the electric motor shaft 19 is measured by means of the tacho-generator 18, and the number of revolutions per minute of the bottom sample (friction force) - by means of the non-contact transducer 2. The pin 4 is used to protect the machine (installation) from overloads.

For testing the „shaft-bushing" tribocouple, the process is carried out in a special chamber according to an open contour scheme. In this case the folding carriage 9 is lifted and fixed in this position (turned upside down). Devices, installed on the panel, *allow for the measurement of* the friction moment, the load force, the number of revolutions, the number of cycles (travel) and the temperature in the contact area of the samples in the tribocouple.

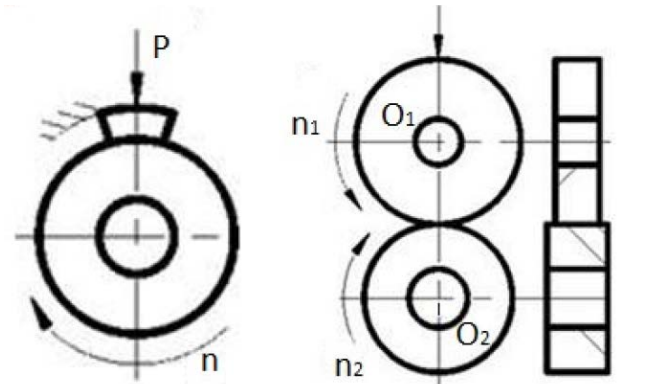

a) b)

Figure 4. Variants of performing the contact.

The contact modelling on the SMT-1 installation is carried out in two variants (fig. 4): a – „roller-shoe"; b – „roller-roller".

The tribomodelling, adapted to the SMT - 1 installation, will be carried out for a precessional gear obtained by mathematical modelling, according to the following parametric configuration Z, δ,β, θ ($Z_1 = 24$, $Z_2 = 25$, $\theta = 3{,}5^0$, $\delta = 22{,}5^0$, r = 6,27 mm și R = 75 mm).

In the mathematical model, *the kinematic analysis was performed* for a series of contact points $k_0, k_1, k_2, \ldots, k_i$ corresponding to crankshaft positioning angles for which the variation of the linear velocities V_{E1} of the contact points E_1 on the profile of the central wheel teeth, V_{E2} of the contact points E_2 on the profile of the satellite teeth and the relative sliding velocity between the flanks V_{al} was established.

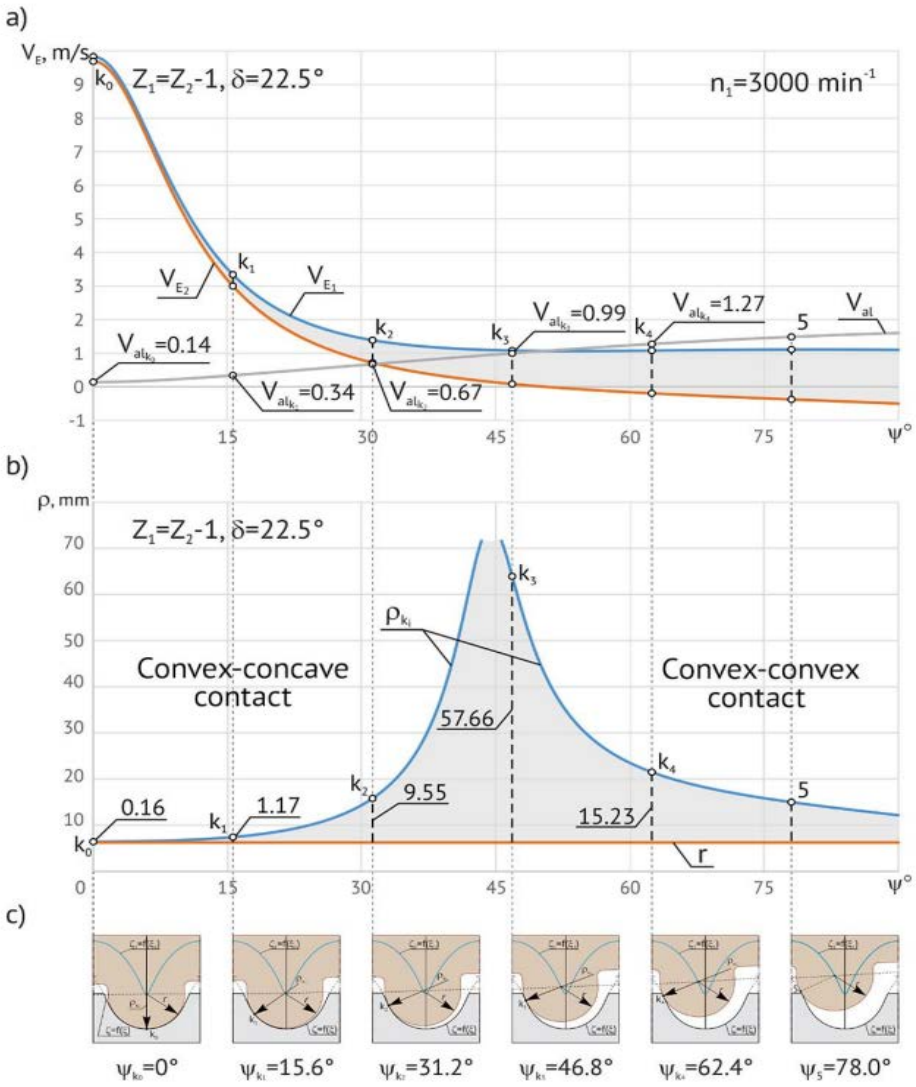

Figure 5. Linear velocities at the contact point V_{E1}, V_{E2}, V_{al} (a) and the difference in the radii of curvature $(\rho_{ki} - r)$ (b) of the conjugated profiles in the contact k_i (c) as a function of ψ for $Z_1 = Z_2 - 1$ and $\delta = 22{,}5°$ ($Z_1 = 24$, $Z_2 = 25$, $\theta = 3{,}5°$, $\delta = 22{,}5°$, r = 6, 27 mm, R = 75 mm) [14].

The tooth contact geometry at the contact point areas is shown by the radii of curvature ρ_{ki} of the central wheel tooth profile and the satellite tooth profile *r* and their difference ($\rho_{ki} - r$). The tooth contact kinematics analysis is performed for the crankshaft

speed frequency $n_1 = 3000min^{-1}$. When rotating the crankshaft by angle ψ, the contact of the teeth in gearing moves from point k_0 within $0^\circ < \psi < 43^\circ$ on the *convex-concave* phase, and then moves to the convex-convex phase.At each point on the tooth profile the geometric and kinematic parameters of the contact change taking concrete values at each position. Thus, for position k_0 of the contact, the linear velocity $V_{E1} = 1\,9{,}83$ m/ s, $V_{E2} = 2\,9{,}69$ m/ s, $V_{al} = 0\,{,}14$ m /s, and the radius of curvature of the profile of the central wheel teeth $\rho_{k0} = 6{,}43mm$, of the satellite teeth r = 6,27 mm and their difference ($\rho_{k0} - r$= 0,16 mm). The calculation results for positions $k_0, k_1, k_2, \ldots, k_i$ are shown in Figure 5. The realization of the experimental tribomodel for the precessional gear is related to the meeting of the constructive aspects of the contact by shape („*convex-concave*" or „convex-convex") and dimensions with the corresponding geometrical parameters (ρ_{ki}, r, $\rho_{ki} - r$) and the values of the kinematic parameters (V_{E1} , $V_{E\,2,}$ V_{al}) for each concrete position of the point k_i.

3. Calculation of the constructive and kinematic parameters of the „roller-shoe" (Figure 6) and „roller-roller" (Figure 7) tribomodels

The tribomodel of the "convex-concave" portion of the contact, according to the kinematic possibilities of the SMT-1 installation, can be realized in the "**roller-shoe**" version (Figure 6) where: $\boldsymbol{r}$ – radius of the roller, $\boldsymbol{\rho_{ki}}$ – radius of curvature of the contact surface of the shoe.

Geometrically the contact is modelled according to the criterion ($\rho_{ki} - r$) - the difference in the radii of curvature of surfaces in the area of points k_i. As a kinematic modelling criterion only the sliding velocity V_{al} can be accepted. Based on these criteria, the values of the constructive and kinematic parameters of the model are concretized for each point k_i (Figure 5) determined by the angle ψ of the position of the crank of the precessional reducer satellite.

From a constructive point of view the roller and shoe triboelements, when interacting, must ensure linear contact with the corresponding difference in radii ($\rho_{ki} - r$) of curvature in the area of the contact points k_1 and k_2 (Figure 5), with corresponding values of the sliding velocity.

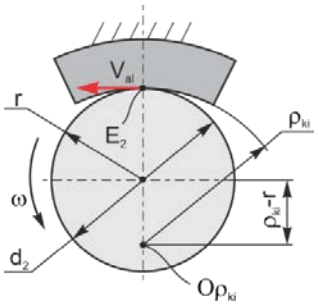

Figure 6. Interaction scheme of the surfaces in contact in the case of the experimental „*roller-shoe*" tribomodel for the „*convex-concave*" portion of the precessional gearing.

Based on the constructive features of the test assembly of the SMT-1 installation, it was accepted that the roller triboelement radius $r = 17mm$ (diameter $d_2 = 2r$).

The radius of curvature of the shoe triboelement is determined according to the relation:

$$\rho_{ki} = r + (\rho_{ki} - r) \tag{1}$$

The rotation speed (revolution) of the guiding roller shaft d_2, required to obtain the sliding velocity with values corresponding to the areas k_i and the contact points (V_{ali}), is determined from the relation:

$$n = {60V_{ali} \cdot 10^3}\Big/{\pi d_2}\ (rot/min) \quad (2)$$

The results of the calculations are shown in Table 1.

Table 1

Constructive and kinematic parameters of the „roller-shoe" tribomodel

Point k_i	r(mm)	$d_2 = 2r$(mm)	$\rho_{ki} - r$(mm)	ρ_{ki}(mm)	V_{al}(m/s)	n(rot/min)
k_1	17	34	1,17	18,17	0,34	191
k_2	17	34	9,55	26,55	0,67	376

In the "roller-shoe" model the influence of the linear reciprocal rolling velocities V_{E1} and V_{E2} on the tribological behavior of the contact is lost.

The "convex-convex" tribomodel of the contact shape. The second variant of experimental modelling of the contact shape of the precessional gearing, possible to perform on the SMT - 1 installation, is the "roller-roller" model with a "*convex-convex*" external contact. In this case the shape of the model contact differs constructively from the shape of the precessional gear contact.

Accepting this compromise, it is possible to realize *the sliding rolling tribosystem model* with which the *tribological behaviour of the contact* under the action of linear reciprocal rolling velocities with relative sliding will be studied with. The sketch of the triboelement interaction in the case of the "roller-roller" contact model is shown in Figure 7, where: r, d_2 – radius and diameter of the *driving* roller; ρ_{ki} and d_1 – radius and diameter of the *driven roller*; V_{E2} and V_{E1} – peripheral linear velocities of the reciprocal rolling surfaces of the driving roller d_2 and the driven roller d_1; ω – angular velocity of rotation of the shafts of the *driving* and *driven* rollers.

The constructive and kinematic parameters required for the experimental model of the precessional gear contact ($\rho_{ki} - r$), V_{E2}, V_{E1} and V_{al} for each point k_i, are shown in Figure 5. Constructively, the radius of the triboelement of the *driving roller* is accepted: $r = 17mm$ (diameter $d_2 = 34mm$). According to the accepted value of the diameter of the driving roller and the peripheral linear velocity V_{E2} the *angular velocity* ω is determined *for the contact position in the area of each point* k_i:

$$\omega = {2V_{E2} \cdot 10^3}\Big/{d_2}\ (\frac{rad}{s}) \quad (3)$$

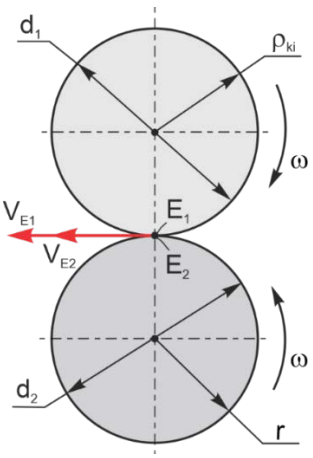

Figure 7. Scheme of the interaction of surfaces in contact for the experimental „*roller-roller*" tribomodel for the „*convex-convex*" shape of the contact.

Knowing the angular velocity, the *diameter of the driven roller triboelement* d_1 is determined:

$$d_1 = {}^{2V_{E1} \cdot 10^3}/_{\omega} \ (mm) \tag{4}$$

To achieve the kinematic regime in the contact area of the tribomodel, similarly to the kinematic regime in the contact area of the precessional gear, the *speed of the driving roller* is determined:

$$n = {}^{60V_{E2} \cdot 10^3}\Big/_{\pi d_2} \ (rot/min) \tag{5}$$

The calculation results for points k_1 and k_2 are shown in Table 2.

Table 2

Constructive and kinematic parameters of the „roller-roller" tribomodel

Contact point	Roller radius r(mm)	Roller diameter d_2(mm)	$(\rho_{ki} - r)$ (mm)	d_{ki} (mm)	V_{E2} (m/s)	V_{E1} (m/s)	V_{al} (m/s)	ω (rad/s)	n (rot/min)
k_1	17	34	1,17	38,02	2,93	3,27	0,34	172	1646
k_2	17	34	9,55	66,55	0,7	1,37	0,67	41,17	393

Conclusions

1. It has been established that, *unlike classical gears, the Precessional Transmission (PT) can have a variable* profile of the central gear teeth, which *leads to* varying the tooth *contact geometry* within the same gear, *changing from one shape to another* (from "*convex-concave*" at the foot of the tooth of the central gear - to "*convex-rectilinear*" towards the middle of the tooth, and "*convex-concave*" towards the tooth tip), and the *manner and limits of its variation* (profile) depend on the configuration of the fundamental parameters of the precessional *gear* (*Z, r, δ* and *ϑ*) by which the *reference front tooth gearing* of *up to 100%* can be ensured.

2. It has been found that this type of gear represents a tribosystem with sliding rolling motion, with a *specific* constructive *tribological structure and behaviour - variable shape of the profile of the central wheel tooth*; small difference in the *radii of curvature* of the conjugated surfaces; high degree of contact multiplicity; contact shape variation – "CVX-CCV", "CVX-RL" and "CVĂ-CVX" - for different teeth *simultaneously* in the gear; relative *spherospatial* motion of *surfaces* in the contact area; *variation* (within large limits) of peripheral linear velocities of the surfaces of the *satellite teeth* and the *central wheel* in the *contact* area during a precession cycle; *variable relative sliding* velocity of the conjugated surfaces for the teeth that are simultaneously in contact; approximately uniform *distribution* of the contact load of the conjugated teeth (on the "CVX-CCV" portion - where the angle of gearing *has values with small deviations from a* constant *value*).

3. From point 2 (*complexity and specificity of the given tribosystem*),described above, we note that a fundamental study of the *tribological behavior* of PT gearing is difficult to carry out, and for this reason we have resorted to modelling on simple (standardized) tribosystems, where tribological processes, similar to tribological processes which occur in the area of PP (precessional plane) gearing contact, can be realized. In order to meet this requirement, tribomodelling is performed on the concrete case of the gear under investigation.

It was proposed that the Experimental modelling of the gear *should be carried out* on the basis of the tribosystematization, developed by Prof. Ion Crudu, which is represented by a

generalized tribosystem (with the setting of input, *command, control and output* parameters), *carried out* on a installation of the 2070 (SMT-1) model, produced according to GRSN RF – 80.

The devices installed on the panel, allow for the measurement of *the friction moment, the load force*, the number of revolutions, *the number of cycles covered* and *the temperature in the contact area* of the elements *("roller-shoe", "roller-roller") of the corresponding tribo-couple. Sample wear shall be assessed by the mass method on the VLA - 2000 electronic scale (accuracy - 0,0001 g).*

4. The constructive and functional parameters of the samples for the experimental tests of the tribocouple elements *"roller-shoe"* and *"roller-roller"* in their concrete test regimes have been calculated and adjusted to the SMT-1 installation.

Acknowledgements: The article was published by the authors by conducting scientific research under the *State Research-Innovation Project*, No. 160-PS of 31.01.2020 *"Increasing the competitiveness of precessional transmissions by developing and capitalizing on the gear with conform contact of the teeth and expanding their application area". Project number 20.80009.700.24*, dated 31.01.2020. *Project leader* - Acad. Ion Bostan.

References

1. Stanovskoy V.V. etc. Eccentric-cycloidal gearing of gear profiles. RF patent No. 2439401, 2007 [in Russian].
2. Radzevich S.P. *High-conformal gearing: A new look at the concept of Novikov gearing.* Proc. of Intern. Conf. on Gears, October 5–7, 2015, Technical University of Munich, Garching, Germany, (2015), 1303–1314.
3. Radzevich S.P. *A possibility of application of Plucker's conoid for mathematical modeling of contact of two smooth regular surfaces in the first order of tangency. Mathematical and Computer Modeling,* Vol. 42, (2004), 999–1022.
4. Stanovskoy V.V. et al. *Toothed wheel gearing and a planetary toothed mechanism based thereon (variants).* USA Patent, no 8157691 B2, 2012.
5. Tsay C.-B., Fong, Z.H. *The mathematical model of Wildhaber-Novikov gears applicable to finite element stress analysis.* Math. Comput. Modeling, Vol. 12, 8, (1989), 939–946.
6. Wildhaber E. *Foundations of Meshing of Bevel and Hypoid Gearings: (a collection of journal papers translated from English and coments by A.V. Slepak).* Mashgiz, Moskow, 1948 (in Russian).
7. Wildhaber E. *Gear tooth shape.* U.S. Patent nr. 3.251.236, 1966.
8. Bostan I., Scaticailov S., Toca A. Mathematical model for determining the line of contact tool-gear bevel gear precessional to machining by grinding. Modern technologies. Quality. Reorganization. Section 7: "Construction and technology for gears". International Conference of Scientific Communications on the 35th Anniversary of the Technical University of Moldova, May 27-29, 1999, Chisinau, Vol. 4, (1999), 419-424 [in Romanian].
9. Bostan I. Creation of planetary precession gears with multi-pair gearing: DSP1, dis. Dr. habilitate. Bulletin of MSTU im. N. Bauman. Moskow, 1989. Volume 1, 511 p. Volume 2 (supplement), 236 p. [in Russian].
10. Bostan I. Precessional gears with multi-pair gearing. Shtiincza, Kishinev 1991. 356 p.
11. Bostan I.A., Drozdov Yu.N., Azhder V., Oprya A.G. Calculation of engagement of precessional gears for wear life. Trends in increasing the load capacity of gears by gearing. KPI, Kishinev, (1989), 67-78 pp.
12. Bostan I. Development of planetary precessional gears [Elaborarea transmisiilor planetare precesionale]. DSP5 Scientific report. KPI. TsNPO "Kometa". Scientific hands Bostan I. Gos. No. GR 01840010860. Inv. No. 2890022721. Moskow, 1988. 29 p.[in Russian].
13. Bostan I. Research, development and development of planetary precessional gears with multi-pair curvilinear-arc gearing. DSP6 Scientific report. KPI. Enterprise G4805. Gos. No. GR 01840010860. Inv. No. 02871143025. Moskow, 1986 [in Russian].
14. Bostan I. Precessional Transmissions. Volume 1 (Synthesis, Kinematics and Calculation Elements). Edit. "Bons Offices", Chisinau, 2019, 477 pp. ISBN 978-9975-87-495-3.
15. Bostan I. Precessional Transmissions. Volume 2 (Contact Geometry, Surface Generation and Applications). Edit. "Bons Offices", Chisinau, 2019, 593 p - ISBN 978-9975-87-525-7.
16. Crudu I. Tribomodeling. AGIR Publishing House, Bucharest, 2011, p. 187.
17. *Maşhina dlya ispytaniya materialov na TRENIE I IZNOS, 2070 SMT-1. Tehnicheskoe opisanie i instruccziya po èxpluataczii.* Gb.2.779.013 TO. Izd. Minist. Priborostr, sredstv avtomotiz. i sistem upravleniya. Moskva – 1980, 15p.

Journal of Engineering Science *Vol. XXIX, no. 2 (2022), pp. 18 - 32*
Fascicle *Industrial Engineering* *ISSN 2587-3474*
Topic *Materials Science and New Technologies* *eISSN 2587-3482*

https://doi.org/10.52326/jes.utm.2022.29(2).02
UDC 656.1.086:614.864

PEDESTRIAN SAFETY ELEMENTS REGARDING CAR CONSTRUCTION

Vasile Plămădeală*, ORCID: 0000-0003-1722-2649,
Vladimir Goian, ORCID: 0000-0002-0031-0389

Technical University of Moldova, 168 Stefan cel Mare Blvd., Chisinau, Republic of Moldova
*Corresponding author: Vasile Plămădeală, *vasile.plamadeala@fimit.utm.md*

Received: 01. 31. 2022
Accepted: 02. 25. 2022

Abstract. Almost a quarter of people killed in road accidents worldwide are the most vulnerable road users – pedestrians. Every year, more than 300000 pedestrians die on the world's roads, which is about 23% of the total number of people killed in road accidents. In addition, millions of pedestrians are traumatized, some of them becoming disabled for life. The article includes a brief description of the driver-pedestrian relationship, road accident statistics involving pedestrians in the Republic of Moldova and in different geographical areas of the globe, modern practices and technologies applied in car construction by manufacturing plants to ensure pedestrian safety.

Keywords: *pedestrian, pedestrian crossing, road accident, traffic accident, pedestrian safety, pedestrian collision, pedestrian collision.*

Rezumat. Aproape un sfert dintre cei decedați în accidentele rutiere din întreaga lume sunt cei mai vulnerabili participanți la trafic – pietonii. Anual pe drumurile lumii mor peste 300000 de pietoni, ceea ce constituie circa 23% din numărul total de persoane decedate în accidentele rutiere. În plus, milioane de pietoni sunt traumatizați, unii dintre ei devenind invalizi pe viață. Articolul cuprinde o descriere succintă a relației conducător-pieton, statistica accidentelor rutiere cu implicarea pietonilor în Republica Moldova și în diferite zone geografice ale globului pământesc, practicile și tehnologiile moderne aplicate în construcția automobilelor de către uzinele producătoare privind siguranța pietonului.

Cuvinte cheie: *pieton, trecere de pietoni, accident rutier, accident de circulație, siguranța pietonului, tamponarea pietonului, coliziunea pietonului.*

Pedestrian, according to the Road Traffic Regulations [1, 2], is considered the person who is on the road outside the vehicle and who does not perform works. Most pedestrians are people who walk, move to or from work, school, shop, etc., perform a physical activity, walk, drive a bicycle, moped, motorcycle, pull or push a car, a toboggan, a freight cart, strollers or wheelchairs for the disabled, carry in their arms, head, shoulders or back loads of different sizes and shapes, run or walk fast, sit or sit on the road platform so that all the world at some point is as a pedestrian, even if some only for short periods of time.

Walking is the most common form of movement, regardless of social groups, in the world. Virtually any route or walk begins and ends with walking. On some routes, walking is the only way to travel, regardless of distance.

It is known that walking has a beneficial effect on human health and contributes to the protection of the environment, as it increases physical activity, which in turn leads to a decrease in the frequency of cardiovascular disease and obesity-related diseases. In this regard, many countries have launched programs that encourage walking [3].

Unfortunately, the promotion and widespread use of pedestrian traffic can, in some cases, lead to an increase in the number of road accidents and injuries. Due to the rapid increase in the number of vehicles (1,2 billion in the world [4, 5], 1,2 million in the *Republic of Moldova* [5, 6]) and their frequency of use, as well as the general neglect of the need to build for pedestrians roads and landscaping, pedestrians are increasingly at risk of getting involved in road accidents. The vulnerability of pedestrians is further amplified in the conditions of unsatisfactory application of the Road Traffic Rules (*RTR*).

The higher share of vehicle-pedestrian conflicts is registered in the urban environment, where with the development of cities, the pedestrian traffic has also increased spectacularly. In urban areas, about half of road accidents occur due to non-compliance with pedestrian traffic rules [7].

According to estimates, more than 300000 pedestrians (about 180000 children) die in road accidents annually in the world, which is about 23% of the total number of deaths in road accidents (Figure 1).

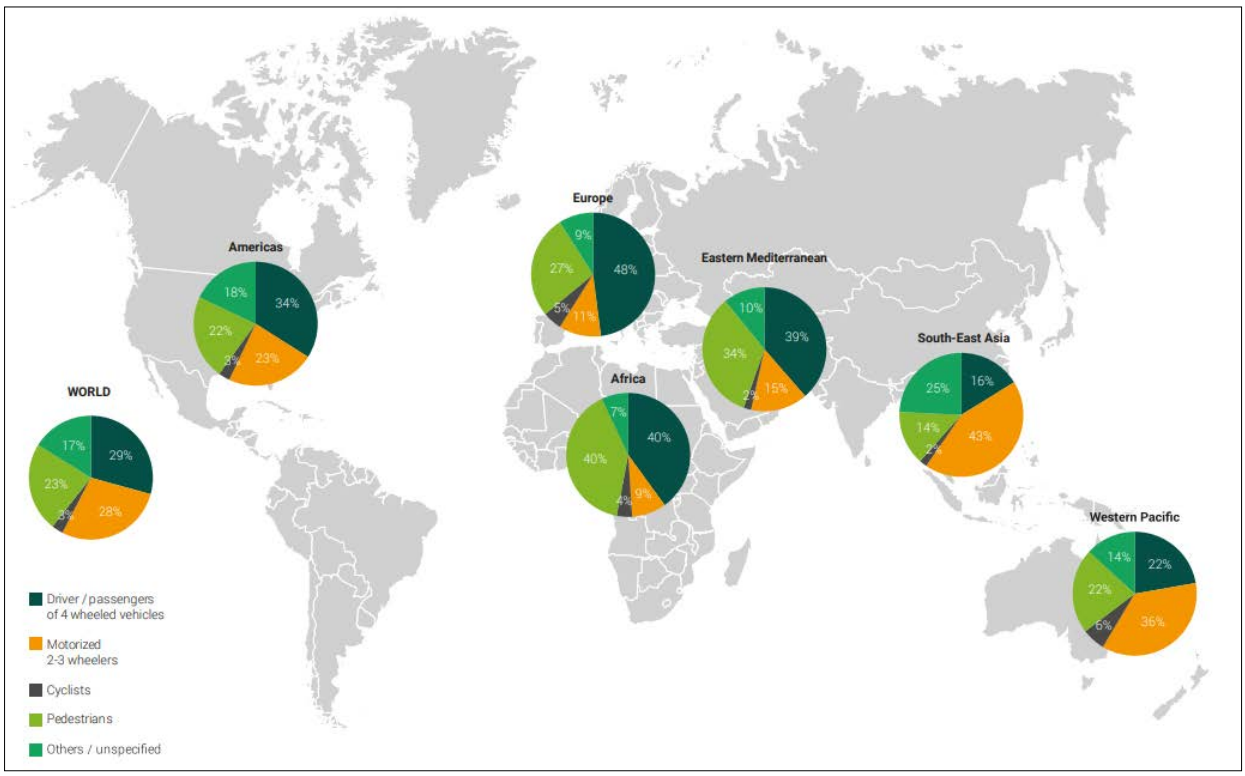

Figure 1. Distribution of deaths by categories of road users by *WHO* regions [11, 12].

29% of those who died in road accidents belong to drivers and passengers of cars, 28% to motorcyclists, and the remaining 20% – to other road users [3, 8-12]. The situation varies significantly between regions of the world. In most low- and middle-income countries, the percentage of road accident victims, such as pedestrians, cyclists, drivers and passengers of two- and three-wheeled motor vehicles, is significantly

higher than in high-income countries. For example, in the *WHO African Region*, 40% of all road accident deaths are due to pedestrians, and in the *WHO West Pacific Region* 36% are to motorcyclists, ie drivers and passengers of 2- or 3-wheel motor vehicles (Figure 1). Drivers and passengers represent between 16% of those killed in road accidents in the *South-East Asia Region* to 48% in the *European Region*.

The *WHO* regions with the highest share of pedestrian deaths in road accidents are the *African Region* with 40% and the *Eastern Mediterranean Region* with 34%, followed by the *European Region* with 27%, the *American Region* and the *Western Pacific Region* with 22% each, and the *Region Southeast Asia* with the lowest share of 14%.

Pedestrian collisions, like other road accidents, cause psychological and socio-economic damage, as well as damage to health. The traumas received as a result of road accidents consume the material resources necessary for the development of the country as a whole and the family in particular. There are no global estimates of the economic impact of road accidents involving pedestrians, but losses in road accidents are estimated at between 1% and 3% of *GDP* [2, 3, 7, 13].

Accidents with pedestrians affect people of all ages, although under certain conditions some age groups may be affected more than others. For example [3]:

- it was found that approximately 57% of pedestrians killed in road accidents in four cities in *South Africa* were between 20 and 44 years old;
- in the *USA* in 2009, the mortality rate among pedestrians over the age of 75 was 2,28 per 100000 inhabitants, which is higher than the mortality rate in any other age group;
- in *Hyderabad* (*India*), the age of 61% of pedestrians who suffered in traffic accidents was between 21 and 40 years;
- in the *Australian* state of *New South Wales* in 2010, 20% of pedestrians who died were under 21 years old, and another 29% – between 21 and 40 years old;
- the results of a study of road injuries among children and adolescents in *African* cities showed that 68% of cases went to pedestrians;
- a study in *Dar es Salaam* (*Tanzania*) found that 45% of traumatized pedestrians were adults.

It has been found that male pedestrians, both children and adults, are more often involved in road accidents with the involvement of pedestrians. For example, a study in the *US* showed that men accounted for 70% of pedestrian deaths, with a mortality rate of 2,19 cases per 100000 population, while in women the mortality rate was 0,91 per 100000 inhabitants. The results of a study conducted in *Mexico* showed that the pedestrian mortality rate was higher among men (10,6 per 100000 inhabitants) than among women (4 per 100000 inhabitants) [3].

Socio-economic status is one of the key determinants of pedestrian road trauma. As a rule, the representatives of the poorer groups of the population are exposed to a higher risk of trauma when walking. For example [3]:

- in the *UK*, the risk of trauma in road accidents in children from lower socio-economic groups was higher more than twice compared to children with a higher socio-economic position;
- in the *US*, in poor areas of *Orange County*, *California*, road accidents involving pedestrians occurred four times more often;
- In *Hyderabad* (*India*), children in the upper quartile of households by income level were much less involved in road accidents.

In general, there are significant differences between countries in terms of places where road accidents involving pedestrians take place. While in high-income countries pedestrian collisions are more common in cities than in rural areas, in low- and middle-income countries the opposite legality is a feature. For example [3], about 70% of all pedestrian deaths in *European Union* countries and 76% in the *US* occur in urban areas. In the *UK*, young pedestrians have been involved in road accidents five times more often in cities than in rural areas, and the death rate has been twice as high. The results of a study conducted in *China* revealed the opposite trend: pedestrians in rural areas suffered more road injuries than pedestrians in cities. A study conducted among university students in *Cairo* (*Egypt*) showed that for those living in rural areas, the probability of suffering road injuries was significantly higher, compared to city dwellers.

Most pedestrian collisions occur when crossing the road. For example [3], a study in *Ghana* showed that 68% of dead pedestrians were hit by vehicles in the middle of the road. Information obtained from 73 pedestrians during a study in *Kenya* showed that 53 people (72,6%) were traumatized when they crossed the road, eight people (11%) – when they were on the sidewalk, six people (8,2%) – when walking along the road and six (8,2%) – in other situations, including when dealing with street trade.

In some countries, there are more road accidents involving pedestrians on weekdays than on weekends, while in other countries, on weekends, there are more fatal collisions with pedestrians. In the *United States*, in December, most pedestrian collisions occur during dusk and in the first hour after dark on all days of the week, and in June during dusk and in the first hour after dark on Fridays and Saturdays [3].

Although child pedestrians are given attention in road education, about one in ten deaths among people aged 5-15 are due to road accidents. Children are vulnerable pedestrians because they are more difficult to see in the driver's field of vision and, conversely, from their low visual position they do not observe or appreciate the movement of vehicles correctly. Also, children show mental lability and do not have the ability to correctly appreciate distances and walking speeds. The statistics of road accidents show that the percentage of elementary school students who died as a result of the impact with moving vehicles is three times higher than that of high school students [7].

The elderly are also the most common victims among pedestrians. They are particularly vulnerable, due to the decrease in their ability to observe approaching vehicles, as well as due to their low agility and speed to avoid vehicles or cross the road more quickly.

In relation to drivers, pedestrians have some essential characteristics:

- are more heterogeneous in terms of age and education on road traffic;
- are more numerous per unit of length or surface of the roads;
- underestimates the effects that their behavior can produce in the development of car traffic;
- know less about the traffic rules and give them less importance;
- are more difficult to follow and constrained to violate traffic rules and signs;
- age is a more important factor in road accidents, young pedestrians due to ignorance, and the elderly due to inattention.

These characteristics determine an unpredictable behavior of pedestrians, the measures of protection and disciplined, comfortable and safe organization of their traffic being much more difficult to achieve.

One of the main problems that arises is the behavior of pedestrians. Usually, when walking, people choose the shortest path, and if they go with a well-established goal they do not want to consume too much time, so they often follow the rules as much as they deem necessary. The shortest route does not require the obligatory use of pedestrian crossings or crossings, especially if this means an additional walking distance. They may also not follow the red traffic light signal if they wait longer. In addition, pedestrians tend to pay less attention to traffic on known routes than in unknown circumstances [14]. When the loss of time becomes substantial, pedestrians become impatient, especially children, and endanger themselves by trying to cross through inappropriate intervals between vehicles. The maximum delay that pedestrians accept must not be greater than that which would be the red signal of a traffic light located at the marked crossing.

An unthinking action of the pedestrian becomes a bad dream for the driver, because in 90% of cases for violations of the pedestrian is responsible to the driver. This happens because the law says the following: even if the pedestrian has violated, the driver must anticipate his actions and not allow the accident.

The main risk factors for pedestrians are well known and include: *the behavior of drivers*, especially in terms of speed and drunk driving; *the level of development of pedestrian infrastructure* in terms of the absence of sidewalks, walkways and elevated dividing lanes, etc.; *vehicle construction* – the presence of a solid and hard front, which does not attenuate and reduce the force of the impact on of the pedestrian and poor visibility of pedestrians. In many countries, emergency services needed to save the lives of traumatized pedestrians are also hampered by their poor functioning.

Other factors that contribute to pedestrian trauma are [3]:

- poor compliance with traffic rules;
- aggressive and unsafe driving;
- stealing the attention of drivers or pedestrians, including by using mobile phones;
- driver fatigue;
- the „*pedestrian-vehicle*" conflict at pedestrian crossings;
- reaction and slow walking speed in the elderly;
- the inability of children to properly assess the speed of vehicles, the distance to them and other appropriate information, which would allow them to cross the street safely without accompanying adults;
- lack of supervision of children, who are still too young to make their own decisions;
- the unwillingness or refusal of the drivers to respect the right and priority of pedestrians in the cases provided by law;
- technical condition of vehicles and their defects (eg defective brakes, poor lighting, damaged windscreen etc.);
- silent (electric) vehicles, the presence of which cannot be detected by hearing.

The following should also be mentioned [14]:

1. Pedestrians represent the largest category of traffic participants, which is characterized by disorganization.
2. Some pedestrians do not know the *Road traffic regulations*. Another part of pedestrians know *RTR* in an insufficient volume and consciously violates them.
3. The pedestrian, who crosses the road and suddenly notices the vehicle, usually gets lost and tends to turn back.

4. Older people are characterized by reduced mobility, poor hearing and sight, delayed reaction and react inappropriately to the dynamic characteristics of vehicles.
5. The group of pedestrians, waiting to cross the road in case of intense transport flow, presents a greater danger than a lone pedestrian.
6. If there are children at the side of the road, it must be taken into account that they are impatient and inattentive.
7. The field of vision of children is one third of the field of vision of adults, and often incorrectly assesses the direction and speed of vehicles.
8. Children can cross the road directly in front of the vehicle, looking only in front of it.
9. The use of umbrellas by pedestrians and the presence of hoods on the head limits visibility and the noise of rain disturbs the noise of vehicles.
10. In winter, pedestrians hear the noise of vehicles worse. They can also slip unexpectedly on the slippery road.
11. Drunk pedestrian behavior is unpredictable. They may suddenly change direction or fall.

Road accidents involving pedestrians in the *Republic of Moldova* constitute about 40% (period 2000-2018) of the total number of accidents (Table 1) [2, 7, 12, 14-22]. Most accident situations happen in localities. They are created in places where pedestrians frequently appear: at pedestrian crossings, road vehicle stations, intersections, markets, places often frequented by children etc.

Every ninth road accident was caused by pedestrians (5357, or 10,75% of the total number of road accidents).

Table 1

Frequency of road accidents (2000–2018)

The year	Total road accidents	Road accidents involving pedestrians	% of the total number of road accidents	Road accidents involving children	% of the total number of road accidents
2000	2580	1269	49,19	491	19,03
2001	2666	1237	46,40	496	18,60
2002	2899	1369	47,22	518	17,87
2003	2670	1289	48,28	440	16,48
2004	2447	1122	45,85	373	15,24
2005	2289	1041	45,48	342	14,94
2006	2298	1006	43,78	316	13,75
2007	2437	1054	43,25	360	14,77
2008	2875	1079	37,53	635	22,09
2009	2755	1066	38,69	536	19,46
2010	2930	1071	36,55	544	18,57
2011	2826	1006	35,60	564	19,96
2012	2712	935	34,48	557	20,54
2013	2603	980	37,65	485	18,63
2014	2564	886	34,56	411	16,03
2015	2527	831	32,88	357	14,13

Continued Table 1

2016	2479	835	33,68	387	15,61
2017	2640	997	37,77	371	14,05
2018	2613	946	36,20	414	15,84
Total	**49911**	**20019**	**40,19**	**8597**	**17,26**

The violations committed by pedestrians that led more frequently to road accidents were:

- crossing the street without being insured beforehand;
- crossing the street in forbidden places;
- irregular driving on the road;
- unexpected exit from vehicles, obstacles.

The number of road accidents in which children suffered is 8597 or 17,26% of the total number of road accidents, as a result of which 602 or 8,11% of the total number lost their lives, and 8757 children were traumatized or 14,46% (Figure 2).

Due to the children's own fault, there were 1810 road accidents (Figure 2). 114 of them died and 1682 children were traumatized.

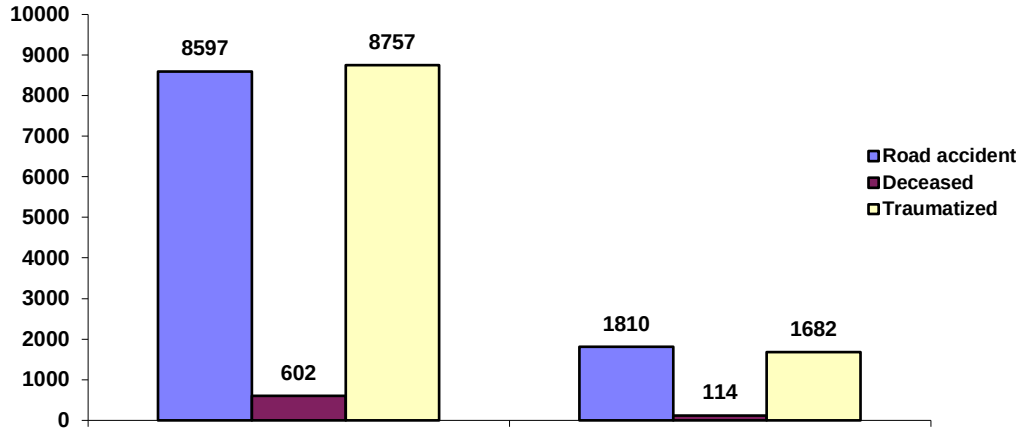

Figure 2. Children who suffered in road accidents (2000–2018).

In order to minimize the number of victims in road accidents, pedestrians are urged to follow some simple but very useful traffic rules [1, 2, 22]:

- make sure at all times, even when you are on the crosswalk, that the crossing can be done safely (vehicles are stopped before marking);
- at pedestrian crossings, drive to traffic light signals for pedestrians, vehicles or traffic officers;
- once engaged in crossing, do not slow down or stop for no reason;
- wait for the route vehicles in the station, on the footway, or on the sideways, as the case may be, on the shelter;
- on undirected crossings, exit the road only when you are convinced of the safety of the crossing even if you have priority over drivers;
- if there are no pedestrian crossings within the visibility limits of 100-150 meters, cross the road only after making sure that no vehicles are approaching;
- move on the right side of the footways, and in their absence – on the sidewalk;
- outside the localities, drive on the left side of the road to meet the flow of vehicles;
- when traveling at night or in low visibility conditions, wear clothing with fluorescent-reflective elements;

- if you are a parent or educator and accompany children – do not allow their unattended exit on the road, and while driving, drive on the outside of the sidewalk or sidewalk;
- children should not be allowed to cross alone – they are unpredictable and cannot appreciate distances and speeds correctly. Do not forget! – children imitate the road behavior of adults.

Pedestrians are also forbidden to engage in road crossing [1, 2, 22]:

- directly in front or behind vehicles stopped or parked on the road;
- on road sectors with limited visual field;
- if a vehicle with a priority traffic regime is approaching, which emits light and sound signals;
- to cross the tracks at level crossings, when the light signal or the position of the barrier prohibits the crossing.

At the same time, in order to avoid road accidents involving pedestrians, drivers are urged to reduce their speed and drive more carefully [22]:

- when approaching the pedestrian crossing, so that it can stop and give priority;
- in the area of educational institutions, socio-cultural or economic objectives, where there is a large flow of pedestrians, especially children;
- when approaching the stations of road vehicles, especially those that are not provided with pedestrian shelters, where some pedestrians can engage in crossing in front of the means of transport;
- when approaching one or more pedestrians moving on the roadway, regardless of the direction of travel.

In order to increase pedestrian safety, attention must be paid to the construction of vehicles, road infrastructure, means of road traffic control, in particular speed limitation, and the application of rules and regulations relating to road traffic.

In the context of the above, car manufacturers since 1960 have set themselves the goal of building vehicles that would reduce the damage and injury to both drivers, passengers and pedestrians in traffic accidents. Since 1967, *General Motors* has used shock-resistant windows. This solution reduced the survival rate for the driver and passengers, but reduced the damage to pedestrians when they collided. The dangers of pedestrian collisions are obvious, and the windshield is one of the most „*favorable*" areas with which it can come into contact.

The impact between the vehicle and the pedestrian is currently a very important issue regarding the active and passive safety of motor vehicles. Data collected from around the world indicate that much more pedestrians die in road accidents than vehicle passengers. A pedestrian bumped at a speed of 60 *km/h* is very likely to die, regardless of the safety solutions incorporated in the vehicle. The separation of pedestrians from road traffic through road infrastructure is the biggest contribution in the field of pedestrian safety, technology having an important word in this area. Currently, car manufacturers are developing equipment to prevent collision, based on radar or ultrasound, which brakes the vehicle in the event of the danger of colliding an obstacle, including a pedestrian, pedestrian protection in the event of a collision, during night hours etc.

The pedestrian protection system [5, 23] is designed to reduce the consequences of a pedestrian collision with the car in the event of a road accident. The system (Figure 3) is developed by *TRW Hodings Automotive* (*Pedestrian Protection System, PPS*), *Bosch* (*Electronic*

Pedestrian Protection, EPP), *Siemens* and since 2011 is installed in series on the cars of European manufacturers. The systems listed have an analog construction.

The principle of operation of the pedestrian protection system is based on the opening of the hood at the collision of the pedestrian with the car, which achieves the increase of the space between the hood and the engine parts and correspondingly the reduction of the pedestrian trauma. In fact, the raised hood participates as a safety cushion.

In addition to the system presented on cars for pedestrian protection, the following constructive solutions are used, that reduce collision trauma:

- „*soft*" hood;
- brushes without housing;
- „*soft*" bumper;
- inclined hood and windshield;
- increased distance between engine and bonnet.

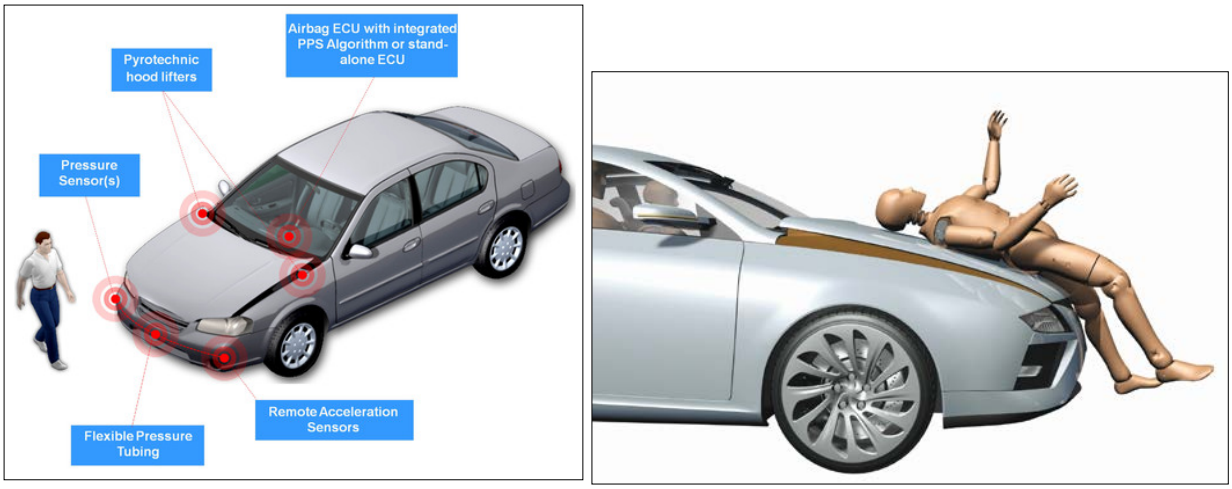

Figure 3. Pedestrian Protection System, PPS.

The further development of the pedestrian protection system is the *Pedestrian Airbag System*, introduced by *Volvo* in 2012 [5, 24]. The system is designed to reduce the degree of pedestrian trauma in a collision with the car. The air cushion (Figure 4) inflates outside the car and covers the bottom of the windscreen and side brackets. At the same time, the rear of the bonnet is raised when the front bumper of the car detects the impact with a pedestrian. Together, the air cushion and the raised hood ensure a significant reduction in trauma to the pedestrian's collision with the car. The pedestrian air cushion works in tandem with another *Volvo* system – the *Pedestrian Detection system*.

The pedestrian air cushion operates at a speed of 20 to 50 *km/h* and cannot be deactivated by the driver. According to statistics, the majority (75%) of road accidents involving pedestrians take place at speeds of up to 40 *km/h*.

The pedestrian detection system [5, 26] is designed to prevent collisions with pedestrians. The system recognizes people near the car, automatically decelerates the car, reduces the impact force and even avoids the collision with the pedestrian. The use of the system allows a 20% reduction in pedestrian mortality, and in the case of road accidents and a 30% reduction in the risk of serious trauma.

The pedestrian detection system was first used in 2010 on *Volvo* cars. The system currently has a number of changes:

Figure 4. Pedestrian Airbag System, PAS [5, 25].

- *PDS (Pedestrian Detection System)* from *Volvo* (Figure 5)*;*
- *APDS (Advanced Pedestrian Detection System)* of the *TRW* (Figure *6*);
- *ES (Eye Sight)* from the *Subaru* (Figure 7).

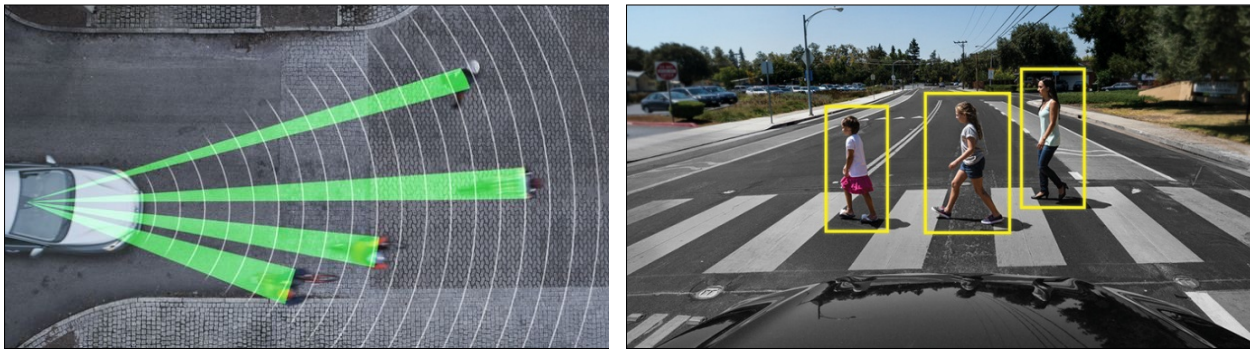

Figure 5. Pedestrian Detection System, PDS [5, 27].

The following interdependent functions are performed in the pedestrian detection system: pedestrian detection, collision warning and automatic braking.

To detect pedestrians, a video camera and a radar are used (two video cameras at *Subaru*), which actually operate at a distance of up to 40 *m*. If the pedestrian is detected by the video camera and the result is confirmed by radar, the system tracks pedestrian movement, predicts subsequent displacement and estimates the probability of a collision with the car. The detection results are displayed on the multimedia system screen. The system also reacts to cars, which are parked or moving in the same direction.

Figure 6. *Advanced Pedestrian Detection System, APDS* [5, 28].

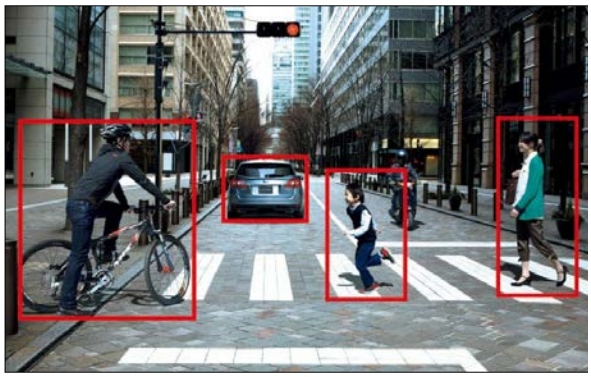

Figure 7. Eye Sight, ES [5, 29].

If the system has determined that a collision with a pedestrian is unavoidable due to the current nature of the car's movement, the driver receives an audible warning. Then, the

system evaluates the driver's reaction to the warning – changing the character of the car's movement (braking, changing direction). If the reaction is missing, the pedestrian detection system automatically stops the car. In this situation, the pedestrian detection system is a derivative of the automatic emergency braking system.

The pedestrian detection system allows complete avoidance of collision at speeds of up to 35 *km/h*. At higher speeds, the system cannot completely prevent the accident, but it can reduce the consequences for the pedestrian by decelerating the car before the collision. The statistical data show that the probability of pedestrian death following the collision with the car at a speed of 65 *km/h* is 85%, 50 *km/h* – 45%, 30 *km/h* – 5%.

The automatic emergency braking system creates partial or maximum braking pressure without the involvement of the driver, ie automatically.

Emergency automatic braking systems include [5, 30]:

- *PSB* (*Pre-Safe Brake*) on *Mercedes-Benz* cars;
- *CMBS* (*Collision Mitigation Braking System*) on *Honda* cars;
- *CBC* (*City Brake Control*) on *Fiat* cars;
- *ACS* (*Active City Stop*) on *Ford* cars;
- *FA* (*Forward Alert*) on *Ford* cars;
- *FCM* (*Forward Collision Mitigation*) on *Mitsubishi* cars;
- *CEB* (*City Emergency Brake*) on *Volkswagen* cars (*figure 8*);
- *CWAB* (*Collision Warning with Auto Brake*) on *Volvo* cars;
- *CS* (*City Safety*) on *Volvo* cars (*figure 9*);
- *PEBS* (*Predictive Emergency Braking System*) from *Bosch*;
- *AEW* (*Automatic Emergency Braking*) of the *TRW*.

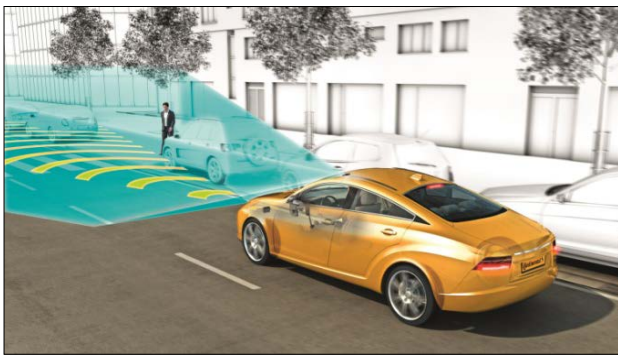

Figure 8. City Emergency Brake, CEB.

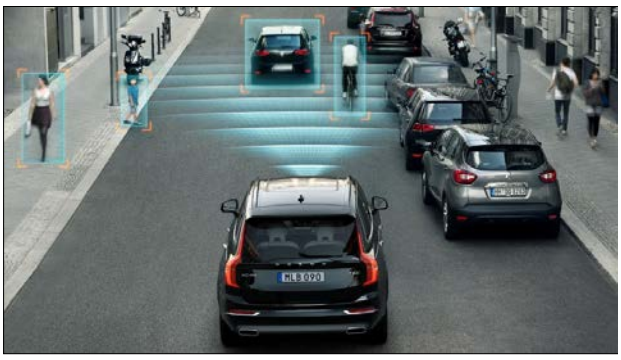

Figure 9. City Safety, CS [5, 31].

Volvo City Safety is an autonomous emergency braking technology that allows you to avoid bumps at low speeds or reduce their consequences. At speeds of 3,6 to 30 *km/h* it uses a transducer, which operates at a distance of up to 10 *m*. If it determines the possibility of an accident, the system prepares the brakes. If the driver does not react, the car's brakes are applied. From a speed of 15 *km/h* the car is able to decelerate to a complete stop. At high speeds it is not possible to avoid buffering, but it will be less serious. In case, if the driver persists to avoid the accident, *City Safety* disconnects.

The night vision system [5, 32] is intended to provide the driver with information on night traffic conditions. The system allows the recognition of all kinds of obstacles, traffic participants, pedestrians on an unlit road, as well as the subsequent trajectory of the road. The system helps to remove the load from the driver in low visibility conditions and thus

ensures an increase in traffic safety. Currently, the night vision system is installed as an option for premium class cars.

The principle of operation of the system is based on fixing the infrared (thermal) radiation of objects with a special camera and projecting it on the screen as a gray scale image.

There are two types of night vision systems: *active* and *passive*. Active systems use an additional car-mounted infrared light source. They are characterized by a high resolution image and an operating length of 150-250 *m*.

Known active night viewing systems are:

- *Night View Assist* from *Mercedes-Benz* (Figure 10);
- *Night View* from *Toyota*.

Passive night vision systems do not have their own source of infrared radiation. The thermal chamber (thermal mirror) captures the infrared radiation of objects at a distance of up to 300 *m*. They have a high level of contrast and a low image resolution.

Passive night vision systems are:

- *Night Vision Assistant* from *Audi* (Figure 11);
- *Night Vision* from *BMW*;
- *Night Vision* from *General Motors*;
- *Intelligent Night Vision System* from *Honda*.

Figure 10. Night View Assist [33].

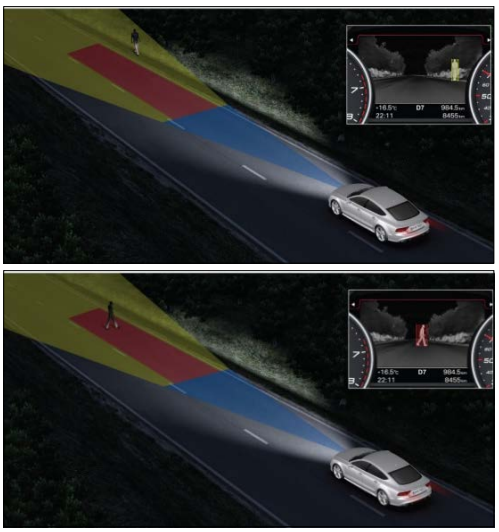

Figure 11. Night Vision Assistant [34].

The most technical and functional night vision system is the latest achievement of *Mercedes-Benz* – the *Night View Assist Plus* system. In addition to the standard driver information functions, the system warns pedestrians of a potential danger. The algorithm of the program is performed at a speed higher than 45 *km/h* and the location of pedestrians at a distance not exceeding 80 *m*.

BMW went further in this direction, presenting an intelligent night-vision system for detecting pedestrians in the immediate dangerous vicinity of the road. The *Dynamic Light Spot* system with the help of heart rate sensors determines the presence of living beings at a distance of up to 100 *m* from the car. For *BMW* cars, the *Dynamic Light Spot* system is also installed in the *Night Vision* viewing system.

Another car manufacturer that draws more attention to the health and life of pedestrians is *Ford* [5, 35]. The latest generation of *Ford Focus* benefits from sophisticated

safety systems designed to prevent or reduce the effects of a road accident on passengers and pedestrians. These systems include a technology especially appreciated by *Euro NCAP*: *Pre-collision Assist* with *Pedestrian and Cyclist Detection*. This system can detect pedestrians and cyclists on or near the road and could intersect the trajectory of the car's movement, applying the brakes automatically, if it detects a potential collision and the driver does not respond to warnings. Detection is now possible at night, with the help of headlights.

The level of protection offered by the car to pedestrians, in case of a frontal impact with them, is 72%. The front parts of the car are soft and if a person is taken on the hood, he will not suffer serious injuries, unless he hits his head in the lower part of the uprights.

Dynamic Light Spot [5, 36], which literally means a „*spot lighting*" dynamic lighting system. The name speaks for itself: automation detects the pedestrian and directs light towards him (Figure 12), thus indicating to the driver the potential danger. Moreover, the hint appears earlier, so that the object appears in the light of the passing headlights. As a result, the driver receives an advantage of a few seconds or tens of meters, which are often not enough to brake or bypass the pedestrian safely.

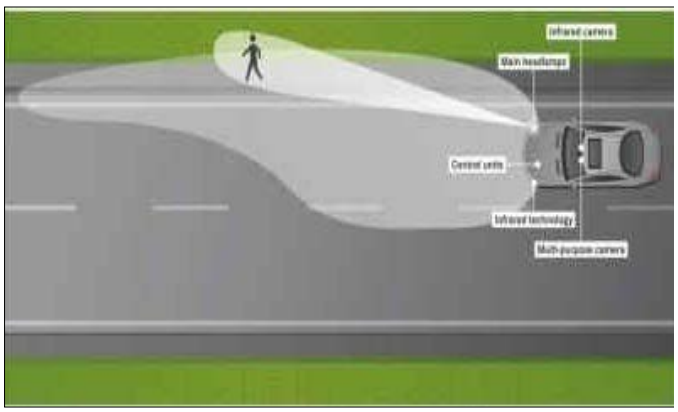

Figure 12. Dynamic Light Spot.

Figure 13. *„Night Guide"* lamp [5, 37].

„*Night Guide* – 3 in 1" lamp – multispectral lamp (Figure 13), which combines the properties of three types of lamps: „*Vision Plus* + 50%", „*Blue Vision*" and „*Weathervision*". The light from this lamp on the road is scattered in three areas:

- in front – white light with 50% amplified brightness, which allows the illumination of the roadway at a distance greater by 10–20 *m*, compared to a halogen lamp;
- on the left – yellow light, which does not blind drivers in the opposite direction;
- on the right – the area with blue daylight, which illuminates well, in particular, the road signs and the sidewalk.

Conclusion. In the end we can conclude that no car manufacturer, no passive or active safety system, no matter how sophisticated it can be, cannot replace man, and to avoid the number of such road accidents. Both drivers and pedestrians must comply with the *RTR*, meet the requirements of traffic behavior, crossing dangerous road areas so as not to endanger his life and health.

Until recently, the driver of the car was fully to blame for road accidents involving pedestrians, thus exempting the pedestrian from legal consequences, which led to an aggressive behavior on the part of pedestrians compared to drivers when crossing the road in forbidden places, sometimes even a few, meters of pedestrian crossings, unlit, without a fluorescent vest or at least some light source, which would make them visible. A draft law is

currently being prepared in several countries for approval, which would provide that in such cases, pedestrians should bear both legal and material liability for the violation of the *RTR* resulting in the tamponade of pedestrians. The neighboring country of the *Republic of Moldova* this year has implemented such a project, if such a law will be reached in the *Republic of Moldova* it remains a question.

Bibliography

1. Government Decision No. 357 of 13.05.2009 regarding the approval of the Road Traffic Regulation. In: *Official Monitor of the Republic of Moldova*, 15.05.2009, no. 92-93, art. 409. Date of entry into force: 15.07.2009 (in Romanian).
2. Ududovici D., Plămădeală V. *Regulamentul şi securitatea circulaţiei rutiere*. Manualul conducătorului auto. Ediţia a 3-a, revăzută şi completată. Chişinău, 2010, 288 p. ISBN 978-9975-109-22-2.
3. *Pedestrian safety. Guide to road safety for managers and professionals*. World Health Organization 2013, 130 p. ISBN 978-92-4-450535-9 (in Russian).
4. *How many cars are there in the world and how many will be in 2050* [online]. Copyright 2020 Ringier Romania [quote 03.02.2020]. Available: https://www.auto-bild.ro/stiri/cate-masini-sunt-in-lume-si-cate-vor-fi-in-2050-72426.html.
5. Plămădeală V., Goian V., Beiu I. *Organizarea și siguranța circulației rutiere. Volumul 2. Siguranţa automobilelor: activă, pasivă, post-crash şi ecologică.* Curs universitar. Editura „Tehnica-UTM". Chișinău 2021, 435 p. ISBN 978-9975-45-721-7, ISBN 978-9975-45-723-1 (PDF).
6. *Statistical data on the composition of the State Register of Transports in profile of the type of means of transport (status as of January 1, 2022)* [online]. Copyright © Public Services Agency, 2022 [quote 23.01.2022]. Available: http://www.asp.gov.md/node/1662.
7. Plămădeală V. *Accidente rutiere și siguranța circulației*, Teză de magistru, Chișinău UTM 2006, 159 p.
8. Shherbakova E. M. *Global trends in road traffic deaths according to WHO estimates 2018* [online]. Demoskop Weekly. 2019. № 819-820 [quote 05.02.2020]. Available: http://demoscope.ru/weekly/2019/0819/barom01.php.
9. *Report on the state of road safety in the world. Time to act*, World Health Organization, 2009, 297 p. ISBN: 978 92 4 456384 7 (in Russian).
10. *Report on the state of road safety in the world 2015. Executive Summary*, World Health Organization, 2015, 12 p. ISBN: 978 92 4 456384 7 (in Russian).
11. *Global status report on road safety 2018*, World Health Organization, 2018, 419 p. ISBN 978-92-4-156568-4.
12. Plămădeală V. *Two decades of accidental situation in the Republic of Moldova.* In: Ingineria automobilului. 2022, nr. 62, p. 19 – 26. ISSN 1842-4074.
13. Plămădeală V., Pădure O. *Analiza accidentelor rutiere*. În: Conferinţa II-a practico-ştiinţifică „Strategii de management, inginerie şi tehnologii în transporturi". Chişinău, 27 octombrie 2006, UTM, p. 62-66.
14. Plămădeală V. *Modern road safety elements of the pedestrians.* În: Journal of Engineering Science. 2019, nr. 1, p. 47 – 60. ISSN 2587-3474, eISSN 2587-3482.
15. Plămădeală V. *Analiza accidentelor rutiere în Republica Moldova în perioada anilor 2000–2014*. În: Materialele conferinţei naţionale ştiinţifico – practice „Transporturi: inginerie, economie şi management". Chişinău, 22-23 mai 2015, UTM, p. 198 – 208. ISBN 978-9975-45-380-6.
16. Goian V., Plămădeală V., Beiu I. *Organizarea și siguranța circulației rutiere. Volumul 1. Acte normative, elemente de siguranță și caracteristici ale circulației rutiere.* Curs universitar. Editura „Tehnica-UTM". Chișinău 2021, 341 p. ISBN 978-9975-45-721-7, ISBN 978-9975-45-722-4 (PDF).
17. Statistics of Moldova [online]. *National Bureau of Statistics of the Republic of Moldova,* © 2020 [quote 14.03.2020]. Available: http://www.statistica.md/.
18. *Information note on the accident situation for the period 01.01.2019 – 31.12.2019* [online]. National Patrol Inspectorate [quote 08.02.2020]. Available: http://politia.md/sites/default/files/situatia_accidentara_12_luni_2019.pdf.
19. *Information note on the accident situation for the period 01.01.2018 – 31.12.2018* [online]. National Patrol Inspectorate [quote 08.02.2020]. Available: http:// politia.md/sites/default/files/accidenta_inp_in_rm_pentru_12_luni_a_anului_2018.pdf.

20. *Information note on the accident situation for the period 01.01.2017 – 31.12.2017* [online]. National Patrol Inspectorate [quote 08.02.2020]. Available: http://politia.md/sites/default/files/nota_informativa_privind_situatia_accidentara_pentru_perioada_a_12_luni_2017.pdf.
21. Plămădeală V. *Alcoolul și volanul – o combinație periculoasă*. În: Materialele conferinţei naţionale ştiinţifico–practice „Transporturi: inginerie, economie şi management". Chişinău, 17-18 noiembrie 2017, UTM, p. 103 – 117. ISBN 978-9975-45-511-4.
22. *More than 400 pedestrian accidents have been reported since the beginning of the year* [online]. *General Inspectorate of Police* [quote 08.02.2020]. Available: http://politia.md/ro/content/peste-400-de-accidente-cu-implicarea-pietonilor-au-fost-inregistrate-de-la-inceputul-anului.
23. *Pedestrian protection system* [online]. Modern car systems © Suslinnicov Alexandr, 2009-2017 [quote 05.01.2020]. Available: http://systemsauto.ru/passive/pedestrian_protection_system.html.
24. *Pedestrian airbag* [online]. Modern car systems © Suslinnicov Alexandr, 2009-2017 [quote 05.01.2020]. Available: http://systemsauto.ru/passive/pedestrian_airbag_system.html.
25. *The device and principle of operation of the pedestrian protection system* [online]. © 2020 Techautoport.ru [quote 05.01.2020]. Available: https://techautoport.ru/sistemy-bezopasnosti/passivnaya/sistema-zaschity-peshehodov.html.
26. *Pedestrian detection system* [online]. Modern car systems © Suslinnicov Alexandr, 2009-2017 [quote 05.01.2020]. Available: http://systemsauto.ru/active/pedestrian_detection.html.
27. *Advanced driver assistance systems (ADAS)* [online]. Copyright © 2020 NVIDIA Corporation [quote 05.01.2020]. Available: https://www.nvidia.com/en-sg/self-driving-cars/adas/.
28. Mosenzov, E., *Pedestrian detection system: device, principle of operation* [online]. Fastmb Avtozhurnal [quote 05.01.2020]. Available: https://fastmb.ru/auto_shem/3402-sistema-obnaruzheniya-peshehodov-ustroystvo-princip-raboty.html.
29. *Subaru EyeSight. Keen eye* [online]. AvtoMir [quote 18.01.2020]. Available: https://www.avtomir.ua/details/tech/subaru-eyesight-zorkiy-glaz/.
30. *System of its emergency braking* [online]. Modern car systems © Suslinnicov Alexandr, 2009-2017 [quote 05.01.2020]. Available: http://systemsauto.ru/active/brake_assist.html.
31. *Automatic braking will be added to the list of recommended safety technologies for cars v SSHA* [online]. dealerON.ru © 2008 - 2020 [quote 09.01.2020]. Available: http://www.dealeron.ru/news/3370-Avtomaticheskoe-tormozhenie-budet-vnesen-v-spisok-rekomenduemy'x-texnologij-bezopasnosti-dlya-avtomobilej-v-SSHA/.
32. *Car night vision system* [online]. Modern car systems © Suslinnicov Alexandr, 2009-2017 [quote 05.01.2020]. Available: http://systemsauto.ru/active/night_view.html.
33. Mosenzov, E., *How does a car's night vision system work* [online]. Fastmb Avtozhurnal [quote 05.01.2020]. Available: https://fastmb.ru/auto_shem/761-kak-rabotaet-sistema-nochnogo-videniya-avtomobilya.html.
34. *Night vision assistant* [online]. © 2020 AUDI AG. All rights reserved [quote 05.01.2020]. Available: https://www.audi-technology-portal.de/en/electrics-electronics/driver-assistant-systems/night-vision-assistant.
35. *The new Ford Focus received five stars following safety tests by Euro NCAP* [online]. autoblog.md © 2014-2019. All Rights Reserved [quote 18.01.2020]. Available: https://autoblog.md/video-noul-ford-focus-a-luat-cinci-stele-in-urma-testelor-de-siguranta-realizate-de-euro-ncap/.
36. *LED pointer* [online]. © 2000-2020 PRESS obozrenie [quote 17.01.2020]. Available: https://press.try.md/item.php?id=123500.
37. *Philips H4 60/55 Night Guide* [online]. © DRIVE2.RU, 2020 [quote 17.01.2020]. Available: https://www.drive2.ru/l/288230376152624075/.

Journal of Engineering Science *Vol. XXIX, no. 2 (2022), pp. 33 - 45*
Fascicle *Industrial Engineering* *ISSN 2587-3474*
Topic *Electrical Engineering and Power Electronics* *eISSN 2587-3482*

https://doi.org/10.52326/jes.utm.2022.29(2).03
UDC 621.314.222

MODES OF THE BOOSTER TRANSFORMER WITH REGULATION IN ZIGZAG

Sveatoslav Postoronca*, ORCID: 0000-0002-6826-4411,
Dmitrii Zaitsev, ORCID: 0000-0001-7207-1754,
Mihai Tirsu, ORCID: 0000-0002-1193-6774,
Irina Golub, ORCID: 0000-0001-8053-9329,
Danila Kaloshin, ORCID: 0000-0001-7194-2175

Institute of Power Engineering, Chisinau, 5 Academiei str., Republic of Moldova
*Corresponding author: Sveatoslav Postoronca, *sveatoslavpostoronca@gmail.com*

Received: 03. 15. 2022
Accepted: 05. 07. 2022

Abstract. The development of power engineering assumes the increasing flexibility of power networks through the use of various kinds of FACTS, controlled by means of power electronics and being elements of the Smart Grid. These kinds of devices can be attributed to controllers such as UPFS and „Sen" Transformer (ST), which provide regulation of voltage and power flows in networks. Due to the relevance of this topic, technical solutions are proposed that perform similar functions, which implies the need for a comparative analysis of such developments in order to optimize energy characteristics of the equipment. The scope of the paper is to develop and study a regulating transformer which belongs to the „Sen" family, but possessing the extended range and higher control accuracy. Carrying out research, mode parameters of the device were treated, as well as typical power was determined.

Keywords: *booster transformer, load, voltage control, active power, reactive power compensation, operation mode control.*

Rezumat. Dezvoltarea domeniului electroenergeticii presupune creșterea flexibilității rețelelor electrice prin aplicarea de diverse instalații FACTS, mijloace comandate ale electronicii de putere, fiind elemente ale Smart Grid. La dispozitivele de asemenea gen pot fi catalogate controlerele de tip UPFC și transformatorul „Sen", care asigură reglarea tensiunii și a fluxurilor de putere în rețea. Reieșind din actualitatea acestei tematici au fost propuse soluții tehnice, care realizează funcții prin analogie, urmate de necesitatea analizei comparative a acestor elaborări, având ca scop optimizarea caracteristicilor energetice ale echipamentelor. Scopul lucrării constă în elaborarea și cercetarea transformatorului de reglaj, ce face parte din familia „Sen", dar care dispune de un diapazon extins și o precizie sporită de reglaj. Pe parcursul cercetărilor au fost analizați parametrii de regim ai dispozitivului și determinată puterea-tip.

Cuvinte cheie: *transformator booster, sarcină, control tensiune, putere activă, compensare putere reactivă, control regim de funcționare.*

Introduction

The present stage of the electric power industry development is characterized by a significant increase of the volumes of generation of energy through the use of renewable energy sources, production of which is significantly subject to daily and seasonal oscillations. Such a circumstance might reflect upon the power quality indicators. Under these conditions the issue of transmission and distribution network's controllability is becoming increasingly relevant. Technical means, destined to the finding of solutions to tasks (provided by FACTS technologies, Smart Grid) of this kind are largely associated with the use of two-stage energy conversion – rectification and inverting.

One of modern devices providing regulation of voltage and power fluxes in networks is UPFC (Unified Power Flow Controller). The device represents itself as a combination of Static Synchronous Compensator (STATCOM) and Static Synchronous Series Compensator (SSSVC) [1–6]. By including the booster longitudinal voltage with regulated phase, the device UPFC is able in the real-time to regulate simultaneously or selectively: the voltage of power lines, impedance, angle or active and reactive power fluxes in the line, to provide independent transversal controllable compensation, active harmonic filtering, as well as other technical procedures to improve the quality of operation of power systems. The topologies of its realization can vary in quite extensive limits. In the case when the role is fulfilled through the use of a regulating transformer, its ends are connected / disconnected by means of electronic keys, which have gained a high performance level due to the fast development of the power electronics domain. Respectively, the area of their utilization extended on majority segments of the power system: power transmission and distribution, local systems of heavy industrial sector, arc furnaces and electric transport infrastructure [7-10].

To the advantages of this technology can be attributed:

- deeper influence on the characteristics of the line mode compared to other means of regulation;
- combination of the properties at once of three devices: static compensator of reactive power, installation of longitudinal compensation and installation for phase rotation.

Disadvantages of UPFC are:

- increasing of the power of regulation devices under the extension of the range;
- significant range of deviations of the output voltage depending on the values of booster voltage and its angle, that can lead to the corona discharge effects of wires and will require the strengthening of insulation;
- decline of the range of regulation of the active power under the increase of the line's length;
- high cost and, as consequence, increased installation and operating costs.

The same control effects can be achieved on the base of direct (one-stage energy conversion), which allows to accomplish much more reliable and less expensive devices. One of such technologies is a booster transformer of various configurations and destinations, well known as ST. [11–19].

By assigning with the help of tap changer needed combination, ST can correct the voltage, controlling its magnitude and phase-angle shifting, i.e. perform the same functions like UPFC. ST disposes the ability to assure the control of crossflow of active and reactive power in most backbone and distribution networks [20–22].

To the advantages of ST can be assigned:

- relative simplicity of design;

- relative not high cost;
- performs the same functions as UPFC.

Disadvantages can be considered:

- limited number of operation states;
- not high control accuracy in a given area due to the limited number of operation states;
- not high operation speed when using the regulation under load mode.

In the process of creating the so-called „intellectual" power grids (Smart Grid) and their transition in the future to the more efficient systems on the highest level, now called Microgrids, certain requirements will be imposed on the power grids to ensure an optimal load factor and a high power factor.

These functions can be realized by means of regulating transformers, controlled by power electronics, belonging to the family Sen.

Common characteristic of the object of research

This paper is dedicated to the development and research of a regulation transformer based on the principle of operation of the ST, but with an extended range and higher control accuracy. In the process of research, methods of mathematical, structural and simulation modeling were applied based on objects built in SPS-models in the Simulink/Matlab environment [23-28]. The principle circuit diagram of research object is shown in Figure 1. Basic elements of the device are two three-winding transformers, one of which performs a function of parallel (magnetizing), the second – functions of series (booster) elements. The index „*p*" marks the windings and the corresponding electrical units characterizing the mode of the magnetizing transformer, the index „*q*" marks the windings and electrical units of the booster transformer.

Elements belonging to the parallel transformer are numbered by Figures 1-30, and elements belonging to the booster transformer are numbered by digits 31-39.

List of designations of elements presented in Figure 1:

A,B,C – nomination of phases of three-phase voltage system;

A1,B1,C1 – electric inputs (input terminal) of the device;

A2,B2,C2 – electric outputs (outputs terminals) of the device;

1,2,3 – primary windings of high voltage phases A,B,C of the magnetizing transformer (W_{1pA}, W_{1pB}, W_{1pC});

4,5,6 – first regulation windings of fine regulations of phases A,B,C of the magnetizing transformer (W'_{2pA}, W'_{2pB}, W'_{2pC});

7,8,9 – first regulation windings of rough regulation of phases A,B,C of the magnetizing transformer (W''_{2pA}, W''_{2pB}, W''_{2pC});

10,11,12 – second regulation windings of fine regulation of phases A,B,C of the magnetizing transformer (W'_{3pA}, W'_{3pB}, W'_{3pC});

13,14,15 – second regulation windings of rough regulation of phases A,B,C of the magnetizing transformer (W''_{3pA}, W''_{3pB}, W''_{3pC});

16,17,18 – blocks of power electronic switches of the first regulation windings of fine regulation of phases A,B,C of the magnetizing transformer;

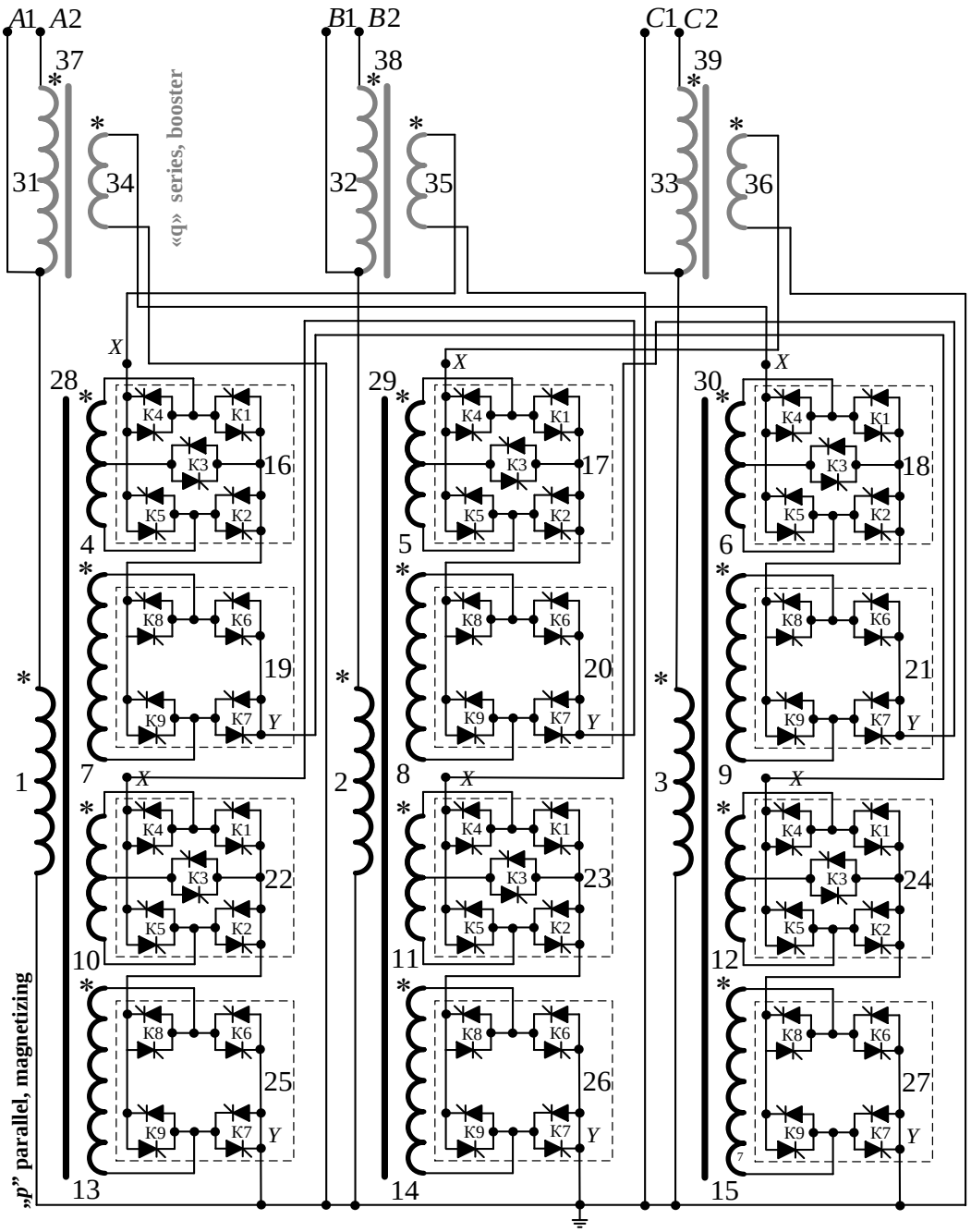

Figure 1. Principle circuit diagram of the device „wye with regulation in zigzag".

19,20,21 – blocks of power electronic switches of the first regulation windings of rough regulation of phases A,B,C of the magnetizing transformer;
22,23,24 – blocks of power electronic switches of the second regulation windings of fine regulation of phases A,B,C of the magnetizing transformer;
25,26,27 – blocks of power electronic switches of the second regulation windings of rough regulation of phases A,B,C of the magnetizing transformer;
28,29,30 – cores of magnetic circuits of phases A,B,C of the magnetizing transformer;
31,32,33 – high voltage windings of phases A,B,C of the booster transformer ($W_{1qA}, W_{1qB}, W_{1qC}$);
34,35,36 – low voltage windings of phases A,B,C of the booster transformer ($W_{2qA}, W_{2qB}, W_{2qC}$);
37,38,39 – cores of magnetic circuits of phases A,B,C of the booster transformer;
K1 ÷ K9 – switchers of power electronics.

As follows from the circuit diagram (Figure 1), high voltage windings ($W_{1pA}, W_{1pB}, W_{1pC}$) of the magnetizing transformer are supplied from the power network through electric inputs A1, B1 and C1. The ends of these windings are grounded. In turn, supply for booster transformer is provided to its low voltage windings ($W_{2qA}, W_{2qB}, W_{2qC}$) in the form of discretely regulated in magnitude and phase (by means of power electronics) voltages, which are generated by the system of regulation windings ($W_{2pA}, W_{2pB}, W_{2pC}, W_{3pA}, W_{3pB}, W_{3pC}$), located on the legs of the magnetic circuit of the magnetizing transformer. The voltages thus formed, being brought to the high-voltage side by transformation into windings ($W_{1qA}, W_{1qB}, W_{1qC}$), are algebraically summed up with the voltages of the corresponding phases of the supply system, thereby providing the necessary action of regulation. Thanks to the application of the sectioning of control windings, the area for regulating the output voltage of the device (Figure 2) consists of 225 points, which significantly improves the accuracy and quality of output voltage regulation. To each position of regulation modules corresponds a definite combination of power keys. The diagram of the sectioning of control windings W_{2p}, W_{3p} and the control law are shown in Figure 3.

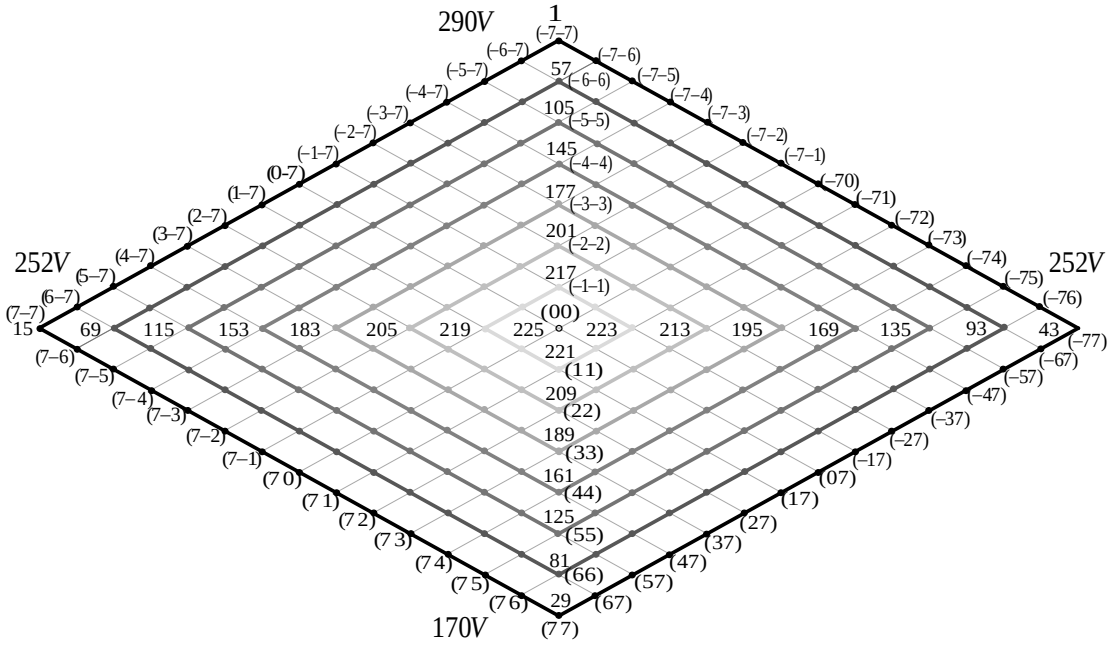

Figure 2. Area of regulation of the output voltage.

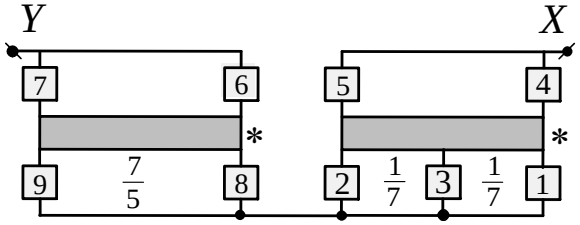

7	6	5	4	3	2	1	0	-1	-2	-3	-4	-5	-6	-7	
				●			●		●			●		●	K1
●		●			●					●					K2
	●		●			●		●			●		●		K3
●	●				●	●	●			●	●	●			K4
		●	●	●				●	●				●	●	K5
					●	●	●			●	●	●	●	●	K6
●	●	●	●	●				●	●						K7
●	●	●	●	●	●	●	●								K8
								●	●	●	●	●	●	●	K9

Figure 3. The diagram and control law of the regulation module.

The mode's parameters of the device

The area of regulation of output voltage of the device can be divided conditionally in four sectors, for each of which vector diagrams and calculation expressions for the mode's parameters are shown below in Figure 4 ÷ 7 and Equations (1 ÷ 20).

The following designations are accepted on vector diagrams:

U_{s0} – voltage at the device input;

β – angle of the vector of booster voltage;

$m = U_{\alpha}$ – magnitude of the booster voltage;

m_0 – magnitude of the longitudinal component of the booster voltage;

U_s – voltage at the device output;

α – angle of the device output voltage.

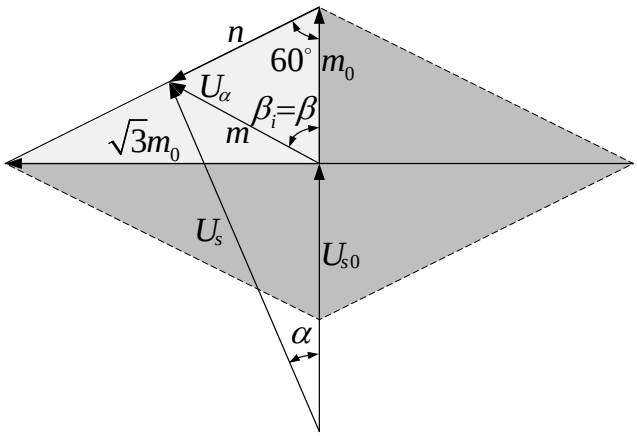

Figure 4. Vector diagram of voltages of the operating device in the first sector.

$$\beta_i = \beta \tag{1}$$

$$m = \frac{\sqrt{3} \cdot m_0}{\sin \beta_i + \sqrt{3} \cdot \cos \beta_i} \tag{2}$$

$$n = \frac{2 \cdot m_0}{1 + \sqrt{3} \cdot ctg\beta} \tag{3}$$

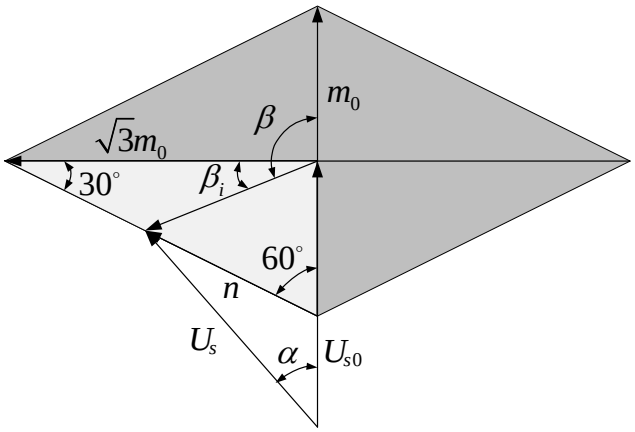

Figure 5. Vector diagram of voltages of the operating device in the second sector.

$$U_S = \sqrt{n^2 + (1+m_0)\cdot(1+m_0-n)}\cdot U_{S0} \tag{4}$$

$$\alpha = \arcsin\frac{\sqrt{3}}{2}\cdot\frac{n}{U_S} \tag{5}$$

$$\beta_i = \beta - 90^\circ \tag{6}$$

$$m = \frac{\sqrt{3}\cdot m_0}{\cos\beta_i - \sqrt{3}\cdot\sin\beta_i} \tag{7}$$

$$n = \frac{2\cdot m_0}{1+\sqrt{3}\cdot tg\beta_i} \tag{8}$$

$$U_S = \sqrt{n^2 + (1-m_0)\cdot(1-m_0+n)}\cdot U_{S0} \tag{9}$$

$$\alpha = \arcsin\frac{\sqrt{3}}{2}\cdot\frac{n}{U_S} \tag{10}$$

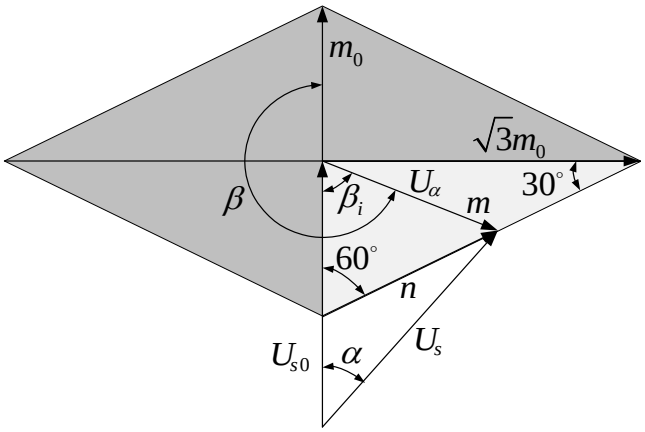

Figure 6. Vector diagram of voltages of the operating device in the third sector.

$$\beta_i = \beta - 180^\circ \tag{11}$$

$$m = \frac{\sqrt{3}\cdot m_0}{\sin\beta_i + \sqrt{3}\cos\beta_i} \tag{12}$$

$$n = \frac{2\cdot m_0}{1+\sqrt{3}\cdot ctg\beta_i} \tag{13}$$

$$U_S = \sqrt{1+m^2-2m\cdot\cos\beta_i}\cdot U_{S0} \tag{14}$$

$$\alpha = \arcsin\frac{\sqrt{3}}{2}\cdot\frac{n}{U_S} \tag{15}$$

$$\beta_i = \beta - 270^\circ \tag{16}$$

$$m = \frac{\sqrt{3}\cdot m_0}{\sqrt{3}\sin\beta_i + \cos\beta_i} \tag{17}$$

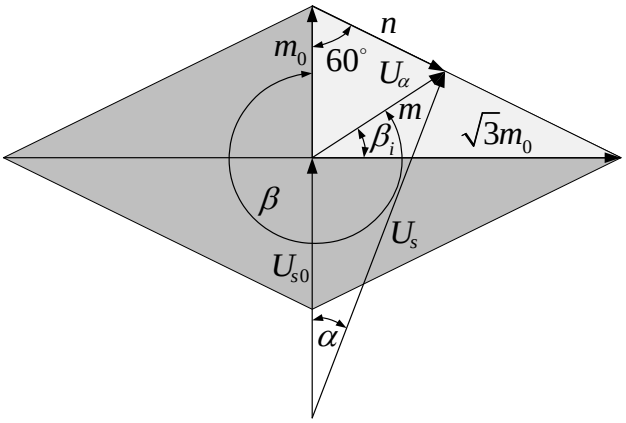

Figure 7. Vector diagram of voltages of the operating device in the fourth sector.

$$n = \frac{2 \cdot m_0}{1 + \sqrt{3} \cdot tg\beta_i} \tag{18}$$

$$U_S = \sqrt{n^2 + (1 + m_0) \cdot (1 + m - n)} \cdot U_{S0} \tag{19}$$

$$\alpha = \arcsin \frac{\sqrt{3}}{2} \cdot \frac{n}{U_S} \tag{20}$$

Values m_0 for various regulation loops according to the Figure 2 are shown in Table 1.

Table 1

The value of longitudinal component of the booster voltage

Loop	Value, m_0
1-15-29-43-1	0.2587
57-69-81-93-57	6/7·0.2587
105-115-125-135-105	5/7·0.2587
145-153-161-169-145	4/7·0.2587
177-183-189-195-177	3/7·0.2587
201-205-209-213-201	2/7·0.2587
217-219-221-223-217	1/7·0.2587

The resulting expressions make it possible to determine the control actions at all regulation points of the mode's parameters of the device.

Device modelling

On the base of Figure 1, a structural simulation model of the device which allowed carrying out research on the object for various operation modes was created in the Simulink/Matlab environment. The device has been modelled in the form of a group of single-phase transformers.

The parameters of the elements of which transformer were determined taking into account nominal voltage $U = 230V$ and the power of device $\approx 2kVA$. Rated currents and voltages of the transformer elements of the device (Figure 1), Table 1 contains accepted for simulation model.

Table 1

The currents and voltages of transformer elements

	Windings of the magnetizing transformer *p*					Windings of the booster transformer *q*	
	W_{1p}	W_{2p}	W_{3p}	W_{4p}	W_{5p}	W_{1q}	W_{2q}
U(V)	3.2	3.2	3.2	10.5	6	9.5	10.5
I(A)	301.7	96.7	96.7	85.7	85.7	120	120

On the base of data contained in Table 1 parameters of SPS-models of the booster and magnetizing elements were calculated and are shown in Table 2.

Table 2

Parameters SPS of transformer's models

Magnetizing transformer	Booster transformer
Normal power and frequency[Pn(VA) fn(Hz)]: [929 50] Winding nominal voltages [U1 U2...Un] (Vrms): [103.18 51.59] Winding resistences [R1 R2...Rn] (Ohm): [0.09 0.0233] Winding leakage inductances [L1 L2...Ln] (H): [0.37e-3 0.009152e-3] Magnetization resistance Rm (Ohm) 1146 Magnetization inductance Lm (H) 1.83 Saturation characteristic [i1(A), phi1(Vs); i2(A), phi2;] [0 0;0.59 0.51;14.75 0.57;29.5 0.59;59.1 0.6; 177.03 0.62]	Normal power and frequency[Pn(VA) fn(Hz)]: [920 50] Winding nominal voltages [U1 U2...Un] (Vrms): [230 4.255 21.275 4.255 4.255 21.275] Winding resistences [R1 R2...Rn] (Ohm): [0.432 0.0019 0.0019 0.0096 0.0019 0.0019 0.0096] Winding leakage inductances [L1 L2...Ln] (H): [1.828e-3 0.00063e-3 0.00063e-3 0.0156e-3 0.00063e-3 0.00063e-3 0.0156e-3] Magnetization resistance Rm (Ohm) 5750 Magnetization inductance Lm (H) 9.16 Saturation characteristic [i1(A), phi1(Vs); i2(A), phi2;] [0 0;0.26 1.14;6.59 1.28;13.17 1.31;26.35 1.35;79.05 1.38]

The modeling's results

The models of the device were tested for both under idle and load modes. When constructing all graphs, the value of the angle of rotation of the booster voltage β as an argument was used. The curves on the graphs correspond to the contours (Figure 2) and are consistent with the numbers of positions of regulation. In Figure 8 dependencies of losses of active power under idling and loaded modes were shown respectively. In the frame of the research related to the above mentioned device the load was modelled as an active resistance $R_L = 19,2Ohm$, which assures the nominal loading of the regulation transformer.

These dependences have a similar complex qualitative structure, differing only in quantitative characteristics.

Thus, active power losses at the idle mode reach 1% during the process of regulation, while load mode losses reach 2,5%. The maximum values of the above listed operating parameters are taken at the angles of the boost voltage $\beta = 90^\circ$ and $\beta = 270^\circ$. The minimum

values can be reached at $\beta = 30^{\circ},150^{\circ},210^{\circ},330^{\circ}$. It should be noted that the shapes of the curves in the load mode change slightly, correlating with characteristics built for the same parameters in the idle mode.

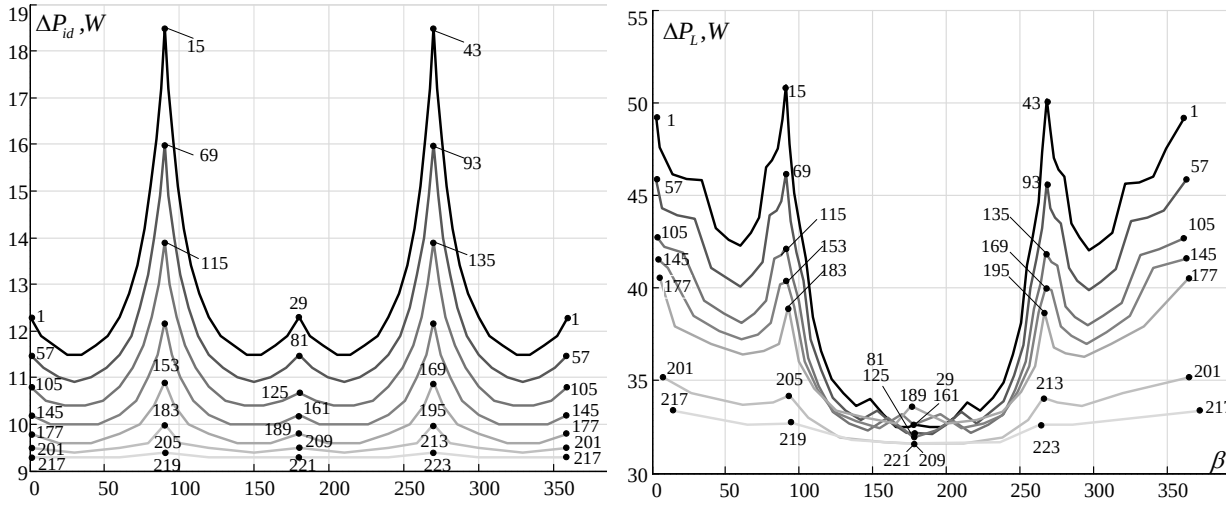

a – for idle mode b – for load mode

Figure 8. Active power losses.

For a more visual perception, the change in the values of active and reactive losses during regulation in the idle and load modes are shown as profiles in Figure 9 in a three-dimensional format. On the surfaces, for better orientation, the location of the characteristic points of the external control loop is applied.

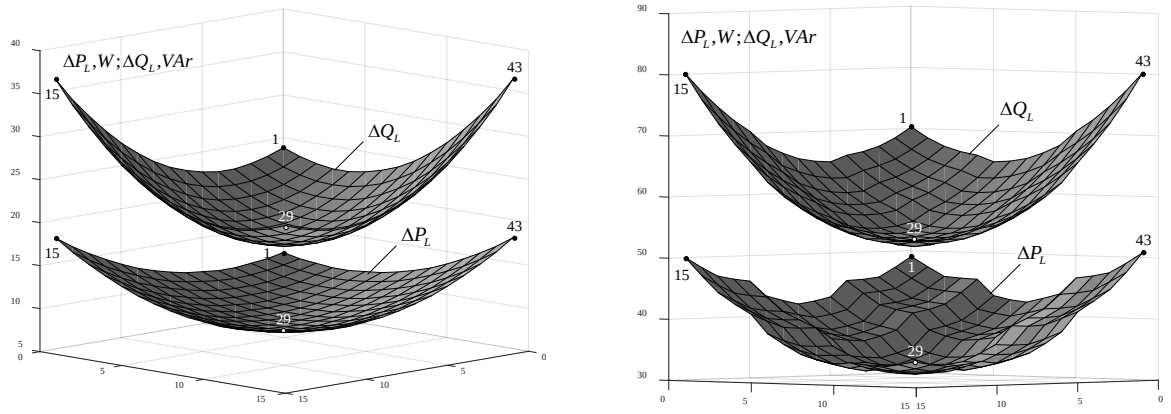

a – for idle mode b – for load mode

Figure 9. Active and reactive power losses in a three-dimensional format.

Figure 10 shows the characteristics of the change in the impedance of the device during regulation in the form of graphs and a surface. The resistance takes on minimum values at the boost voltage angles, respectively $\beta = 90^{\circ}$ и $\beta = 270^{\circ}$. The maximum values can be reached at $\beta = 30^{\circ},150^{\circ},210^{\circ},330^{\circ}$. The range of impedance change during regulation is $\approx 46\%$.

The characteristics of the change in voltage at the output of the device are shown in Figure 11 as an example for three typical loops of regulation.

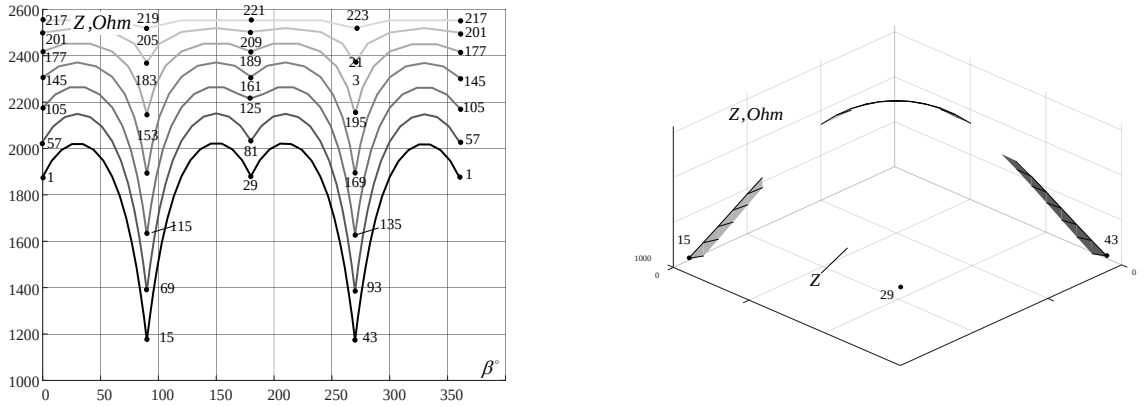

Figure 10. Change of impedance of the device.

The solid lines refer to the idle mode, and the dotted lines refer to the load mode. Analysing the given graphs and the surfaces corresponding to them it can be concluded that the characteristics are close in the considered modes. This confirms the fact that the device holds the mode perfectly. In the course of work, the values of the output voltage were calculated based on mathematical formulas (Figures 4-7), which fully correspond to those obtained in the SPS simulation in the idle mode.

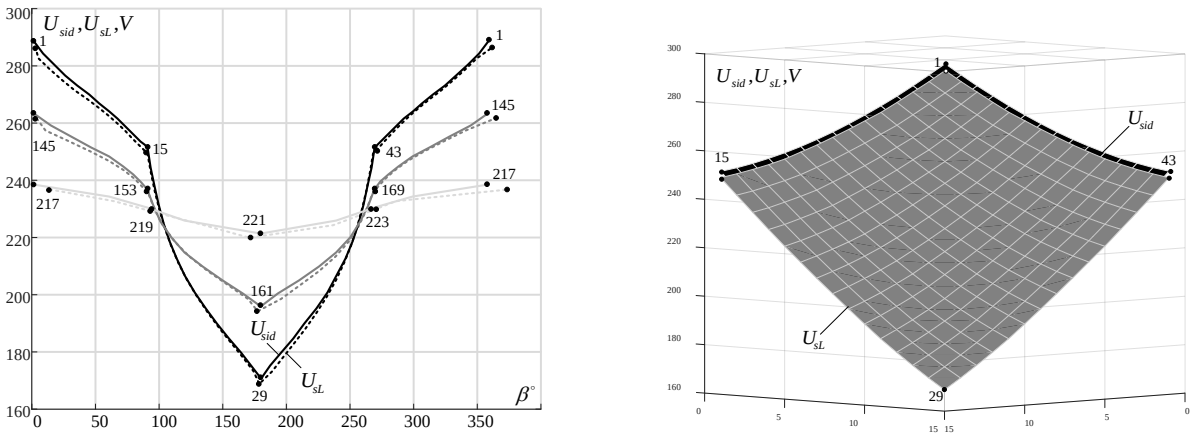

Figure 11. Voltage on the device output.

Based on the results of the experiments, the typical powers of the circuit's elements version of the regulating transformer in zigzag were calculated and are shown in Table 3.

Table 3

The power of the device elements	
Winding designation	**Power, W/(p.u)**
W1q	939.8
W2q	935.4
W1p	874.9
W2p	540.2
W3p	542.4
In all:	**1916.4/0.581**
Power of regulation:	**541.3/1.16**

The data in Table 1 can be used further for the comparative analysis of power characteristics of booster transformers, developed in the prospective future.

Conclusion

Based on the results of the research, the following conclusions can be drawn:

1. The principle diagram of the device, in force to provide the same control actions in the form of booster regulation voltage like FACTS controllers of UPFC and ST types, but on the basis of a simpler and more affordable base of practical accomplishment has been proposed.
2. The techniques of sectioning the regulation windings, as well as laws for its controlling were developed. Control strategy has been formulated and formalized.
3. It is shown that the proposed technical solution provides more opportunities for voltage regulation by phase (relative to UPFC and ST) with the same standards for the allowable limits of its change in module.
4. Vector diagrams are constructed and expressions are obtained that characterize the operating parameters of the device under study.
5. Compliance of the steps with the given positions of the switches during the regulation process was checked.

7. The typical power of the booster transformed with regulation in the zigzag has been calculated.

Acknowledgement: These results were obtained in the frame of *State Program project* no. 20.80009.7007.18: *Eco-friendly technical solutions for efficient energy consumption in buildings and development of smart grid options with advanced renewable energy integration in Moldova*.

References

1. Kim S. Y., Yoon J. S., Chang B. H., Baek D. H. The Operation Experience of KEPCO UPFC. 2005 International Conference on Electrical Machines and Systems. 27-29 Sept. 2005. pp. 2502 – 2505.
2. Schauder C. D., Gyugyi L., Lund M.R., Hamai D.M., Rietman T.R., Torgerson D.R., Edris A. A. Operation of the unified power flow controller (UPFC) under practical constrains. IEEE Transactions on Power Delivery, vol. 13, no. 2, April 1998; pp. 630–639.
3. Ashwani K., and Gao W. Power Flow Model of Sen Transformer for Loadability Enhancement and Comparison with UPFC in Hybrid Electricity Markets. Electric Power Components and Systems, vol.37, no. 2, Feb. 2012; pp. 189-209.
4. Nabavi-Niaki A., Iravani M.R. Steady-state and dynamic models of unified power flow controller (UPFC) for power system studies. IEEE Transactions on Power Systems. 11 (4): (2018-12-18), pp. 1937–1943. doi:10.1109/59.544667.
5. Fuchs Ewald F., Masoum Mohammad A. S. Unified Power Quality Conditioner (UPQC)". Power Quality in Power Systems and Electrical Machines: (January 2008), pp. 443–468. doi:10.1016/B978-012369536-9.50012-7. ISBN 9780123695369. Retrieved 2019-01-16.
6. Sen K.K., Stacey E.J. UPFC-unified power flow controller: theory, modeling, and applications". IEEE Transactions on Power Delivery. 13 (4): pp. 1453–1460. (2018-12-18) doi:10.1109/61.714629.
7. Gyugyi L., Schauder C.D., Williams S.L., Torgerson T.R.R D.R., Edris A. The Unified Power Flow Controller: A New Approach to Power Transmission Control, IEEE Trans.on Power Delivery April 1995, pp.1085- 1097.
8. Yathisha L., Davoodi K., Kulkarni S.P. Optimal Switching Control Strategy For UPFC For Wide Range Of Operating Conditions In Power System, Indian Control Conference, ICC 2017 - Proceedings. 3. 2017, pp. 225-232.
9. Baskaran S., Karpagam N., Devaraj D. Optimization Of UPFC Controllable Parameters For Stability Enhancement With Real-Coded Genetic Algorithm, IEEE-International Conference on Advances in Engineering, Science and Management, ICAESM-2012. 2012, pp. 250-255.
10. Sen K. K. and Sen M. L. Introduction to FACTS Controllers: Theory, Modeling, and Applications , IEEE Press and John Wiley & Sons, 2009.

11. Fentie D. Transient Modeling and Protection of "Sen" Transformer. University of Saskatchewan, 2010.
12. Fentie D., Garcia J. C., Gokaraju R. and Faried S. O. EMT Model of the "Sen" Transformer for Fault Analysis Studies" International Conference on Power Systems Transients (IPST 2015), Cavtat, Croatia, Jun. 2015
13. Kalyan K. Sen, Mey Ling Sen. Introducing the Family of "Sen" Transformers: A Set of Power Flow Controlling Transformers, IEEE Transactions on power delivery, vol. 18, No. 1, January 2003, pp. 149-157.
14. Kumar A. and Kumar J. Comparison of UPFC and "Sen" transformer for ATC enhancement in restructured electricity markets, Int. J. Electr. Power Energy Syst., vol. 41, no. 1, Oct. 2012, pp. 96–104.
15. Kumar A., and Sekhar C. Comparison of sen transformer and UPFC for congestion management in hybrid electricity markets, Int. J. Electr. Power Energy Syst., vol. 47, May 2013, pp. 295-304.
16. Sen K. K., and Mey Ling S. Comparison of the "Sen" transformer with the unified power flow controller," IEEE Trans. Power Del., vol. 18, no. 4, Oct. 2003, pp. 1523–1533.
17. Mohamed S. E. G. Power flow control capability of the power transistor assisted "Sen" transformer and the unified power flow controller: A close comparison, IET Gener., Transmiss. Distrib., vol. 14, no. 15, 2020, pp. 3033-3041.
18. Gasim Mohamed S. E., Jasni J., Radzi M. A. M., and Hizam H. Power transistor-assisted "Sen" transformer: A novel approach to power flow control, Electric Power Syst. Res., vol. 133, pp. 228_240, Apr. 2016.
19. Behera T. and De D. ``Enhanced operation of "Sen" transformer with improved operating point density/area for power flow control, IET Gener., Transmiss. Distrib., vol. 13, no. 14, pp. 3158_3168, 2019.
20. Faruque M. O., and Dinavahi V. A tap-changing algorithm for the implementation of Sen transformer", IEEE Trans. on Power Delivery, vol. 22, no. 3, July 2007, pp. 1750-1757.
21. Song H. and Na R. Out-of-phase technique based few-step type extended "Sen" transformer and its practical tap selection algorithm, Chinese Patent CN5 262 079 A, Sep. 18, 2017.
22. Faruque M. O., and Dinavahi V. A tap-changing algorithm for the implementation of "Sen" transformer, IEEE Trans. Power Del., vol. 22, no. 3, Jul. 2007, pp. 1750–1757.
23. Asghari B., Faruque M. O., and Dinavahi V. Detailed real-time transient model of Sen transformer, IEEE Trans. on Power Delivery, vol. 23, no. 3, July 2008; pp. 1513-1521.
24. Feng J., Han S., Pan Y., and Hu X. Steady-state modelling of extended "Sen" transformer for unified iterative power flow solution, Electric Power Syst. Res., vol. 187, Oct. 2020, Art. No. 106492.
25. Pan Y., Han S., Zhou C., and Guo X. On switching transient modeling and analysis of electronic on-load tap-changers based "Sen" transformer, Int. J. Electr. Power Energy Syst., vol. 130, Sep. 2021, Art. No. 107024.
26. Pan Y., Han S., Feng J., and Hu X. An analytical electromagnetic model of "Sen" transformer with multi–winding coupling, Int. J. Elect. Power Energy Syst., vol. 120, Sep. 2020, Art. No. 106033.
27. Asghari B., Faruque M. O., and Dinavahi V. Detailed real-time transient model of the "Sen" transformer, IEEE Trans. Power Del., vol. 23, no. 3, Jul. 2008, pp. 1513-1521.
28. Liu J., and Dinavahi V. Nonlinear magnetic equivalent circuit-based real-time "Sen" transformer electromagnetic transient model on FPGA for HIL emulation, IEEE Trans. Power Del., vol. 31, no. 6, Dec. 2016, pp. 2483–2493.

Journal of Engineering Science *Vol. XXIX, no. 2 (2022), pp. 46 - 53*
Fascicle *Industrial Engineering* *ISSN 2587-3474*
Topic *Electrical Engineering and Power Electronics* *eISSN 2587-3482*

https://doi.org/10.52326/jes.utm.2022.29(2).04
UDC 621.372:004.3:621.31

DEVELOPMENT OF SIX-PHASE SYMMETRICAL COMPONENTS FILTERS FOR SELF-COMPENSATING POWER LINES

Natalya Turturica, ORCID: 0000-0003-3013-9508

Institute of Power Engineering, Chisinau, 5 Academiei str., Republic of Moldova
*Corresponding author: Natalya Turturica, *departpe@gmail.com*

Received: 02. 27. 2022
Accepted: 05. 15. 2022

Abstract. The paper deals with elaboration of hexaphase symmetrical components filters and their modeling to create microprocessor-assisted relay protection of self-compensating power lines. The theory is presented and the basic principial electrical schemes and mathematical models in the Matlab/Simulink of the filters of the hexaphase symmetric components are elaborated. The results of their simulation and testing at the computer are presented. The obtained results demonstrate the possibility of creating in the base on the elaborated filters of hexaphase symmetrical components the modern, efficient and high-sensitivity microprocessor-assisted relay protection of self-compensating power lines. What reacted not to phase electrical values, but symmetrical components of them.

Keywords: *modeling of current filter, power transmission line, relay protection, transfer capacity of the line.*

Rezumat. Lucrarea este dedicată elaborării filtrelor cu componente simetrice hexafazate și modelarea acestora pentru crearea protecției prin relee asistată de microprocesor a liniilor electrice cu autocompensare. Este prezentată teoria și sunt elaborate schemele electrice principiale și modelele matematice în Matlab/Simulink a filtrelor cu componente simetrice hexafazate. Sunt prezentate rezultatele simulării și testării lor la calculator. Rezultatele obținute demonstrează posibilitatea creării în baza filtrelor cu componente simetrice hexafazate a unei protecții eficiente, bazată pe microprocesor de înaltă sensibilitate, care reacționează la diferite deteriorări ale liniilor electrice cu autocompensare nu la mărimi electrice de fază, ci la componentele simetrice.

Cuvinte cheie: *modelare filtru de curent, linie electrică de transport, protecție prin relee, capacitatea de transport a liniei.*

Introduction

From the viewpoint of maximum saving the consumers' electric power supply, fault tolerance of the self-compensating power lines (SCL) [1], increasing the efficiency and sensitivity of a relay protection [2] and selective switching off of a certain faulted phase or several phase circuits, depending on the short-circuit type or a phase break [3], it is necessary to create a relay protection (RP) [4, 5] responsive to the appearance of certain six-phase

symmetrical components [6]. Considering the SCL as a six-phase line, the creation of the relay protection responsive to the six-phase symmetrical components simplifies the identification of the short-circuit and phase break types, as well as the protection detuning and enhances its sensitivity, since the occurrence of certain six-phase symmetrical components comply with some sorts of faults.

For the development of the RP and the SCL automatics responsive to the occurrence of various six-phase symmetrical components in fault conditions (of short-circuits and phase breaks), the filters of the symmetrical components [7] of the six-phase expansion [8, 9] are necessary.

For the modern numerical and microprocessor protections the most expedient is mathematic 'emphasizing' of the data on symmetrical components at various nonsymmetrical short-circuits, including complex types of failures, for which the combined filter of six-phase symmetrical components of currents and voltages 0, 1, 2, 3, 4, 5 of consequences at computer using complexes Matlab-Simulink environment has been modeled [10].

1. Theoretical bases for the development of the filters of six-phase symmetrical components

The phase currents, which are supplied to the current filter $\dot{I}_A, \dot{I}_{C'}, \dot{I}_B, \dot{I}_{A'}, \dot{I}_C, \dot{I}_{B'}$ of the SCL six-phase system, whose phase A symmetrical components will be designated, using $\dot{I}_0, \dot{I}_1, \dot{I}_2, \dot{I}_3, \dot{I}_4, \dot{I}_5$. The elements, which the filter consists of, are the linear function of Hence, the current at the filter output is

$$\dot{I}_p = \dot{n}_A \cdot \dot{I}_A + \dot{n}_{C'} \cdot \dot{I}_{C'} + \dot{n}_B \cdot \dot{I}_B + \dot{n}_{A'} \cdot \dot{I}_{A'} + \dot{n}_C \cdot \dot{I}_C + \dot{n}_{B'} \cdot \dot{I}_{B'} \tag{1}$$

where the coefficients $\dot{n}_A, \dot{n}_{C'}, \dot{n}_B, \dot{n}_{A'}, \dot{n}_C, \dot{n}_{B'}$ are complex or real values, which characterize the magnitude and phase changes of the currents, supplied to the filter.

The substitution of full currents for their symmetrical components can be described using the following formula:

$$\dot{I}_p = \dot{k}_0\dot{I}_0 + \dot{k}_1\dot{I}_1 + \dot{k}_2\dot{I}_2 + \dot{k}_3\dot{I}_3 + \dot{k}_4\dot{I}_4 + \dot{k}_5\dot{I}_5 \tag{2}$$

where the coefficients of the filter are presented as complex or real values in accordance with the matrix of transition from the phase coordinates to the symmetrical components in the matrix form:

$$\begin{vmatrix} \dot{k}_0 \\ \dot{k}_1 \\ \dot{k}_2 \\ \dot{k}_3 \\ \dot{k}_4 \\ \dot{k}_5 \end{vmatrix} = \begin{vmatrix} 1 & 1 & 1 & 1 & 1 & 1 \\ 1 & e^{j300} & e^{j240} & e^{j180} & e^{j120} & e^{j60} \\ 1 & e^{j240} & e^{j120} & 1 & e^{j240} & e^{j120} \\ 1 & e^{j180} & 1 & e^{j180} & 1 & e^{j180} \\ 1 & e^{j120} & e^{j240} & 1 & e^{j120} & e^{j240} \\ 1 & e^{j60} & e^{j120} & e^{j180} & e^{j240} & e^{j300} \end{vmatrix} \cdot \begin{vmatrix} \dot{n}_A \\ \dot{n}_{C'} \\ \dot{n}_B \\ \dot{n}_{A'} \\ \dot{n}_C \\ \dot{n}_{B'} \end{vmatrix} \tag{3}$$

Using the inverse transformation of matrix Eq. (3), we can obtain the expression for coefficients *n* via coefficients *k*:

$$\begin{vmatrix} \dot{n}_A \\ \dot{n}_{C'} \\ \dot{n}_B \\ \dot{n}_{A'} \\ \dot{n}_C \\ \dot{n}_{B'} \end{vmatrix} = \frac{1}{6} \begin{vmatrix} 1 & 1 & 1 & 1 & 1 & 1 \\ 1 & e^{j60} & e^{j120} & e^{j180} & e^{j240} & e^{j300} \\ 1 & e^{j120} & e^{j240} & 1 & e^{j120} & e^{j240} \\ 1 & e^{j180} & 1 & e^{j180} & 1 & e^{j180} \\ 1 & e^{j240} & e^{j120} & 1 & e^{j240} & e^{j120} \\ 1 & e^{j300} & e^{j240} & e^{j180} & e^{j120} & e^{j60} \end{vmatrix} \cdot \begin{vmatrix} \dot{k}_0 \\ \dot{k}_1 \\ \dot{k}_2 \\ \dot{k}_3 \\ \dot{k}_4 \\ \dot{k}_5 \end{vmatrix} \quad (4)$$

Based on Eq (3). and Eq. (4), Table 1 was built up of arguments of complex coefficients of $\dot{n}_A, \dot{n}_{C'}, \dot{n}_B, \dot{n}_{A'}, \dot{n}_C, \dot{n}_{B'}, \dot{n}_{AB}, \dot{n}_{BC}, \dot{n}_{A'B'}, \dot{n}_{B'C'}$ depending on the argument of complex coefficient of filter *k*.

Table 1

Complex coefficients' arguments

k	$\dot{n}_A$	$\dot{n}_{C'}$	$\dot{n}_B$	$\dot{n}_{A'}$	$\dot{n}_C$	$\dot{n}_{B'}$	$\dot{n}_{AB}$	$\dot{n}_{BC}$	$\dot{n}_{A'B'}$	$\dot{n}_{B'C'}$
0°	0°	120°	-120°	0°	120°	-120°	0°	-60°	0°	-60°
30°	30°	150°	-90°	30°	150°	-90°	30°	-30°	30°	-30°
60°	60°	180°	-60°	60°	180°	-60°	60°	0°	60°	0°
90°	90°	-150°	-30°	90°	-150°	-30°	90°	30°	90°	30°
120°	120°	-120°	0°	120°	-120°	0°	120°	60°	120°	60°

For realization the filters of symmetrical components, according to Table 1, it is necessary to sum up the currents or voltages, which are in definite ratios with the electric values supplied to the filter. The phase shift in currents or voltages can be performed using different methods by a relevant choice of the circuits' elements of the filter: active, inductive, capacitive, mixed type and those inductively connected.

The potential diagrams of the six-phase filter are obtained (Figure 1). Upon feeding to the filter the 5-th sequence of voltages (currents), the 1-st sequence voltage (current) equals to 0 at the filter output.

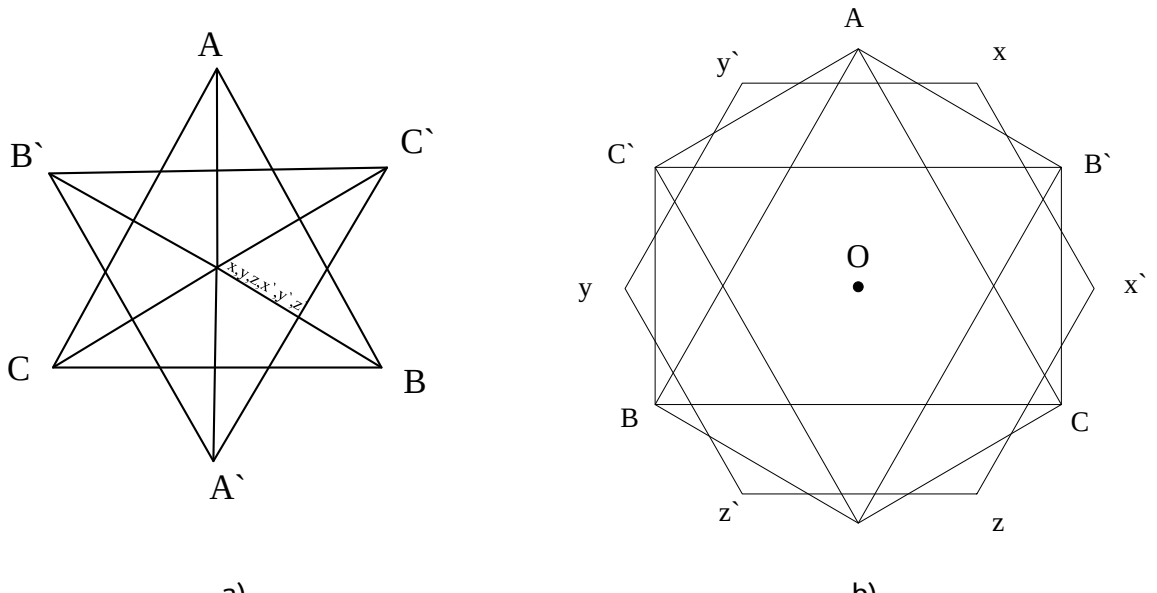

a) b)

Figure 1. Potential diagrams of six-phase filter of voltages: a) for the supplied voltage of direct sequence; b) for the supplied voltage of the 5-th sequence.

Relatively, potentials of points *x, y, z* and *x', y', z'* coincide. On the potential diagram (Figure 1a), points *x, y, z, x', y', z'* are in the center of the potential polyhedron A, C', B, A', C, B'. Whereas upon the supply of the 5-th sequence voltage to the filter, points B` and C`, B and C of the hexagon change their places, and side AA' occupies the position of AC' side, and together with the latter, triangle AA'x potential shifts. If we treat similarly the remaining sides of the hexagon, the potential diagram will look like as in Figure 1.

Six-phase filters, which were created according to the above principle, can serve as a source of symmetrical voltages (currents) at any kind of nonsymmetrical SCL short-circuits, provided that the load resistances are symmetrical and exceed significantly the internal resistance of the filter itself.

2. Modeling the combined filter of six-phase symmetrical components of currents (voltages) in the Mutlab-Simulink environment

For realization the above filters using computer and Matlab-Simulink environment, the equations' solution was performed, which described the obtaining of phase currents (voltages) via the symmetrical components and vice versa, by means of the use of the library SimPowerSystem of the Matlab-Simulink package. Figure 2 shows the simulation model of filter of six symmetrical components, which was realized in the Matlab-Simulink package.

To realize the filter model methods in the library Math Operation the following blocks with their functional capabilities were used:

- block Constant – forms the constant value: a system operator of $a = e^{j120^\circ}$ and $-a = e^{-j60^\circ}$;
- block Math – performs mathematical functions: raises to the square operator a and $-a$;
- block Product – derives the result of multiplication of two input data, according to the matrix expression:

$$\begin{vmatrix} \dot{F}_{A0} \\ \dot{F}_{A1} \\ \dot{F}_{A2} \\ \dot{F}_{A3} \\ \dot{F}_{A4} \\ \dot{F}_{A5} \end{vmatrix} = \frac{1}{6} \begin{vmatrix} 1 & 1 & 1 & 1 & 1 & 1 \\ 1 & e^{j60^\circ} & e^{j120^\circ} & e^{j180^\circ} & e^{j240^\circ} & e^{j300^\circ} \\ 1 & e^{j120^\circ} & e^{j240^\circ} & 1 & e^{j120^\circ} & e^{j240^\circ} \\ 1 & e^{j180^\circ} & 1 & e^{j180^\circ} & 1 & e^{j180^\circ} \\ 1 & e^{j240^\circ} & e^{j120^\circ} & 1 & e^{j240^\circ} & e^{j120^\circ} \\ 1 & e^{j300^\circ} & e^{j240^\circ} & e^{j180^\circ} & e^{j120^\circ} & e^{j60^\circ} \end{vmatrix} \begin{vmatrix} \dot{F}_A \\ \dot{F}_{A'} \\ \dot{F}_B \\ \dot{F}_{B'} \\ \dot{F}_C \\ \dot{F}_{C'} \end{vmatrix} \quad (5)$$

- block Sum – summarizes the phase components at the inputs;
- block Gain – multiplies the input signal by the constant value.

Subsystems 1, 2, 3, 4 and 5 are responsible for the processing of the measuring information terms of the matrix Eq. (5). Subsystems, which realize emphasizing the relevant sequences, are presented in Figure 3.

The modules, which are presented in Matlab/Simulink (Figure 3), based on the preset values $\dot{F}_A, \dot{F}_{A'}, \dot{F}_B, \dot{F}_{B'}, \dot{F}_C, \dot{F}_{C'}$, allow emphasizing symmetrical components $\dot{F}_0, \dot{F}_1, \dot{F}_2, \dot{F}_3, \dot{F}_4, \dot{F}_5$ of sequences in accordance with Eq. (5). The Matlab-model of the filter can be used to obtain the SCL symmetrical components, which can further be used by certain organs of the microprocessor relay protection as the input data at various short-circuits and nonsymmetrical modes.

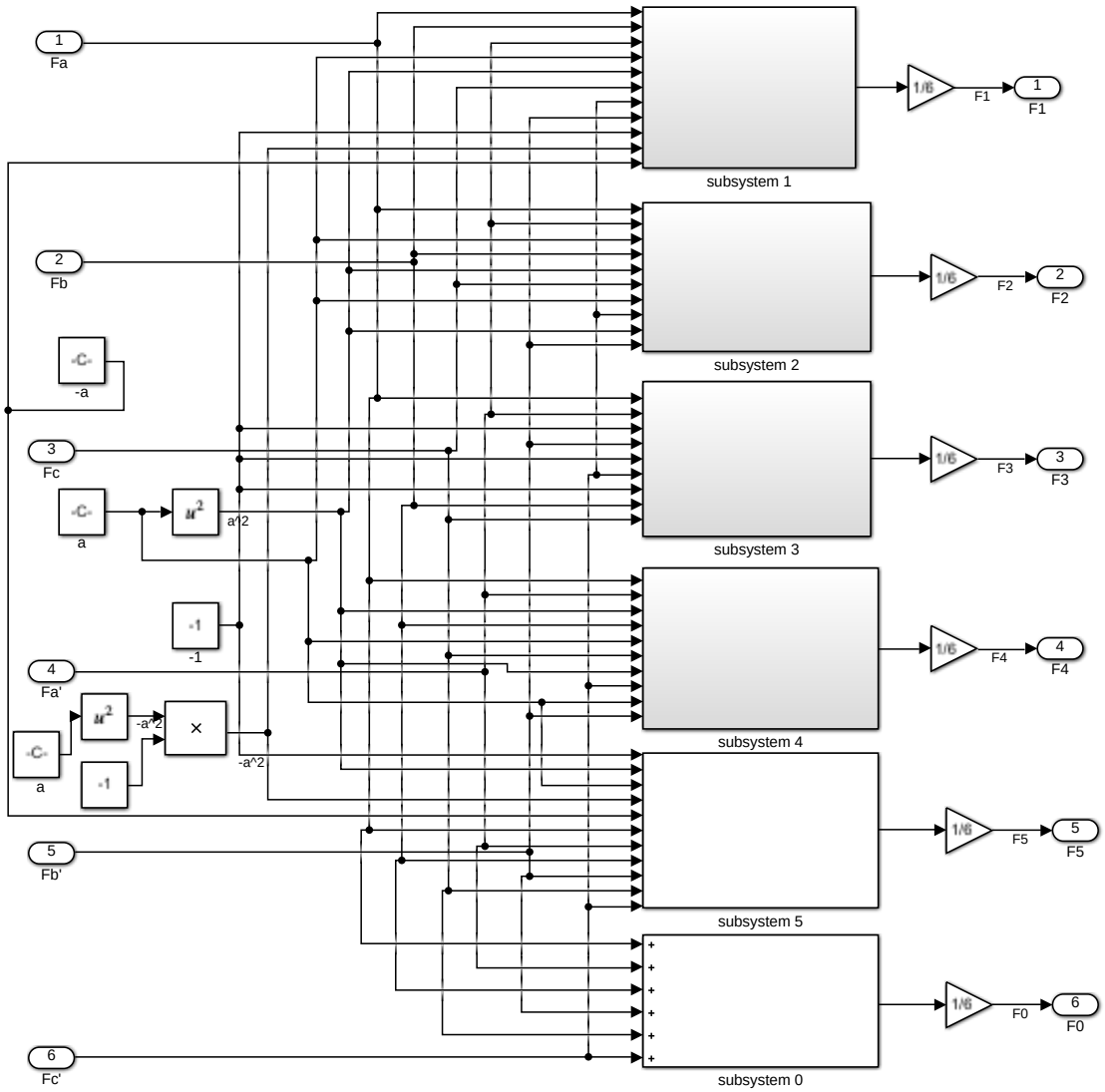

Figure 2. Simulation model of filter of six symmetrical components realized in Matlab-Simulink environment.

3. Results of modelling

For testing the developed model (Figure 2), the complex model was composed of the six-phase transmission line (SCL) with a two-way feed and a filter with six-symmetrical components of currents (voltages). Figure 4 is a short-circuit of phase A.

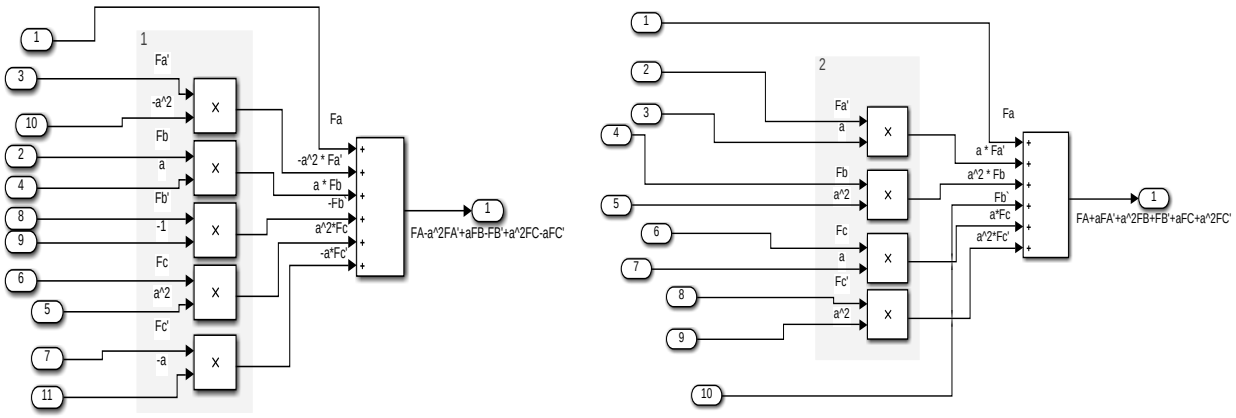

a) b)

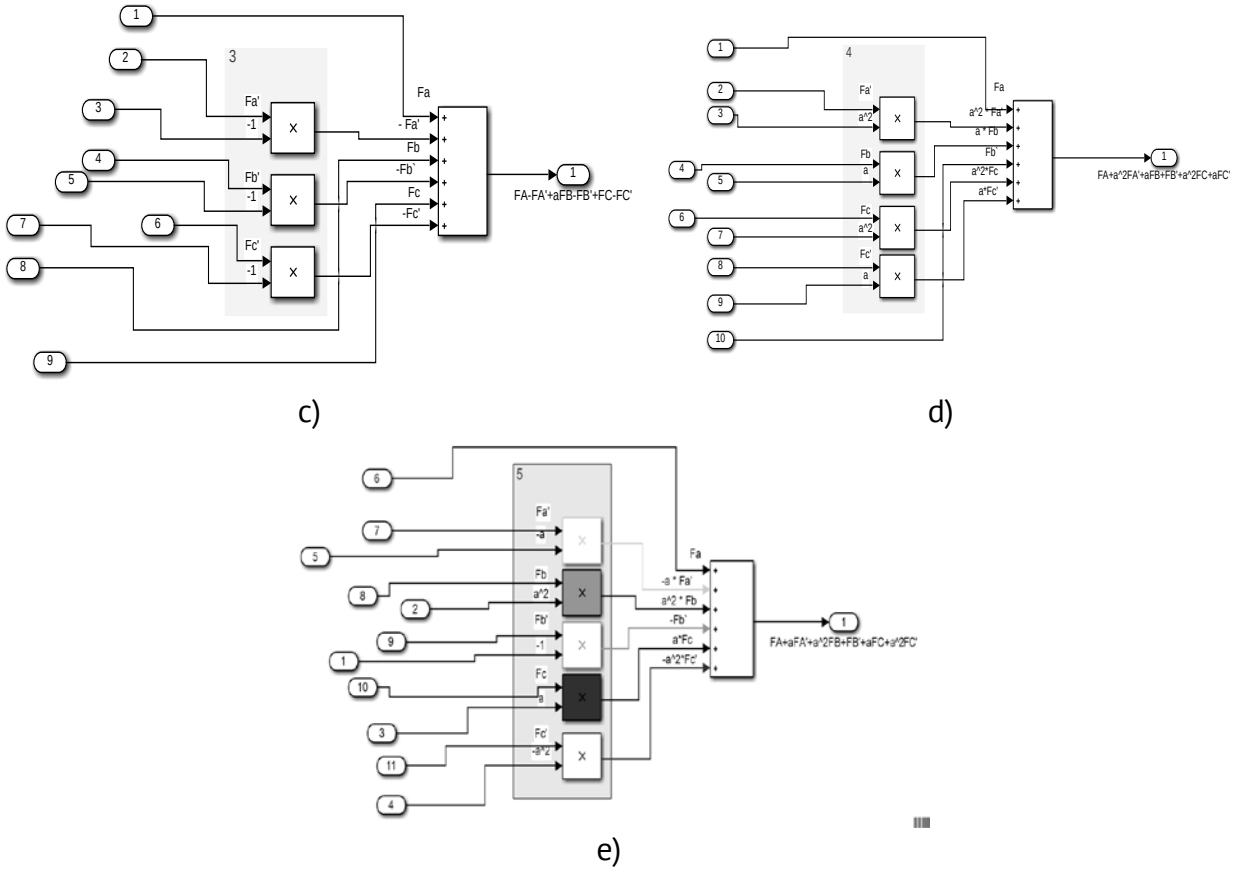

Figure 3. Subsystems of components: a) subsystem of the 1-st sequence; b) subsystem of the 2-nd sequence; c) subsystem of the 3-rd sequence; d) subsystem of the 4-th sequence; e) subsystem of the 5-th sequence.

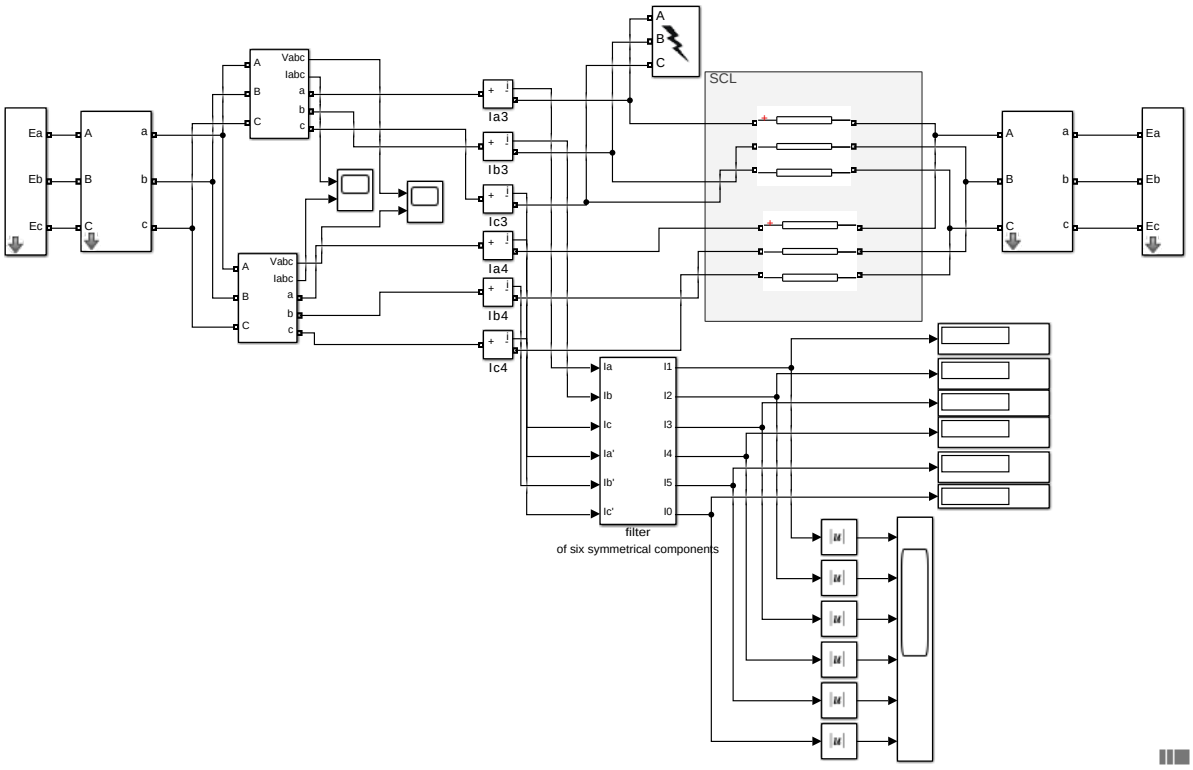

Figure 4. Model for testing the filter of symmetrical components at phase A short-circuit.

Figures 5, 6 show oscillograms of phase and current symmetrical components at phase A short-circuit. The initial time interval of oscillograms (up to 0.3 s) corresponds to a normal mode; finite interval is the occurrence of emergency condition.

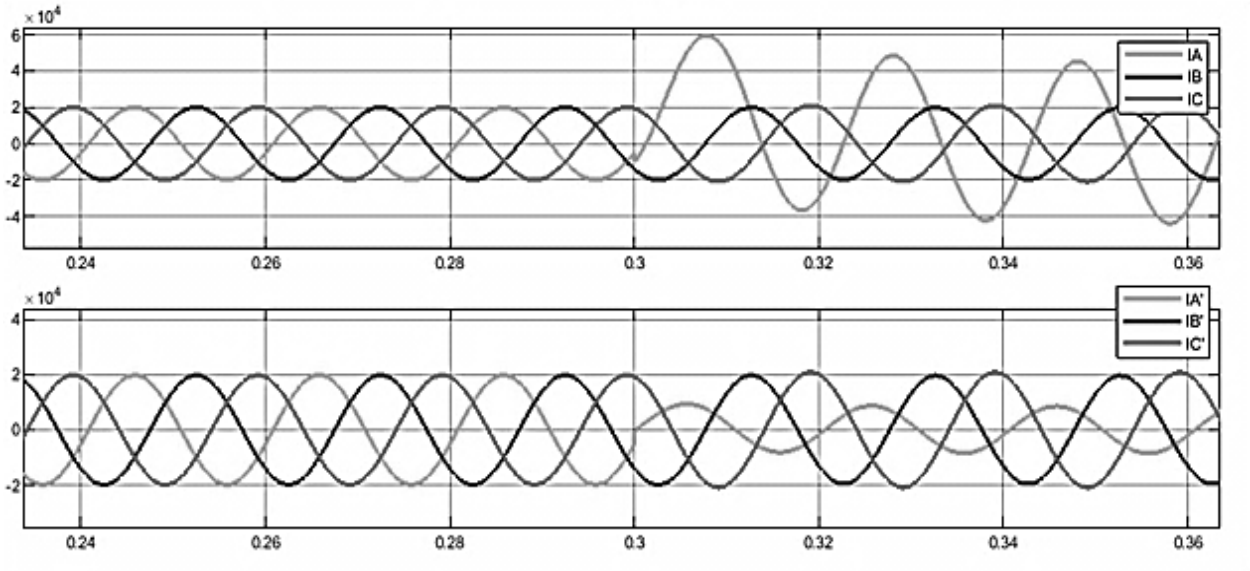

Figure 5. Oscillograms of phase currents at phase A short-circuit.

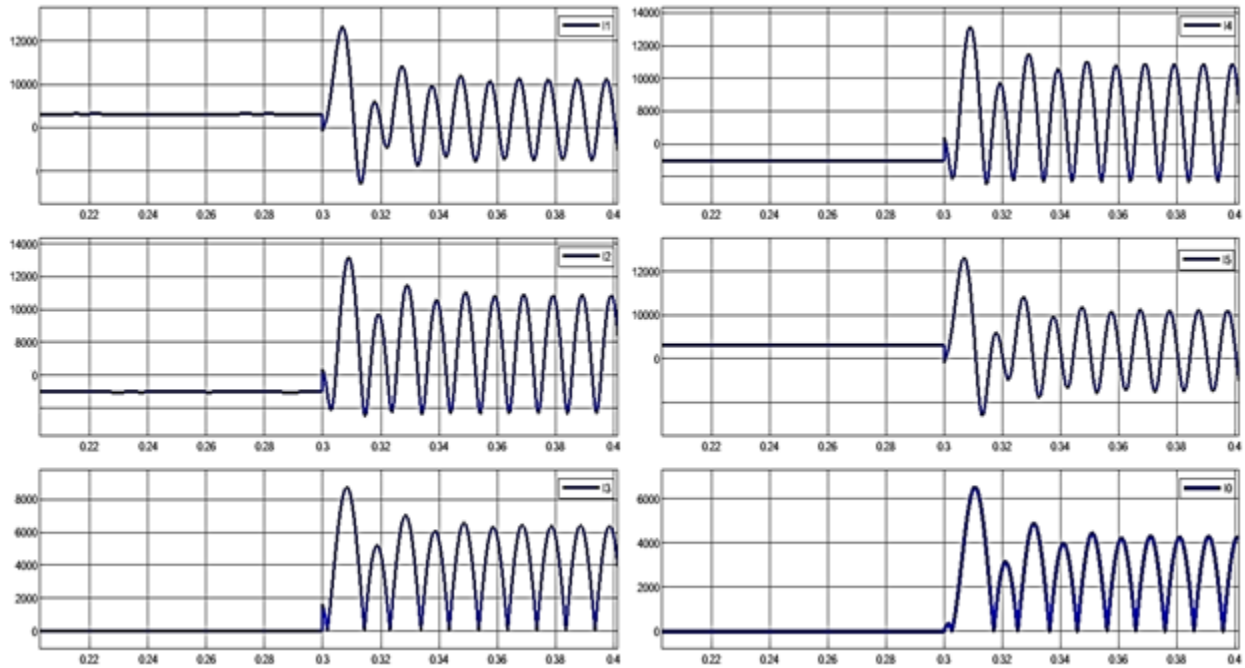

Figure 6. Oscillograms of current symmetrical components at phase A short-circuit.

At a normal mode of current 0, 1, 2, 3, 4 and 5, the sequences at the current filter output equal to zero (Figure 6, time interval from 0 to 0.3 s). Upon phase A short-circuit at a time moment of 0.3 s, current 0, 1, 2, 3, 4, 5 of sequences appears at the filter output.

4. Conclusions

Based on the study results, the following conclusions can be drawn:

1. The theoretical bases and generalized method for creation filters of six symmetrical components for the six-phase transmission line of type SCL are considered.

2. This method makes it possible to calculate the electric values of not only simple, but of complex kinds of faults as well in order to create the efficient relay protection of the required sensitivity, which responses not to the phase values, but to their symmetrical components.
3. The mathematic model is obtained through the program realization of six symmetrical components filters, using the computer and Matlab-Simulink environment, which can be used for creation of the SCL microprocessor relay protection.
4. The results of this work can be used to perform theoretic and experimental studies as well as for the development of the relay protection devices on SCL and ordinary double-circuit transmission lines.

References

1. Postolatij V.M. *Teoreticheskie osnovy i principy sozdaniya upravlyaemyh samokompensiruyushchihsya linij elektroperedachi*. Dissertaciya na soiskanie uchenoj stepeni doktora tekhnicheskih nauk. Chișinău (Kiev), 1987.
2. Waikar D. L., Liew A. C., and Elangovan S. Performance comparison of symmetrical component based fault impedance estimation methods for digital distance relay applications. In: *2nd International Conference on Advances in Power System Control, Operation and Management*, 1993, pp. 83-90.
3. Ciontea C. I., C. L. Bak, F. Blaabjerg, C. I. Ciontea, K. K. Madsen and C. H. Sterregaard. A feeder protection method against the phase-phase fault using symmetrical components. In: *Electric Ship Technologies Symposium (ESTS)*, 2017, pp. 56-63.
4. Kiorsak M.V., Fejgis SH.L. *Fil'try simmetrichnyh sostavlyayushchih shestifaznogo razlozheniya*. Sb. Rezhimy samo-kompensiruyushchihsya linij elektroperedachi. – Chișinău: Shtiinca, 1980.
5. Chiorsac M., Tertea Gh., Sidelnicov V., Turcuman L. Metoda componentelor simetrice în calculul circuitelor polifazate. In: *Conferința tehnico-ştiinţifică a colaboratorilor, doctoranzilor şi studenţilor UTM*, 19 noiembrie 2010, pp.427-430.
6. Kiorsak M., Turturica N. Methodology for Assessment the Possibility of Transfer Six-Phase Power Line into the Mode of Operation with Incomplete Number of Phases. In: *Problemele Energeticii Regionale* , 2020, pp.51-58
7. Kiorsak M.; Turturica N., Simulation of Filters of Six Symmetrical Components of Currents (Voltages) of Controlled Self-Compensating Power Lines. In: *2021 International Conference on Electromechanical and Energy Systems (SIELMEN)*, 2021, pp. 371-375.
8. Kiorsak M., Turturica N. Methodology for Assessment the Possibility of Transfer Six-Phase Power Line into the Mode of Operation with Incomplete Number of Phases. In: *Problemele Energeticii Regionale*. 2020, nr. 1(45), pp. 51-58
9. Kiorsak M., Turcuman L., Turturica N. Natalia. Principiul de elaborare a protecţiei prin relee a liniilor electrice aeriene cu autocompensare la scurtcircuite nesimetrice dintre fazele apropiate. In: *Problemele Energeticii Regionale*. 2015, nr. 3(29), pp. 63-66
10. MathWorks is the leading developer of mathematical computing software for engineers and scientists. [online]. © 1994-2022 The MathWorks, Inc. [accesat 10.11.2021]. Disponibil: https://www.mathworks.com/.

Journal of Engineering Science *Vol. XXIX, no. 2 (2022), pp. 54 - 61*
Fascicle *Industrial Engineering* *ISSN 2587-3474*
Topic *Electrical Engineering and Power Electronics* *eISSN 2587-3482*

https://doi.org/10.52326/jes.utm.2022.29(2).05
UDC 620.92:621.31

INTEGRATION OF VARIABLE ENERGY SOURCES IN ENERGY SYSTEMS

Corina Guțu-Chetrușca*, ORCID: 0000-0001-6090-4421,
Dumitru Braga, ORCID: 0000-0002-5500-2033

Technical University of Moldova, 168 Stefan cel Mare Blvd., Chisinau, Republic of Moldova
Corresponding author: Corina Guțu-Chetrușca, *Corina.gutu@tme.utm.md*

Received: 03. 16. 2022
Accepted: 05. 15. 2022

Abstract. The main global concern in the energy sector is the substitution of fossil fuels and the mitigation of climate change - the transition to the carbon neutrality of the economy. For the power sector, the main solution for this transition is to use hydro, wind and solar energy sources, which have a high energy potential, including in the Republic of Moldova. Variable renewable energy sources, wind and solar, due to their intermittent nature have a significant impact on the power system and the quality of electricity. The necessary measures to reduce the impact of the variability of these sources are presented. The most appropriate measure would be to use pumped storage hydropower plants. The water losses from their accumulation lakes were appreciated. That constitutes approx. 1 ... 2 m^3/MWh which is considerably lower than the losses from the Thermal Power Plants with steam turbines.

Keywords: *variable renewable energy sources, energy storage, water losses.*

Rezumat. Principala preocupare la nivel mondial în sectorul energetic este substituirea combustibililor fosili și atenuarea fenomenului schimbărilor climatice – tranziția către neutralitate de carbon a economiei. Pentru sectorul electroenergetic principala soluție pentru această tranziție constă în utilizarea surselor hidro, eoliene și solare de energie, care au un potențial energetic înalt, inclusiv în Republica Moldova. Sursele regenerabile variabile de energie, eoliene și solare, din cauza caracterului intermitent au impactul semnificativ asupra sistemului electroenergetic și calității energiei electrice. Sunt prezentate măsurile necesare pentru diminuarea impactului variabilității acestor surse. Măsura mai potrivită ar fi folosirea Centralelor Hidroelectrice cu Acumulare prin Pompare. S-au apreciat pierderile de apă din lacurile de acumulare ale acestora. Ele constituie cca. 1...2 m^3/MWh ceea ce este considerabil inferior pierderilor din Centralele Termoelectrice cu turbine cu abur.

Cuvinte cheie: *sursele regenerabile variabile de energie, acumularea energiei, pierderi de apă.*

Introduction

In recent years, Renewable Energy Sources (RESs) are occupying a growing important place in the global electricity mix, reaching a share of 29% by 2020 [1]. In the future, the volume of renewable energy generation will have a continuously growing trend. In the recent period, the investments in renewable energy systems had a share of around 70% of total

energy investments. The installed capacity of the renewable energy systems increased by more than 256 gigawatts (GW) during the pandemic, the largest increase ever [1, 2]. The COVID-19 pandemic has had a significant impact on the power sector, with total production declining by 4%, while its production from renewable sources, which is less affected by restrictions and largely unaffected by demand, has increased worldwide in 2020, compared to 2019, by 6.3% [3]. Over the next decade, the commitments announced by governments will lead to an expansion of renewable sources, that is fast enough to keep pace with rising electricity demand and reduce the share of fossil fuels to meet electricity needs. It is estimated that the share of renewable energy sources will increase from almost 30% of global electricity generation in 2020 to about 45% in 2030 according to the Announced Pledges Scenario (APS) and could exceed 60% in the Net Zero Emissions Scenario (NZE) [4].

Recently, RESs have also increased in the Power sector of the Republic of Moldova: from 17.2 million kWh in 2015, production has increased to 81.4 million kWh in 2020, but their share in the total volume of energy is quite small - 9.6% of domestic product and less than 2% of electricity consumption per republic [5].

Depending on the primary source, electricity generated by RESs has different particulars. Although, if hydraulic, geothermal, biomass energy can be used at the necessary time and in the required quantity, so-called variable energy generated by variable renewable energy sources (VREs), as solar and wind, being intermittent and sometimes unpredictable over time, can have a negative impact on the operation of power systems. At the same time, these sources have a number of advantages. They are more environmentally friendly compared to other RESs, require less operating and maintenance costs, and as result, the cost of generated energy is lower, and has a continuous downward trend, while for other types of RES these costs increase.

The specific investments for power plants using RESs and the Levelized Cost of Energy are presented in Table 1 [6]. It is noted that the specific investments for geothermal and hydraulic energy increased significantly during the last 10 years. At the same time, the specific investments for solar PV and wind systems decreased considerably. The price of solar PV electricity is slightly higher than that of hydraulic electricity, but, given the nature of their change, the reversal of this ratio is expected. It should be noted that these prices are in a favorable ratio with those of fossil fuel energy which are in the range of 0.05 - 0.15 USD / kWh [1, 6].

Table 1

Total cost of investment in RES and levelized cost of energy produced for 2010 and 2020*

Type of renewable energy source	Total installed costs			Levelized cost of electricity		
	2020 USD/kW		Percent change	2020 USD/kWh		Percent change
	2010	2020		2010	2020	
Bioenergy	2619	2543	-3	0,076	0,076	0
Geothermal	2620	4468	71	0,049	0,071	45
Hydropower	1269	1870	47	0,038	0,044	18
Solar PV	4731	883	-81	0,381	0,057	-85
Wind (onshore**)	1971	1355	-31	0,089	0,039	-56

**After [6]; ** wind offshore and ocean systems being unavailable for the Republic of Moldova, as well concentrated solar energy requiring large installation areas are not considered.*

Being the cheapest and most competitive, VRESs - solar PV and wind, far exceed the other sources in their growth and, according to [4], will ensure about 75% of the increasing electricity demand by 2030 in the Stated Policies Scenario (STEPS) and 90% in APS. This means that the share of solar PV and wind energy in electricity balance for 2030 will increase from below 10% in 2020 to 23% in STEPS and 27% in APS. The energy generated by hydropower, bioenergy, geothermal and concentrated solar systems is expected to grow much lower by 2030 in all scenarios, as they have longer project deadlines and require favorable site conditions and resources.

Problems of variable renewable energy sources and solutions

Intermittency, variability, and unpredictability of solar and wind energy are serious challenges for the power system's operation and control, affecting its stability, reliability, flexibility, and resilience. They also cause a reduction of the load factor of the respective systems, which leads to the increase of the payback period for power plants using VRESs. For the European area, the capacity factor for wind systems is 17 ... 22%, and for PV systems 5 ... 11% [7], while for conventional power plants using fossil or renewable fuels it is 60 ... 80 %. The values of capacity factors in the conditions of the Republic of Moldova are: for PV systems - 8 ... 9%, for wind systems - 9 ... 13% [5].

According to the mentioned above, it can be concluded that the massive use of solar PV and wind systems requires alternative energy sources or other measures, such as interconnection with other power systems, hybrid generators, synergy generation - consumption, energy storage.

Alternative sources at the present stage are mainly represented by conventional power plants using fuels. The NZE scenario envisages replacing them with power plants using invariable renewable sources (hydro, bio, geothermal) and nuclear power. Connections to other systems allow to take advantage of different climatic conditions in different geographical regions and alternative sources from neighboring power systems.

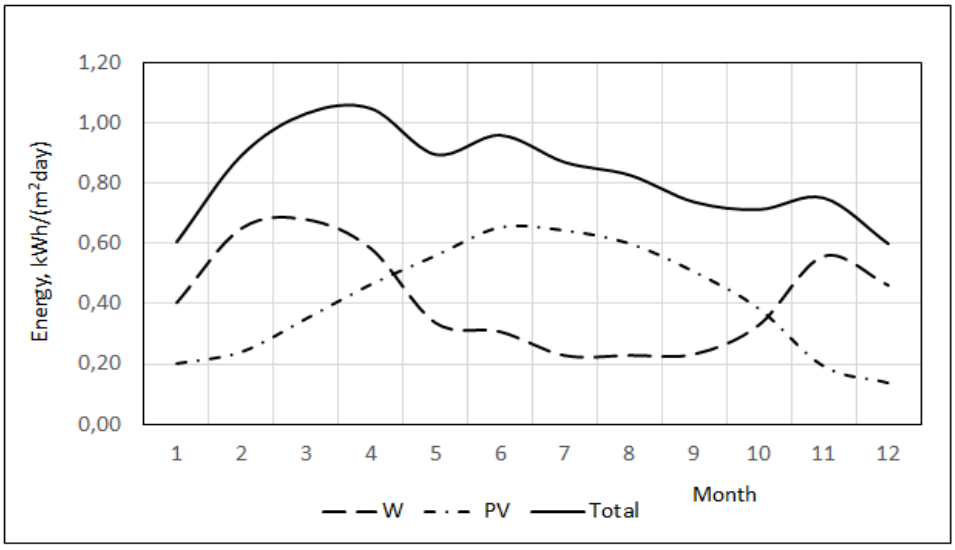

Figure 1. Operation dynamics of a hybrid PV-wind installation in climatic conditions in the central part of Republic of Moldova [8].

The PV-wind hybrid systems present a promising solution due wind and solar energy are complementary to each other, which makes this type of system generate electricity throughout the year, and in some cases, they also provide the diurnal load curve. For the

climatic conditions in the center of the Republic of Moldova, this is demonstrated by the graph in Figure 1 which shows the dynamics of operation of a hybrid installation [8] The monthly production is at the level of 0.8 kWh / (m^2 day) and varies in the limits of -26.1% (in January-December) and +27.2% (in March).

Some cases of system imbalance can also be avoided by synergy between generating and consumption, or the concordance of energy production with the consumers electricity load. For example, agrovoltaic systems can be used for irrigation pumping stations. Approx. 40% of the energy can be produced by PV systems installed on 15% of their roof surface [9]. Another example is residential buildings. The energy produced by the PV systems installed on the roof in summer can be used for air conditioning, and in winter - for heat pumps. In addition, the pandemic, which introduced and developed online work and home learning, led to an increase in household energy consumption during the day, which coincided with the peak of electricity generation by PV systems [10]. Working from home has proven to be convenient for both employees and employers and is expected to remain so after the pandemic crisis is resolved. The most common method of solving the problems created by the variability of Renewable Energy Sources is the storage of electricity.

Energy storage

Energy Storage Systems (ESS) can provide safe and cost-effective answers to the problems facing power grids today - in the SMART GRID development phase that they are going through [11, 12]:

- starting the equipment after the fault, ensuring without resorting to the network for the necessary energy (cases of black-out/start or brown-out/start);
- energy storage during periods of low load and low prices and supplying consumers with energy during peak periods and higher cost;
- ensures due to the associated power electronics, the control and the fast variation of the active and reactive power, maintaining the optimal parameters of the network;
- reducing the need to provide conventional units, the ESS providing the function of "spinning reserve";
- fast provision through stored energy, at additional demand requested by the consumer;
- facilitating the integration of VRES, by storing energy when time allows and returning it when it needs to be delivered;
- storage of excess energy in case of favorable weather conditions, in conditions where there are no demands and efficiency of wind farms, photovoltaic.

Since there is no possibility to directly store electricity, a wide range of storage methods are used by converting it into other forms of energy. Possible solutions for storage systems include:

1. Mechanical storage:
   a. pumped hydro,
   b. compressed air,
   c. flywheels;
2. Electrochemical storage:
   a. batteries with internal storage (eg Pb-acid, NiCd, Li-ion),
   b. externally stored batteries,
3. Electrical storage
   a. superconducting magnetic energy storage,

b. supercapacitors (different technologies).

4. Thermal storage
   a. cryogenic storage systems, liquid air energy storage (LAES)
   b. molten salts.
5. Chemical storage:
   a. hydrogen;
   b. ammonia

and other.

The choice of the appropriate system can be made on the basis of several factors, such as required storage capacity, minimum storage period, loading and unloading conditions, available space and environment, type of compensated fluctuations, required energy density, lifespan required, the minimum number of cycles and the properties of the energy system.

Overall, the global operational energy storage capacity reached 191.1 GW in 2020, reflecting 3.4% growth year on year. The largest market was China (18.6% of the global total), which reached 35.6 GW by year's end, up 4.9% from 2019. The United States added 1.5 GW due to a record fourth quarter in the deployment of front-of-the-meter storage, to reach an estimated 23.2 GW by year's end. The European market grew 54%, adding 1.7 gigawatt-hours of storage capacity for a cumulative capacity of 5.4 GWh. In addition, 4 GW was either announced or under construction across the region. The structure of the installed power according to the technology is shown in Figure 2. Pump storage continued to present the largest part of the installed capacity, over 90%.

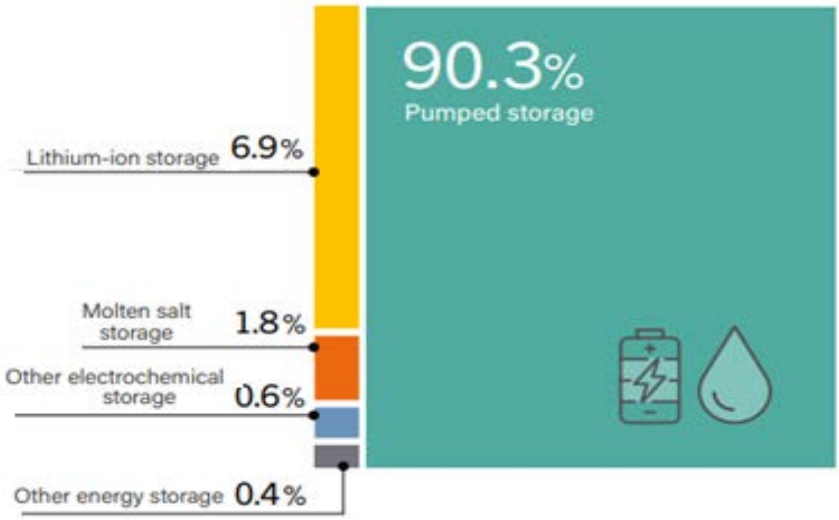

Figure 2. The installed capacity structure of global electricity storage units at the end of 2020 [1].

Pumping storage: use possibilities in the Republic of Moldova

According to [13 and 14], pumping storage is the only commercially proven technology available for the large-scale storage of energy in a power system, from which the Republic of Moldova could benefit fully. On the other hand, in the media of the republic, there is a concern that the accumulation lakes of the Pumped Storage Hydro Power Plants (PSHPP) can significantly affect the hydrological balance of the republic [15, 16, 17].

In order to assess the degree of influence of PSHPP on the hydrological regime, the calculations of water losses from the accumulation lake of a 50 MW Power Plant were performed. The characteristics of PSHPP are presented in Table 2. Load adjustment shall be provided for one day with a turbine operating time of 8 hours.

Table 2

The analyzed PSHPP characteristics

Power plant capacity, MW	50
Pumping efficiency	0,7
Generation efficiency	0,8
Day time load adjustment type	Day time
Operating time, h/day	8
Energy generation, MWh/day	400
Net fall height, m	100
Turbine water flow, m^3/s	63,71

The sizing of the storage lake is carried out, considering the useful volume equal to the amount of water required for the operation of PSHPP at nominal power during the daily operation. The calculation scheme of the lake is shown in Figure 3. The characteristics of the lake are presented in Table 3. Water losses in the lake consist mainly of evaporation losses E from the water surface and filtration F through the water-covered part of the lake cuvette. They are partially offset by atmospheric deposits D that occur during the year on the surface of the soil occupied by the lake basin.

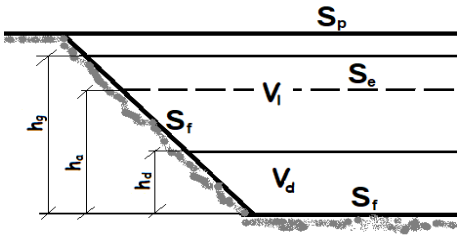

Figure 3. PSHPP reservoir calculation scheme:

V_l – live storage volume, V_d – dead storage volume, S_p - precipitation surface, S_e - evaporation surface, S_f - infiltration surface, h_g- depth of the brut gross volume, h_a- average depth, h_d- depth of the dead volume.

Table 3

Characteristics of the CHEAP accumulation lake

Volume of water consumed, Mm^3/ day	1,83
Volume of water consumed, Mm^3/ year	669,72
Quotation useful tank	0,85
Gross volume of tank, Mm^3	2,45
Talus angle, degrees	45,00
Maximum depth of tank, m	20,00
Medium depth of tank, m	16,6
Surface of deposits, m^2	122 224
Vaporization surface, m^2	115 671
Filter surface, m^2	123 610

Thus, the losses ***P*** will be determined by the formula [18, 19]:

$$P = E + F - D, \text{ m}^3/\text{year} \quad (1)$$

In turn:

$$E = S_e \cdot e; \quad (2)$$

$$F = S_f \cdot f; \quad (3)$$

$$D = S_p \cdot p. \quad (4)$$

In these formulas:

$\boldsymbol{S_e}$ is the evaporation surface;

$\boldsymbol{S_f}$ - the filtering surface, equal to the water-covered surface of the lake cuvette;

$\boldsymbol{S_p}$ - the cross-sectional area of the upper part of the cuvette;

$\boldsymbol{e}$ - Evaporation layer from the surface of the water, according to [18], for the corresponding area of RM $\boldsymbol{e}$ = 0.8 ... 1.0 m / year, consider $\boldsymbol{e}$ = 0.9 m / year;

$\boldsymbol{f}$ - water filtration layer in the soil, according to [19], $\boldsymbol{f}$ = 0.4 ... 1.0 m / year, consider f = 0.8 m / year;

$\boldsymbol{p}$ - precipitation in the territory of RM, according to [20], $\boldsymbol{p}$ = 0.49 ... 0.62 m / year, consider p = 0.53 m / year;

The values of the surfaces are given in Table 3. The calculations were performed for two types of CHEAP: open cycle and closed cycle. Open-cycle CHEAPs are built on the banks of large rivers, from which water is pumped into the upstream reservoir. The closed cycle CHEAP is equipped with two lakes, upstream and downstream, one of which is supplied with additional water from a smaller source.

The results of the calculations are presented in Table 4.

Table 4

Water loss values in CHEAP reservoirs

Characteristic		Value	
		Open cycle	**Closed cycle**
Cycle losses	m^3/day	379	757
	% from the cycle	0,021	0,041
Annual losses	m^3/year	138 213	276 427
	% from the lake volume	11,1	11,1
Specific losses	m^3/MWh	0,96	1,92

As can be seen from the table, the current losses are insignificant - hundredths of percentages, but the annual ones related to the volume of accumulated water are significant - over 11%. The specific losses, per production unit, are 0.96 m^3 / MWh and 1.92 m^3 / MWh, respectively. It should be mentioned that they are 2 ... 3 times smaller than the water losses from the cooling towers of the Thermoelectric Power Plants with steam turbines which is 2.7... 4.2 m^3 / MWh [21].

Conclusions

Power plants using variable Renewable Energy Sources, in the future, will occupy a predominant place in the production of electricity in the Republic of Moldova. Their intermittency, variability, and unpredictability will affect the stability, reliability, flexibility, and resilience of the National Power System of the Republic of Moldova. To counteract this damage, it is necessary to apply a number of main measures, including the storage of electricity. For this, the Republic of Moldova could fully benefit from the technology of

accumulating electricity by pumping. Water losses, in this case, would be much lower than in conventional electricity generation technologies such as steam turbines from combined heat power plants.

Acknowledgment: This paper was written as study including in the project "*Eco-Innovative Technical Solutions for Energy Efficiency in Buildings and Developing Smart Grid Development Options with Advanced Renewable Energy Integration in R.M. (SYNERGY)*".

References

1. RENEWABLES 2021. GLOBAL STATUS REPORT. GSR2021_Full_Report.pdf (ren21.net)
2. RENEWABLES 2020. GLOBAL STATUS REPORT. https://www.ren21.net/wp-content/uploads/2019/05/gsr_2020_full_report_en.pdf
3. Hannah Ritchie, Max Roser. Electricity Mix.https://ourworldindata.org/electricity-mix. https://iea.blob.core.windows.net/assets/4ed140c1-c3f3-4fd9-acae-789a4e14a23c/WorldEnergy2021.pdf
4. Report on the activity of the National Agency for Energy Regulation in 2017-2020. https://www.anre.md/raport-de-activitate-3-10
5. Renewable Power Generation Costs in 2020, IRENA (2021), Abu Dhabi. Renewable Power Generation Costs 2020 (irena.org)
6. https://www.eia.gov/todayinenergy/detail.php?id=22832#
7. Chiorsac M., Guţu C. Feasibility of PV/wind power system in the Moldavian Republic conditions. Conferinţă Internaţională de Sisteme Electromecanice şi Energetice SIELMEN 2003. Chişinău.
8. Bostan I., Guțu A. and Guțu-Chetruşca C. "The photovoltaic greenhouses - a challenge for Republic of Moldova," International conference on electromechanical and energy systems SIELMEN 2019,Craiova, Romania, 2019, pp. 1-4., Doi: 10.1109/ SIELMEN.2019.8905838 Electronic ISBN: 978-1-7281-4011-7.USB ISBN: 978-1-7281-4010-0
9. Guțu-Chetrușca C., Guțu A. *Republic of Moldova Power Energy in the Pandemic*. Journal of Engineering Science. Vol. XXVIII, no. 4 (2021), pp. 27 – 33. ISSN 2587-3474, eISSN 2587-3482 https://doi.org/10.52326/jes.utm.2021.28(4).02
10. Braga D. "Optimal Capacity and Feasibility of Energy Storage Systems for Power Plants Using Variable Renewable Energy Sources," 2021 International Conference on Electromechanical and Energy Systems (SIELMEN), 2021, pp. 087-091, doi: 10.1109/SIELMEN53755.2021.9600392.
11. Tănăsescu F. T. Energy storage systems, a solution for optimizing the operation of electrical networks to which intermittent renewable sources are connected. https://www.agir.ro/buletine/2222.pdf [in Romanian].
12. Arion V., Efremov C. „Increasing flexibility of the National Energy System by Building up Hydro Pumped Storage Plants", Quarterly publication of Romanian National Committee of World Energy Council (Wec/Rnc) and The General Association Of Engineers in Romania (Agir) – Emerg 3 (Energy, Environment, Efficiency, Resources, Globalization, Volume VII, Issue 3) – ISSN 2668-7003, ISSN-L 2457-5011; An V / 2021 – p.p. 48-61. DOI: 10.37410/EMERG.2021.2.1. https://emerg.ro/files/increasing-flexibility-of-the-nationalenergy-system-by-building-up-hydro-pumped-storage-plants
13. Braga D. "*Integration of Energy Storage Systems into the Power System for Energy Transition towards 100% Renewable Energy Sources*," 2021 10th International Conference on ENERGY and ENVIRONMENT (CIEM), 2021, pp. 1-5, DOI: 10.1109/CIEM52821.2021.9614778
14. Dniester Hydropower Complex: Impact on the hydrological status of the Dniester River. 02.12.2021 https://www.mesaj.md/news/society/5391-complexul.
15. Ukraine's energy ambitions could leave Moldova without water. https://agrotv.md/ambitiile-energetice-ale-ucrainei-pot-lasa-moldova-fara-apa [in Romanian].
16. Study commissioned by UNDP: Dniester Hydropower Complex - impact on the hydrological status of the Dniester River. https://replicamedia.md/ro/article/IEeJM4zjA/ [in Romanian].
17. Scaveleva D.S.Ispolizovanie vodnoi energii. Pod red. d.t.n.,prof.
http://lib.hydropower.ru/books/doc_00032783.pdf
18. Rascet poteri vody iz vodohraniliscea. https://studfile.net/preview/7402285/page:2/
19. http://www.meteo.md/images/uploads/gis/meteo/Caracterizarea_climei_RM.pdf
20. Grigoriev V.A. Teplovye i atomnye electriceskie stanzii: Spravocinic. Kniga3/ V.A. Grigoriev, V.M. Zorin – M.: Kniga po trebovaniu, 2013. – p.604. ISBN 978-5-458-37558-0.

Journal of Engineering Science *Vol. XXIX, no. 2 (2022), pp. 62 - 67*
Fascicle *Electronics and Computer Science* *ISSN 2587-3474*
Topic *Electronics and Communication* *eISSN 2587-3482*

https://doi.org/10.52326/jes.utm.2022.29(2).06
UDC 621.37.001

THE INFLUENCE OF A RESIDUAL REFLECTIVITY AT THE FRONT FACET OF A MULTISECTION MASTER-OSCILLATOR POWER-AMPLIFIER

Eugeniu Grigoriev[1]*, ORCID: 0000-0002-0665-7500,
Vasile Tronciu[1], ORCID: 0000-0002-9164-2249,
Nils Werner[2], ORCID: 0000-0002-3055-6670,
Hans Wenzel[2], ORCID: 0000-0003-1726-022

[1]*Technical University of Moldova, 168 Stefan cel Mare Blvd., Republic of Moldova*
[2]*Ferdinand-Braun-Institut, Gustav-Kirchhoff-Straße 4, 12489 Berlin, Germany*
*Corresponding author: Eugeniu Grigoriev, *eugeniu.grigoriev@fiz.utm.md*

Received: 03. 05. 2022
Accepted: 04. 28. 2022

Abstract. This paper reports on the theoretical end experimental investigation of the output characteristics of a multisection master-oscillator power-amplifier (MOPA). It consists of a master oscillator (MO) composed by a gain section surrounded by two DBR sections monolithically integrated with a power amplifier (PA). We use a traveling wave equation model to calculate the optical output power in dependence on the current injected into the PA. The experimental results can be well explained with our theoretical analysis. For a finite front facet reflectivity of the PA the system is acting as a compound cavity.

Keywords: *distributed Bragg reflector laser, DBR, master oscillator power amplifier, MOPA, feedback.*

Rezumat. Articolul prezintă rezultatele finale ale investigației teoretice și experimentale a caracteristicilor de ieșire ale unui amplificator de putere master-oscilator multisecțional (MOPA). Amplificatorul este format dintr-un oscilator master (MO) compus dintr-o secțiune de câștig înconjurată de două secțiuni DBR integrate monolitic cu un amplificator de putere (PA). Este aplicat un model de ecuație a undelor de călătorie pentru a calcula puterea optică de ieșire în funcție de curentul injectat în PA. Rezultatele experimentale pot fi bine explicate prin analiza teoretică. Pentru o reflectivitate finită a fațetei frontale a PA, sistemul acționează ca o cavitate compusă.

Cuvinte cheie: *laser reflector Bragg distribuit, DBR, amplificator de putere master oscilator, MOPA, feedback.*

Introduction

Over the last years, master oscillator power amplifiers have been requested by several applications such as LIDAR, free space optical communications, and spectroscopy. These applications need spatially diffraction limited and spectral narrow-band emission at several hundreds of milliwatts or even watts output power [1-4]. A monolithically integrated master oscillator power amplifier at 1.5 μm is presented in [2]. The three-section device includes a

distributed feedback (DFB) laser, a modulation section, and a high power tapered amplifier. In order to mitigate the coupling effects of the light reflected at the facets, the device has been designed with a bent cavity axis and a tilted waveguide at the front facet. Such devices emit more than 400 mW output power. The dynamical behavior of a 1.5-μm DFB tapered MOPA was reported in [3]. Three different emission regimes such as stable amplified DFB laser emission with wavelength jumps when sweeping the injection currents, multimode Fabry–Perot (FP) operation of the complete MOPA cavity, and self-pulsing operation at frequencies between 5 and 8 GHz were observed. In Ref. [4] the physical origins of these phenomena were investigated in the framework of a time-dependent travelling wave (TW) model which phenomenologically incorporates thermal effects via self and cross-heating of the different sections of the device similarly as proposed in [5] for the first time.

This paper is concerned with numerical and experimental investigations of a multisection monolithically integrated distributed Bragg reflector (DBR) MOPA emitting at 1120 nm using a TW model [5-8]. We report the output characteristics of such device varying the front facet reflectivity. In Section 2 we introduce the device under study and the theoretical model. Section 3 presents experimental and numerical results. Finally, conclusions are given in Section 4.

Laser structure and equations

A schematic representation of the multisection DBR MOPA device is shown in Figure 1. The MO consists of three sections. The gain section G having a length of 0.5 mm is complimented by 1 mm and 0.5 mm long DBR sections on left- and right-hand sides, respectively. The MO is connected to the 4 mm power amplifier PA. The reflectivity R at the front facet for the PA is varied from 0 to 10^{-1}. The entire length of the device is 6 mm, and the emission wavelength is 1120 nm. The width of the ridge providing lateral fundamental mode operation is 4 μm. Electrical currents are injected into the gain section (I_{MO}) and the power amplifier (I_{PA}). The investigated structure is like to the one reported in [9]. The layer structure was grown by metalorganic vapor phase epitaxy. The active layer is formed by an InGaAs double quantum well which is embedded asymmetrically into a 4.8 μm thick vertical waveguide core [10, 11].

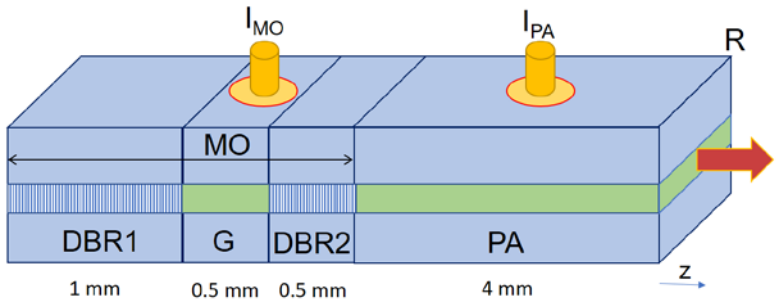

Figure 1. Setup of multisection DBR MOPA. The current injected into the MO is fixed. The current injected into the PA and the front facet reflectivity of the PA are varied.

The laser dynamics is analyzed using traveling wave equations for the slowly varying complex amplitudes $E^{+}(z,t)$ and $E^{-}(z,t)$ of the counter-propagating optical fields within each section of the device [7, 8] incorporated in [12]

$$\frac{n_g}{c_0}\frac{\partial}{\partial_t}E^{\pm} = [\mp\frac{\partial}{\partial_z} - i\Delta\beta(N,I)]E^{\pm} - i\kappa E^{\pm} + F_{sp}^{\pm} \quad (1)$$

where c_0 is the vacuum light speed and κ is the field coupling coefficient due to the Bragg grating. We also use the rate equation for carrier density:

$$\partial_t N = \frac{I}{edWl_A} + \frac{U_F^{'}}{edr_s}\left(\overline{N} - N\right) - \left(\frac{N}{T} + BN^2 + CN^3\right), \\ -\frac{c_0}{n_g}\Re\sum_{\nu=\pm} E^{\nu *}\left[g(N) - D\right]E^{\nu} \tag{2}$$

where d and W are the thickness and width, respectively, of the active region. The relative propagation factor, the modal peak gain, and the change of the modal index with carrier density are given by following expressions

$$\Delta\beta = \delta_0 - i\frac{\alpha_0}{2} + k_0\left[\Delta n_N\left(N\right) + \Delta n_T\left(I\right)\right] + i\frac{g\left(N\right) - D}{2},$$

$$g(N) = \Gamma g' N_{tr} \ln\left(\frac{N}{N_{tr}}\right), \quad \Delta n_N = \tilde{\alpha}_H \frac{\Gamma g' N_{tr}}{k_0}\sqrt{\frac{N}{N_{tr}}}.$$

The values of main laser parameters used in our simulations are collected in Table 1. For a detailed description of the remaining model equations and parameters, we refer to [6-8].

Table 1

Symbol	Description	Unit	Value
λ_0	reference wavelength	m	$1.12 \cdot 10^{-6}$
L_G	length of active section	m	$0.5 \cdot 10^{-3}$
L_{DBR1}	length of DBR section	m	$1.0 \cdot 10^{-3}$
L_{DBR2}	length of DBR section	m	$0.5 \cdot 10^{-3}$
L_{PA}	length of PA section	m	$4.0 \cdot 10^{-3}$
R_r	rear facet intensity reflectivity		0
R_f	front facet intensity reflectivity		0···0.1
n_g	group refractive index		3.6
κ	coupling coefficient	m^{-1}	$10 \cdot 10^{2}$
α_H	linewidth enhancement factor		-0,8
α_0	internal absorption	m^{-1}	$3 \cdot 10^{2}$
Γ	optical confinement factor		$0.68 \cdot 10^{-2}$
g’	differential gain	m^2	$2555 \cdot 10^{-22}$
ε_g	gain compression factor	m^3	$1 \cdot 10^{-24}$
N_{tr}	transparency carrier density	m^{-1}	$1.5 \cdot 10^{-24}$
d	thickness of active layer	m	$10 \cdot 10^{-9}$
W	width of active layer	m	$4 \cdot 10^{-6}$
A	recombination parameter	s^{-1}	$3.4 \cdot 10^{-9}$
B	recombination parameter	m^3s^{-1}	$1.5 \cdot 10^{-16}$
C	recombination parameter	m^6s^{-1}	$5 \cdot 10^{-42}$
U'_F	derivative of Fermi level separation	V m^3	$0.03 \cdot 10^{-24}$

Results and discussions

In what follows we discuss the output characteristics of the multisection device shown in Figure 1. We use the equations (1)-(2) and parameters listed in Table 1 for numerical calculations. The experiment was done at room temperature. Figure 2 illustrates both numerical and experimental output power versus injected current into PA characteristics for a fixed current of 200 mA injected into MO.

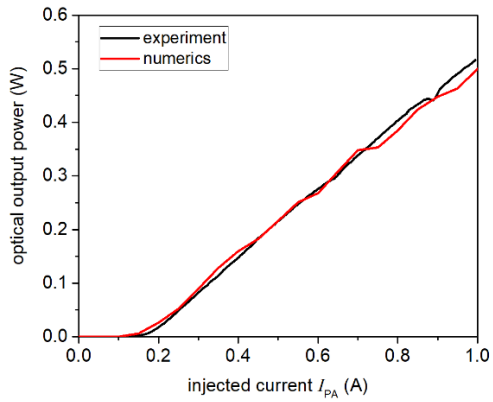

Figure 2. Dependence of output power on current injected into power amplifier PA: red – numerics, black – experiment. The current injected into the MO is 200 mA. The front facet reflectivity R =0.

From the characteristics a threshold of 0.15 A, and a slope of 0.6 W/A can be determined. The experimental investigations were performed at room temperature [9]. This figure indicated a good agreement between numerical calculations and experimental results. We next examine the same dependence as in Figure 2 what happens if the front facet reflectivity in increased to 10^{-2}. Figure 3a shows the measured characteristics. As mentioned before, for zero reflectivity the threshold current is 0.16 A. On the other hand, an increase of front facet reflectivity reduces the threshold current to 0.09 A (red curve in Figure 3a). One can observe an increase of the slope to 0.78 W/A. This is due to the fact that for a finite front facet reflectivity the system acts as compound cavity. However, for high currents one observes undulations of the output power with injected current.

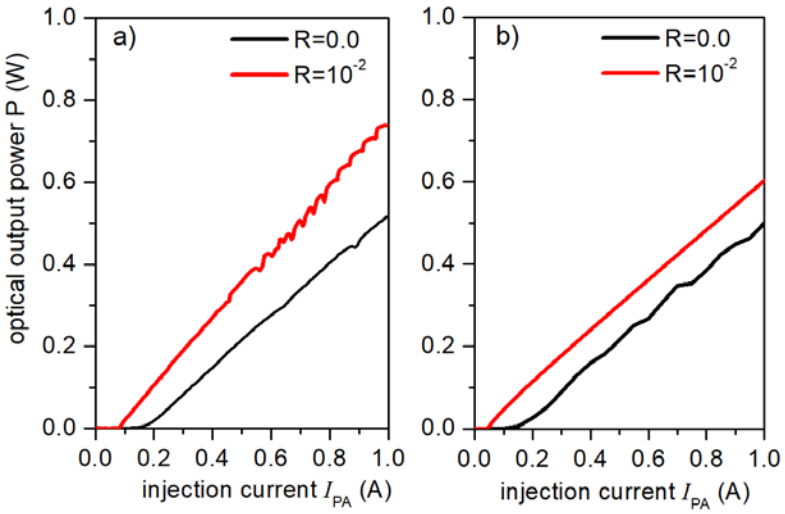

Figure 3. Output power versus injection current injected into the PA for two front facet reflectivities. The current injected into the MO is fixed to 200 mA: a) experiment, b) numerics.

Usually, this region with undulations is characterized by instabilities, which are not the subject of present investigations. The right panel of Figure 3 shows the numerically obtained results. We observe a good agreement between experiment and numerics regarding the decrease of the threshold current (0.05 A), However the slope (0.60 W/A) remains only constant in the simulation. In what follows, we show in Figure 4 how the front facet reflectivity affects the output power. An increase of the reflectivity from zero (black line) to 10^{-3} (red line) leads to a parallel shift of the characteristics to lower currents keeping the slope efficiency almost unaffected. A further increase of the front facet reflectivity to 10^{-1} remains the threshold current almost unchanged (I_{th}= 0.05 A) but reduces the slope to a value of 0.42 W/A due to a reduction of the outcoupled power.

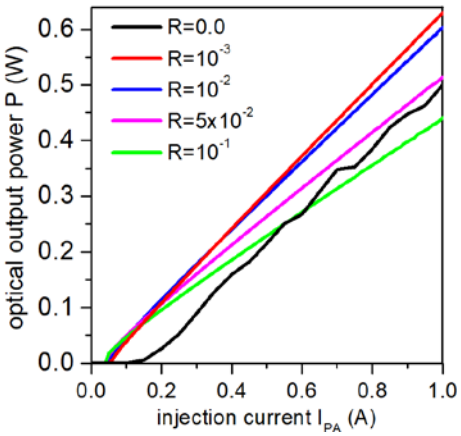

Figure 4. Simulated power–current characteristics for different front facet reflectivities.

Conclusions

We have carried out experimental and theoretical investigations of the output characteristics of multisection master-oscillator power-amplifier. The MO is designed to be composed of a gain section and two DBR sections. Both simulations and experiment show a good quantitative agreement between output laser characteristics for zero front facet reflectivity. When the front facet reflectivity is increased the MOPA works as a compound cavity. We believe that our work provides a good basis for future study and provides some hints for more detailed investigations of mechanisms behind the MOPA effects.

Acknowledgments: This work was supported by the National Agency for Research and Development of Moldova within the project 20.80009.5007.08 *"Study of optoelectronic structures and thermoelectric devices with high efficiency"*. We thank M. Radziunas for providing his LDSL code.

References

1. Crump P., Brox O., Bugge F., Fricke J., Schultz C., Spreemann M., Sumpf B., Wenzel H., Erbert G. High power, high effciency monolithic edge-emitting GaAs-based lasers with narrow spectral widths. In: *Advances in Semiconductor Lasers*, 2012, No. 49.
2. Faugeron M. et al. High Power Three-section integrated master oscillator power amplifier at 1.5 µm. In: *IEEE Photonics Technology Letters*, Jul. 1st 2015, V. 27, No. 13, p. 1449
3. Vilera M., Pérez-Serrano A., Tijero J. M. G., Esquivias I. Emission Characteristics of a 1.5-µm All-Semiconductor tapered master oscillator power amplifier. In: *IEEE Photon. Journal*, Apr. 2015, V. 7, No. 2.
4. Perez-Serrano A., Vilera Mariafernanda, Javaloyes Julien, Tijero Jose Manuel G., Esquivias Ignacio, Baile Salvador Wavelength jumps and multimode instabilities in integrated master oscillator power amplifiers at 1.5 µm. Experiments and theory. In: *IEEE J. Sel. Top. Quantum. Electron.*, Nov./Dec. 2015, V. 21, No. 6, 1500909

5. Spreemann M., Lichtner M., Radziunas M., Bandelow U., Wenzel H. Measurement and simulation of distributed feedback tapered master oscillator power amplifiers. In: *IEEE J. Quantum Electron.*, 2009, 45(6), 609-616
6. Mindaugas R., Tronciu V., Bandelow U., Lichtner M., Spreemann M., Wenzel H. Mode transitions in distributed-feedback tapered master-oscillator power-amplifier: theory and experiments. In: *Opt Quant Electron* 2008, 40, 1103-1109
7. Radziunas M., Wünsche H. J. Multisection lasers: Longitudinal modes and their dynamics. In: J. Piprek, *Optoelectronic Devices*, 2005, Springer: New York, p. 121-150
8. Radziunas M.: Traveling wave modeling of nonlinear dynamics in multisection laser diodes', in: J. *Piprek (Ed.), Handbook of Optoelectronic Device Modeling and Simulation: Lasers, Modulators, Photodetectors, Solar Cells, and Numerical Methods,* 2017, V. 2, CRC Press, Ch. 31
9. Werner N., Wegemund J., Gerke S., Feise D., Bugge F., Paschke K., Tränkle G. Comparison of distributed Bragg reflector ridge waveguide diode lasers and monolithic master oscillator power amplifiers. In: *Proceedings SPIE,* Volume 105531D, 2018, Novel In-Plane Semiconductor Lasers XVII.
10. Paschke K., Wenzel H., Fiebig C., Blume G., Bugge F., Fricke J., Erbert G. High brightness, narrow bandwidth dbr diode lasers at 1120 nm. In: *IEEE Phot. Techn. Lett.*, 2013, No. 25 (20) 1951-1954
11. Bugge F., Erbert G., Fricke J., Gramlich S., Staske R., Wenzel H., Zeimer U., Weyers M. 12 W continuous-wave diode lasers at 1120 nm with InGaAs quantum wells". In: *Appl. Phys. Lett.*, 2001, No. 79 (13) 1965-1967.
12. A software package LDSL-tool. Longitudinal Dynamics of multisection Semiconductor Lasers. http://www.wias-berlin.de/software/ldsl.

Journal of Engineering Science *Vol. XXIX, no. 2 (2022), pp. 68 - 75*
Fascicle *Electronics and Computer Science* *ISSN 2587-3474*
Topic *Electronics and Communication* *eISSN 2587-3482*

https://doi.org/10.52326/jes.utm.2022.29(2).07
UDC [004.7:621.39]:001.89

5G AND 6G EVOLUTION

Titu-Marius I. Băjenescu*, ORCID ID: 0000-0002-9371-6766

Swiss Technology Association, Electronics Group Switzerland
*Corresponding author: Titu-Marius I. Băjenescu, *tmbajenesco@gmail.com*

Received: 03. 07. 2022
Accepted: 04. 28. 2022

Abstract. The constant evolution in telecommunications is recognized both as a market driver and as a driver for R&D, since R&D activities are built to support consumer and business demands. The market pressures and recent past recessions have considerably shifted the focus of companies to product development and incremental research. This current focus on short term gains has paved the way for applied research to the furthest extent. Research and technological development, which is a founding block of any field of science and technology, was explained from the point of view of ICT with a primary focus on the telecom industry. The research ecosystem along with its shortcomings were also presented. It is important that governments and the ICT industry re-evaluate the R&D ecosystem and consider having both a 3 to 5-year view along with a 30 to 40-year long vision. 5G technology started to roll out effectively to ordinary users in 2019 (development of this technology started in April 2008), and in 2020 it was expected to spread to even more countries, and then in a few years it will be global. This is despite various studies that point out that 5G radiation will have negative effects on human health (which has also been claimed for 4G and 3G), while organisations such as the *US Communications Commission* (US FCC) and almost all similar organisations state that 5G radiation has no significant effects on human health. Another concern is the security of communications over 5G networks, especially equipment sold by China. Australia and the UK - in early 2019, took steps to restrict or eliminate the use of Chinese-sourced equipment in their 5G networks. Also in 2019 the US via the FBI and the UK via *Government Communications Headquarters* (GCHQ) other intelligence services, began to get more involved in changing surveillance standards. Including at the NATO meeting in London in December 2019, 5G network security and development was discussed. In addition to high download speeds, the 5G network also has a low "air latency" (between phone and antenna) of 8-12 milliseconds.

Keywords: *5G mobile communication, robust research ecosystem, 6G, wireless network, NTT DOCOMO, R & D process, significantly faster speeds, Nokia 2G 6G, making 6G a reality.*

Rezumat. Evoluția constantă în telecomunicații este recunoscută atât ca un motor de piață, cât și drept un motor pentru cercetare și dezvoltare, construite pentru a susține cerințele consumatorilor și ale afacerilor. Presiunile pieței și recesiunile recente au mutat considerabil concentrarea companiilor către dezvoltarea de produse și cercetarea incrementală. Accentul actual asupra câștigurilor pe termen scurt a deschis larg calea cercetării aplicate. Cercetarea

și dezvoltarea tehnologică, care este un bloc fondator al oricărui domeniu al științei și tehnologiei, a fost explicată din punctul de vedere al TIC, cu accent primar pe industria telecomunicațiilor. Au fost prezentate și ecosistemul de cercetare împreună cu deficiențele acestuia. Este important ca guvernele și industria TIC să reevalueze ecosistemul de cercetare și dezvoltare și să ia în considerare atât o viziune pe 3 până la 5 ani, cât și o viziune pe o perioadă de 30 până la 40 de ani. Tehnologia 5G a început să se răspândească în mod eficient către utilizatorii obișnuiți în 2019 (dezvoltarea acestei tehnologii a început în aprilie 2008), iar în 2020 era de așteptat să se răspândească în mai multe țări, iar apoi în câțiva ani să devină globală. Acest lucru se întâmplă în ciuda diferitelor studii care subliniază că radiațiile 5G vor avea efecte negative asupra sănătății umane (care a fost revendicată și pentru 4G și 3G), în timp ce organizații precum Comisia de Comunicații din SUA (US FCC) și aproape toate organizațiile similare declară că 5G radiațiile nu au efecte semnificative asupra sănătății umane. O altă preocupare este securitatea comunicațiilor prin rețelele 5G, în special echipamentele vândute de China. Australia și Regatul Unit al Marii Britanii au luat măsuri pentru a restricționa sau elimina utilizarea echipamentelor provenite din China în rețelele lor 5G. De asemenea, în 2019, SUA prin intermediul FBI și Marea Britanie prin intermediul cartierului general de comunicații guvernamentale (GCHQ) și alte servicii de informații, au început să se implice mai mult în schimbarea standardelor de supraveghere. Și la reuniunea NATO de la Londra din decembrie 2019 s-a discutat despre securitatea și dezvoltarea rețelei 5G. Pe lângă viteze mari de descărcare, rețeaua 5G are și o „latență a aerului" scăzută (între telefon și antenă) de 8-12 milisecunde.

Cuvinte cheie: *comunicații mobile 5G, ecosistem robust de cercetare, 6G, rețea fără fir, NTT DOCOMO, proces de cercetare și dezvoltare, viteze semnificativ mai mari, Nokia 2G 6G, transformând 6G în realitate.*

Introduction

As stated earlier, the 5G vision has been mainly focused on serving three applications: eMBB, uRLLC, and mMTC. These three applications however, require focused network planning around optimizing throughput, latency, and coverage respectively. The eMBB application is particularly challenging in dense urban environments where there is expected to be a massive installation of outdoor small cells as well as an extensive underground fiber optic network to support the traffic and throughput demands from the urban center [1]. Because of this, there has been a major effort around realizing millimeter-wave (mmW) communications technology for mobile networks—a spectrum space that was traditionally exclusively utilized for military and science purposes for radar and imaging [2].

This has proliferated mmW-based research in antennas, RF transceivers, and fabrication processes so that they are more readily integrated into user equipment. This all comes with the typical power (EIRP) and propagation requirements/considerations that are native to cellular components and networks. This has been particularly challenging considering the path loss at mmW frequencies—the high frequency signal attenuates greatly over distance causing the need for line-of-sight (LoS) links at close distances [3, 4]. Moreover, mmW frequency signals tend to scatter at an obstacle as opposed to its low frequency counterpart that can often diffract around an obstacle.

The uRLLC applications rely upon a highly synchronized network, at low-to-medium throughputs, with a very high device density [5-8]. Table 1 shows some sample uRLLC scenarios, often in an industrial automation setting. However, public safety and medical

applications are also required to have low latency and reliable communications. For instance, in a remote surgery application where a surgeon must be little time delay between the controller and equipment. This type of communications requires a dedicated backhaul backbone, low time errors in the synchronization path/clock chain from the primary reference time clock (PRTC) down to the telecom transparent clock (T-TC), with stringent end-to-end quality of service (QoS) goals.

Table 1

URLLC applications

Table 1 Performance requirements for uRLLC use cases							
Scenario	Max Allowable E2E Latency (ms)	Survival Time (ms)	Reliability (%)	User Experience Data Rate (Mbps)	Payload Size	Traffic Density (Gbps/km^2)	Connection Density (/km^2)
Discrete Automation	10	0	99.99	10	Small to large	1000	100,000
Process Automation - Remote Control	60	100	99.9999	1 to 100	Small to large	100	1,000
Process Automation - Monitoring	60	100	99.9	1	Small	10	10,000
Electricity Distribution - Medium Voltage	40	25	99.9	10	Small to large	10	1,000
Electricity Distribution - High Voltage	5	10	99.999	10	Small	100	1,000
Intelligent Transport Systems - Infrastructure Backhaul	30	100	99.999	10	Small to large	10	1,000

The mMTC applications almost directly correspond to the proliferation of IoT devices in industry vertices from commercial to industrial. This is supported by the ever-growing presence of new IoT protocols and the marketplace for IoT development platforms, bringing previously unknown data to the cloud for complex analysis and feedback [9, 10]. The network for this type of communication does not have the bandwidth constraints of eMBB nor the stringent latency requirements of uRLLC, rather, strict battery life/node maintenance expectations along with coverage in the unconnected areas of the globe [11-13]. Power saving protocols and energy harvesting techniques are used in these compact nodes with smart placement in order to ensure ideal connectivity along with OTA firmware updates for minimal maintenance after installation.

NTT DOCOMO R&D (Nippon Telegraph and Telephone do communications over the mobile network) has been in the forefront of mobile technology, not only in Japan, but also at a global scale. During 2014, it created one of the first labs dedicated to conducting R&D on 5G and to speeding up work on its standardization. It contributes about 2.5% of its revenue to research and development. It is evident that the vendor community spends over 10% of its revenue on R&D, whereas operators' spending hovers around 2% (if any). R&D spending by some of the largest operators is on the order of a few hundred million dollars, whereas it runs into billions for large-scale manufacturers [14]. Orange Labs and DOCOMO are the two key R&D spenders in the operator community, whereas the vast majority of the service providers do not set aside a budget for R&D.

R & D process (telecom)

Established vendors and start-ups are always seeking to bring research and innovations to their customers, that is, the operators. In the majority of cases, operators have the final say as to whether or not to take the supplier's innovation to the next level [15]. The established suppliers, big or small, have deeper pockets and more leverage over operators as compared to start-ups. The start-ups spend considerable time seeking funding from venture capital firms and endorsements from operators for their technology incubation. As the research starts to mature, suppliers start working to sell their ideas, which leads to technology

development (or technology incubation for start-ups). Technology development enables development and enhancement of practical solutions. Technologies are first normally standardized and then utilized during product development.

Nothing is more normal than to project oneself into the future when one works in tech. The telecom pros are already well advanced in their thinking. The planning has already been done: 6G is expected to be launched in 2028 and commercialised in 2030, and these few years will not be too long for telecom research, patenting and agreement on new standards.

We have gone from SMS to interactive video to IoT in a few years and 6G will propel us into another world [16].

Telecoms companies are working hard to implement 5G connectivity into our everyday lives, and some are reportedly already working on the upcoming 6G network. Samsung released a white paper called "*The Next Hyper-Connected Experience for All*" in which it detailed what the key areas for development are and what the hurdles are.

According to Samsung, 6G could launch in 2028 at the earliest, while mass adoption could happen ten years from now, or 2030. The timeframe is similar to the eight years it took the 5G network to develop from concept to reality. In comparison, the 3G network was developed in 15 years.

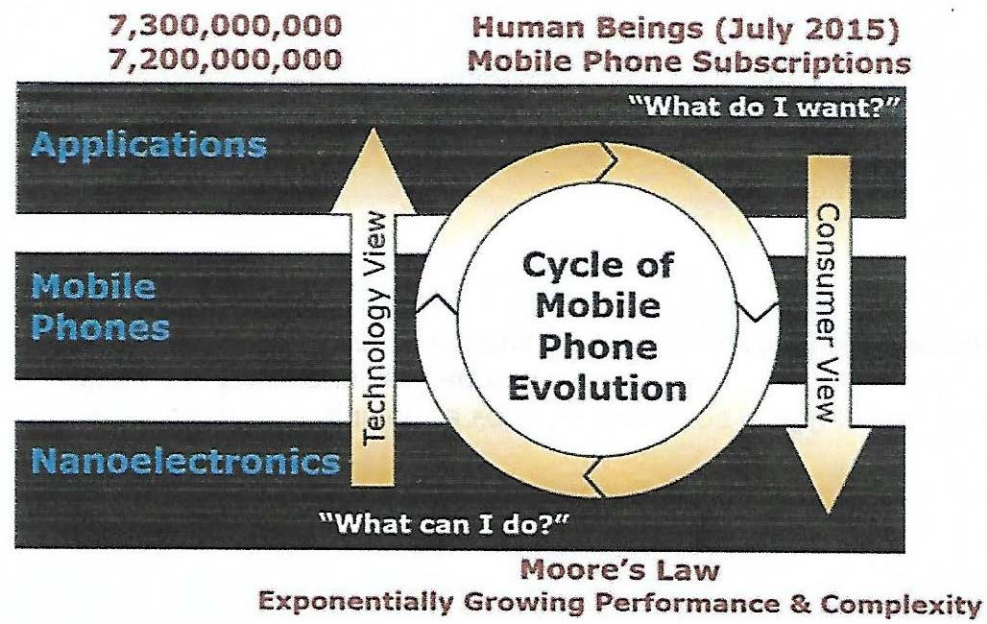

Figure 1. Cycle of mobile phone evolution.

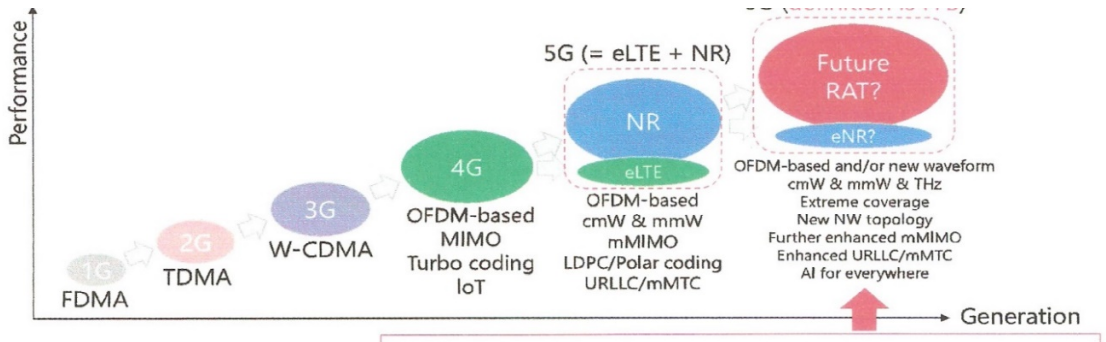

Figure 2. Technological evolution up to 5G in mobile communications.

Robust research ecosystem

A robust research ecosystem comprises strong government policies, energetic university and industrial research institutions, emerging start-ups, mature technology companies, funding for both basic and applied technologies from government and private institutions (including venture capital firms), and a large pool of talented researchers [17]. Only a few countries have all of the ingredients required to establish and maintain a dynamic ICT research ecosystem. Thus, strong collaboration is required at the global level so that one country can address the missing elements of another nation. A critical element for continuation of this ecosystem is investment in basic research, which is almost nonexistent, particularly in the ICT sector, worldwide. Most of the investment since the last decade has been pouring into applied research for immediate returns. This trend is expected to continue as ICT companies operate in a highly competitive and commoditized environment, which is forcing them to quickly bring products to market with razor thin margins.

Samsung also suggests that both people and machines will use 6G, which will enable a truly immersive extended reality (XR) experience, lead to high-fidelity holograms and digital replicas.

Figure 2 shows the technological evolution up to 5G in mobile communications.

What is 6G?

The applications have a natural progression to more a ubiquitous virtual experience with AR/VR applications, tactile internet along with intensive predictive analysis/modeling via the proliferation of artificial intelligence (AI) processing within said devices [18]. These push current technologies to the next level. The mixed reality (MR) experience uses 3D objects and AI to provide a seamless, immersive experience with a high integrity 6G connection.

An example of this would be holographic communications where conventional video conferences are augmented with a realistic projection for a three-dimensional image. The concept of connected robots and autonomous systems to provide basic services such as mail/package delivery also requires a high-fidelity wireless connection to enable the proper feedback necessary to control the destinations of such equipment.

Other future wireless applications include a brain-computer interface (BCI) where appliances can be controlled via a communication path between the user's brain and the device's RF front-end. This can be extended to the medical field with medical wearables tracking/monitoring a patient's health while they are in hospice [19]. Entirely automated industrial facilities with intensive computing will require a reliable connection to the cloud in order to perform the complex data analytics necessary for remote control and predictive analysis.

The 6G infrastructure is expected to be built upon 5G with some critical additions that diverge from the traditional contemporary cellular technologies. One major aspect of 6G is the incorporation of the terahertz spectrum from 0.1 THz to 10 THz [20]. This massive block of additional spectrum has the bandwidth to support the connectivity needed through the use of photonic and hybrid electronic-photonic transceivers. The benefit of this technology over most mmW technology is that a line-of-sight (LoS) link is not required. A cell-less architecture is called upon to support 6G where user equipment (UE) is connected to the RAN as opposed to a singular cell. This can be realized through the tight integration of difference communication technologies (e.g., sub-6 GHz, mmW, THz, and visible light communications

(VLC) where 6G devices can support all these heterogeneous radios within the device. This eliminates the gaps in coverage that come with handovers.

Figure 3 shows an Image of technological development toward 6G.

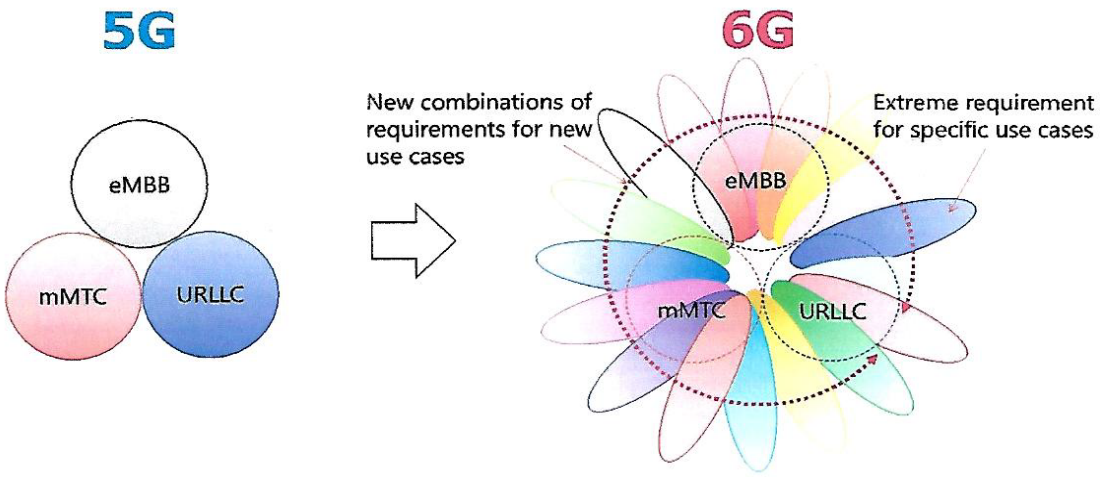

Figure 3. Image of technological development toward 6G (after NTT DOCOMO)
eMBB: enhanced mobile broadband; **mMTC**: massive machine type communication; **URLLC**: ultra-reliable and low latency communications.

Significantly faster speeds

As for the future of 6G technology, the future is looking bright, with data transfer speeds of 1 §TB per second that would, in theory, make it possible to download 142 hours of content at the highest resolution currently possible - 4K - every second. If these figures seem abstract, it's easiest to imagine a show like Supernatural, which will have 15 seasons of around 20-21 episodes each when it's finished, being downloadable using 6G in less than two minutes.

Despite the performance this technology could achieve, it's still a long way off before it can be integrated into the devices we use every day. Clearly, the physical limits of communications networks need to be overcome to support such a data flow [21-23].

As for the launch date of 6G technology, it will be available on the market after 2030, which means that it will take a few more years before it becomes dominant in the smartphone market.

Some reports also suggest that China is not alone in the race for 6G, with Japan already working to achieve this communications speed standard.

6G will not arrive before the end of the decade, but it will not only be a new increase in speeds and a reduction in latency. It is a true fusion of the real and digital worlds that is coming, with the human being always at the center [23].

5G is being rapidly deployed around the world and brings its share of new features with even more throughput, reduced latencies opening new possibilities (autonomous cars, industry 4.0, fine control at a great distance...) and an infrastructure that starts to be aware of its environment by adapting its capacities in real time according to the needs or emergencies [24, 25].

These elements will be found in 6G, the next generation of mobile technology that will take its first steps by the end of the decade and deploy more widely during the 2030s.

It will take these notions further by enabling a fusion between the real and digital worlds to create digital duplicates of the physical elements, filled with a whole set of data provided by multiple sensors and information bases.

Nokia 2G 6G

This fusion of the two worlds could endow humans with "superpowers" and analytical capabilities that go beyond their vision of the physical world by accessing a whole new set of information on their surrounding environment.

The equipment manufacturer Nokia is among the pioneers preparing this revolution through its Nokia Bell Labs research centers and talks about this upcoming transformation.

Every aspect introduced with 5G will be improved in 6G, with an intermediate evolution 5G-advanced that will prepare the ground around 2025 (as there was a 4G-advanced before 5G) [25]. The big theme of 6G is about creating these digital doubles, or "Digital Twin", of cities, infrastructure and factories. This trend is already underway with 5G, but it will take on a new dimension with the next generation by enabling much faster detection and response to out-of-the ordinary conditions and phenomena, whether it's an incident or a need to redirect resources to a specific point [26].

What remains now is to identify/finalize the technologies and put in place the intellectual property that will create this vision. Nokia estimates that the first 6G systems will be operational by 2030, following a classic 10-year cycle between generations of cellular communications, with the first phase of standardization by 2026, within 3GPP Release 20.

5G-Advanced will pave the way through 3GPP Release 18, with a rollout from 2025. As a reminder, Nokia is the project leader of the Hexa-X program, which should put Europe back at the heart of 6G developments [27].

Nokia for NASA

Nokia to develop a 4G network on the Moon for NASA. Nokia has received funding from NASA to study the possibility of designing a 4G network on the Moon as part of the human colonization project of our natural satellite [28].

5G: Nokia to build its own experimental mobile network in Finland. Nokia plans to build an experimental 5G mobile network in Finland that could be up and running by early next year.

Making 6G a reality

There are already research initiatives kicked-off in different countries in order to realize 6G. In Finland, the University of Oulu kickstarted Finnish 6G research in 2018. The FCC opened up the 95 GHz to 3 THz spectrum for experimental licenses, opening up research opportunities for optical/photonic communication links in the U.S. As of 2019, South Korea and China began putting together working groups dedicated to 6G research between companies, government departments, and universities [29]. It goes without saying that 6G is very much a nascent platform. However, between the potential new technological solutions and the KPIs, it will become the new goalpost for innovation beyond 5G [30].

Conclusion

Hyperconnectivity, the trend towards online work and communication has been fueled by both technical and social trends. Entire companies and even industries have moved to online working. And after the workday is over, people switch from video calls to online gaming. From virtual reality games to massively multiplayer immersive experiences,

participation in online games has skyrocketed. People no longer come together at an office building to work or at a sports stadium to watch a game. They go online, in millions of homes, to meet colleagues, drive virtual race cars, or cheer on their favorite rock stars at a virtual concert.

References

1. Holma H., Toskala A., and Nakamura T. "5G technology: 3GPP new radio," Wiley, Dec. 2019.
2. Newsletter of the MIC, Japan, "Announcement of the Local 5G implementation guidelines - Institutional development for Local 5G implementation," Dec. 2019.
3. Government of Japan, "The 5th Science and Technology Basic Plan," Jan. 2016.
4. Kishiyama Y. and Nakamura T. "Real and future for 5G evolution and 6G," MWE2018 Workshop FR2A-1, Nov. 2018.
5. Saad Z. Asif. "5G Mobile Communications - Concepts and Technologies", CRC Press, 2019.
6. Erik Dahlman, Stefan Parkvall, and Johan Sköld, "5G NR: The Next Generation Wireless Access Technology", Academic Press, 2018.
7. Fa-Long Luo, Charlie (Jianzhong) Zhang (Eds.), "Signal Processing for 5G Algorithms and Implementations" Wiley, 2016.
8. Ji M., Caire G., and Molisch A. F. "Wireless device-to-device caching networks: basic principles and system performance," IEEE JSAC, vol. 34, no. 1, pp. 176-189, Jan. 2016.
9. Teyeb O., Muhammad A., Mildh G., Dahlman E., Barac F., and Makki B. "Integrated access backhauled networks," IEEE VTC2019-Fall, Sept. 2019.
10. Onizawa T., Tatsuda T., Kita N., and Yamashita F. "Recent research and developments focusing on fixed wireless and satellite communication systems," IEICE Tech. Rep., RCS2019-32, pp. 53-58, May 2019.
11. FCC News Release, "FCC takes steps to open spectrum horizons for new services and technologies," Mar. 2019.
12. Paulo Sergio, Rufino Henrique, and Ramjee Prasad (Eds.), "6G The Road to the Future Wireless Technologies, 2030", River Publishers Alsbjergvej 10 9260 Gistrup Denmark.
13. Rappaport T. S. "Wireless beyond 100 GHz: opportunities and challenges for 6G and beyond," IEEE COMCAS Keynote, Nov. 2019.
14. Sawahashi M. "Views on technical challenges of physical layer for integrated wireless access and backhaul," IEICE Society Conference 2018, BS4-1, Sept. 2018.
15. M. Taromaru, "A view of digital modulation technologies beyond 5G – Are we still to use IFFT/FFT-based modulations for the new radio?," IEICE Society Conference 2018, BS4-3, Sept. 2018. 17
16. Sasaki H., Lee D., Fukumoto H., Yagi Y., Kaho T., Shiba H., and Shimizu T. "Experiment on over-100-Gbps wireless transmission with OAM-MIMO multiplexing system in 28-GHz band," IEEE GLOBECOM2018, Dec. 2018.
17. J. A. Lucciardi, N. Thomas, M. L. Boucheret, C. Poulliat, and G. Mesnager, "Trade-off between spectral efficiency increase and PAPR reduction when using FTN signaling: Impact of non linearities," IEEE ICC2016, May 2016.
18. T. Murakami, R. Ohmiya, T. Nakahira, K. Ishihara, and T. Hayashi, "Proposal of virtual massive MIMO (VM-MIMO)," IEICE General Conference 2019, B-1-123, Mar. 2019.
19. https://www.5g-acia.org/
20. Fujino Y., Fukumoto H., Nakano M., Tsubaki T., and Sakamoto K. "Challenge to Mbps-class high-speed acoustic communication for wireless remote operation of underwater vehicles," IEICE Tech. Rep., RCS2019-232, pp. 163-168, Nov. 2019.
21. Harada H., Murayama D., and Nagata S. "3GPP study on 5G NR based access to unlicensed spectrum," IEICE Tech. Rep., SRW2018-70, pp. 61-65, Mar. 2019.
22. Ye N., Li X., Yu H., Wang A., Liu W., and Hou X. "Deep learning aided grant-free NOMA toward reliable low-latency access in tactile internet of things," IEEE Trans. on Industrial Informatics, vol. 15, no. 5, pp. 2995-3005, 2019.
23. Arai T., Goto D., Iwabuchi M., Iwakuni T., and Maruta K. "AMAP: adaptive movable access point system for offloading efficiency enhancement," IEICE Tech. Rep., RCS2016-43, pp. 107-112, May 2016.
24. Murakami T., Miyazaki M., Ishida S., and Fukuda A. "Wireless LAN based CSI monitoring system for object detection," MDPI Electronics, vol. 7(11), no.290, Nov. 2018.
25. Murakami T., Otsuki S., Hayashi T., Takatori Y., and Kitamura K. "Wildlife detection system using wireless LAN signals," NTT technical review, vol.17, no.6, pp.45-48, Jun. 2019.
26. Zhao N., Zhang S., Yu F. R., Chen Y., Nallanathan A., and Leung V. C. M. "Exploiting interference for energy harvesting: a survey, research issues, and challenges," IEEE Access, vol. 5, pp. 10403–10421, May 2017.
27. Angeliki Alexiou (Ed.), "5G Wireless Technologies", published by The Institution of Engineering and Technology, London, United Kingdom, 2017.
28. Băjenescu T.-M. "5G: Future Opportunities and Challenges", Journal of Engineering Science, Vol. XXVII, no. 4 (2020), pp. 120 – 127.
29. Dang S., Amin O., Shihada B. et al. What should 6G be?. Nat Electron 3, 20–29 (2020). https://doi.org/10.1038/s41928-019-0355-6.
30. Giordani M., Polese M., Mezzavilla M., Rangan S., and Zorzi M. "Toward 6G Networks: Use Cases and Technologies," in IEEE Communications Magazine, vol. 58, no. 3, pp. 55-61, March 2020.

Journal of Engineering Science *Vol. XXIX, no. 2 (2022), pp. 76 - 90*
Fascicle *Electronics and Computer Science* *ISSN 2587-3474*
Topic *Computers and Information Technology* *eISSN 2587-3482*

https://doi.org/10.52326/jes.utm.2022.29(2).08
UDC 004.056:004.4

SECURE SOFTWARE DEVELOPMENT AWARENESS: A CASE STUDY OF UNDERGRADUATE DEVELOPERS

Murimo Bethel Mutanga*, ORCID: 0000-0002-6021-8613

Mangosuthu University of Technology, Umlazi, Durban, South Africa
*Corresponding author: Bethel Mutanga, *mutangamb@mut.ac.za*

Received: 03. 23. 2022
Accepted: 05. 08. 2022

Abstract. As ubiquitous computing becomes an increasingly inherent component of everyday life due to the rapid growth of communication technologies and globalization, threats against information systems have taken a more latent yet lethal dimension. This emergent digital security challenge has correspondingly motivated a proactive change in the software engineering process in recent decades. This change has inspired more intense research scrutiny on security as a crucial component of any software system. Moreover, in today's virtual world of hyperconnectivity, the most significant vulnerabilities in modern information systems security are software centred. Nevertheless, research shows that software developers often lack the required knowledge and skills in secure software systems development (SSD). Such knowledge ensures that all the resultant software components of each development lifecycle are correctly implemented rather than merely following the SSD lifecycle. Also, the knowledge engenders software security consciousness as a professional attitude amongst developers. Therefore, investigating students' awareness of SSD principles can generate insight into evolving the undergraduate software development curriculum – a path to building future career developers. The study used a voluntary online survey to recruit a sample of 76 undergraduate developers and employed a descriptive approach to data analysis. Among other findings, the study revealed that participants' perception of the threat of software vulnerability impacts their attitude towards security on online and mobile platforms. And that though over 90% of the undergraduate developers took software vulnerability threats either "serious" or "extremely serious", this disposition did not reflect the depth of their knowledge and experience in SSD.

Keywords: *Cyber-security, Framework, Software, threat, ubiquitous-computing, vulnerability.*

Rezumat. Pe măsură ce computerul omniprezent devine o componentă din ce în ce mai inerentă a vieții de zi cu zi datorită creșterii rapide a tehnologiilor de comunicare și globalizării, amenințările la adresa sistemelor informaționale au luat o dimensiune mai latentă, dar letală. Această provocare emergentă de securitate digitală a motivat în mod corespunzător o schimbare proactivă în procesul de inginerie software în ultimele decenii. Această schimbare a inspirat o cercetare mai intensă a securității ca componentă crucială a oricărui sistem software. Mai mult, în lumea virtuală de astăzi a hiperconectivitatii, cele mai

semnificative vulnerabilități în securitatea sistemelor informatice moderne sunt centrate pe software. Cu toate acestea, cercetările arată că dezvoltatorii de software nu au adesea cunoștințele și abilitățile necesare în dezvoltarea sistemelor software securizate (SSD). O astfel de cunoaștere asigură că toate componentele software rezultate ale fiecărui ciclu de viață de dezvoltare sunt implementate corect, mai degrabă decât să urmărească pur și simplu ciclul de viață SSD. De asemenea, cunoștințele generează conștiința securității software ca atitudine profesională în rândul dezvoltatorilor. Prin urmare, investigarea gradului de conștientizare de către studenți a principiilor SSD poate genera o perspectivă asupra evoluției curriculum-ului de dezvoltare software pentru licență - o cale către construirea viitorilor dezvoltatori de carieră. Studiul a folosit un sondaj online voluntar pentru a recruta un eșantion de 76 de dezvoltatori de licență și a folosit o abordare descriptivă a analizei datelor. Printre alte constatări, studiul a arătat că percepția participanților asupra amenințării vulnerabilității software influențează atitudinea lor față de securitate pe platformele online și mobile. Și că, deși peste 90% dintre dezvoltatorii de licență au considerat amenințările de vulnerabilitate software fie „serioase" fie „extrem de grave", această dispoziție nu a reflectat profunzimea cunoștințelor și experienței lor în SSD.

Cuvinte cheie: *Securitate cibernetică, arhitectură, software, amenințare, tehnica de calcul omniprezentă, vulnerabilitate.*

Introduction

Traditionally, security in software development is often viewed either as a remedy or patch deployed to solve security breaches or as an enhancement to a wholly developed software package [1]. As further emphasized by Alkussayer and Allen [1], developers only pay attention to security considerations as they approach the end of the development lifecycle, which is why such security solutions often come as add-on mechanisms and techniques before software systems deployment. Therefore, security issues were often reactively addressed when prompted by some undetected vulnerability or when such vulnerability may have even been exploited [1, 2].

However, in recent decants, there has been a pragmatic change away from this mundane approach for security in software development to embrace a more proactive approach that advocates the deliberate injection of forethought security ramifications into all stages of the software development lifecycle [1–4]. The emergent alternative to secure software development primarily recognizes security requirements as an integral element of the software design and development process; therefore, rather than treating security requirements as an ad-on or a corrective measure, it is implemented as a "designed-in" component.

It has become increasingly imperative to strengthen or reengineer the existing processes for developing secure software. The advancement of the internet and the proliferation of other related sophisticated technologies have escalated the scale of cyber threats against information systems [5]. For instance, as ubiquitous computing becomes an increasingly inherent component of everyday life, it has become increasingly easy to use these technologies in complex ways [6]. However, cyber adversaries who thrive on exploiting information systems vulnerabilities take undue advantage of this ease-of-use and the pervasiveness of the internet [7, 8].

Furthermore, in the broad context, information security research focuses on two fundamental drivers of vulnerability: people-oriented and software-oriented factors [9]. While

the former can constitute a potential loophole in information systems security [9, 10], faulty software development in utilizing the appropriate security requirements represents the core weakness in the landscape of information system security. According to Luo et al. [11], such weaknesses are "defects in software's specific implementation or system security policy, which can enable attackers to access or damage the system without authorization".

On the other hand, research on how students undertake software development abound. For example, in the context of this study, the work reported in [12] discussed students' software development knowledge at a more general level. However, current literature suggests that there has been more emphasis on improving students' programming skills and optimising teaching programming techniques [13–15]. But scanty investigations tend to probe students' awareness of emergent security challenges and the state-of-the-art software development principles designed to guarantee secure systems development.

The fact is, as the world becomes more and more interconnected, the landscape and implications of information systems security have drawn more concerns than ever. For instance, amongst other technological evolutions, the emerging trend of the Internet of Things (IoT) has gained momentum in recent years. In conjunction with mobile communication technologies, IoT facilitates the design and supports the deployment of intelligent and ambient devices [16], which essentially makes it possible for things and objects to interact and cooperate between themselves [17] autonomously. With these advances, society will get smarter and smarter with the gradual shift in focus to adopting innovative software-driven systems as the hub of critical resource management to ensure convenient and efficient resource administration and service delivery [8]. At an industrial level, the popularity and reliance on IoT are already rising with critical applications such as smart grids, smart cities, IoT connected factories, smart supply chain management, connected healthcare systems, and smart farming.

The dominant role of software systems is not limited to the industrial sector as governments, research, and other corporate establishments are also heavily reliant on information technology these days. Therefore, software security breaches can have far more reaching consequences.

Because of the essential nature of the global challenge of securing information systems, this study investigates awareness of secure software development principles among South African undergraduate students. This study is motivated first because South Africa has one of Africa's most funded educational systems, the government's strategic interest in advancing local technological content. Second, according to Vadra [18], South Africa's inclusion into the four-member grouping of fast-emerging economies of the world, namely, Brazil, Russia, India, and China, is both a mark of the country's development strides in the African continent and most importantly, a call for a potential shift in focus knowledge-based economy in alignment with the other countries with the block.

As a whole, the findings of this study provide helpful insight into the level of preparedness of upcoming undergraduate programmers to effectively contribute toward secure software development in the industry. Such understanding also contributes to improving the current computer programming teaching curriculum to sufficiently equip undergraduate students with the expertise to address the information system security challenge through secure application development. This study surveyed 2nd and 3rd undergraduate information technology students from a South African University of Technology and qualitatively analyzed the data.

Research Methodology

This section presents the entire research design, which includes the description of the population, sample categorization, data collection instrument, and the approach to data analysis.

Study Participants

This study targets undergraduate 2nd and 3rd-year Information and Communication Technology students. On the one hand, it was assumed that the 2nd year students have enough exposure to software development training because their three-year study curriculum is highly streamlined to specialize in software development or network engineering. And on the other hand, aside from being in their final year of study, the 3rd year students were undergoing their compulsory work-integrated learning program (WIL), which exposes them to various real-life industry experiences. These two scenarios make the selected population most appropriate for this investigation.

The study used a sample of 76 students drawn up from the study population as described above. Table 1 presents the characterization of the study's participants.

Table 1

Characterization of the study's population

Gender		Year of Study	
Male	56	2nd	43
Female	20	3rd	33
Total		76	

Data collection and Analysis

This study employed an online questionnaire-based survey for gathering data. This data collection method utilized Google Forms – a customizable virtual survey tool that allows researchers to create suitable questionnaires following an existing template. The instrument's suitability was ascertained using a closed-ended questionnaire designed and subjected to evaluation by an independent expert. The validated questionnaire was then used to create a customized questionnaire on Google Forms. This questionnaire elicited demographic and other information related to students' awareness of secure software development principles.

Due to the nature of the information collected, a descriptive approach was used to analyze the data. And a question-by-question analysis was performed to ascertain the level of students' awareness of secure software development principles.

Results and discussion

In this section, a summary of the study's results is presented. First, the data were quantitatively analyzed and presented section-by-section according to the questionnaire design. Second, the results are then interpreted in the discussion subsection section.

In this section, a summary of the study's results is presented. First, the data were quantitatively analyzed and presented section-by-section according to the questionnaire design. Second, the results are then interpreted in the discussion subsection section.

How students perceived the threat of software vulnerability

This investigation asked two background questions to explore students' understanding of and, by extension, their attitude towards the critical issue of software security as a global and professional challenge. These questions were as follows:

Question 1(a): How would you describe the threat posed by software vulnerability to information system security? As stated earlier, this question was asked to enable the researcher to elicit information that can help make the existing software development curriculum more robust and better aligned with current software security realities. Most importantly, such a curriculum can improve the quality of graduate developers in South Africa by ensuring that they are well-grounded in the ethical, theoretical, and professional responsibility of being security conscious when developing commercial systems. Figure 1 illustrates the outcomes.

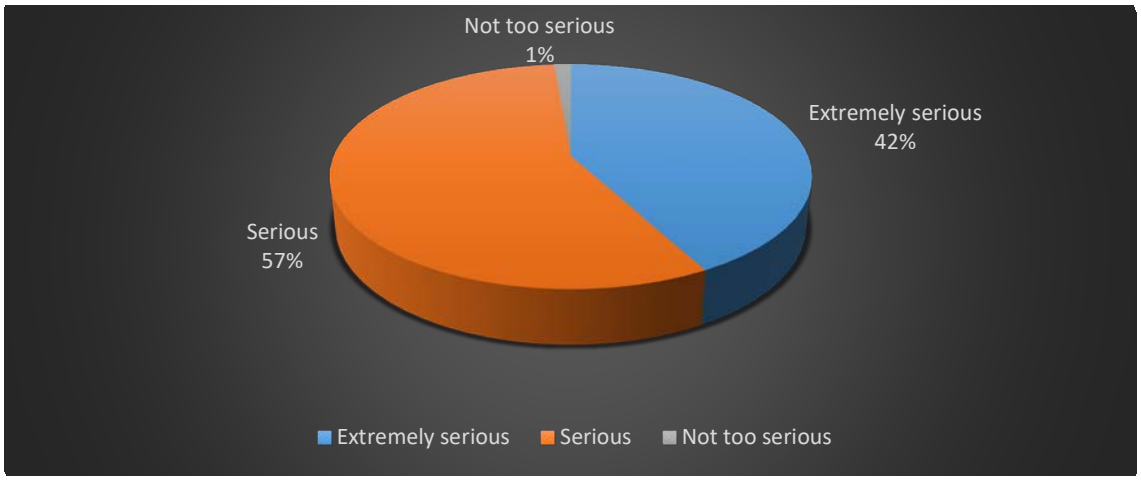

Figure 1. Perception of software vulnerability threat.

From the analysis illustrated in Figure 1, more than 90% of the surveyed population said they took software vulnerability threats either "serious" or "extremely serious". The implication of this outcome is that majority of the undergraduate developers are fully aware of the threat posed by software vulnerability and, therefore, take it as a severe threat to information systems.

Question 1(b): As a developer, which of these types of systems would give you the most security concerns? i) Web/online systems, ii) Mobile systems, iii) Desktop systems.

Understanding the threat posed by software vulnerability to information systems is one thing and knowing the implication of this threat to different information systems is another thing. Therefore, the second question highlighted the students' understanding of the information systems most at risk.

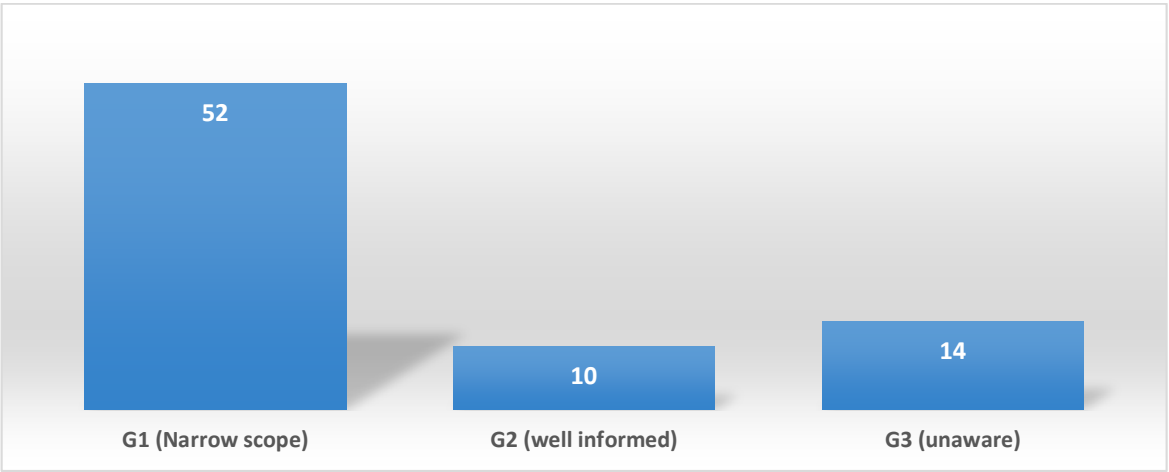

Figure 2. The Scope of information Vulnerability.

The responses to the second question provided an exciting perspective of the software security awareness of the respondents. This perspective evoked the categorization of the respondents into three groups (G1 – G3), as shown in Figure 2. G1 represents participants that only picked either Web/online systems or Mobile systems as a security concern. While the responses under the G1 category are not wrong, in the context of the study, such responses reflected a narrow scope of the software vulnerability landscape. On the contrary, participants who believed that both Web/online systems and Mobile systems post the most security concerns were labelled G2. This group was described as "well informed" because their view reflected an accurate understanding of the reality of software systems' vulnerability. Still, the other category of participants, labelled G3, captured responses that included Desktop systems. Such respondents were tagged "unaware" because desktop systems pose the most minimal security risk than the other systems listed in question 2.

The consequences of having a narrow scope of software security can equally potentially undermine information systems as being unaware. In this regard, it can be argued that it essentially makes no difference for a developer to have a narrow scope or be unaware of software security vulnerabilities. Therefore, when interpreted in this sense, Figure 2. above translate to Figure 3 below:

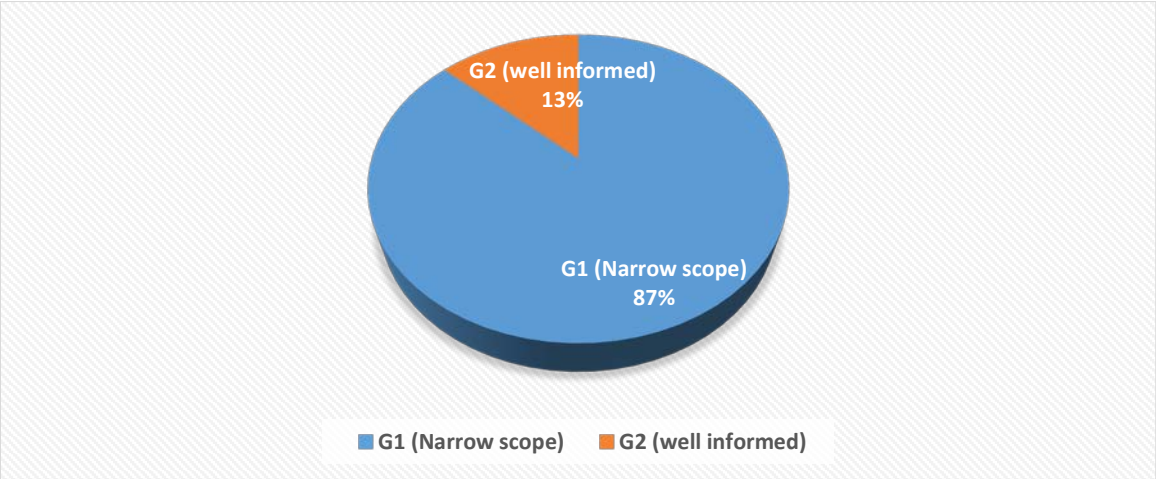

Figure 3. A translation of Figure 2.

From the illustration in Figure 3, it becomes striking to note that the result revealed a 74% gap between the developers who are well abreast of the scope of the software system's vulnerability and others who are still unaware. Only 13% of the sample demonstrated an adequate understanding of what software systems they, as future developers, must design with utmost security concerns.

Examining participants' knowledge of state-of-the-art industry standards for secure software development

The need for developers to be informed about the nature and scope of the threat of software vulnerability is hugely critical but being a future career developer requires more knowledge about existing standards for developing secured systems. Therefore, the study poses three sub-questions aimed at helping the study examine how participants are consciously aligning their undergraduate software development experiences and skills with professional standards.

Question 2(a): Do you know about any existing secure software development frameworks (SSDF)? This question tested the extent of the participants' familiarity with existing and most popular professional standards guiding secure software systems development. The outcome is as presented in Figure 4.

The results depicted in Figure 4 suggest that a significant number (42% of the sample) of undergraduate developers have either not theoretically or practically interacted with the fundamental frameworks of secure software development. This number is significant because it is only 16% less than the number of participants who reported that they knew about some existing frameworks for developing secure software.

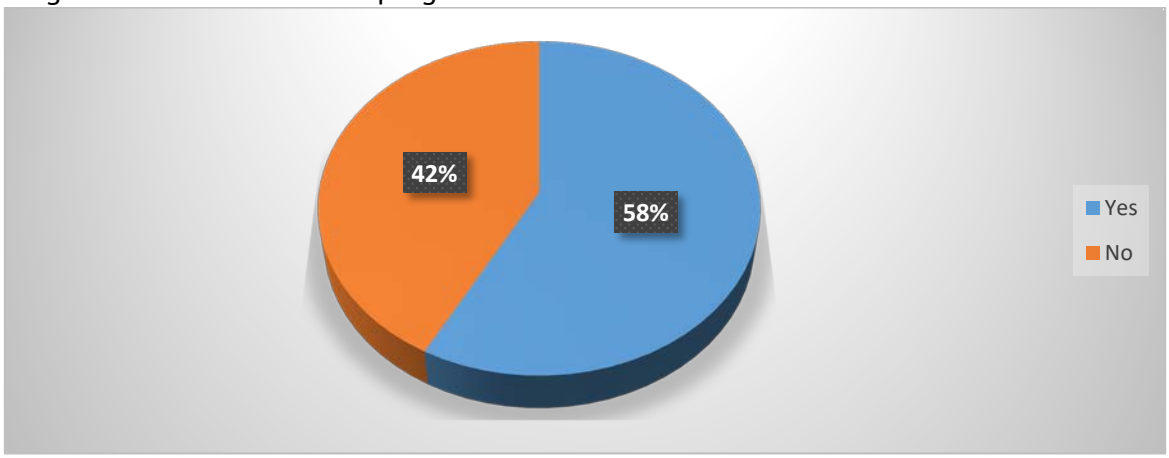

Figure 4. Familiarity with secure software development frameworks.

Question 2(b): If you answered "yes" to 3(a), then select all the frameworks that you have known from the list below and continue with 3(c): i) The Fundamental Secure Software Development Guide, ii) The Microsoft SDL, iii) The Integrated Security Development Framework (ISDF), iv) The OWASP's CLASP, v) Software Security TouchPoints.

With this question, the study validates the participants' knowledge depth. The findings enabled the researcher to understand whether the participants can demonstrate classroom knowledge leading to experiential or applicational knowledge (practical experience) or just classroom knowledge. This goal aligns with Kolb's learning framework, which argues that learning is only proven successful when the learners can try out whatever has learned (active experimentation) [19].

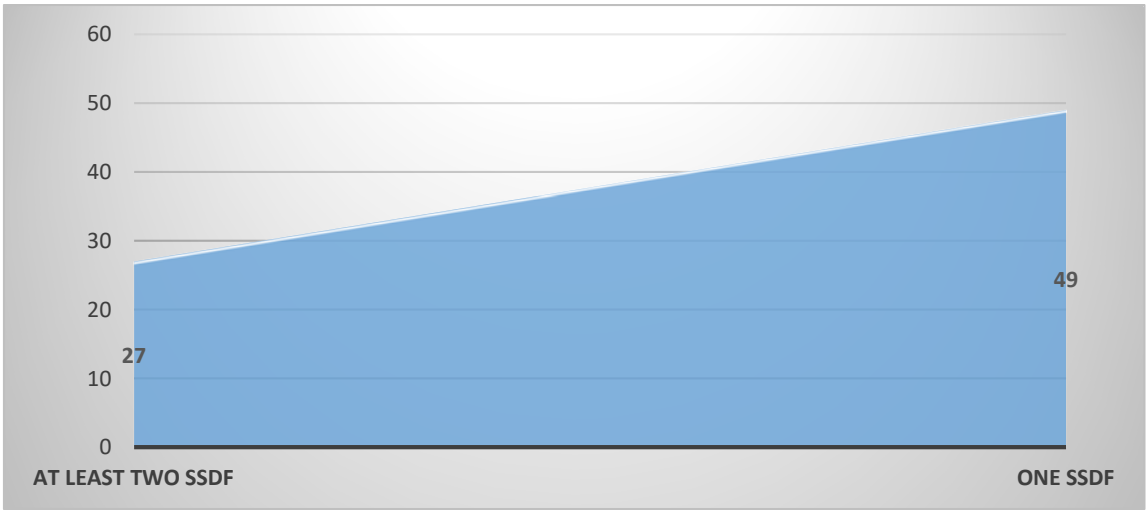

Figure 5. Extent of classroom knowledge about specific SSDFs.

As presented in Figure 5, the results show that fewer participants had a broad understanding of the existing SSDFs. For example, only 36% of the sampled developers know at least two existing SSDFs or have applied them. Whereas 49 participants, representing 64% of the sample, learned only one SSDF or had used it.

Question 2c: Choose the option below that best suits your knowledge of the framework(s) that you selected in 3b above: i) I have only learned about the framework(s), ii) I learned about the framework(s) and applied its outlined best practices.

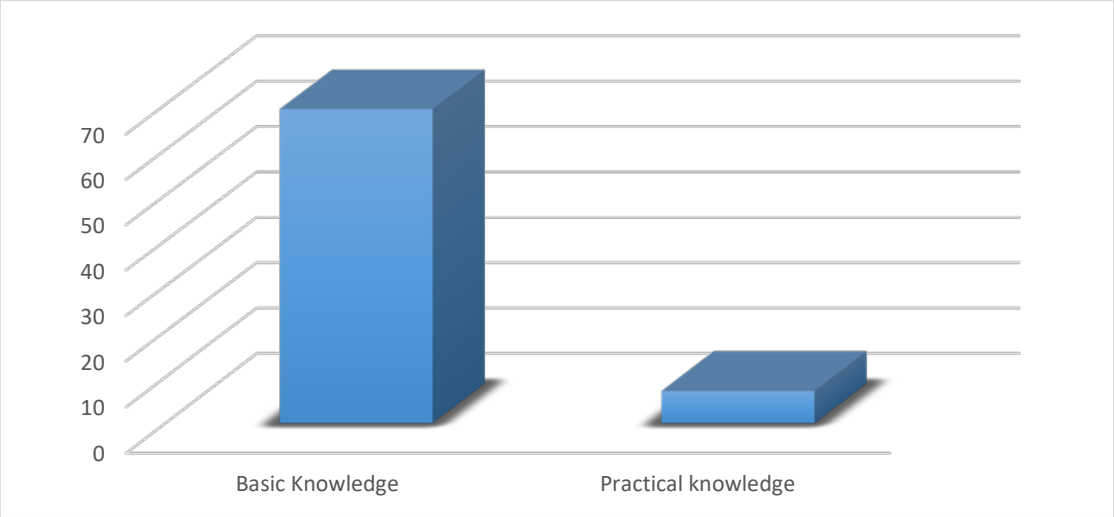

Figure 6. Applicational knowledge of specific SSDFs.

The results in Figure 5 show that 64% of the sample knew at least one SSDF or have applied it. However, as demonstrated in Figure 6, a further investigation revealed that 69 out of the 76 (91%) admitted that they had only learned about some of the SSDFs. But have not practically applied any of the SSDFs in their software development practice. This finding, therefore, suggests that just 9% of the sampled undergraduate developers have experiential knowledge of software development frameworks in context.

Attitude towards software systems security

Xie et al. [20] show a disconnect between developers' conceptual understanding of security and their attitudes regarding their responsibility and practices for software security". Consequently, the next question provided insight into whether the participant's attitude towards online and mobile platforms relates to the way they perceive and may likely handle software security as developers. This aim was achieved in this study by asking the following four questions:

Question 3(a): Choose all the online and mobile platforms (OMPs) that you often use from the list below: i) Facebook, ii) Twitter, iii) Instagram, iv) WhatsApp, v) Linkedln, vi) Email, vii) LMS.

With this question, the researcher sought to understand the participant's level of involvement in the use of various online and social media platforms. This question is motivated by the fact that these platforms constitute software systems' vulnerability tipping point.

From Figure 7, all the participants widely used online and mobile platforms. For instance, the results indicate that 62 of the 76 (83%) participants used at least three of the listed OMPs. And the remaining 18% of the sample used at least one but not more than three OMPs.

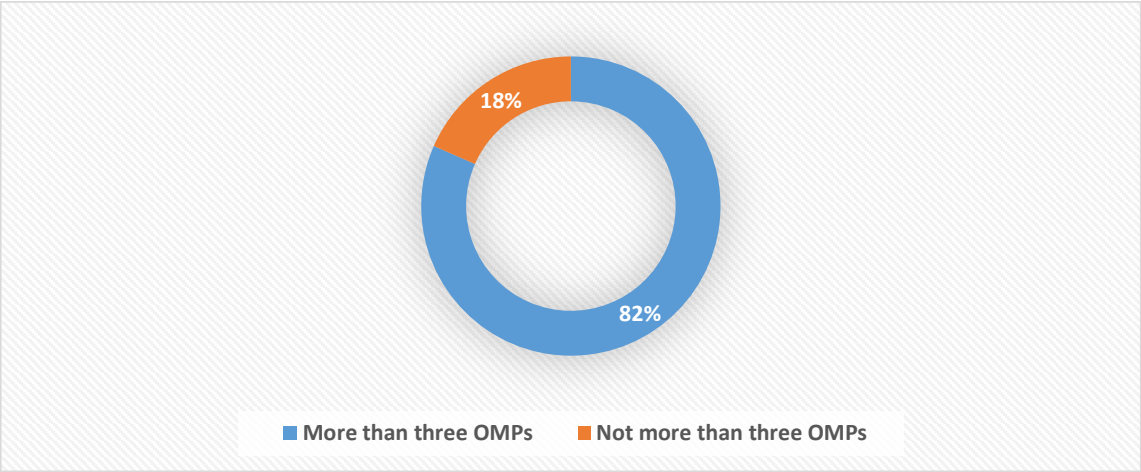

Figure 7. Perception about software security threat vs attitude toward software security – A.

Question 3(b): Indicate what you usually do when using social media and other online platforms? i) Use personal security settings (UPSS) ii) Use the same password across more than one platform (USPAP) iii) Share password (SP) iv) Use personal security settings, Use the same password across more than one platform (UPSS/SPAP).

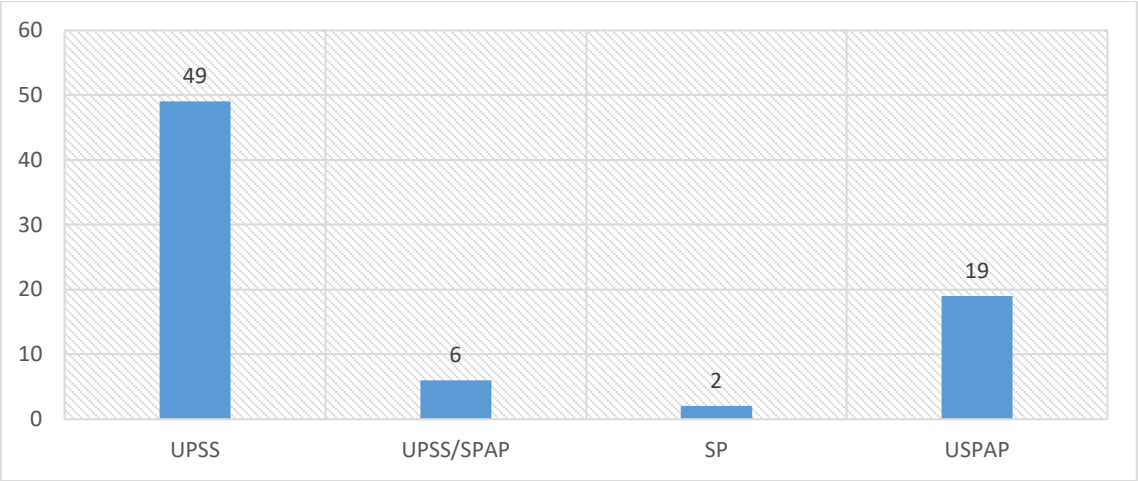

Figure 8. Personal responsibility when using OMPs – A.

Responses to question 3(b) above, as given in Figure 8, indicate that most participants showed an attitude of security consciousness. For instance, 54 out of the 76 participants used personal security settings, representing 72% of the sampled population. At a personal level, this approach shows that such participants often take personal responsibility to prevent software security breaches. On the contrary, the result also indicates that 21 participants do not use personal security settings. Instead, these participants indicated sharing their passwords or using the same password across different OMPs.

Based on the latter finding, further investigation became apparent. Therefore, as depicted in Figure 9, the outcome of Figure 8 was linked to the participants' earlier response to question 1(a).

As presented in Figure 9, the results suggest that the participant's attitude towards security on online and mobile platforms is influenced by their perception of the threat of software vulnerability. This claim substantially supports the above findings showing that all the participants who either took the threat of software security "serious" or "extremely serious" were found to use personal security settings.

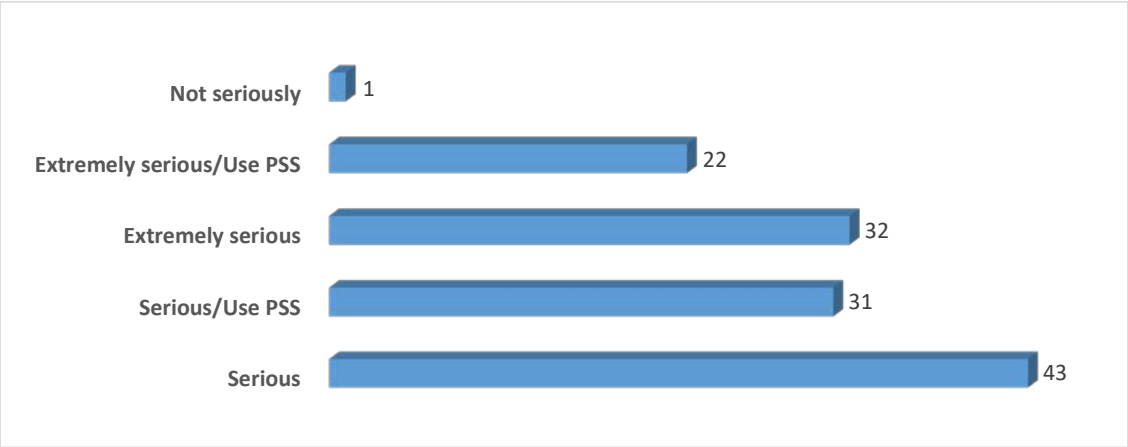

Figure 9. Perception about software security threat vs attitude toward software security – A.

Specifically, only 12 out of the 43 participants who took software security threats "serious" did not use personal security settings when using various OMPs. And only 10 out of 32 of those who took the threat "extremely serious" did not use personal security settings when using OMPs.

Question 3(c): When using social media platforms, do you change the security and privacy settings or change your passwords regularly? This question provided more information on how the participants explored existing software security features on OMPs. Such information further reveals participants' attitudes towards the threat of software vulnerability.

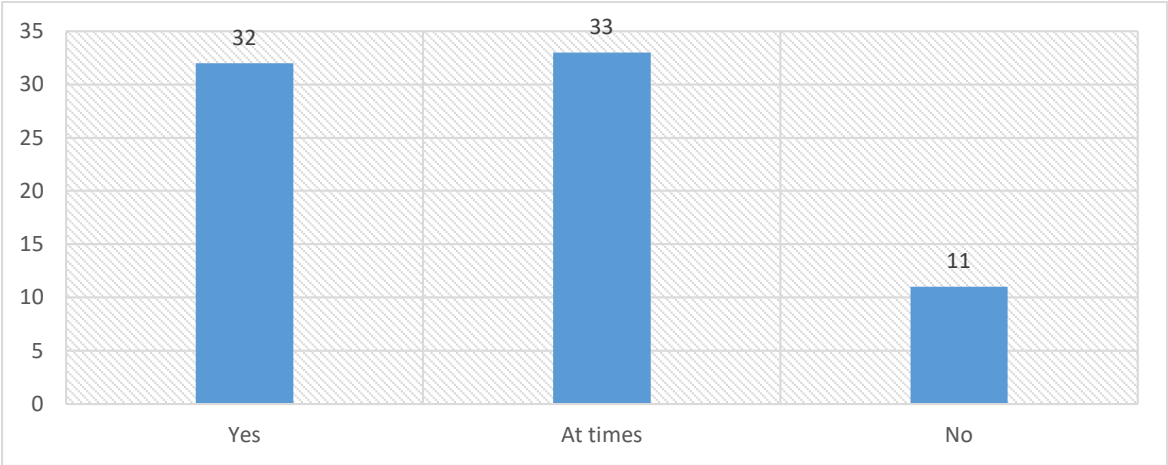

Figure 10. Personal responsibility when using OMPs – S.

As illustrated in Figure 10, the questions' responses show that most (65 out of 76, that is over 85%) of the respondents either change their passwords regularly or at times. When the results in Figure 10 were linked to the participants' earlier response to question 1(a), the outcome in Figure 11 the study further linked participants' attitude towards cyber security to how they perceived the threat of software vulnerability.

For example, as depicted in Figure 11, the findings suggest that out of 43 participants that claimed to take the threat of software security either "serious", 35 also admitted that they change their password regularly (20) or at times (15). Similarly, of the 32 participants that admitted to taking software security threats "extremely serious", 30 change their password at least sometimes.

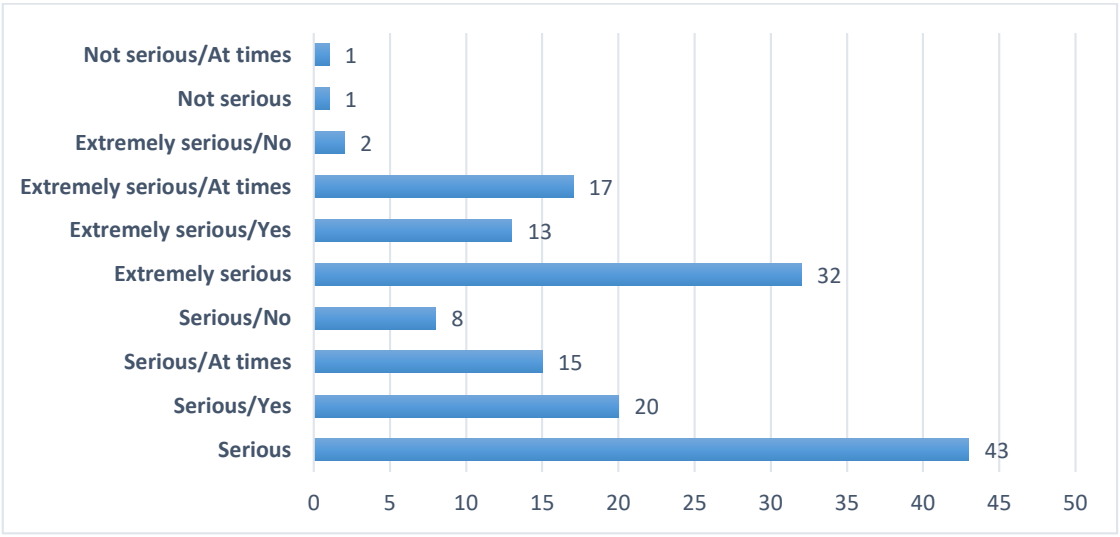

Figure 11. Perception about software security threat vs attitude toward software security – B.

Self-confidence in the knowledge of secure software development (SSD)

Another factor investigated in this study was the participants' confidence in the fundamentals and practices of secure software development. Therefore, in this question, the participants were required to assert their confidence level and provide a personal assessment of their current curriculum with regard to software security.

Question 4: Do you think you have sufficient knowledge in secure software development? If not, what do you think is lacking in your current curriculum?

The above question became imperative because this study sought to enhance the existing software development curriculum. Therefore, the data elicited from the question helped shape the study's contribution.

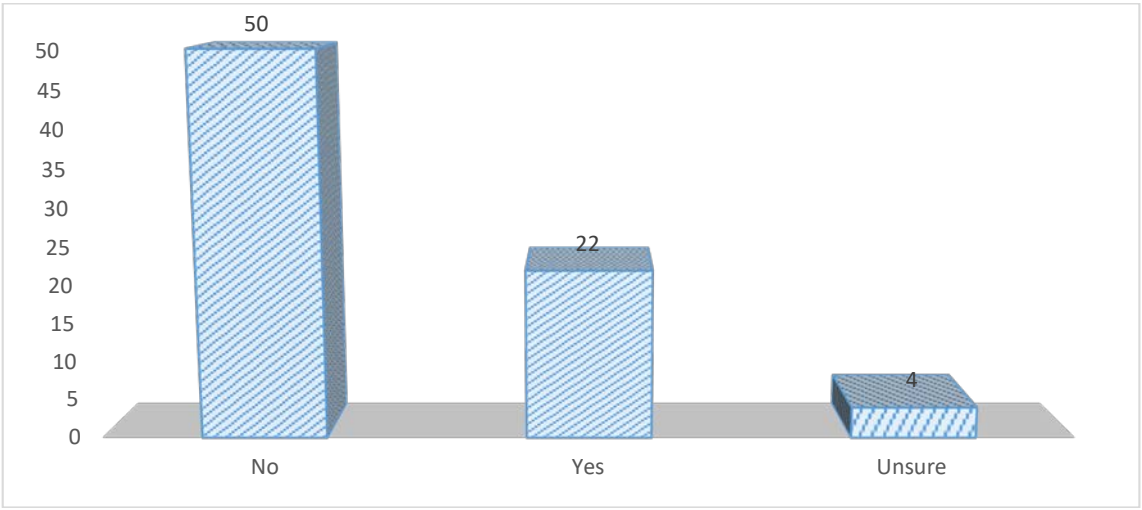

Figure 12. Self-confidence in the knowledge of SSD.

Although earlier findings, as shown in Figure 5, show that 64% of the participants knew at least one of the SSDF, the analysis in Figure 12 indicates that the majority of the respondent somewhat low confidence in their knowledge of SSD. For instance, concerning question 4 above, only 22 participants responded in the affirmative, while 50 participants admitted they had no confidence in their SSD knowledge.

The responses to the second part of question 4 helped capture the participants' expectations or verdict or their current curriculum, as illustrated in Figures. 13 and 14.

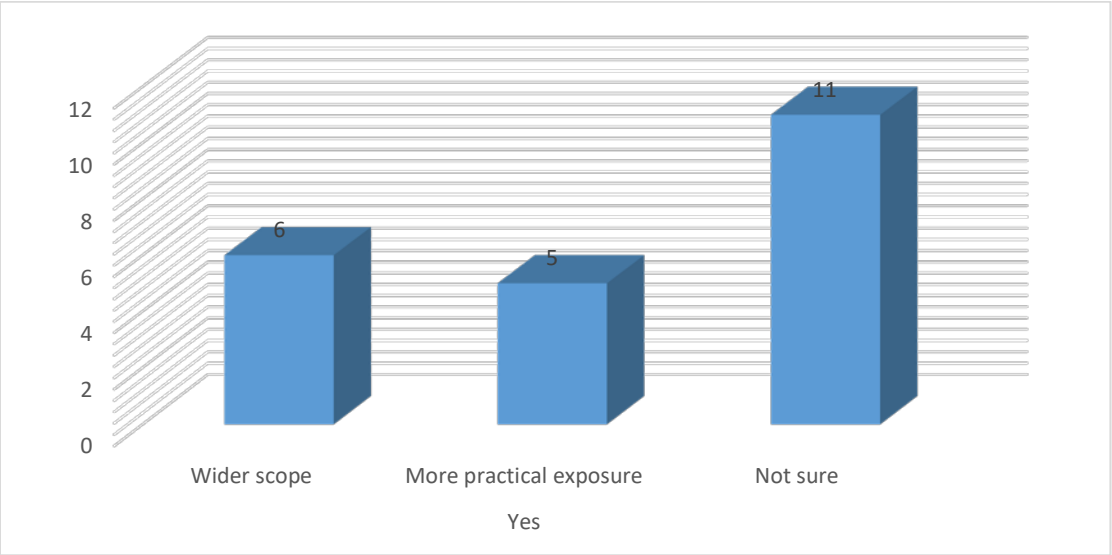

Figure 13. Personal assessment of software development curriculum A.

Figure 13 presents further analysis of the results in Figure 12. The first part of the analysis focused on the participants who answered "Yes" to the question: Do you think you have sufficient knowledge in secure software development? As illustrated in Figure 13, the result indicates that half the number of the participants who acknowledged the confidence in their SSD knowledge were unsure of what may be required to enhance the existing curriculum. But the rest of the participants either believed that extending the scope of the current curriculum on SSD or providing a platform or practical exposure can make a huge difference, as one of the participants stated:

"Yes, I can say I have the knowledge, but it is not much enough. When it comes to the topic of secure software development, we need to dive deeper and learn everything because they are very important."

Similarly, another participant admitted: "Yes, I do have knowledge on secure software development even though it is just basic knowledge. I don't really know a lot of detail in the concept, but I have knowledge."

Concerning the participant that responded "No" to the question in retrospect, Figure 14 demonstrates the findings. And the results suggest that 44, representing 88% of the participants, saw the need to enhance the existing SD curriculum.

In responding to what may be lacking in the current curriculum, 37 wants the curriculum to be expanded by explicitly adding a module on SSD. In that respect, the participants quoted below seemed most explicit and representative of the entire feedback.

Participant A: "No, Security has only been scratched on the surface, but we haven't really dived deep into it and implemented the necessary practices for secure systems outside the obvious sign in and login password."

Participant B: "No, I think we need a specific module or course that teaches practically secure software development".

Participant C: "No, because the technology industry is always evolving, so the knowledge that I have on security might be outdated. So, the curriculum must keep up with the times in terms of security updates as a developer."

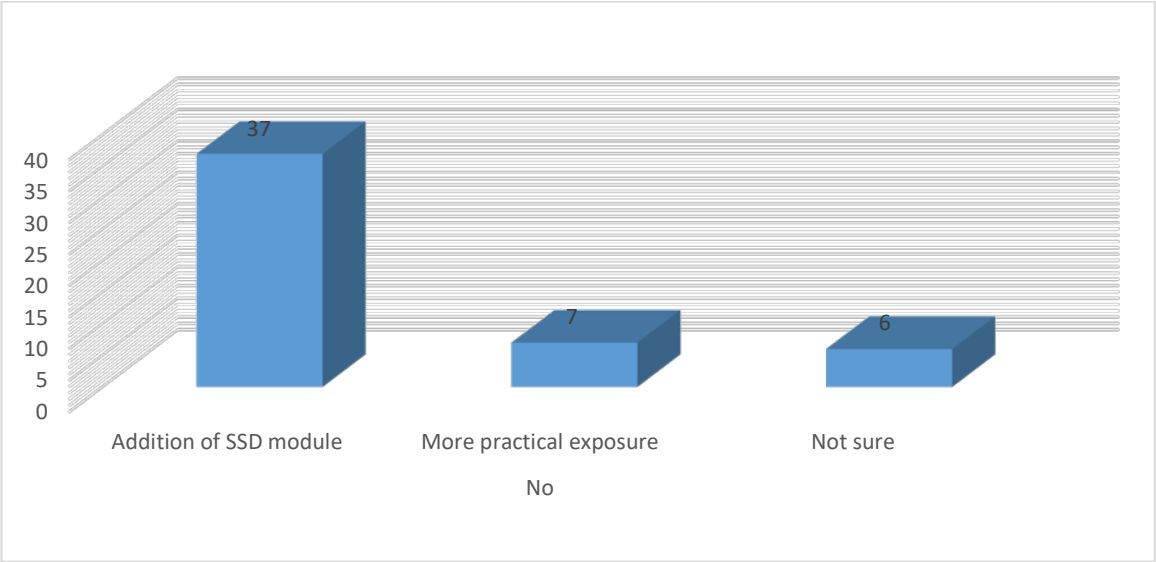

Figure 14. Personal assessment of software development curriculum 2.

On the contrary, though the remaining 7 participants admitted their SSD inadequacy, they opined that the current curriculum would serve them better if it offered them adequate provision for practical exposure.

Discussion and conclusion

This research attempted to understand undergraduate software developers' perception of software vulnerability threats and the developer's response to information system security. Essentially, the study explored the participants' knowledge of secure software development standards and principles and demonstrated how the developers' sense of personal responsibility in leading a professional attitude of software security consciousness impacts their perception of software security threats.

The study is motivated by the fact while the demand for software is rapidly growing, the risk of software vulnerabilities equally increases proportionately. Therefore, it has become pertinent to ensure that future career developers are adequately armed with the relevant knowledge and skills in secure software development.

Despite the study's relatively moderate sample (76), primarily due to employing a voluntary online survey, the key findings still offered valuable insights that informed the recommendations made.

An overview of and reflection on some key findings is as follows:

i. An overwhelming majority of over 90% of the surveyed undergraduate developers took the threat of software vulnerability either "serious" or "extremely serious". Nevertheless, subsequent results suggested that such a majority did not necessarily reflect the depth of their knowledge and experience in secure software development.

ii. Regarding the awareness software system's vulnerability, the gap between the well abreast undergraduate developers and the others who are still unaware constituted a striking 74% of the sample. The implication is that lack of adequate practical or simulated secure software development experience may undermine undergraduate developers' understanding of the software vulnerability threat.

iii. The participants' theoretical knowledge of secure software development framework was constrained by their lack of experiential knowledge, as 91% of the participants

admitted that they had only learned about some of the SSDFs but had not applied them.

iv. The participant's attitude towards security on online and mobile platforms was influenced by their perception of the threat of software vulnerability. Therefore, it can be argued that unless professional training or ethics override the developers' perception of software vulnerability threats, their handling of security in software development may be compromised.

v. A vast majority of the sampled undergraduate developers feel dissatisfied with the current software development curriculum. Of this majority, 74% advocate the addition of a module that would explicitly deal with secure software development, while 14% expressed the need for more practical exposure.

Centrally, the study's findings, as a contribution, echoed the need to redesign the undergraduate software development curriculum of South African universities of technology in a manner that would guarantee two things. First, to incorporate and facilitate the use of state-of-the-art platforms that can enable undergraduate developers to gain real-life exposure in software security programming. Second, formulate standard curricula review mechanism to ensure the curriculum evolves in alignment with current trends in the industry.

References

1. Alkussayer A, Allen WH. The ISDF Framework: Towards Secure Software Development. J Inf Process Syst. 2010, 6 (1) pp. 91-106.
2. Bafandeh Mayvan B, Rasoolzadegan A, Ghavidel Yazdi Z. The state of the art on design patterns: A systematic mapping of the literature. J Syst Softw. 2017, 125 pp. 1339-1351.
3. Baig ZA, Szewczyk P, Valli C, et al. Future challenges for smart cities: Cyber-security and digital forensics. Digit Investig. 2017, 22 pp. 3-13.
4. Bassey I, Afuro D, Munienge M. An Investigation of Software Engineering Knowledge of Undergraduate Students. Int J Mod Educ Comput Sci. 2015, 7 (12) pp. 42-50.
5. Biju S. Benefits of Working in Pairs in Problem Solving and Algorithms - Action Research. Athens J Educ. 2019, 6 (3) pp. 223-236.
6. Changsheng Y, Kaibin H, Hyukjin C. Energy Efficient Mobile Cloud Computing Powered by Wireless Energy Transfer - IEEE Journals & Magazine. Sci World J. 2016, 34 (5) pp. 1757-1771.
7. Davis N, Humphrey W, Redwine ST, Zibulski G, McGraw G. Processes for producing secure software: Summary of US national Cybersecurity Summit subgroup report. IEEE Secur Priv. 2004, 2 (3) pp. 18-25.
8. Faily S, Faily S. Usable and Secure Software Design: The State-of-the-Art. In: Designing Usable and Secure Software with IRIS and CAIRIS. Springer International Publishing, 2018 pp. 9-53.
9. Ghafur S, Grass E, Jennings NR, Darzi A. The challenges of cybersecurity in health care: the UK National Health Service as a case study. Lancet Digit Heal. 2019, 1 (1) pp. e10-e12.
10. Gunduz MZ, Das R. Analysis of cyber-attacks on smart grid applications. In: 2018 International Conference on Artificial Intelligence and Data Processing (IDAP). IEEE; 2018 pp. 1-5.
11. Heitzenrater C, Simpson A. A case for the economics of secure software development. In: ACM International Conference Proceeding Series. Vol 26-29-Sept. Association for Computing Machinery; 2016, pp. 92-105.
12. Isong B, Ifeoma O, Gasela N. On the integration of agile practices into teaching: An approach to overcoming teaching and learning challenges of programming. In: Proceedings - 2015 International Conference on Computational Science and Computational Intelligence, CSCI 2015. Institute of Electrical and Electronics Engineers Inc.; 2016 pp. 264-270.
13. Isong B. A Methodology for Teaching Computer Programming: first year students' perspective. Int J Mod Educ Comput Sci. 2014, 6 (9) pp. 15-21.
14. Luo C, Bo W, Kun H, Yuesheng L. Study on Software Vulnerability Characteristics and Its Identification Method. Math Probl Eng. 2020;2020.
15. Morris TH. Experiential learning – a systematic review and revision of Kolb's model. Interact Learn Environ. 2019, 28 (8) pp. 1064-1077.

16. Omar S, Frimpong T, J. B. Hayfron-Acquah. Information System Security Threats and Vulnerabilities: Evaluating the Human Factor in Data Protection. Int J Comput Appl. 2016, 143 (5) pp. 0975 – 8887.
17. Sharma M, Kaur S. Cyber Crimes Becoming Threat to Cyber Security. Acad J Forensic Sci. 2019, 2 (1) pp. 2581-4273.
18. Stergiou C, Psannis KE, Kim BG, Gupta B. Secure integration of IoT and Cloud Computing. Futur Gener Comput Syst. 2018, 78 pp. 964-975.
19. Vadra R. Knowledge Economy in BRICS: a Case of South Africa. J Knowl Econ. 2017, 8 (4) pp. 1229-1240.
20. Xie J, Lipford HR, Chu B. Why do programmers make security errors? In: Proceedings - 2011 IEEE Symposium on Visual Languages and Human Centric Computing, VL/HCC 2011, 2011 pp. 161-164. doi:10.1109.

Journal of Engineering Science *Vol. XXIX, no. 2 (2022), pp. 91 - 107*
Fascicle *Electronics and Computer Science* *ISSN 2587-3474*
Topic *Computers and Information Technology* *eISSN 2587-3482*

https://doi.org/10.52326/jes.utm.2022.29(2).09
UDC 004.8/.9:576

COMPUTER SYSTEMS SYNTHESIS INSPIRED FROM BIOLOGIC CELLS STRUCTURES

Silvia Munteanu*, ORCID: 0000-0003-0749-8457,
Viorica Sudacevschi, ORCID: 0000-0003-0125-3491,
Victor Ababii, ORCID: 0000-0002-0769-8144

Technical University of Moldova, 168 Ștefan cel Mare Blvd., Chișinău, Republic of Molodova
*Corresponding author: Silvia Munteanu, *silvia.munteanu@calc.utm.md*

Received: 02. 20. 2022
Accepted: 03. 25. 2022

Abstract. This paper deals with a synthesis method of membrane computer systems inspired from the biological cells structure. The functional concept of the computer system is based on the internal structure, chemical transformations and the way of interaction between living cells. Thus, the computer system is composed of a set of autonomous, homogeneous or heterogeneous computing cells, which communicate with each other in synchronous or asynchronous mode. The algorithmic complexity of the solved problem depends on the knowledge gained, the rules of data processing and the computer system topology. It is proposed the sequence of operations for the synthesis of membrane computer systems with implementation in reconfigurable FPGA architectures which includes: analysis of behavioural models of living organisms and their interpretation in artificial intelligence models; structure and functional description of the computing cell; cell modelling and performance evaluation using Petri nets; Van diagram of the membrane computer system topology; formal description of the membrane computer system topology by applying the JSON formatting language; validation, functional modelling and performance evaluation of the membrane computer system topology using Petri nets; Hardware Description Language (HDL) code of the cell from which the principle electrical diagram and the time diagrams are obtained; implementation of the computer system in the FPGA circuit.

Keywords: *computational topology, cognitive properties, evolutionary computing, FPGA, HDL, knowledge, membrane computing, nature-inspired computing, natural computing, P-Systems, Petri nets, swarm intelligence, JSON.*

Rezumat. În lucrare se propune o metodă de sinteză a sistemelor de calcul membranar inspirate din structura celulelor biologice. Conceptul funcțional al sistemului de calcul este bazat pe structura internă, transformările chimice și modul de interacțiune dintre celulele vii. Astfel, sistemul de calcul este compus dintr-o mulțime de celule de calcul autonome, omogene sau eterogene, care comunică între ele în regim sincron sau asincron. Complexitatea algoritmică a problemei soluționate depinde de cunoștințele acumulate, regulile de procesare a datelor și topologia sistemului de calcul. Este propusă secvența de

operații pentru sinteza sistemelor de calcul membranar cu implementare în arhitecturi reconfigurabile FPGA care include: analiza modelelor comportamentale ale organismelor vii și modele de interpretare a acestora în inteligența artificială; dezvoltarea structurii și descrierea funcțională a celulei de calcul; modelarea și evaluarea performanțelor celulei prin Rețele Petri; sinteza diagramei Van a topologiei sistemului de calcul membranar; descrierea formală a topologiei sistemului de calcul membranar prin aplicarea limbajului de formatare JSON; validarea, modelarea funcțională și evaluarea performanțelor topologiei sistemului de calcul membranar prin Rețele Petri; elaborarea codului de descriere hardware a celulei în baza căreia sunt obținute schema electrică de principiu și diagramele de timp; implementarea sistemului de calcul în circuitul FPGA.

Cuvinte cheie: *topologii de calcul, proprietăți cognitive, calcul evolutiv, FPGA, HDL, cunoștințe, calcul membranar, calcul inspirat din natură, calcul natural, P-Systems, rețele Petri, inteligență de grup, JSON.*

Introduction

The theory of evolution is the most important theory in biology. Evolution can add an extra dimension to a lot of aspects of natural history, give new sense to living facts and social change. Evolution means change, change in the form and behaviour of organisms between generations. The forms of organisms, at all levels from DNA sequences to macroscopic morphology and social behaviour, can change from those of ancestors during evolution. Adaptation is another crucial concept of the theory of evolution and refers to life design and those properties of living being that allow them to survive and reproduce in nature. Natural selection, also an important concept of evolution, means that some individuals in the population tend to contribute with more descendants to the next generation than others, being better adapted to the conditions of the environment in which they live [1, 2].

In 1998, academician Gheorghe Păun laid the foundations of a new field in computer science called membrane computing. Membrane computing is a branch of natural computing, being defined as a field of computer science with two major objectives: to be inspired by nature for the benefit of computer science - data bases, data operations, computer architectures, in the most general way - and vice versa, to provide new tools to those who study nature by other means, such as biologists or physicists. Natural calculus is a field that contains genetic algorithms, evolutionary calculus, with ideas from the genome area, neural algorithms. Computing inspired by the area of DNA - DNA Computing, also proposes a new hardware, the DNA molecule. Membrane computing aims to teach from the example of the cell and create cell-like systems by the help of mathematics and computer science [3].

Nature has served as a source of inspiration for many areas of the exact sciences, including computer science, artificial intelligence and related fields [4, 5]. Because most modern technological systems that have been and are being developed are extremely complex, distributed and interconnected, they depend on efficient communication, require high flexibility, adaptability and the ability to meet quality and performance requirements.

Carrying out a more detailed analysis of natural systems, we can see that they are usually characterized by a very high level of complexity. This complexity indicates that the behaviour of natural systems may be unpredictable and inaccurate, but at the same time living organisms and the ecosystems in which they are living have a substantial degree of survival. Examples of such resistant systems can be colonies of social organisms, nervous systems, etc. The survivability of the system is determined by a number of parameters: a large

number of objects in each system that can be replaced by others; free but flexible interconnections between objects; differences between objects in the system that allow flexible responses to a changing environment; the complex environment in which all components interact and produce various responses / actions [4]. Natural organisms have demonstrated by their existence the ability to cope with exceptional situations and to adapt to the environment through the ability to learn throughout life and by evolving over several generations [5].

It follows that natural systems have several properties that form the basis for many nature-inspired applications, namely dynamics, flexibility, robustness, self-organization, simplicity of basic objects and decentralization. Another important aspect of living organisms is that they always live in conditions of extreme competition. Therefore, they can be subject to actions that may partially or completely destroy the population, but in most cases they can be fully recovered. The ability to recover is determined by the presence of the immune system of individuals or interactions within and between populations. Resource limitation is one of the selection criteria that can ultimately lead to more efficient self-organization and recovery [1-3].

Underlying the definition of natural computation is the concept of P-System which is a computational model based on processes inspired by the behaviour and structure of biological cells. P-System is an abstraction model of computational processes by applying the interaction mode of chemicals and the cell membrane. This idea was first proposed by Gheorghe Păun in 1998 [6], which were later developed as a new branch of theoretical informatics [7, 8].

In the process of membrane computer systems (P-Systems) developing were designed some components that are functionally present in biological cells. The activity of a P-System can only be analysed in an environment that is the provider of input data and respectively the consumer of the results of their processing. Membranes are the main components of a P-Systems structure. A computational membrane is an autonomous functional logical unit that includes a set of objects, a set of rules, and / or a set of other membranes. The outer membrane that interacts with the environment is also called the "container membrane". A membrane may dissolve itself and in this case its contents migrate to the membrane to which it belongs or divide while retaining all or part of its properties [7, 8].

The functional logic of membrane computer systems is determined by a set of rules. A rule is validated for a lot of objects or input conditions that are applied, is consumed and produce a lot of objects or output conditions. In order to exclude internal competition, a rule may take precedence over other rules (dominant rules), so that priority computational models can be developed with priority in which less dominant rules (with low quality parameters) will be applied only in critical or exceptional conditions [9-11].

The algorithmic complexity of a P-System depends on the set of rules defined for each membrane and their topological structure. The main objective of applying membrane computation models is the optimal distribution of computational tasks in order to obtain a parallel computing process with maximum efficiency. Membrane computer systems with both asynchronous and synchronous processing can be defined [13, 14]. A topology of a P-System can be defined in the form of Ven diagram, tree or formal description [12].

Membrane computing models offer the possibility to formally and structurally describe computing and control systems of varying complexity, for example specialized logic structures and processors, reconfigurable computer systems, complex computing

architectures, which include functional elements with hierarchical interaction, parallel and concurrent computing architectures and network topologies for distributed computer systems.

Membrane computing cells being considered systems with artificial intelligence and cognitive properties implement as rules for data processing both mathematical and logical models, as well as models based on neural networks, Fuzzy logic and evolutionary computation.

The paper [15] presents a study of the interaction between membrane computation and Fuzzy logic theory. Theoretical research is focused on the processing of uncertainties in P-Systems, the fusion, representation and reasoning of unclear knowledge. Applications of Fuzzy-membrane computing focus on the representation of Fuzzy knowledge and the identification of its uncertainties.

Another example is described in paper [16] which examines the use of membrane computing models to control a group of mobile robots. The topics addressed in the paper are oriented towards the complexity of the robot and the tasks performed, the development of a genetic algorithm that uses a high level of abstraction, the design of swarm algorithms using a top-down approach with real-time operation.

P-Systems computing architectures represent a multitude of homogeneous or heterogeneous units for data processing. In the paper [17] it was shown that the synchronous interaction between them plays a decisive role, especially for real-time systems. The paper investigates synchronous membrane computer systems with communication and division rules, using the strategy of evolving parallelism together with the synchronization between uncooperative rewriting rules. As mentioned in the paper [18], in order to achieve maximum parallelism, a strategy for evolving the topology of the membrane computer system is used by applying synchronization between the applied rules. The most efficient are the membrane computer systems that operate in standby or event mode. The efficiency of the synchronization process is demonstrated by simulating the basic operations (addition, subtraction, multiplication, and division).

An essential factor in the evolution of membrane computer systems is their cognitive abilities. The paper [19] explored two methods of applying associative memory for knowledge storage. In the first method, associative memory is considered a device for memorizing the process of objects evolution, in which they are constantly updated to monitor the evolution and circumstances in which they were produced. This model allows the study of the evolution of the membrane. In the second method, associative memory is considered as a device for storing previously consumed objects. This model allows describing the dynamics of the object allocation process.

The field of use of membrane computer systems and models is very wide. The scientific papers for the last 20 years specify the advantages of applying membrane computation in such areas as image processing [20], biology, ecology, robotics or engineering [21, 22], decision-making systems [23, 24], collaborative systems and swarm intelligence [24, 25], reliable diagnostic systems [26], etc.

In this paper, the authors propose a new method for membrane computation models implementation in reconfigurable hardware architectures. In order to achieve the established objectives, were elaborated the algorithm for the synthesis of hardware membrane computer systems, the functional scheme of the data processing cell based on membrane computing models, the Petri net model for performance evaluation, the functional model for membrane

computing structures with complex topology, the model for the formal description of membrane computing structures with complex topology, the HDL code for cell implementation in hardware architecture. The validation of the obtained results is performed based on the diagrams generated as a result of the modelling and simulations of membrane computing cells implemented into FPGA circuits.

1. Algorithm for synthesis of membrane computer systems implemented in hardware architectures

The basis of proposed algorithm (Figure 1) for synthesis of the membrane computer systems implemented in hardware architectures is the multitude of knowledge gained from various fields of natural sciences (biology, genetics, natural intelligence, etc.) and exact sciences (physics, mathematics, artificial intelligence, engineering and computer science).

The synthesis of membrane computer systems implemented in hardware architectures includes the following steps:

Nature Inspired Computing - includes the analysis and mathematical and behavioural description of Swarm Computing models and the association of physiological and chemical processes performed in living cells with models and the formal description of computational processes for the implementation of membrane architecture in hardware architecture;

Artificial Intelligence - includes providing mathematical and logical models based on neural networks and Fuzzy logic to implement the knowledge and rules of data processing performed by the cell. At this stage, optimization models based on genetic algorithms can be applied, which will ensure the optimization of knowledge and data processing rules;

Cells Computing - based on the accumulated information and specifications for the membrane computing system, the synthesis of the cell structure scheme is performed. As a result of this stage, the cell architecture is obtained at the level of functional elements and data flows;

Cell: Petri Net Modelling - modelling and performance evaluation of the membrane computing cell through Petri nets [27, 28, 29]. At this stage, parallel and concurrent processes, resource access conflicts, and the efficiency of the rules synchronization model are identified. As a result of the performance analysis, graphs are generated that will highlight the strengths and weaknesses of the cell architecture;

Membrane Computing (P-Systems) - based on the mathematical model or formal description is developed the topology of the membrane computer system in the form of a Van diagram which specifies the set of rules made by each membrane and the relationships between them;

XML (JSON) - based on the Van diagram, a formal description of the topology of the membrane computer system is presented applying the XML (JSON) formatting language [30]. The result of this operation is a text file that describes the system topology, the inputs and outputs for each cell, and the identifiers of the cell hardware description files;

P-Systems: Petri Net Modelling - at this stage the performance modelling and evaluation of the membrane computer system through Petri nets is performed [31, 32, 33]. The purpose of these models is to optimize the synchronization process between the system cells and their rules. As a result of modelling, time graphs and diagrams are generated;

P-Systems: HDL - cell implementation (P-Systems) in hardware architecture based on HDL [34]. As a result of code compilation in the Intel Quatrus Prime 19.1 Design Software

[35] design tool, the wiring diagram, the files for the configuration of the FPGA circuit and the time diagrams of the membrane computer system are obtained;

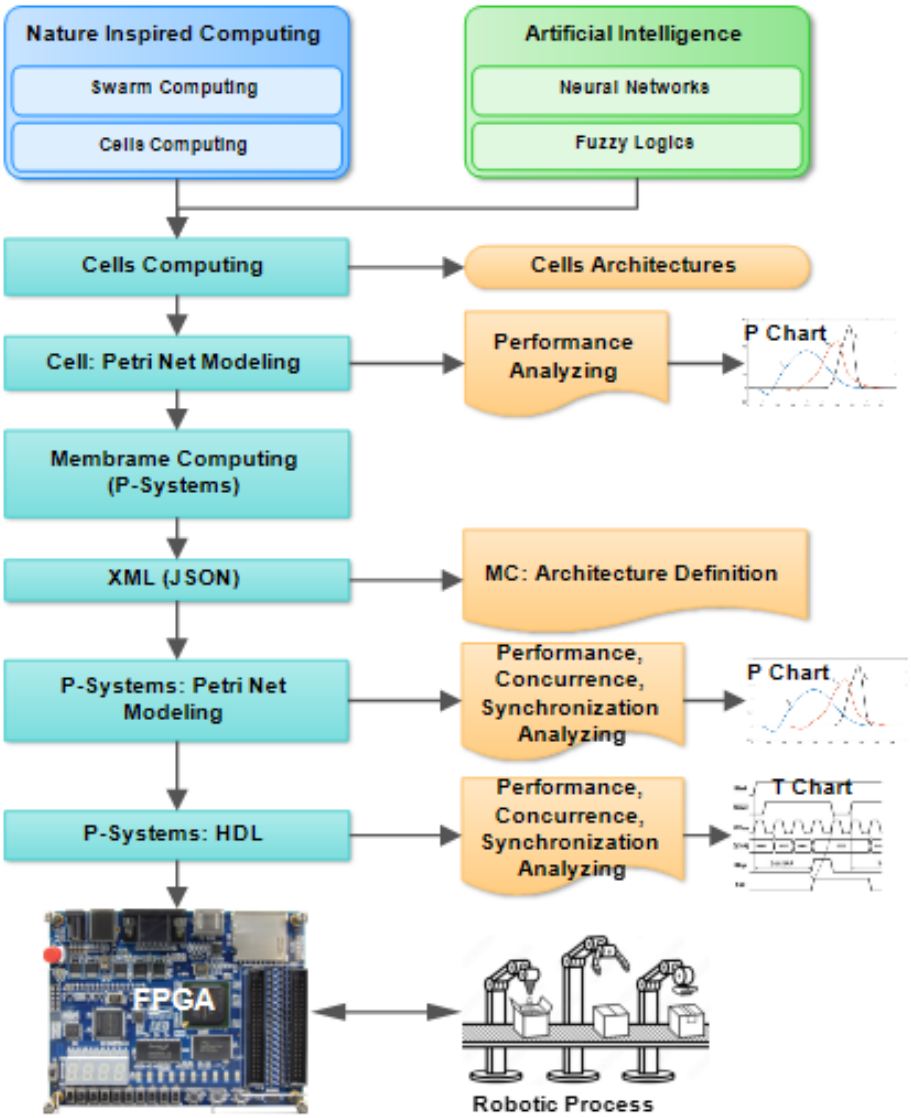

Figure 1. Algorithm for synthesis of membrane computer systems implemented in hardware architectures.

FPGA - loading the configuration code into the FPGA circuit [36] which is then used to control a robotic process which was used to formulate the specifications of the synthesis process of membrane computer systems.

2. Synthesis and modelling of computing cells

Computing cells represent a set of smart and autonomous elements for data processing. The data processing algorithm is determined by the set of rules obtained as a result of adapting the knowledge gained during the evolution of the cell. The interaction between the cells and the topological structure determines the algorithmic complexity of the membrane computing system. The synthesizing process of the computing cell structure requires the analysis of the chemical and physiological processes that take place in living cells and the tasks that are performed by it. A membrane computing system forms a collective intelligence (Swarm Intelligence) and can be composed of homogeneous or heterogeneous

computing cells. In the paper the synthesis of a general cell structure that can serve as a model for the synthesis of cells oriented towards certain specific fields of application is proposed.

The computing cell (Figure 2) consists of the following components:

Environment - the cell activity environment that delivers input data for the cell activity and reacts to the actions applied as a result of data processing;

$X(t)$ - input data or activity environment state;

Filtering (I) - the input data filtering mechanism that selects only certain data and allows them to enter into the cell to be processed;

Fuzzification – Fuzzy operations for input data that generate the set of events for processing;

Associative Memory (I) - associative memory for storing the list of input events;

$X[T]$ - the list of events waiting to be processed;

Knowledge - the set of knowledge that forms the rules of data processing;

$Op[T]$ - the set of elementary operations defined by the set of rules for data processing (events);

ALU - the block for performing arithmetic and logic operations according to the set, defined by the applied rule;

$Y[T]$ - list of events (decisions and actions) obtained as a result of data processing;

Associative Memory (O) - associative memory for storing the list of output events. After processing the input and output events they are removed from the lists;

Filtering (O) - the output data filtering mechanism that selects events to be moved at the output of the computing cell;

De-Fuzzification - turns the list of output events into action data or communication with the environment;

$Y(t)$ - action or communication data with the environment;

Synchronization - the synchronization block of the operations performed by the computing cell.

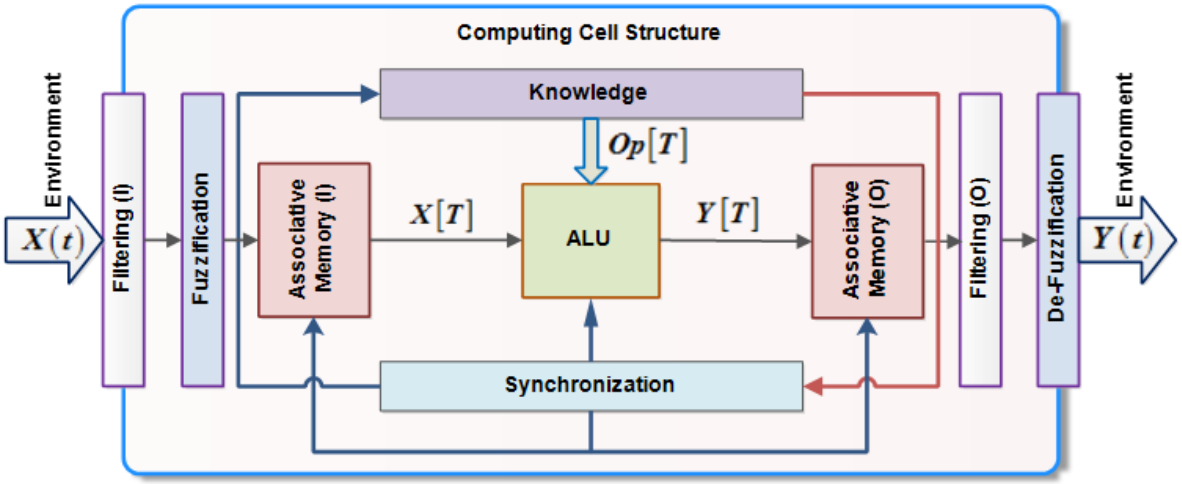

Figure 2. Computing Cell diagram.

Functional validation and performance evaluation of computing cells was performed based on the Petri net model shown in Figure 3. For this purpose, the following functions performed by the model cell were identified:

1. The cell receives from the activity *Environment* two state values $X(t)=\{x_1(t), x_2(t)\}$ modelled by timed transitions $\{t_1, t_2\}$;

2. The events $X_1[T]|x_1(t)\geq 4$ and $X_2[T]|x_2(t)\geq 6$ are identified by the *Fuzzification* which are modelled by transitions $\{t_3, t_4\}$ and arcs $\{p_1, t_3\}$ with weights 4 and 6, respectively;

3. *Associative Memory (I)* stores two values of events $X[T]=\{X_1[T], X_2[T]\}$ and is modelled by places $\{p_3, p_4\}$;

4. Places p_{12} and p_{13} monitors the waiting time to serve the events $X_1[T]|Time\ Delay(1)$ and $X_2[T]|Time\ Delay(2)$, being synchronized by timed transitions $\{t_{13}, t_{14}\}$;

5. The *ALU* block is modelled by place p_5 and synchronized by $\{t_5, p_8, t_7\}$ to serve the events $X_1[T]$, and respectively synchronized by $\{t_6, p_9, t_8\}$ to serve the events $X_2[T]$, where t_7 and t_8 are timed transitions;

6. The places p_{14} - *Event Processing (1)* and p_{15} - *Event Processing (2)* monitor the served events $X_1[T]$ and $X_2[T]$;

7. The places $\{p_6, p_7\}$ model the *Associative Memory (O)* in which two values of the output events are stored $Y[T]=\{Y_1[T], Y_2[T]\}$;

8. The *De-Fuzzification* block is modelled by combinations $\{p_{10}, t_{11}\}$ and $\{p_{11}, t_{12}\}$ which transforms the output events $Y_1[T]$ and $Y_2[T]$ into pulse sequences $y_1(t)|n=8$ and $y_2(t)|n=10$, where t_{11} and t_{12} there are timed transitions.

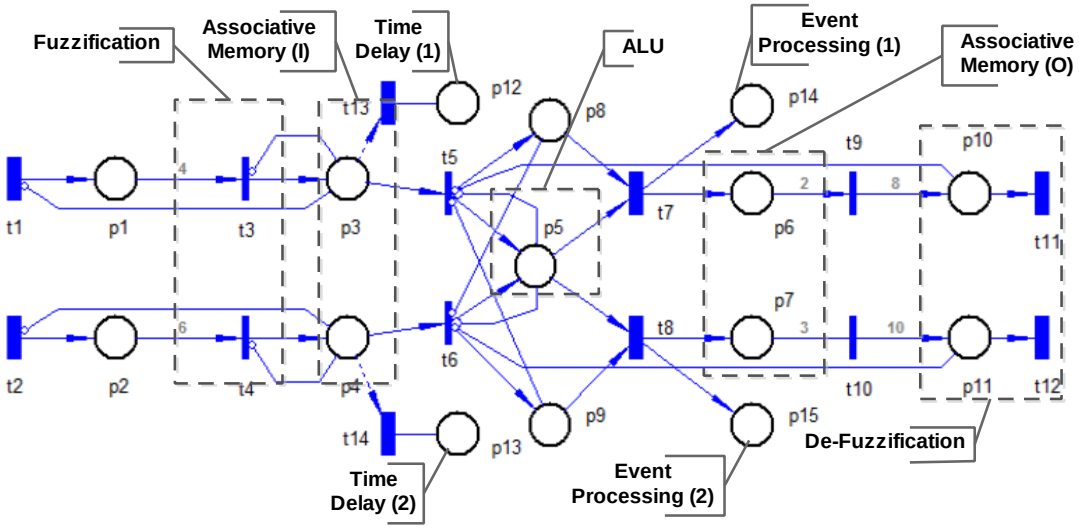

Figure 3. Petri Net model for Computing Cell validation and performance evaluation.

The VPNP application, developed at the Department of Computer Science and Systems Engineering by the university professor Emilian Guțuleac [37], was used for the functional validation and evaluation of the computing cell performance.

3. Synthesis and modelling of the membrane computing (P-Systems) architecture

As mentioned above, the synthesis of the membrane computing system topology (P-Systems) depends on the specific of the solved problem and its algorithmic complexity. The purpose of the synthesis is to obtain a computing architecture with maximum parallelism and minimal concurrency in data processing and resources accessing.

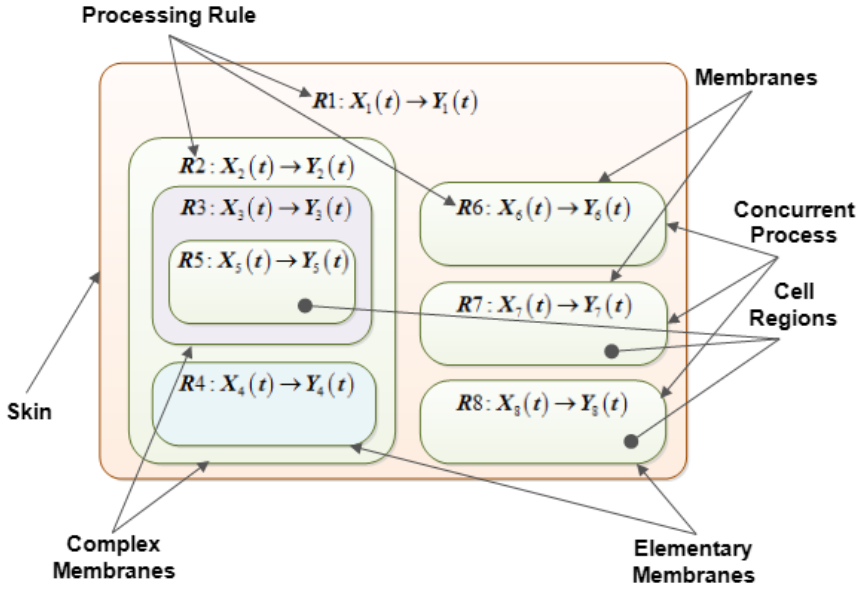

Figure 4. Membrane computing (P-Systems) architecture.

Figure 4 shows the synthesis result of a calculation membrane topology using Van diagram format that includes the following specifications:

1. The set of rules for data processing $R = \{R_1, R_2, ..., R_8\}$ that also determine the name of the calculation cell;
2. The set of elementary membranes $\{R_4, R_5, R_6, R_7, R_8\}$;
3. The set of complex membranes $\{R_1, R_2, R_3\}$;
4. Concurrent / parallel processes $\{R_2, R_6, R_7, R_8\}$ and $\{R_3, R_4\}$;
5. Sequential processes $\{R_1 : \{R_2 : \{R_3 : \{R_5\}, R_4\}, R_6, R_7, R_8\}\}$;

Skin external membrane that communicates with the business environment.

The Petri net model for validation and performance evaluation of the membrane computing architecture is presented in Figure 5.

The Petri net model includes the following elements:

1. The calculation cell R_1 modelled by the timed transition t_1 (generator of external events) and place p_1 (memory for the accumulation of events generated by the activity environment);

2. The set of computing cells $R_2 : \{t_2, p_2, t_6, p_6\}$, $R_6 : \{t_3, p_3, t_7, p_7\}$, $R_7 : \{t_4, p_4, t_8, p_8\}$ and $R_8 : \{t_5, p_5, t_9, p_9\}$, which operate in parallel / concurrently, where: $\{t_2, t_3, t_4, t_5\}$ are transitions

for validating event processing, $\{p_2, p_3, p_4, p_5\}$ are places for events modelling accepted for processing by that cell, $\{t_6, t_7, t_8, t_9\}$ are timed transitions that model the data processing time required for each calculation cell, $\{p_6, p_7, p_8, p_9\}$ are places that model the end of the data processing performed by the respective cell;

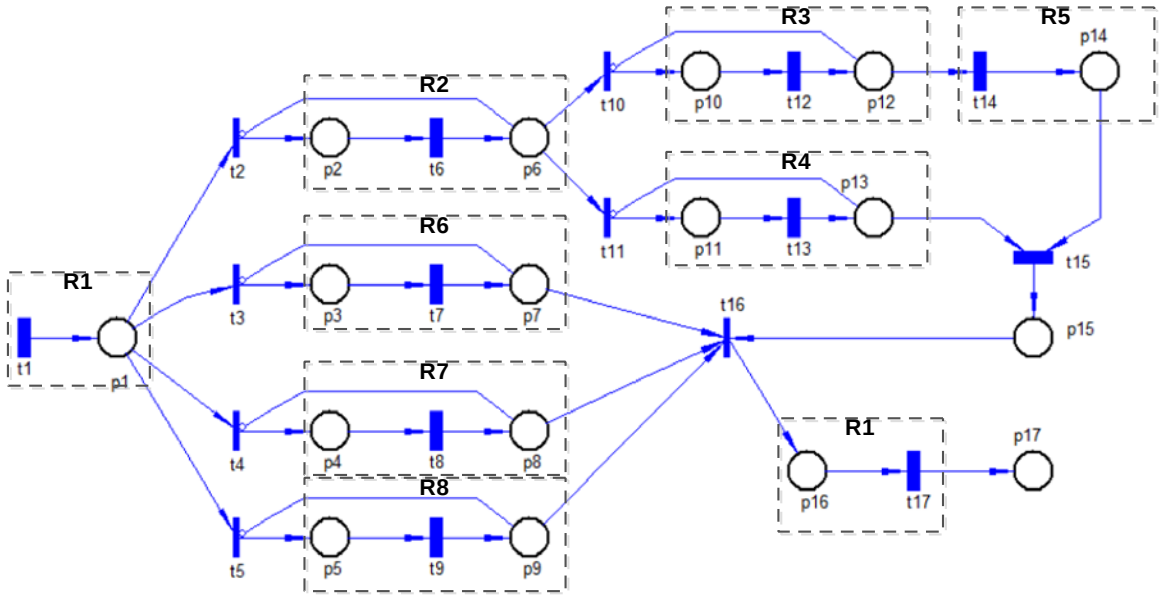

Figure 5. Modelling of membrane computing (P-Systems) architecture.

3. The set of computing cells $R_3 : \{t_{10}, p_{10}, t_{12}, p_{12}\}$ and $R_4 : \{t_{11}, p_{11}, t_{13}, p_{13}\}$, where: $\{t_{10}, t_{11}\}$ there are transitions that model the distribution of events to those cells, $\{p_{10}, p_{11}\}$ there are places that indicate that the cell is processing the data, $\{t_{12}, t_{13}\}$ there are timed transitions that model the data processing time by that cell, $\{p_{12}, p_{13}\}$ are places that model the end of data processing by that cell;

4. The cell $R_5 : \{t_{14}, p_{14}\}$ where t_{14} is a timed transition that models the data processing time and p_{14} is the place that models the end of the cell data processing;

5. Timed transition t_{15} and place p_{15} model the synchronization process between cells $\{R_3, R_4, R_5\}$;

6. The cell $R_1 : \{t_{16}, p_{16}, t_{17}\}$ model the action of the membrane computing architecture on the activity environment, where the place p_{17} indicates the number of processed events.

In order to achieve the circuit of the membrane computing system presented in the form of a Van diagram, it is proposed to use a formal description model in JSON format [30]. The purpose of these transformations is to gradually move from the Van diagram presentation of the membrane computing system to the HDL hardware description code. Figure 6 shows the result of this operation for the example analysed in Figure 4.

Description of the JSON code for membrane computing system formatting:

1. *"Membrane_Computing"* - the name of the main object that integrates the architecture of the membrane computing system in a logical structure;
2. *"Cell_Name"* - the name of the cell, obtained from the Van diagram that describes the topology of the membrane computing system;

```
{ // JSON model for Membrane Computer systems
// Synthesis Inspired from Biologic Cells Structures
"Membrane_Computing" : { // Cell_R1 definition
        "Cell_Name" : "Cell_R_1",
                "Cell_Type" : "Cell_Type_1",
        "Input" : {"Input_1" : "IValue_1"},
        "Output" : {"Output_1" : "OValue_1"},
        "Knowledge" : {
                "Data" : ["KData_1"],
                "Methods" : "e:/Cells_Device/R_1.inc"
        },
        "Cell_2" : { // Cell R2 definition
        "Cell_Name" : "Cell_R_2",
        "Cell_Type" : "Cell_Type_2",
        "Input" : {"Input_1" : "IValue_1"},
        "Output" : {"Output_1" : "OValue_1"},
        "Knowledge" : {
                "Data" : ["KData_2"],
                "Methods" : "e:/Cells_Device/R_2.inc"
        },
        "Cell_3" : { // Cell R3 definition
        "Cell_Name" : "Cell_R_3",
        "Cell_Type" : "Cell_Type_3",
        "Input" : {"Input_1" : "IValue_1"},
        "Output" : {"Output_1" : "OValue_1"},
        "Knowledge" : {
                "Data" : ["KData_3"],
                "Methods" : "e:/Cells_Device/R_3.inc"
                },
        "Cell_5" : { // Cell R5 definition
        "Cell_Name" : "Cell_R_5",
        "Cell_Type" : "Cell_Type_5",
        "Input" : {"Input_1" : "IValue_1"},
        "Output" : {"Output_1" : "OValue_1"},
        "Knowledge" : {
                "Data" : ["KData_5"],
                "Methods" : "e:/Cells_Device/R_5.inc"
                }}},
"Cell_4" : { // Cell R4 definition
        "Cell_Name" : "Cell_R_4",
        "Cell_Type" : "Cell_Type_4",
        "Input" : {"Input_1" : "IValue_1"},
        "Output" : {"Output_1" : "OValue_1"},
        "Knowledge" : {
                "Data" : ["KData_4"],
                "Methods" : "e:/Cells_Device/R_4.inc"
                }}},
        "Cell_6" : { // Cell R6 definition
        "Cell_Name" : "Cell_R_6",
        "Cell_Type" : "Cell_Type_6",
        "Input" : {"Input_1" : "IValue_1"},
        "Output" : {"Output_1" : "OValue_1"},
        "Knowledge" : {
                "Data" : ["KData_6"],
                "Methods" : "e:/Cells_Device/R_6.inc"
        }},
        "Cell_7" : { // Cell R6 definition
        "Cell_Name" : "Cell_R_7",
        "Cell_Type" : "Cell_Type_7",
        "Input" : {"Input_1" : "IValue_1"},
        "Output" : {"Output_1" : "OValue_1"},
        "Knowledge" : {
                "Data" : ["KData_7"],
                "Methods" : "e:/Cells_Device/R_7.inc"
        }},
        "Cell_8" : { // Cell R6 definition
        "Cell_Name" : "Cell_R_8",
        "Cell_Type" : "Cell_Type_8",
        "Input" : {"Input_1" : "IValue_1"},
        "Output" : {"Output_1" : "OValue_1"},
        "Knowledge" : {
                "Data" : ["KData_8"],
                "Methods" : "e:/Cells_Device/R_8.inc"
        }}}}
```

Figure 6. JSON format for membrane computing architecture description.

3. *"Cell_Type"* - the type of cell that represents a specification of it (ordinary, complex, etc.);
4. *"Input"* – specification of the input variables for the respective cell;
5. *"Output"* - specification of the output variables for the respective cell;
6. *"Knowledge"* - the specifications of the object for the description of the knowledge that will present the rules of data processing;
7. *"Date"* - the list of knowledge set for the initial state of the cell;
8. *"Methods"* - the name of the file and the path to it for implementing the rules of data processing.

4. HDL synthesis of membrane computing architecture

As an example for the synthesis of a membrane computing architecture using HDL code, it is proposed to design a computing cell with input variable $X\ (t)$ and output variable $Y(t)$, where:

$$X\ (t) = \left\{ X_1[T] \in \{0000,...,0111\}, X_2[T] \in \{1000,...,1111\} \right\},$$

$$\forall X_1[T]: Op[T] \to Y_1[T] \text{ and } \forall X_2[T]: Op[T] \to Y_2[T].$$

As a result of the application of the broadcasting operations, the transformations $Y_1[T] \rightarrow Y_1(t)$ and $Y_2[T] \rightarrow Y_2(t)$ will take place, where $Y_1(t)$ and $Y_2(t)$ are the sequence of synchronization signals with a number proportional to the respective variables $X_1[T]$ and $X_2[T]$. The HDL description code of the computing cells is shown in Figure 7.

```
SUBDESIGN Celula
(
        clk, load, ena, clr, fuzzy[3..0]   : INPUT;
        yt1, yt2, q_yt1[3..0], q_yt2[3..0]          : OUTPUT;
)
VARIABLE
        xt1, xt2                    :       NODE;
        z_yt1, z_yt2        :               NODE;
        count_yt1[3..0]     :               DFF;
        count_yt2[3..0]     :               DFF;
BEGIN
                TABLE               -- Fuzificztion
                        fuzzy[3..0]                 =>      xt1,            xt2;
                                B"0XXX"             =>      1,              0;
                                B"1XXX"             =>      0,              1;
                END TABLE;
                        count_yt1[].clk = clk;
                        count_yt1[].clrn = !clr;
                        count_yt2[].clk = clk;
                        count_yt2[].clrn = !clr;
        -- Function 1
                        IF      (xt1 & load) THEN
                                        count_yt1[].d = fuzzy[];
                        ELSIF ((count_yt1[3].q # count_yt1[2].q # count_yt1[1].q # count_yt1[0].q) & ena) THEN
                                count_yt1[].d = count_yt1[].q - 1;
                        ELSE
                                count_yt1[].d = count_yt1[].q;
                        END IF;
                        yt1 = count_yt1[0].q;
                        q_yt1[] = count_yt1[].q;
        -- Function 2
                        IF      (xt2 & load) THEN
                                count_yt2[].d = fuzzy[];
                        ELSIF ((count_yt2[3].q # count_yt2[2].q # count_yt2[1].q # count_yt2[0].q) & ena) THEN
                                count_yt2[].d = count_yt2[].q - 1;
                        ELSE
                                count_yt2[].d = count_yt2[].q;
                        END IF;
                        yt2 = count_yt2[0].q;
                        q_yt2[] = count_yt2[].q;
END;
```

Figure 7. The HDL code of Cell.

Figure 8 shows the logic diagram of the cell obtained as a result of compiling the HDL code using the Intel Quatrus Prime 19.1 development environment.

Figure 9 shows the graphical symbol of the cell with the input and output signals of the cell obtained as a result of HDL code compilation in the Intel Quatrus Prime 19.1 development environment.

Specification of the input signals (Figure 8 and 9):

1. *clk* - clock signal synchronizes the data processing;
2. *load* - loading data into the associative input memory of the cell;
3. *ena* - validation of data processing;
4. *clr* - deleting data from associative memory;
5. *fuzzy [3..0]* - the binary code of the input data.

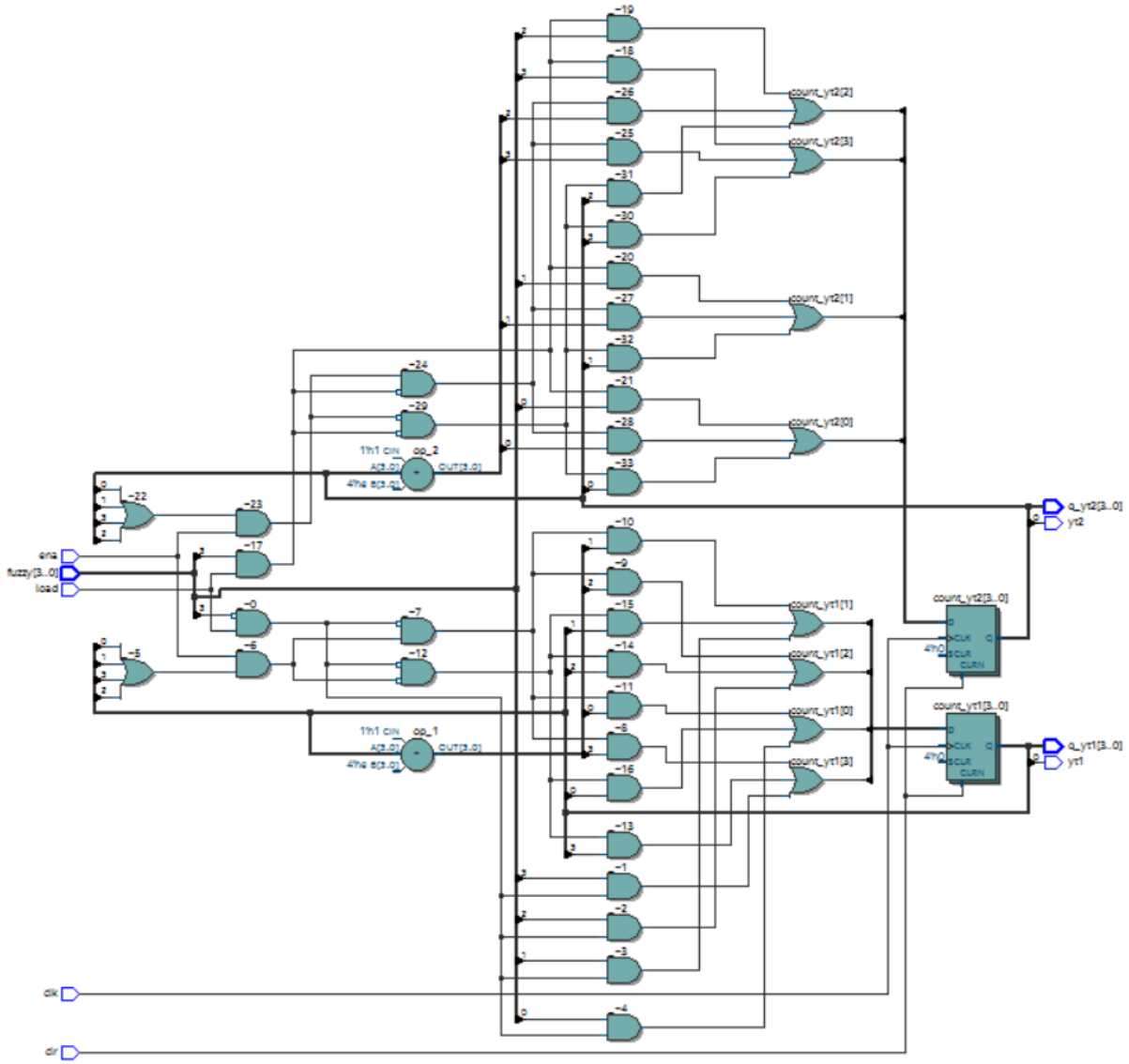

Figure 8. The logic circuit obtained from HDL code.

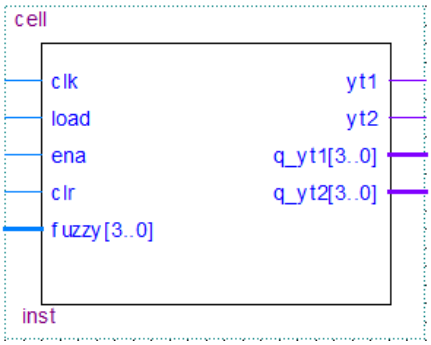

Figure 9. The Cell symbol.

Specification of the output signals (Figure 8 and 9):

1. *yt1* - pulse sequence;
2. *yt2* - pulse sequence;
3. q_*yt1 [3..0]* - the binary code from the associative output memory;
4. *q_yt2 [3..0]* - the binary code from the associative output memory.

The values of the variables *fuzzy [3..0]*, *q_yt1 [3..0]* and *q_yt2 [3..0]* are used to interconnect the cells according to the JSON file format.

The result of the functional validation of the computing cell, in the form of time diagram, is shown in Figure 10.

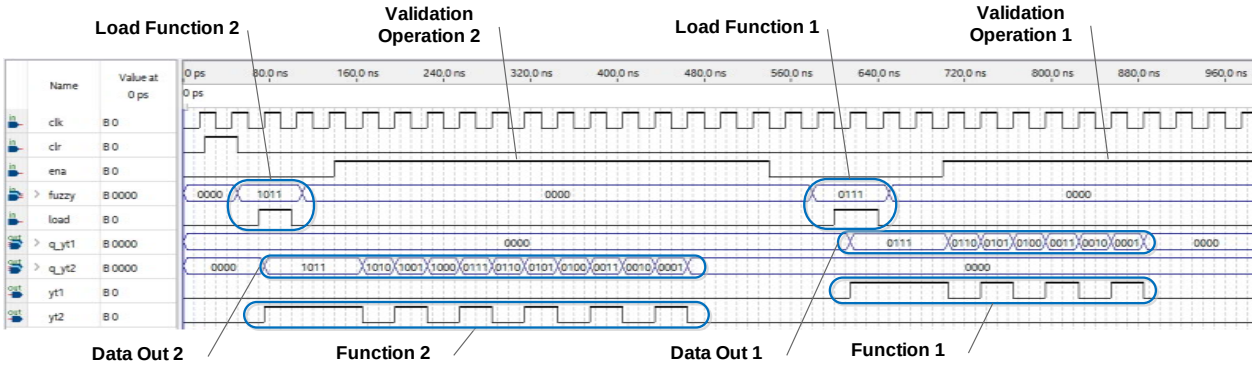

Figure 10. The Time diagram.

Specification of the signals grouped by function:

1. *Load Function 2* - uploading data for the function according to the condition $X(t) = X_2[T] \in \{1000,...,1111\}$;
2. *Data Out 2* - binary code output data $Y_2[T]$;
3. *Function 2* - pulse sequence $Y_2(t)$;
4. *Load Function 1* - uploading data for function according to the condition $X\ (t) = X_1[T] \in \{0000,...,0111\}$;
5. *Data Out 1* - binary code output data $Y_1[T]$;
6. *Function 1* - pulse sequence $Y_2(t)$.

5. Functional testing of membrane computing cells implemented in HDL models

Functional testing of membrane computing cells implemented in HDL models was performed based on the Altera DE0 Board kit [38].

This development kit is equipped with an Altera Cyclone III 3C16 FPGA circuit that provides the user (designer) with 15,408 LEs and 346 Input / Output pins, enough to test the example proposed in the paper.

Figure 11 shows the functional structure of the stand for testing membrane computing models that includes: a personal computer with *Intel Quartus Prime* development environment installed and the USB cable for connecting the Altera *DE0 Board* kit.

The development kit highlights the areas used in the process of functional testing of membrane computing models: *Binary Switches x 10* - used to enter the input code (variable values $X[T]$); *Binary LEDs x 10* - for displaying in binary code the result of processing the data performed by the cell (variable values $Y[T]$); *4x7-Segment Display* - for displaying the result of data processing in decimal or hexadecimal code; *Extension Headers* - for connecting external input devices and assistive or action devices.

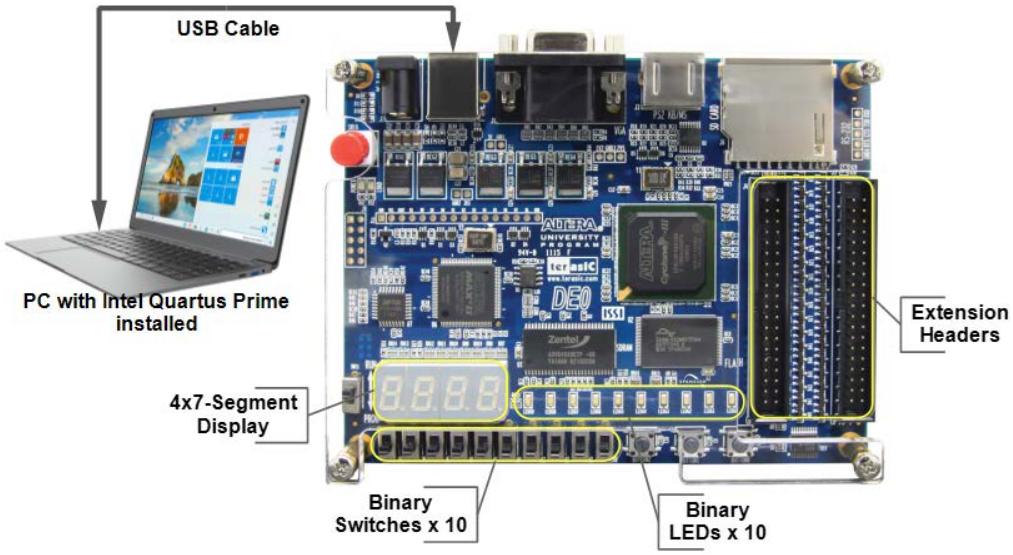

Figure 11. Functional structure of stand for testing of membrane computing models.

Acknowledgments: The results obtained in this paper are part of the research conducted under the PhD topic *"Distributed computational structures based on intelligent algorithms with cognitive properties"*.

Conclusion

The paper describes an application proposed by the authors for the design and implementation of membrane computing systems based on FPGA reconfigurable devices. The synthesis algorithm of membrane computing systems includes a sequence of activities involving knowledge in the fields of biology, nature-inspired computing, artificial intelligence, system modelling, formatting languages, hardware description languages, and systems design based on FPGA reconfigurable devices. The operating model of the computer system is inspired by the functioning and interaction of living cells.

The synthesis process includes the following steps: development of the cell structure diagram for data processing; modelling and evaluating the performance of computing cells and the topology of the membrane computing system through Petri nets; elaboration of the Van diagram for the membrane computing system; formal description of the membrane computation model based on the JSON formatting language; development of the hardware description code of the cells for data processing and implementation of the cells in reconfigurable FPGA computing architectures.

For the future, the development of membrane computing systems for the control of a mobile robot and a robotic arm is planned. The objectives of the research are aimed to highlight the possibilities of performing operations in parallel, the use of methods of synchronization and control of concurrency inside the cells and at the level of topology of the membrane computing system.

References

1. Ridley M. *Evolution*. Third edition, Blackwell, 2004, 751p. ISBN: 1-4051-0345-0.
2. Futuiama D.J. *Evolution*. Third edition, Sinauser Associates, 2013, 655p.
3. Păun G., Rozenberg G., Salomaa A. *DNA Computing: New Computing Paradigm*. Texts in Theoretical Computer Science (An EATCS Series). Springer, Berlin, Heidelberg. 1998, 409p. ISBN: 978-3-540-64196-4.
4. Siddique N., Adeli H. Nature Inspired Computing: An Overview and Some Future Directions. *Cognitive Computing*, 2015, 7: 706-714. DOI: 10.1007/s12559-015-9370-8.

5. De CASTRO, L.N. Fundamentals of natural computing: an overview. *Phys Life Rev.* 2007; 4: 1–36. DOI: 10.1016/j.plrev.2006.10.002.
6. Păun Gh. *Computing with Membranes*. TUCS Report 208. Turku Centre for Computer Science. 1998. ISBN: 978-952-12-0303-9.
7. Păun Gh., Rozenberg G. A guide to membrane computing. *Theoretical Computer Science*. 287 (1): 73-100, 2002. DOI: 10.1016/S0304-3975(02)00136-6. ISSN: 0304-3975.
8. Păun Gh. Introduction to Membrane Computing. *Applications of Membrane Computing*. Springer Berlin Heidelberg. pp. 1-42. ISBN: 978-3-540-29937-0.
9. Alhazov A. *Communication in Membrane Systems with Symbol Objects*. Ph.D. Thesis. Tarragona, Spain: Universitat Rovira i Virgili, 2006, 218p.
10. Alhazov A. Small Abstract Computers. Habilitation Thesis. Chișinău (RM): Academy of Sciences of Moldova, 2013, 255p.
11. Aman B., Ciobanu G. Membrane Systems with Surface Objects. In: *Proceedings of the International Workshop on Computing with Biomolecules*, Wien, Austria, August 27th, 2008, pp. 17-28.
12. Giovitto J.-L., Michel O. *The Topological Structures of Membrane Computing*. LaMI technical report Nr. 70-2001. November 2001, France.
13. Dinneen M. J., Kim Y.-B. and Nicolescu R. Synchronization in P Modules. In: *Unconventional Computation, volume 6079 of Lecture Notes in Computer Science,* Springer-Verlag, Berlin Heidelberg, 2010, pp. 32–44.
14. Dinneen M. J., Kim Y.-B. and Nicolescu R. An Adaptive Algorithm for P System Synchronization. In: *Proceedings of the Twelfth International Workshop on Membrane Computing, (CMC11),* Fontainebleau/Paris, France, 2011, pp. 1–26.
15. Wang T., Zhang G., Perez-Jimenez M.J. Fuzzy Membrane Computing: Theory and Applications. *International Journal of Computers Communications & Control,* 2015, Vol. 10(6), pp. 144, DOI: 10.15837/ijccc.2015.6.2080.
16. A Generic Guide for Using Membrane Computing in Robot Control. *Advances in Computational Intelligence and Robots – Membrane Computing for Distributed Control of Robotic Swarms,* 2017, pp.86-96. DOI: 10.4018/978-1-5225-2280-5.ch005.
17. Aman B. On the Efficiency of Synchronized P-Systems. *Journal of Membrane Computing,* 2022, Springer, ISSN: 2523-8914, DOI: 10.1007/s41965-021-00091-1.
18. Aman B., Ciobanu G. Synchronization of Rules in Membrane Computing. *Journal of Membrane Computing*, 1, 233-240, 2019, ISSN: 2523-8914, DOI: 10.1007/s41965-019-00022-1.
19. Ciobanu G., Pinna G.M. Memory Associated with Membranes Systems. *Journal of Membrane Computing*, 3, 116-132, 2021, ISSN: 2523-8914, DOI: 10.1007/s41965-020-00066-8.
20. Diaz-Pernil D., Gutierrez-Maranjo M.A., Peng H. Membrane computing and Image Processing: a Short Survey. *Journal of Membrane Computing*, 1(1), pp. 58-73, 2019, ISSN: 2523-8914, DOI: 10.1007/s41965-018-00002-x.
21. Sanchez-Karhunen E., Valencia-Cabrera L. Modelling Complex Market Interaction using PDP Systems. *Journal of Membrane Computing*, 1(1), pp. 40-51, 2019, ISSN: 2523-8914, DOI: 10.1007/s41965-019-00008-z.
22. Ababii V., Sudacevschi V., Munteanu S., Borozan O., Nistiriuc A., Lasco V. IoT based on Membrane Computing Models. In: *Proceedings of the 13th International Conference on Electromechanically and Energy Systems (SIELMEN-2021),* 7-8 October, 2021, Chisinau, Republic of Moldova, pp. 010-014, ISBN: 978-1-6654-0078-7. DOI: 10.1109/SIELMEN53755.2021.9600341. (IEEE Catalog Number: CFP21L58-ART).
23. Sosik P. P-Systems Attacking Hard Problems Beyond NP: a survey. *Journal of Membrane Computing,* 1(3), pp. 198-208, 2019, ISSN: 2523-8914, DOI: 10.1007/s41965-019-00017-y.
24. Munteanu S., Sudacevschi V., Ababii V., Borozan O., Ababii C., Lasco V. Multi-Agent Decision Making System based on Membrane Computing. In: *The 11th IEEE International Conference on Intelligent Data Acquisition and Advanced Computer systems: Technology and Applications*. 22-25 September, 2021, Cracow, Poland, Vol. 2. pp. 851-854. ISBN: 978-1-6654-4210-7, DOI: 10.1109/IDAACS53288.2021.9660971.
25. Orellana-Martin D., Valencia-Cabrera L., Riscos-Nunez A., Perez-Jimenez M.J. Minimal Cooperation as a way to Achieve the Efficiency in Cell-Like Membrane Systems. *Journal of Membrane Computing,* 1(2), pp. 85-92, 2019, ISSN: 2523-8914, DOI: 10.1007/s41965-018-00004-9.
26. Zhou N., Wang A. Fault Diagnosis of Transmission Circuit Based on Triangular Interval Valued Fuzzy Spike Neural Network P-System. *Energy Reports,* 2022, Vol. 8, pp. 776-784. DOI: 10.1016/j.egyr.2021.11.086.
27. Desel J., Esparsa J. *Free Choice Petri Nets*. Cambridge University Press, 1995, 244 p. ISBN: 0-521-46519-2.
28. Guțuleac E. *Modelarea și Evaluarea Performanțelor Sistemelor de Calcul prin Rețele Petri*. UTM, 1999, 267p.

29. Diaz M. *Petri Nets: Fundamental Models, Verification and Applications*. Wiley, 2009, 613p. ISBN: 978-1-84821-079-0, DOI: 10.1002/9780470611647.
30. JSON. [online]. [accessed 17.11.2021]. Available: https://www.json.org/json-en.html.
31. Bernardini F., Gheorghe M., Romero-Compero F., Walkinshaw N. A Hybrid Approach to Modeling Biological Systems. *WMC8 2007, LNCS 4860*, Springer-Verlag, pp. 138-159.
32. Liu F., Heiner M., Yang M. Modeling and Analyzing Biological Systems using Colored Hierarchical Petri Nets Illustrated by C. Elegans Vulval Development. *Journal of Biological Systems,* Vol. 22, No. 3, 2014, pp. 463-493, DOI: 10.1142/S0218339014500181.
33. Liu F., Heiner M. Modeling Membrane Systems using Colored Stochastic Petri Nets. *Natural Computing,* 2013, Nr. 12, pp. 617-629, DOI: 10.1007/s11047-013-9367-8.
34. Harris S.L., Harris D. *Digital Design and Computer Architecture. RISC-V Edition*. ScienceDirect 2021, 564p., ISBN: 978-0-12-820064-3, DOI: 10.1016/C2019-0-00213-0.
35. Intel Quartus Prime Software Suite. [online]. [accessed 21.12.2021]. Available: https://www.intel.com/content/www/us/en/software/programmable/quartus-prime/overview.html.
36. Cofer R.C., Harding B.F. *Rapid System Prototyping with FPGAs. Accelerating the Design Process*. ScienceDirect 2006, 301p., ISBN: 978-0-7506-7866-7, DOI: 10.1016/B978-0-7506-7866-7.X5000-8.
37. Guţuleac E., Boşneaga C., Railean A. VPNP-Software tool for modeling and performance evaluation using generalized stochastic Petri nets, *In: Proceedings of the 6-th International Conference on DAS-2002*, 23-25 May 2002, Suceava, România, p. 243-248, ISBN: 973-98670-9-X.
38. Altera DE0 Board. [online]. [accessed 11.01.2022]. Available: https://www.terasic.com.tw/cgi-bin/page/archive.pl?No=364.

Journal of Engineering Science *Vol. XXIX, no. 2 (2022), pp. 108 - 115*
Fascicle *Electronics and Computer Science* *ISSN 2587-3474*
Topic *Biomedical Engineering* *eISSN 2587-3482*

https://doi.org/10.52326/jes.utm.2022.29(2).10
UDC [621.397.424:772.96+004.93]:616.98:578.834.1

TEMPERATURE CAPTURE AND IMAGE PROCESSING SYSTEM: A CASE STUDY

Daniela Istrati*, ORCID: 0000-0002-1607-9273

Technical University of Moldova 168 Ștefan cel Mare Blvd, Chișinău, Republic of Moldova
*Corresponding author: Daniela Istrati, *daniela.istrati@ia.utm.md*

Received: 04. 14. 2022
Accepted: 05. 12. 2022

Abstract. This paper describes a technical solution to stop the spread of COVID-19 by creating a system consisting of a video camera with a thermal sensor connected to a web-based platform, which would help to manage to restrict access of people who have fever into a building. The main purpose of the project system is to measure body temperature, to detect and to recognize the person that has at the moment or had fever in the past 14 days, the registration in the database of both the fever and the person, and validate the access of the person in the building if it has a temperature below 37 degrees Celsius. The technical details as analysis and determination of the domain of interest, development of the new system design, functional and non-functional requirements, interface, project planning, technical specification and quality of the proposed solution are discussed. The proposed system aims to reduce the number of employees responsible for collecting the temperature, thus no longer exposing them to the risk of infection.

Keywords: *covid-19, thermal camera, body temperature, OpenCV library, activity diagram, user interface.*

Rezumat. Prezenta lucrare descrie o soluție tehnică de stopare a răspândirii COVID-19 prin crearea unui sistem ce constă dintr-o cameră video cu un senzor termic conectat la o platformă web, care ar ajuta la gestionarea și restricționarea accesului persoanelor cu febră într-o clădire. Scopul principal al sistemului propus este măsurarea temperaturii corpului, recunoașterea persoanei care a avut febră în ultimele 14 zile, înregistrarea în baza de date atât a febrei, cât și a persoanei și validarea accesului persoanei în clădire dacă are o temperatură sub 37 de grade Celsius. În lucrare se discută detaliile tehnice precum analiza și determinarea domeniului de interes, dezvoltarea noului proiect de sistem, cerințe funcționale și nefuncționale, cerințe față de interfață, planificarea proiectului, specificația tehnică și calitatea soluției propuse. Sistemul propus urmărește reducerea numărului de angajați responsabili cu colectarea temperaturii, astfel nu îi mai expune riscului de infecție.

Cuvinte cheie: *covid-19, camera termica, temperatura corpului, biblioteca OpenCV, diagrama de activitate, interfața utilizator.*

Introduction

On December 31, 2019, people with unknown form of pneumonia have been diagnosed in Wuhan, China. The World Health Organization announced a virus outbreak which led to a global pandemic [1]. The infection caused by the SARS-CoV-2 virus, called COVID-19 [2] is still contagious with a high spread rate from person to person, with a predominance of asymptomatic forms [3]. Fever has proved to be the main symptom of this infectious disease, causing outbreaks such as severe acute respiratory syndrome SARS, coronavirus (COVID-19) previously tracked in influenza A H1N1 and Ebola virus disease (EVD). Fever screening is a medical countermeasure used at international borders, public transport hubs and hospitals to lessen the spread of these diseases [4].

Globally, there has been launched a huge number of projects aiming to identify and provide solutions, tools and methods to stop the spreading of the pandemic [5, 6, 7].

A large variety of digital solutions were proposed worldwide, from communication within the community to supervision of population for new cases identification [8]. A diversity of mobile contact tracing apps in the EU Member States have been created. Most of these applications (Coronalert in Belgium, CovTracer-EN in Cyprus, Smittestop in Denmark, etc.) are based on Bluetooth technology, available on GooglePlay and Appstore, based on anonymity, provide information to users of the applications about those tested positive and their location for period of 14 days [9]. However, users are asked to inform their relatives and family about a possible infection.

The EU 30+ satellites system is involved in monitoring the impact of the outbreak during the COVID-19 pandemic, within the EU Space Programme [10].

Supercomputer platforms from 4 countries (Spain, Italy and Germany), along with pharmaceutical companies and top research centers within an EU-funded project named EXSCALATE4CoV are searching the best treatments for the disease [11].

In this context, the Technical University of Moldova applying for several projects, was selected as the first beneficiary for *"Scanner thermique intelligent – IntelST"* project launched by AUF (Agence Universitaire de la Francophonie) in May 2020 as part of its special COVID-19 action plan [12].

The particular objective of this project was to provide a technical solution to stop the COVID-19 pandemic by creating a system that would help both the medical system and the entire population of the Republic of Moldova. The main purpose of the project system is to measure body temperature, to recognize the person that have had a fever in the past 14 days, the registration in the database of both the fever and the person, and validate the access of the person in the building if it has a temperature below 37 degrees Celsius. All of this will help implement public health measures to prevent the rapid spread of infection and increase the readiness of the health system and replace the person measuring the fever at the entrance to the building. As a result of the system, students will be able to slowly return to offline classes. The system requires security measures other than those recommended for the operating system.

The team of students of Technical University of Moldova and mentors of the project's partners came with a solution that could allow students to return to classes. One of the solutions to achieve this goal is a temperature capture and image processing system, allowing students to return to courses openly and quietly [13].

Thus, the system provides for prevention, preparedness and intervention measures for public health emergencies, risk assessment, declaration / cancellation of public health

emergency, special powers of attorney for rooms and property, including containment measures and / or quarantine, the establishment of entry / exit rules for the area subject to isolation or quarantine, by informing the population of the public health emergency, the mechanisms for coordination and mobilization of emergency funds.

It is important to mention that the processing of registered data occurs in accordance with the legislation of the Republic of Moldova and Technical University of Moldova, being registered as an operator that meets the requirements of personal data protection legislation, respects the rigors of the normative framework related to the protection of personal data.

Infrared thermo-scanners are widely used in airports, public facilities and hospitals because their non-invasive nature allows massive screening. In the created situation, we would need a modern and comfortable tool to use to detect potentially sick people and monitor the number and frequency of illnesses in each closed building or public place separately.

The body temperature is imperative to be checked in countering transmission of the COVID-19 virus. The main effective weapon applied in combating infection, as professionals require, is restraining of contact with infected people [14].

1. Analysis and determination of the domain of interest

The application is an innovation for people who would visit any public space, and it will replace the person who identifies the temperature of the people entering the building.

This project is split into three modules:

1. The part of facial recognition and fever measurement thanks to the thermo-camera using the OpenCV library and the transmission of people detected in the database for 14 days.
2. The front-end part that will allow to set the camera, the interface parameters, to view statistics and identified cases, to allow entry for people identified with negligible fever, to view covid information, etc.
3. The backend part which will create the database with the detected people who will be in quarantine and the creation of functionalities such as the statistics of the detected people with fever, the creation of notifications, the possibility of defining the days and the temperature in the interface, etc.

General objective: development of a solution with immediate technological and social impact for:

- help the health system not to reach a critical level of saturation. The proposed solution aims to identify the sick or infected people and prohibit their access to common areas, thus reducing their contact with many people.
- help the population cope with the difficulties caused by the COVID-19 pandemic, in particular the fear of going to common access areas, by setting up a system that reduces the risk of infection.
- replacing the person taking temperature measurements and is exposed themselves to the risk of being infected with the temperature collection device.

The direct beneficiaries of the project are economic actors (shops, pharmacies, companies), employers, hospitals, universities (including the Technical University of Moldova) – all of which aim to ensure a safe environment for customers / employees / students and

reduce the possibility of infection in their spaces. In such way the population that will be exposed to less risk of being infected.

The indirect beneficiaries of the project are the health system because the solution aims to reduce the possibility of spreading the virus, thus avoiding the saturation of the medical system.

2. Development of the new system design

In terms of design, this system is developed using technologies such as:

- Vue.js on the front end that the general user will interact with, i.e., the institution administrator who will allow access to people;
- Symphony for the functional backend where data will be stored;
- OpenCV for facial recognition and fever measurement of people entering the building [15].

The proposed solution highlights the knowledge of the students but also come with the possibility of hosting new experiences such as:

- innovation: the implementation of a solution that is less expensive compared to existing solutions - therefore accessible for universities, theaters, shops;
- engineering: the construction of the temperature collection device;
- algorithmic: the definition of the decision-making algorithm based on the data collected.

3. Functional Requirements/ Non-Functional Requirements

The software solution meets the following functional and organizational requirements:

a. The application has to contain a system configuration allowing users shared access to system resources.
b. The security of the application has to be ensured by the rights offered by the application's administrator, which gives access to the registration for users and user groups.
c. The application will guarantee the ability to work in an open multi-level structure, using database management systems.
d. The application must have an ergonomic interface in which the user can view all the information relating to the identified persons.
e. The application will provide viewing permissions of people with a fever above 37 degrees Celsius and prohibit entry into the building.

4. Project planning requirements:

User requirements must be clear, verifiable, complete, precise, achievable. Requirements' analysis is the first step in the product development cycle in which the requirements of the application are established, from the requirements of the end user, the functions of the future software product are identified as well as the data involved. This step answers the question of what will be achieved by developing the software product [16].

5. Interface requirements:

The system should have a graphical interface through which it will be convenient and easy to perform operations for the building administration [17]. Thus, the application must

have an ergonomic interface in which the user can view all information related to case statistics:

1. the list of identified persons
2. notices
3. application settings
4. covid information
5. access to live view of camera data.

6. Quality requirements:

- The system must have high stability, security and safety, as it is to store a person's data.
- The application must contain a configuration system that allows internal access only for institution-specific administration to SL resources. To be comfortable to be used by an administrator.
- The security of the application concerning the inaccessibility to other pages of the site by the manual change of the link as well as the impossibility of following from the browser the data entry for the connection / registration.

Elaboration of the Technical Specifications necessary for the realization of the information system.

General objectives;

1. the destination and objectives of the creation / modernization of the information system;
2. description of the object of automation;
3. system requirements;
4. the composition and content of the work to create the system;
5. how to test/check and hand over/receive the system;
6. requirements for the composition and content of work for the preparation of the object of automation for the launch of the information system

In the diagram represented on the Figure 1, it can be visualized the appearance and physical component of the elements in the IntelST system. There can be observed the bearings and the data transmission wire for processing and its return.

At the entrance of the building the kit of the system has to be installed: the Hikvision camera the TV, a Raspberry Pi and a computer. The camera here has the role of measuring the temperature of the people who enters the building. The thermal camera sends data which are automatically added to the database and deleted after a certain period of time.

The temperature measurement process: the person who measures the temperature is replaced by the camera, which facilitates data processing and saving. The system will display a list of people who do not have access to the building. After that, a person can be allowed to enter. After giving permission, it can be seen if the given person is in the building or not.

The transmission of processed data: this is the component of the system. The processed data (temperature and person identifier) are transmitted to the display screen, then to the administrators.

An administrator being a part of the company has the right to modify certain configurations. So, the administrator can change the temperature limit and restriction for entering to the building.

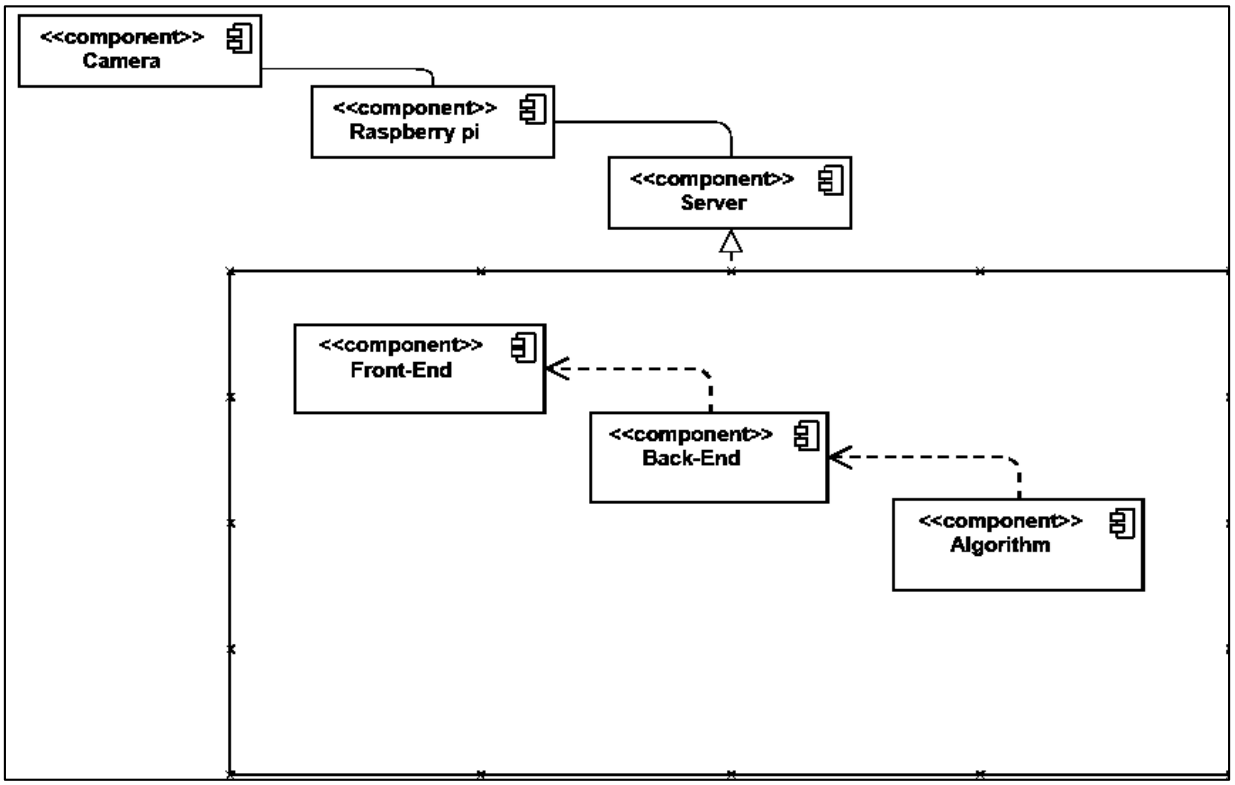

Figure 1. IntelST System Components Diagram.

The system allows the administrator to change the settings of a company as well. To edit a company, he must fill in a form with the data of the company he will edit.

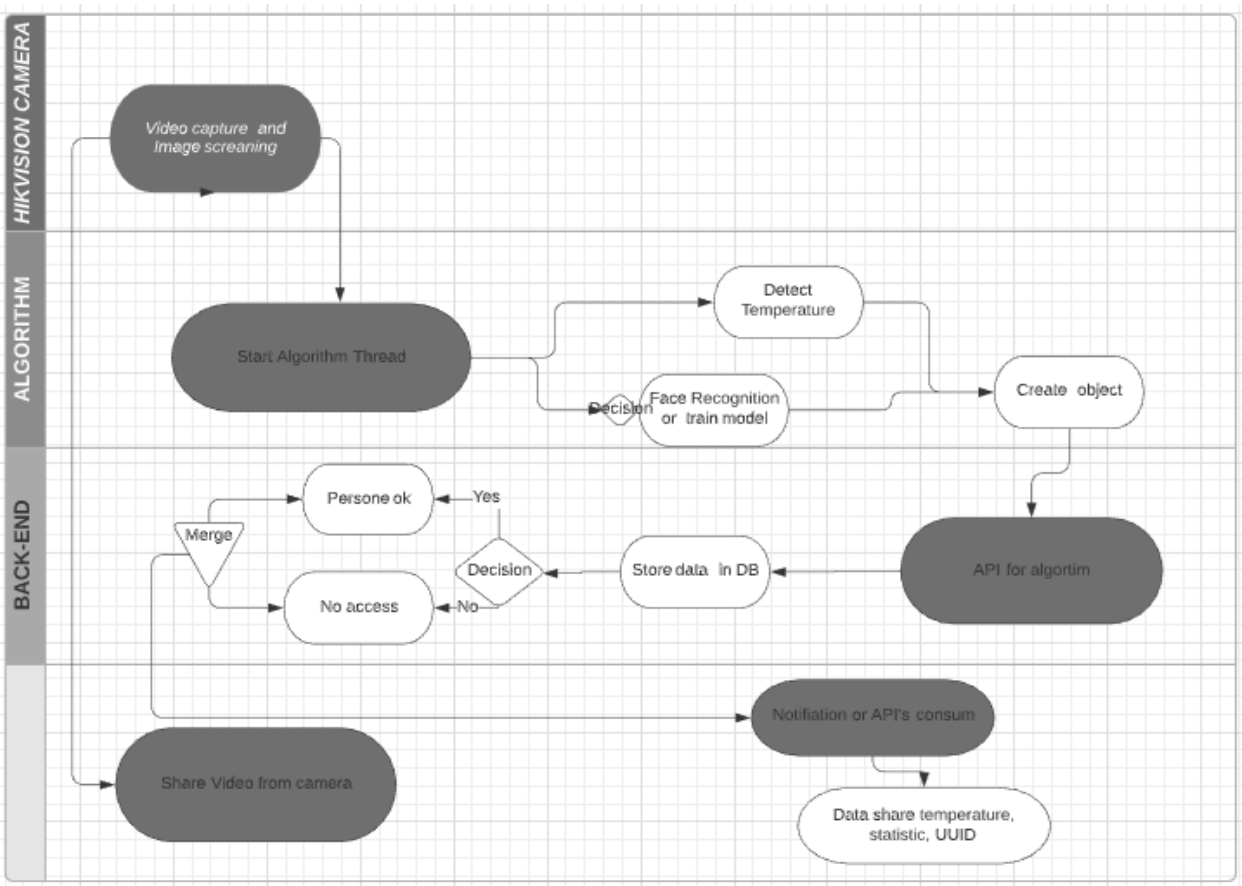

Figure 2. The activity diagram of the system.

In the activity diagram presented in Figure 2 it can be seen the followed steps by the system's data, i.e., it can be seen how the algorithm processes the obtained data and then sent to the back-end and then to the front-end to be monitored and perceived by users of the new system. *The algorithm that processes and saves data:* If a person has a temperature above 37 degrees Celsius, its access is prohibited in the building for a period of 14 calendar days [18]. The access is allowed in the building only if people show normal body temperature, below 37 degrees ºC and are without fever. Depending on the restrictions imposed, these data can be changed in the system, according to the rules of the moment.

The system allows sensors to add a newly identified case. To add a new case, it is necessary for the thermal camera to receive an image of a person and record his/her temperature. Once the two steps are completed and everything goes well, the system automatically saves the request in the database. If the person is already in the database, the data will still be added again.

To add an identified case of a person that has a temperature above 37 degrees Celsius, it is mandatory to detect the person and determine his temperature. This is the moment where it is assigned an ID, images, date, time and input temperature. Depending on the temperature, it will be specified whether or not the person has access to the building. The personal identifier will be assigned depending on whether the person is for the first time or has been identified before. The case is first registered in the database and then it is decided whether the person has access to it or not based on the rest of the cases. The automatic system deletes older cases based on the date they were identified. An important role in this system is played by the statistical part. In order to keep the situation under control it is necessary on daily and weekly bases to present graphs which will show the number the number of registered cases of people who have been detected with fever compared to the total number of people who have entered into the building. The administrator can thus compare and make a decision based on the result of the statistics. The total number of people whose access was restricted due they were detected with fever can be indicated separately. The *IntelST* system is a more complex system, but being a free resource, it can be viewed and installed by anyone, if he has a personal server with the physical capacities necessary for the work and the processing of data for the algorithm, the only difficulty is the server and resources for data processing.

Conclusions

This work presents the proposed solution for the protection against the COVID-19 pandemic spread, for people who want quickly to enter into the stores, hospitals, schools or other institutions. The system purpose is to ensure a safe environment for customers / employees / students and reduce the possibility of infection in their spaces and for the population who will have a lower risk of being infected overall. The system aims to reduce the possibility of the virus spreading, thus avoiding the saturation of the medical system. It offers a much cheaper solution compared to existing solutions, thus offering the possibility to a greater number of actors to benefit from it, to identify patients, but also, to replace the person carrying out temperature measurements and risk to infect himself from the temperature collection device.

Acknowledgments: This paper reflects the main results obtained within the framework of the *"IntelST – Scanner thermique Intelligent"* project, implemented by the Technical University of Moldova in partnership with the company *"PENTALOG CHI" SRL* - the Moldovan subsidiary of the French Group *PENTALOG* and the *Micro Lab Student Engineering Club*, financed by *Agence Universitaire de la Francophonie*.

References

1. WHO Director-General's opening remarks at the media briefing on COVID-19 - 11 March 2020 https://www.who.int/director-general/speeches/detail/who-director-general-s-opening-remarks-at-the-media-briefing-on-covid-19---11-march-2020
2. Naming the coronavirus disease (COVID-19) and the virus that causes it 11.02.2020 https://www.who.int/emergencies/diseases/novel-coronavirus-2019/technical-guidance/naming-the-coronavirus-disease-(covid-2019)-and-the-virus-that-causes-it
3. Kronbichler A., Kresse D., Yoon S., Lee K. H., Effenberger M., Shin J. Il. Asymptomatic patients as a source of COVID-19 infections: A systematic review and meta-analysis. International Journal of Infectious Diseases, Volume 98, 2020, Pages 180-186, ISSN 1201-9712, https://doi.org/10.1016/j.ijid.2020.06.052
4. Kuthyar S., Anthony C. L., Fashina T., Yeh S., & Shantha J. G. (2021). *World Health Organization High Priority Pathogens: Ophthalmic Disease Findings and Vision Health Perspectives*. *Pathogens* [online]. (Basel, Switzerland), 10(4), 442. [accessed 10.01.2022]. Available: https://doi.org/10.3390/pathogens10040442
5. European Comission. *Coronavirus response. Digital solutions during the pandemic*. Available : https://ec.europa.eu/info/live-work-travel-eu/coronavirus-response/digital-solutions-during-pandemic_en
6. PRESS RELEASE, *World Bank Group's $157 Billion Pandemic Surge Is Largest Crisis Response in Its History,* 19.07.2021, [online]. Available: https://www.worldbank.org/en/news/press-release/2021/07/19/world-bank-group-s-157-billion-pandemic-surge-is-largest-crisis-response-in-its-history
7. PRESS RELEASE, *Plan d'actions de l'AUF : spécial pandémie COVID-19, [AUF COVID-19 PANDEMIC SPECIAL PLAN P],* march 2020. [online]. Available: https://www.auf.org/nouvelles/actualites/plan-dactions-de-lauf-special-pandemie-covid-19/
8. Budd J., Miller B.S., Manning E.M. *et al*. Digital technologies in the public-health response to COVID-19. *Nat Med* 26, 1183–1192 (2020). https://doi.org/10.1038/s41591-020-1011-4
9. European Commission website. *Mobile contact tracing apps in EU Member States*. [online]. Available: https://ec.europa.eu/info/live-work-travel-eu/coronavirus-response/travel-during-coronavirus-pandemic/mobile-contact-tracing-apps-eu-member-states_en
10. Breton Th. *EU Space response to Coronavirus*. [online]. Available: https://www.copernicus.eu/en/coronavirus
11. European Commission website. *Supercomputers versus coronavirus*. [online]. Available: https://ec.europa.eu/info/strategy/recovery-plan-europe/recovery-coronavirus-success-stories/digital/supercomputers-versus-coronavirus_en
12. *Le scanner thermique intelligent : une solution à l'aide du système de santé moldave, [The intelligent thermal scanner: a solution using the Moldovan health system]*. [online]. 30.07.2020. [accessed 10.01.2022]. Available: https://www.auf.org/europe-centrale-orientale/nouvelles/actualites/le-scanner-thermique-intelligent-une-solution-laide-du-systeme-de-sante-moldave/
13. Ignatiuc A., Buftea M., Istrati D. Module de traitement et d'affichage des données en temps réel pour le système intellST. In: Conferinţa tehnico-ştiinţifică a studenţilor, masteranzilor şi doctoranzilor. Vol.1, 23-25 martie 2021, Chișinău. Chișinău, Republica Moldova: Tehnica-UTM, 2021, pp. 386-389. ISBN 978-9975-45-699-9. http://cris.utm.md/handle/5014/935
14. Güner R., Hasanoğlu I., & Aktaş F. (2020). *COVID-19: Prevention and control measures in community*. Turkish journal of medical sciences, 50(SI-1), 571–577. https://doi.org/10.3906/sag-2004-146
15. Prasanna, D. Mary, Reddy, Ch. Ganapathy, *Development of Real Time Face Recognition System Using OpenCV* in International Research Journal of Engineering and Technology (IRJET), Volume: 04, Issue: 12, Dec-2017, e-ISSN: 2395-0056, p-ISSN: 2395-0072, pag. 791-798. shorturl.at/dDJ03
16. Sutcliffe A., Gulliksen J. *Chapter 18*- User-Centered Requirements Definition. In Buie E., and Murray D., (Editors) *Usability in Government Systems,* Morgan Kaufmann, Elsevier 2012, Pag. 285-300. *ISBN 9780123910639*. https://doi.org/10.1016/B978-0-12-391063-9.00050-X
17. Stone D., Jarrett C., Woodroffe M., Minocha S., *User interface design and evaluation*, Morgan Kaufmann 2005, 669 p. ISBN: 0-12-088436-4.
18. World Health Organization Guidelines *PANDEMIC AND EPIDEMIC DISEASES Infection prevention and control of epidemic- and pandemic-prone acute respiratory infections in health care*. Geneva, 2014.133 p. ISBN 9789241507134 https://apps.who.int/iris/bitstream/handle/10665/112656/9789241507134_eng.pdf?sequence=1&isAllowed=y

Journal of Engineering Science *Vol. XXIX, no. 2 (2022), pp. 116 - 122*
Fascicle *Architecture, Civil and Environmental Engineering* *ISSN 2587-3474*
Topic *Civil Engineering and Management* *eISSN 2587-3482*

https://doi.org/10.52326/jes.utm.2022.29(2).11
UDC 691.32:006

COMPRESSION STRENGTHS CORRESPONDENCE OF CONCRETES ACCORDING TO THEIR CLASSES AND MARKS

Gheorghe Croitoru*, ORCID: 0000-0001-6289-8897

Technical University of Moldova, 168 Stefan cel Mare Blvd., Chisinau, Republic of Moldova
*Corresponding author: Gheorghe Croitoru, *gheorghe.croitoru@dmmc.utm.md*

Received: 03. 22. 2022
Accepted: 05. 12. 2022

Abstract. The article presents the problems related to the application of the provisions of the new European standards EN for concrete production, after the withdrawal of the obsolete national standards GOST regarding the correspondence of the classes to the concrete marks. In the context of the application of harmonized standards, there has been a need to establish the correspondence of classes to concrete marks, in order to help design and construction companies to correctly establish the strength mark of concrete to the corresponding class of concrete. The concrete class establishes the normative resistance of concrete for the calculation of constructions, for the service limit state, the prismatic resistance to compression adopted as normative resistance. The ratio between concrete classes and marks, in terms of compressive strength, is determined by the normative coefficient of variation V = 13.5%. The degree of homogeneity of the quality of the concrete is determined according to the values of the standard deviation σ and the average compressive strength of the concrete. As a result of the research, intermediate classes of concrete have been identified, which are not indicated in the normative documents, related to the production of concrete.

Keywords: *basic parameters, coefficient of variation*, *compliance criteria*, *concrete class*, *concrete mark*, *compression strength*, *correspondence, medium values*, *standard deviation.*

Rezumat. Articolul analizează problemele legate de aplicarea prevederilor noilor standarde europene EN pentru producția de beton, după retragerea standardelor naționale învechite (GOST) privind corespondența claselor cu mărcile de beton. În contextul aplicării standardelor armonizate a apărut necesitatea stabilirii corespondenței claselor cu mărcile din beton, pentru a ajuta firmele de proiectare și construcții să stabilească corect marca de rezistență a betonului la clasa corespunzătoare de beton. Clasa de beton stabilește rezistența normativă a betonului pentru calculul construcțiilor, pentru starea limită de serviciu, rezistența prismatică la compresiune adoptată ca rezistență normativă. Raportul dintre clasele și mărcile de beton, în ceea ce privește rezistența la compresiune, este determinat de coeficientul normativ de variație V = 13,5%. Gradul de omogenitate al calității betonului se determină în funcție de valorile abaterii standard σ și rezistența medie la compresiune a betonului. În urma cercetărilor au fost identificate clase intermediare de beton, care nu sunt indicate în documentele normative, legate de producția de beton.

Cuvinte cheie: *parametri de bază, coeficient de variație, criterii de conformitate, clasa betonului, marca betonului, rezistență la compresiune, corespondență, valori medii, abatere standard*.

Introduction

This article deals with issues related to the application of new European standards for concrete production, following the cancellation of obsolete national standards, regarding the correspondence of concrete classes to marks. The fields of design and construction are strictly regulated by provisions regarding concrete and reinforced concrete constructions, through normative documents and standards, in which the class and mark of concrete are very important.

The ratio between the class and the mark of concrete determines the engineering calculations for the production and construction of concrete elements, in which, as basic parameters are taken the data of laboratory tests on strength, using a concrete cube or cylinder of certain dimensions. The notion of "concrete class" is necessary for establishing the normative strength of concrete when calculating constructions at the service limit state, ie the prismatic compressive strength, adopted as normative strength.

The class according to SM EN 206 [1] and the mark according to GOST 26633-91 [2] characterize the strength of the concrete, but when designing the composition of the concrete mixture, the frost-thaw resistance (F), the impermeability of concrete to water (W) and other indicators must also be taken into account considering the individual characteristics of construction projects.

The strength of concrete depends on the ratio between water and cement (W/C), where the proportions W/C = 0.3 ÷ 0.5 are considered an ideal composition. If the ratio is lower - the concrete loses its plasticity, if the proportion of water increases - the resistance decreases, but the plasticity of the mixture becomes higher.

The compressive strength class according to SM EN 206 [1] is denoted by "C" being expressed in N/mm^2, and the compression strength mark according to GOST 26633-91 [2] is denoted by "M", expressed in kgf/cm^2. The difference between these concepts is that if the mark is an average indicator, then the class assumes guaranteed compliance with the specified level of strength of the concrete.

The methodological part

With the implementation of the standard on the specification, performance, production and conformity of concrete SM EN 206 [1], the need arose to expose the correspondence of concrete classes with concrete marks, established by the standard on heavy concrete and fine-grained concrete GOST 26633-91 [2]. The correspondence between concrete classes and marks according to GOST 26633-91 [2] has the value of compressive strength (tensile) evaluated by the normative coefficient of variation V = 13.5% which is not found in SM EN 206 [1]. This value of the coefficient is used in the case of initial tests and when there is no statistical data on the actual uniformity of the concrete, according to GOST 27006-86 [3]. The strength mark of the concrete is an average value of the compressive strength expressed in kgf/cm^2 by the normative coefficient of variation V.

According to the provisions of the standard SM EN 206 [1], the conformity of the compressive strength of concrete is evaluated on samples tested at 28 days, and each individual test result on the cube f_{ci} must satisfy the relationship:

$$f_{ci} \geqslant (f_{ck} - 4)\ \text{N/mm}^2 \quad (1)$$

In the case when, the production of a concrete family starts, for the first time, the average strength of the groups of three consecutive results, performed on the samples, which overlap or not, must satisfy the relationship (Compliance Criterion 1, according to SM EN 206 [1]):

$$f_{cm} \geqslant (f_{ck} + 4)\ \text{N/mm}^2 \quad (2)$$

When we have a continuous production of concrete, the conformity assessment will be made on the results of the tests over an evaluation period of at least 15 results and not more than 35 consecutive results obtained over a period not exceeding 6 months, in case when the number of results of the tests is less than 35 per quarter, and over a period not exceeding 3 months in cases when the number of test results is more than 35 per quarter. The degree of homogeneity of the concrete quality is determined according to the values expressed in N/mm^2 of the standard deviation σ and the average compressive strength f_{cm} of the concrete (Conformity criterion 1 according to SM EN 206 [1]):

$$\text{fcm} \geqslant (\text{fck} + 1{,}48\sigma)\ \text{N/mm}^2 \quad (3)$$

The standard deviation σ is determined for a minimum of 15 results recorded in a period of maximum 6 months, according to the relation:

$$\sigma = \sqrt{\frac{1}{N}\sum_{i-1}^{N}(f_{ci-1}f_{cm})^2} \quad (4)$$

where:

σ - standard deviation;

N – number of results;

f_{ci} – individual result of compressive strength;

f_{cm} – average compressive strength.

It is also important to note that testing larger specimens provides more information about concrete. The standard SM EN 206 [1] specifies two types of samples, cubes with a side of 150 mm and cylinders of 150 mm diameter and 300 mm height, while the standard GOST 26633-91 [2] specifies cubes with a side of 100 mm, according to GOST 22685-89 [4]. When testing samples with a side of 100 mm, the volume of the concrete under test decreases and the variation of the resistance on the samples increases, which can be solved by increasing the number of samples or their dimensions.

The experimental part

For the preparation of concrete mixtures with different cement dosages, crushed aggregates of sand and gravel sort (fraction) 0-4, 4-8 and 8-16 mm and plasticizer/superplasticizer additive were used. The experimental tests, performed on concrete, were performed in accordance with the national standard SM EN 206 [1] and the canceled standard GOST 26633-91 [2].

In the preparation of concrete, for both cases, the effective W/C ratio was used, which took into account the water absorption of the aggregates (determined in accordance with SM EN 1097-6 [5]), the cement dosages being 260 kg/m^3, 280 kg/m^3, 300 kg/m^3, 320 kg/m^3, 340 kg/m^3, 380 kg/m^3, 420 kg/m^3, 440 kg/m^3 to which appropriate amounts of plasticizer/superplasticizer were added.

The concrete mixtures were designed so that the compaction class was S3 (100-150 mm), the test being performed according to SM EN 12350-2 [6]. After stripping, the concrete samples according to SM EN 206 [1] were immersed in water and the samples according to GOST 26633-91 [2] maintained in laboratory conditions, at a humidity of 95 %, at a temperature of plus 20 °C up to the trial period of 28 days. The determination of the compressive strength of the concrete samples (Figure 1) was performed on cubes with a side of 150 mm, according to SM EN 206 [1] and with a side of 100 mm, according to GOST 26633-91 [2], and SM EN 12390-1 [7], these being manufactured and stored in accordance with SM EN 12390-2 [8].

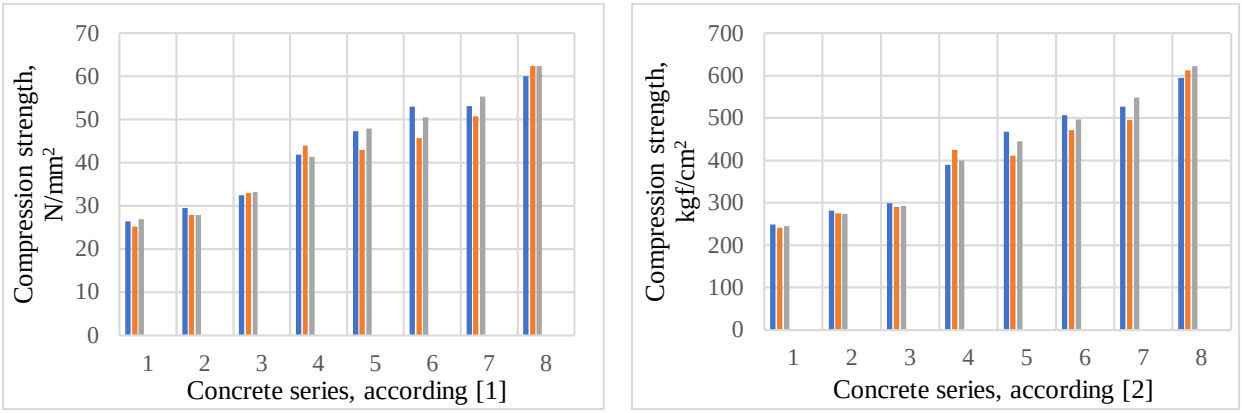

a) b)

Figure 1. Average values of compressive strengths of concrete batches with different cement dosages: a) tests performed on eight series of cubes, with a side of 150 mm, according to SM EN 206 [1]; b) tests performed on eight series of cubes, with side 100 mm, according to GOST 26633-91 [2].

The average values of the tests on the cubes are presented in Table 1. Concrete classes were established based on the application of different compliance criteria for compressive strength, depending on the number of test results (f_{cm}), for a concrete in the family, applying the criterion ($f_{cm} \geq f_{ck} + 4$). In this case, the relation $f_{ck} + 8$ N/mm^2 was applied, the concrete classes obtained being presented in Table 2.

Table 1

Average values of compressive strengths obtained on concrete samples

Series	Cement dosage, kg/m^3	Average compressive strength, N/mm^2 [1]	Series	Cement dosage, kg/m^3	Average compressive strength $\overline{R}$, kgf/cm^2 [2]
1	260	26,17	1	260	244,73
2	280	28,46	2	280	276,93
3	300	32,86	3	300	293,62
4	320	42,39	4	320	404,70
5	340	44,21	5	340	441,05
6	380	49,71	6	380	491,47
7	420	53,05	7	420	523,30
8	440	61,58	8	440	609,65

Table 2

Determination of concrete classes according to SM EN 206 [1] and marks according to GOST 26633-91 [2]

Series	Criterion 1, N/mm²	Concrete class, C, [1]	Series	Deviation of the nearest concrete mark from the average strength of the class, % $(M - \bar{R})/\bar{R}\times 100$	Concrete marks, *M*, [2]
1	26,17 – 15 = 11,17	C12/15	1	200 – 244,73/244,73 × 100 = –18,3	M200
2	28,46 – 20 = 8,46	C16/20	2	250 – 276,93/276,93 × 100 = –9,7	M250
3	32,86 – 25 = 7,86	C20/25	3	300 – 293,62/293,62 × 100 = +2,2	M300
4	42,39 – 30 = 12,39	C25/30	4	400 – 404,70/404,70 × 100 = –1,2	M400
5	44,21 – 37 = 7,21	C30/37	5	400 – 441,05/441,05 × 100 = –9,3	M400
6	49,71 – 37 = 12,71	C30/37	6	450 – 491,47/491,47 × 100 = –8,4	M450
7	53,05 – 45 = 8,05	C35/45	7	550 – 523,30/523,30× 100 = +5,1	M550
8	61,58 – 50 = 11,58	C40/50	8	600 - 609,65/609,65 × 100 = –1,5	M600

From Table 2 it is observed that the series 3 and 5 of concrete samples, executed according to SM EN 206 [1], with cement dosages of 300 kg and 340 kg respectively, did not satisfy the relation f_{ck} + 8 N/mm² (Figure 2 a) or were close to the default values. Therefore, these series can be classified in intermediate concrete classes, respectively C18/22 and C28/35.

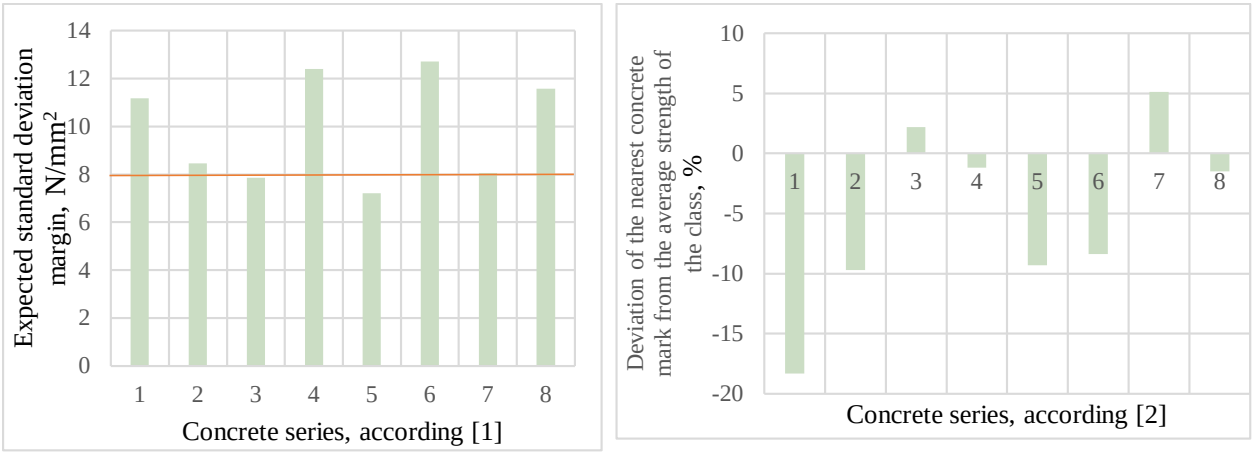

a) b)

Figure 2. Criteria for accepting the initial tests of f_{ck} + 8 N/mm² concrete: a) expected standard deviation margin; b) deviation of the nearest concrete mark from the average strength of the class.

The values of the deviations of the closest concrete marks from the average strength of the class (Figure 2 b), differ insignificantly from those indicated in GOST 26633-91 [2], exceeding the allowed deviation of 5 %, which can be explained by deviation from the average values at compression, due to model uncertainties, variations in geometric and material properties, as well as the required level of safety.

Based on the results obtained and the concrete marks established, in "Table V.1" of the normative document CP H.04.04 [9], appropriate concrete classes and intermediate marks can be introduced (Table 3).

Table 3

Marks and classes of compressive strength for concrete, according to GOST 26633 [2] and SM EN 206 [1]

Compression strength marks according to GOST 26633, kgf/cm^2	Compression strength classes according to SM EN 206	Minimum characteristic resistance on cylinders, $f_{ck,cil}$ N/mm^2	Minimum characteristic resistance on cubes, $f_{ck,cub}$ N/mm^2
M150	C8/10	8	10
M150	**C10/12**	**10**	**12**
M200	C12/15	12	15
M250	C16/20	16	20
M300	**C18/22**	**18**	**22**
M350	C20/25	20	25
M350	**C22/27**	**22**	**27**
M400	C25/30	25	30
M450	**C28/35**	**28**	**35**
M500	C30/37	30	37
M550	C32/40	32	40
M600	C35/45	35	45

According to the SM EN 1992-1-1 standard [10], the strength of the concrete is obtained by applying the formula:

$$f_{cd} = \frac{\alpha_{cc} f_{ck}}{Y_c} \tag{5}$$

where:

Y_c – partial safety factor, set as 1.5.

$$Y_c = Y_M \cdot Y_{conv} \tag{6}$$

where:

Y_M has a value of 1.3 and is a factor, which takes into account the deviation from the value f_{ck}, due to model uncertainties, variations in geometric and material properties, and the level of safety established.

Y_{conv} has a value of 1.15 and is a factor, which takes into account the possible decrease in the strength of concrete in its application.

Figure 3 presents the conformity criteria for the compressive strength of concrete in different stages, starting from the determination of the concrete composition for initial tests (stage I), to the accepted resistance, in case of in situ tests (stage VII), taking - into consideration the acceptance criteria for fresh concrete on the construction site.

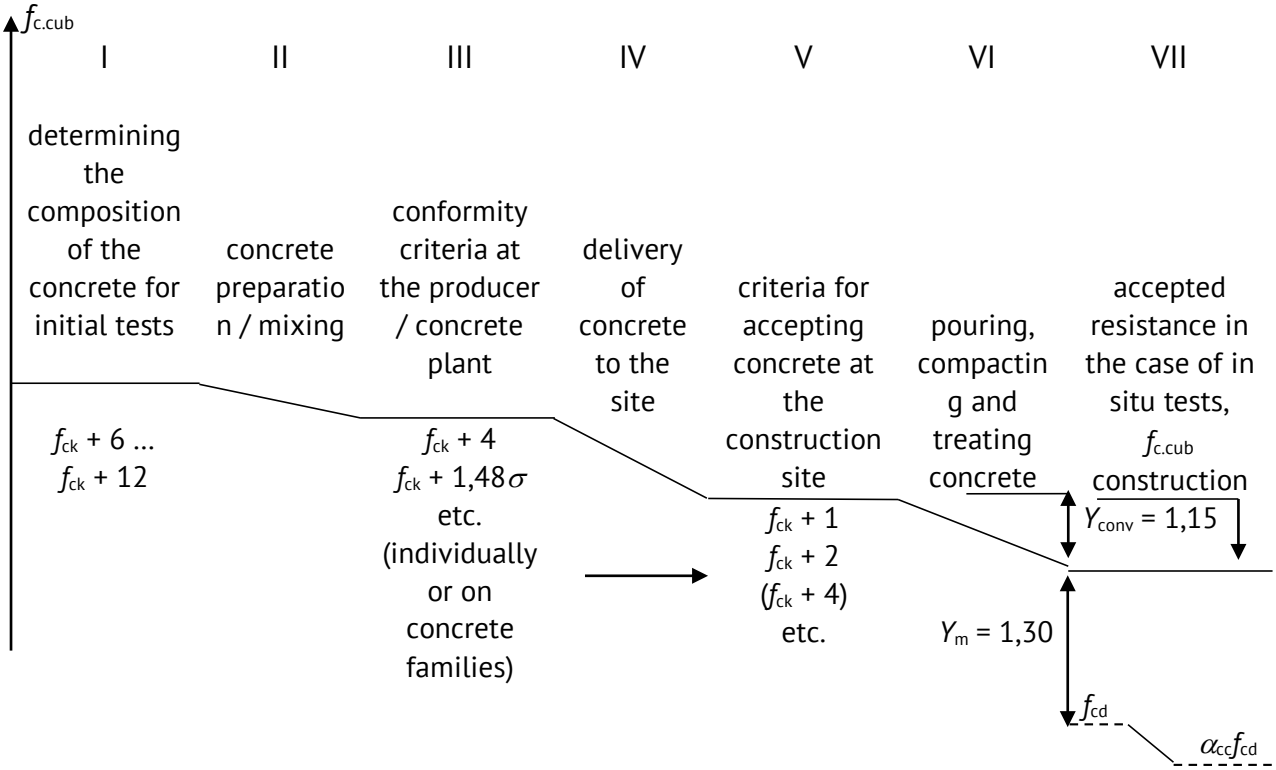

Figure 3. Conformity criteria for the compressive strength of concrete in different stages.

Conclusions

Assessing the compressive strength of concrete is an important activity, as it provides data on the most important characteristic of concrete, - the strength class.

In the context of the application of harmonized standards, within [10], there was a need to establish the correspondence of classes with concrete marks, in order to help design and construction companies to correctly establish the strength mark of concrete with the corresponding class of concrete.

Not all concrete marks, according to GOST 26633-91 [2] have corresponding classes, according to SM EN 206 [1], hence the need for their establishment, by introducing intermediate classes of concrete.

References

1. SM EN 206:2013+A2:2021 Concrete. Specification, performance, production and conformity.
2. GOST 26633-91 Heavy-weight and sand concretes. Specifications.
3. GOST 27006-86 Concretes. Rules for mix proposing.
4. GOST 22685-89 Moulds for making control specimens of concrete. Specifications.
5. SM EN 1097-6:2016 Tests for mechanical and physical properties of aggregates - Part 6: Determination of particle density and water absorption.
6. SM EN 12350-2:2019 Testing fresh concrete - Part 2: Slump test.
7. SM EN 12390-1:2015 Testing hardened concrete Shape, dimensions and other requirements for specimens and moulds.
8. SM EN 12390-2:2019 Testing hardened concrete - Part 2: Making and curing specimens for strength tests.
9. CP H.04.04:2018 Concretes and mortars. Concrete. Specification, performance, production and conformity.
10. SM EN 1992-1-1:2004/A1:2017 Eurocode 2: Design of concrete structures – Part 1-1: General rules and rules for buildings.
11. Government Decision no. 913 of 25.07.2016 on the approval of the Technical Regulation on the minimum requirements for the sale of construction products (Published: 05.08.2016 in the Official Gazette No. 247-255 art. 997, with application from 05 August 2018).

Journal of Engineering Science *Vol. XXIX, no. 2 (2022), pp. 123 - 132*
Fascicle *Architecture, Civil and Environmental Engineering* *ISSN 2587-3474*
Topic *Civil Engineering and Management* *eISSN 2587-3482*

https://doi.org/10.52326/jes.utm.2022.29(2).12
UDC 332.87:311.21:04.6+312] (478)

UPDATING THE STATISTICAL REGISTER OF HOUSING IN THE REPUBLIC OF MOLDOVA USING OPEN-SOURCE GIS TECHNOLOGIES

Mihail Spataru[1], ORCID ID: 0000-0003-2547-6171,
Ana Vlasenco[2]*, ORCID ID: 0000-0002-5017-6392,
Livia Nistor-Lopatenco[2], ORCID ID: 0000-0003-3509-648X,
Vasile Grama[2], ORCID ID: 0000-0002-2100-2756

[1]*National Bureau of Statistcis of the Republic of Moldova, 106 Grenoble street, Chisinau, Republic of Moldova*
[2]*Technical University of Moldova, 168 Stefan cel Mare Boulevard, Chisinau, Republic of Moldova*
*Corresponding author: Ana Vlasenco, *ana.vlasenco@gcg.utm.md*

Received: 02. 18. 2022
Accepted: 04. 23. 2022

Abstract. This article describes the possibilities of promoting and implementing open-source geoinformation technologies in the field of statistical activity in the Republic of Moldova, which will simplify and streamline the process of analysis, collection, systematization of data, as well as their dissemination. Since 2019, the National Bureau of Statistics of the Republic of Moldova, according to the recommendations of the United Nations, has proposed the creation of the geo-coded Statistical Register of Housing (SRH). With the creation of the National Spatial Data Infrastructure (NSDI), this goal can be achieved, as SRH will form the basis of the Population and Housing Census (PHC) from the 2020 round. The geospatial data from SRH will be used to delimit the census enumeration areas, and the reviewed population will be attached to the geographical coordinates of the dwelling. These enumeration areas will cover the entire territory of the Republic of Moldova and will serve to plan human resources, organize field activities and ensure the full coverage of census units (for people, households and dwellings).

Keywords: *Statistical Register of Housing (SRH), Geographic Information Systems (GIS), Population and Housing Census (PHC), QGIS, QField.*

Rezumat. Articolul descrie posibilitățile de promovare și implementare a tehnologiilor de geoinformație open-source în domeniul activității statistice în Republica Moldova, care vor simplifica și eficientiza procesul de analiză, colectare, sistematizare a datelor, precum și difuzarea acestora. Din 2019, Biroul Național de Statistică al Republicii Moldova, conform recomandărilor Națiunilor Unite, a propus crearea Registrului Statistic al Locuințelor (SRH) geocodat. Odată cu crearea Infrastructurii Naționale de Date Spațiale (NSDI), acest obiectiv poate fi atins, întrucât SSR va sta la baza Recensământului Populației și Locuințelor (PHC) din runda 2020. Datele geospațiale de la SRH vor fi utilizate pentru delimitarea zonelor de enumerare a recensământului, iar populația revizuită va fi atașată la coordonatele geografice ale locuinței. Aceste zone de enumerare vor acoperi întreg teritoriul Republicii Moldova și vor servi pentru planificarea resurselor umane, organizarea activităților de teren și

asigurarea acoperirii integrale a unităților de recensământ (pentru persoane, gospodării și locuințe).

Cuvinte cheie: *Registrul Statistic al Locuințelor (SRH), Sisteme Informaționale Geografice (GIS), Recensământul Populației și Locuințelor (PHC), QGIS, QField.*

Introduction

Numerous real-world examples, with clear explanations of the methodology, demonstrate the usefulness of geographic information systems (GIS) for solving practical problems in various fields of activity [1, 2].

In the field of statistics, high quality data are of particular importance for a contemporary country. They are essential for solid decision-making, which will affect the daily lives of citizens. The implementation of geo-informational technologies in statistics will simplify and streamline the data collection process as well as their dissemination [3, 4].

Given that the update of the Statistical Register of Housing (SRH) in the Republic of Moldova is a very important database for the future census in 2023, the use of GIS technologies, especially open-source, are welcome. SRH is a database of all dwellings, regardless of the form of ownership, including specialized houses (dormitories, boarding houses, penitentiaries and others), apartments, service rooms and other houses in other useful constructions for living. Until 2019 there was no such register, an alternative used being the Lists of Buildings and Housing (LBH), prepared by the Local Public Authorities (LPA) together with the Territorial Statistics Offices (TSOs). These lists were difficult to use because not all dwellings had an address, and even if they did, they were not standardized [5].

According to the recommendations of the United Nations, our country has proposed the creation of the geo-coded Statistical Register of Housing (each dwelling must have x and y coordinates).

In this sense, in order to achieve the proposed goal, the following objectives have been outlined:

- analysis, collection and systematization of housing data, from official sources of administrative data;
- presenting the structure of the SRH layers and explaining the variables;
- choosing and establishing methods for collecting and storing data in a database, using the open-source applications QGIS [6,7] and QField [8];
- populating, validating and processing housing data in SRH.

Data collected and structuring of SRH layers

When updating the SRH for the study area were served the following sources of geospatial data:

- Real Estate Register (RER), managed by the Public Services Agency (ASP) [9];
- State Register of Administrative-Territorial Units and Addresses (SRATUA), Public Services Agency (ASP) [9];
- Linear Map 2017, State Enterprise Institute of Geodesy, Engineering Research and Cadastre "INGEOCAD" under the coordination of the Agency for Land Relations and Cadastre of the Republic of Moldova (ARFC) [10];
- Orthoimages (Orthophoto) 2007/2016/2020, State Enterprise Institute of Geodesy, Engineering Research and Cadastre "INGEOCAD" under the coordination of the Agency for Land Relations and Cadastre of the Republic of Moldova (ARFC) [10];

For areas that were not covered by the geospatial data listed above or whose source is obsolete, field data were collected.

The database that will contain the homes which we are going to update will be of the *SpatiaLite* type [11] and will be called *"ActRSL_Ialoveni"*. It will consist of the *"Buildings"* layers, of point type (Table 1) and *"Dwellings"*, of table type (Table 2) [5, 12].

Table 1

Structure of the "Buildings" layer

No.	Name	Type	Description	Values
1	Commune	Text, 150 char.	Commune name	
2	Locality	Text, 150 char.	Locality name	
3	ID_ea	Text, 12 char.	Enumeration area code	
			Address data	
4	ID_Entry	Integer, 3 char.	Building entry ID	
5	CODE_ Building	Integer, 3 char.	Building code	
6	JID_ Entry	Text, 20 char.	Building-entrance code	
7	Street_ type	Text, 15 char.	Street type	1) Street; 2) Stradella; 3) Boulevard; 4) Road; 5) City Square; 6) Blind alley; 7) Other.
8	Street	Text, 150 char.	Street name	
9	Number	Integer, 3 char.	Building number	
10	Slash	Text, 10 char.	Slash	
11	Stair	Integre, 2 char.	Stair number	
			Building data	
12	Build_Cond.	Text, 150 char.	Building condition	1) With all structural components 2) Under (re)construction 3) Damaged / ruined 4) Demolished

Continued Table 1

13	Build_Use.	Text, 150 char.	Building use	1) For residential purposes only 2) Residential and other purpose 3) Non-residential
14	Build_Type.	Text, 150 char.	Building type	1) Detached house 2) Row house 3) Apartment building 4) Collective living quarter 5) Accessory building for the main building 6) Industrial 7) Commercial 8) Educational 9) Health 10) Institutional 11) Others
15	Nr_ Floors	Integer, 2 char.	Total number of floors in the building	
16	Nr_ Dwell.	Integer, 3 char.	Total number of dwellings in the building	
17	List_ Dwell.	Text, 254 char.	Dwelling list	
18	Notes	Text, 254 char.	Notes	

Table 2

Structure of the "Dwellings" layer

No.	Name	Type	Description	Values
1	ID_ Dwell.	Integer, 3 char.	Dwelling ID	
2	CODE_ Entry	Text, 20 char.	Building-entrance code	
3	Floor	Integer, 2 char.	Floor number	
4	Apartment	Text, 10 char.	Apartment number	
5	DirectAccess	Text, 2 char.	Presence of a direct access from outside the building	1) Yes 2) No

Continued Table 2

6	Type Dwelling	Text, 15 char.	Dwelling type	1) Conventional dwelling 2) Unconventional dwelling 3) Collective living quarter 4) Business unit 5) Unit for Institutional or cultural use 6) Unit used as accessory of the building 7) Ruined unit 8) Others 9) Non-existent
7	Notes	Text, 254 char.	Notes	

Results - Case study

For the case study, two pilot enumeration area from the Republic of Moldova were chosen, namely from Ialoveni district:

- 552000002061 from the village of Milestii Mici [13] (Figure 1 (a)), where it took place massive primary real estate registration, and in the Population and Housing Census (PHC-2014) 126 dwellings were identified [14];
- 552300004023 from the village of Pojareni [13] (Figure 1 (b)), where it did not take place massive primary real estate registration, and at PHC-2014, 87 dwellings were identified [14].

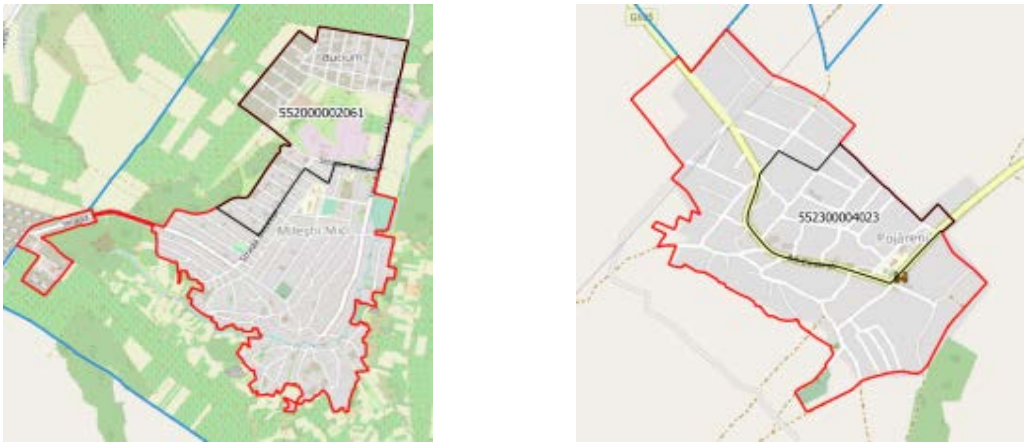

a) b)

Figure 1. Excerpt from the enumeration area boundaries:
a) 552000002061 Milestii Mici; b) 552300004023 Pojareni

Source: [5].

The process of updating the SRH will include three stages: population of the register; data validation; data processing.

Population of the register.

In the first stage, using the open-source application QGIS, SRH was populated based on administrative data and orthophoto images, as follows:

- Pilot enumeration area of the Population and Housing Census (PHC) - 2014, defined the work area [14];
- Address point of the building from SRATUA, was used to complete the variables for the address;
- Land and buildings from Real Estate Register, were needed to define the boundaries between the properties and to identify the buildings and their use;
- Roof Area from the Linear Map 2017, completed the *Buildings* layer, especially in the areas where it did not take place massive primary real estate registration;
- Orthophoto images have completed the *Buildings* layer and Roof Area, especially in high-speed construction areas.

The database in QGIS will contain the dwellings to be updated and will be named "ActRSL_Ialoveni", which will consist of the *Buildings* layer, of point type and *Dwellings* of table type (Tables 1 and 2).

Following this stage, there were obtained a total of 917 buildings: 613 in the enumeration area 552000002061 from Milestii Mici (Figure 2 (a)) and 304 in the enumeration area 552300004023 from Pojareni (Figure 2 (b)).

a) b)

Figure 2. Excerpt from the distribution and classification of buildings after the population of the SRH from administrative data and orthophoto images:
a) 552000002061 Milestii Mici; b) 552300004023 Pojareni
Source: [5].

In the village of Pojareni 97% of the buildings are with all the structural components, of which 38% are used only for residential purposes and another 59% for non-residential purposes. 100% of the residential buildings are of the individual house type, and in the

category of non-residential buildings 53% are auxiliary buildings of the household and another 40% are buildings without capital walls.

In the village of Milestii Mici 94% of the buildings are with all the structural components, of which 38% are used only for residential purposes and another 56% for non-residential purposes. 99% of the residential buildings are of the individual house type, and in the category of non-residential buildings 62% are auxiliary buildings of the household and another 32% are buildings without capital walls.

Data validation.

Given that administrative data, used in the SRH population, is not always current and it is necessary to go to the field and validate the data obtained directly from the source.

The QField open-source mobile application was used to accomplish this step. The QField application uses the same graphical editing controls as the QGIS desktop [8].

To create a project in the QField application, we will use the *"QFieldSync"* plugin, which will help us to prepare and package QGIS projects for QField. The QField project will be based on the QGIS project *"ActRSL_Ialoveni"*

In this case, a copy of this project will be created with the name *"ActRSL_Ialoveni_QField"*, where only the necessary layers from the field will be kept.

Thus, in the QGIS platform, this project was created for data collection in the QField application (Figure 3).

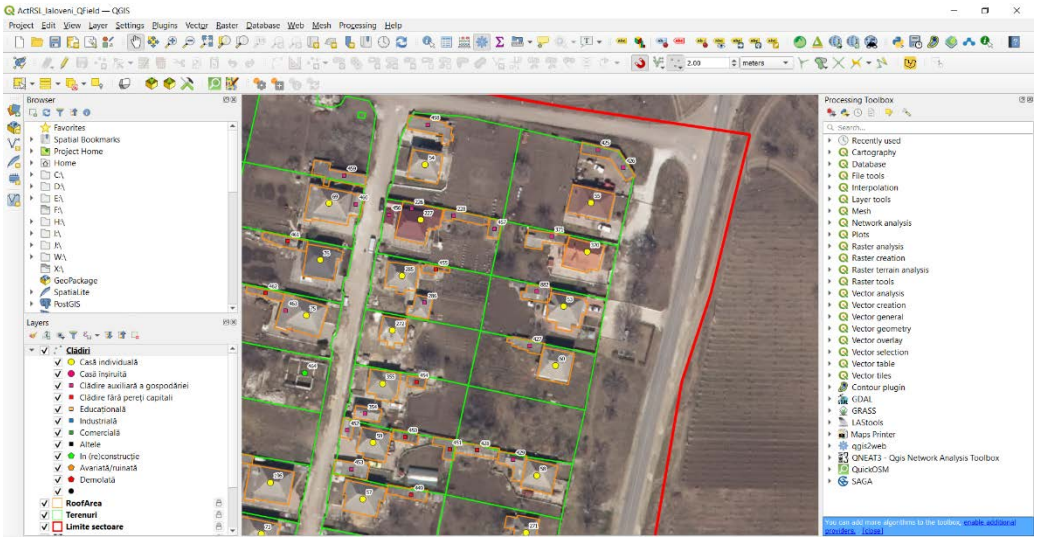

Figure 3. Creating the project for collecting data from the field.
Source: [5].

This project is exported and uploaded to the mobile device via a USB. To open the project in the QField application, will be performed the following steps from Figure 4: (1) *„Open local file"*; (2) choosing the location of the file; (3) opening the project with the terminations "*qgs*".

With the help of the tools for enlarging, reducing and finding the user's location, the pilot area will be navigated. So, when we are in the field, we will visit each building and check the correctness of the classification using the QField application (Figure 5).

To view the data of a building, is accessed the geometry of the building (1), and from the *"Features"* window (2) is selected from the list the desired building, based on the code *"pkuid"* (3). To edit the existing data, go to the *"Enable editing"* button (4), and from the list (5) you will find the move buttons *"Move Feature"* (6), move duplication *"Duplicate Feature"* (7) or

delete the object *"Delete Feature"* (8). And by accessing the check mark (9) we will save the created changes.

Figure 4. Opening of the *"ActRSL_Ialoveni_QField"* project.
Source: [5]

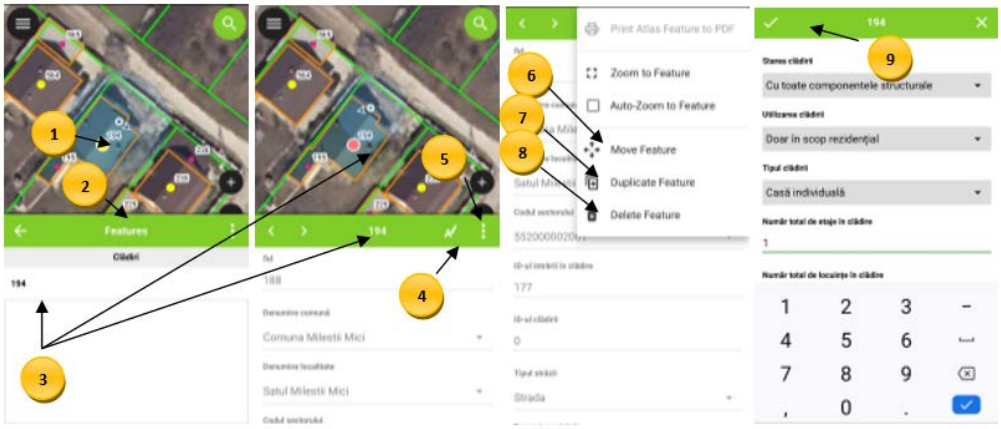

Figure 5. Visualization, editing and saved an object in QField.
Source: [5].

Data processing.

After the field verification, we move on to the third stage, that of data processing. The data processing step involves downloading the data collected in the field, from the mobile device to the computer, with their repeated verification and uploading as a final variant in the SRH database.

Following the data analysis, were obtained a total of 916 buildings: 615 in the 552000002061 enumeration area in Milestii Mici (Figure 6 (a)) and 301 in the 552300004023 enumeration area in Pojareni (Figure 6 (b)).

In Pojareni village 92% of the buildings are with all the structural components, of which 39% are used only for residential purposes and another 53% for non-residential purposes. 100% of the residential buildings are of the individual house type, and in the category of non-residential buildings 54% are auxiliary buildings of the household and

another 40% are buildings without capital walls. At the same time, 1% of the buildings are in (re) construction, 6% are damaged and 1% are demolished.

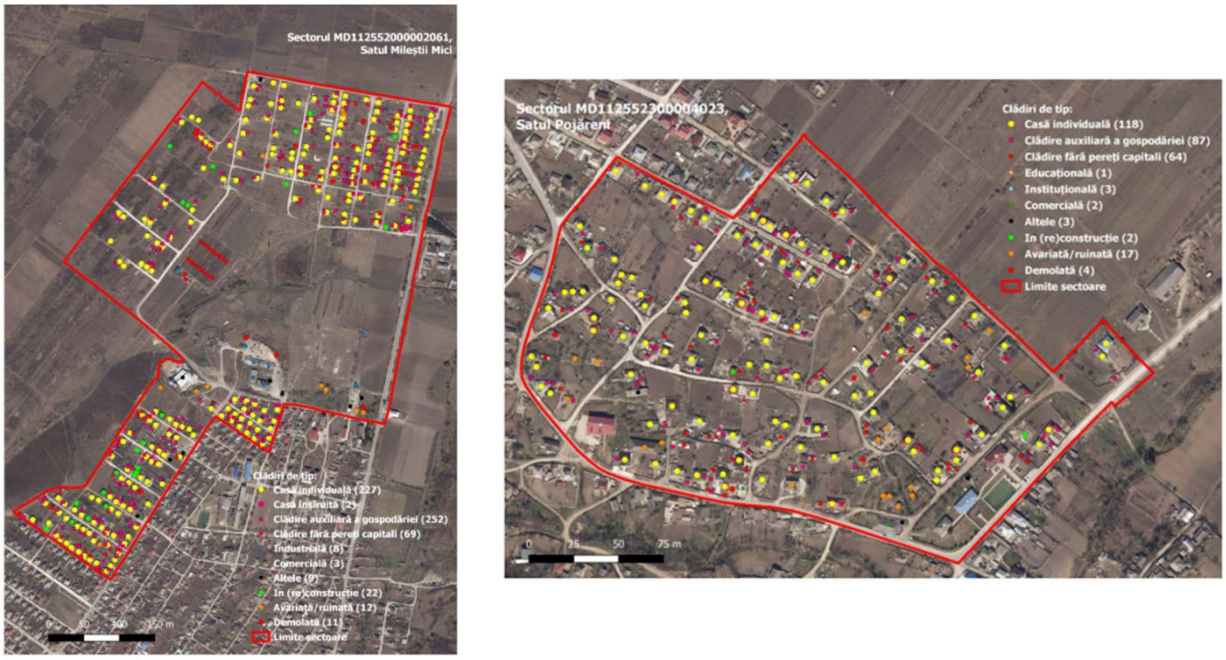

a) b)

Figure 6. Excerpt from the distribution and classification of buildings according to the field data validation process: a) 552000002061 Milestii Mici; b) 552300004023 Pojareni.
Source: [5].

In the village of Milestii Mici, 93% of the buildings are with all the structural components, of which 37% are used only for residential purposes and another 55% for non-residential purposes. 99% of the residential buildings are of the individual house type, and in the category of non-residential buildings 74% are auxiliary buildings of the household and another 20% are buildings without capital walls. At the same time, 4% of the buildings are in (re) construction, 2% are damaged and 2% are demolished.

Conclusions

Comparing the number of dwellings registered at PHC-2014 with those collected in this paper, there is an increase of 26% in the case of Pojareni village, from 87 dwellings registered at PHC-2014 to 118 recently identified. And in the case of the village of Milestii Mici, an increase of 45%, from 126 dwellings in the PHC-2014 to 229 recently identified.

The increase in the number of dwellings is largely influenced by two factors: the first factor would be the spatial mismatch of the dwellings in the census enumeration area in the spatial base with those in the database collected at the census. And the second reason is due to a positive dynamics of various constructions in the localities near the municipality of Chisinau.

The implementation of open-source GIS technologies are recommended in the field of statistical activity in the Republic of Moldova. Their use will lead to an increase in the quality of data collected and disseminated, will reduce the team involved in data collection and monitoring, while reducing the cost of statistical work.

References

1. Peter A. Burrough, Rachael A. Mcdonnel, Cristopher D. LLOYD. *Principles of Greogrphical Information Systems*, Oxford, University Press, 1998.
2. Davis D. E. *GIS for everyone*. Third Edition, ESRI Press, Redlands, California, 2003, 152 p.
3. Spătaru M., Iacovlev A. *Reflectarea distribuției grafice a populației pe localități în proces și la finalizarea recensământului populației*. In: Materials of the Technical-Scientific Conference of Students, Master and Doctoral Students TUM, March 23-25, 2021, Chisinau, Vol. II. ISBN 978-9975-45-701-9, pp. 35-38.
4. Grama V., Dilan V., Cepoi E. *Tehnologii geoinformaționale avansate*. TUM, 2013, 260 p.
5. Spătaru M. *Utilizarea tehnologiilor GIS open-source pentru actualizarea Registrului Statistic al Locuințelor din Republica Moldova*. Master Thesis. Chisinau, TUM, 2022.
6. QGIS User Guide. [online], [access 14.12.2021]. Available: https://docs.qgis.org/2.18/pdf/en/QGIS-2.18-UserGuide-en.pdf. 6
7. User Manual - QGIS. Version 2.0. [online], [access 16.12.2021]. Available: http://adrnord.md/public/files /publication /GIS_manual_dhv_final.pdf
8. QField Documentation. [online], [access 20.12.2021]. Available: https://qfield.org/docs/ro/
9. Geoserver. [online], [access 15.10.2021]. Available: https://moldova-map.md/geoserver/web/
10. Geoportal INDS. [online], [access 15.10.2021]. Available: http://www.geoportalinds.gov.md/
11. SpatiaLite. [online], [access 21.12.2021]. Available: https://www.gaia-gis.it/fossil/libspatialite/home
12. Galer L. *Manual metodologic privind efectuarea procedurii de actualizare a hărților (colectare date georeferențiate referitor la clădiri și locuințe).* Chisinau: NBS, 2021.
13. National Bureau of Statistics of the Republic of Moldova: *Clasificări şi nomenclatoare*. [online], [access 31.10.2021]. Available: https://statistica.gov.md/pageview.php?l=ro&idc=385
14. National Bureau of Statistics of the Republic of Moldova: *Solicitare de informații statistice*. [online], [access 31.10.2021]. Available: https://statistica.gov.md/solicitare_informatii_statistice.php?l=ro

Journal of Engineering Science *Vol. XXIX, no. 2 (2022), pp. 133 - 143*
Fascicle *Architecture, Civil and Environmental Engineering* *ISSN 2587-3474*
Topic *Environmental Engineering* *eISSN 2587-3482*

https://doi.org/10.52326/jes.utm.2022.29(2).13
UDC 620.95:633.282

PERSPECTIVES FOR THE USE OF BIOMASS GENERATED BY SOME MISCANTHUS GENOTYPES IN THE PRODUCTION OF DENSIFIED SOLID BIOFUELS

Nicolae Daraduda*, ORCID: 0000-0001-5683-0431,
Grigore Marian, ORCID: 0000-0002-9975-2522

State Agrarian University of Moldova, 44 Mircesti Str., Chisinau, Republic of Moldova
*Corresponding author: Daraduda Nicolae, *n.daraduda@uasm.md*

Received: 03. 22. 2022
Accepted: 05. 12. 2022

Abstract. Miscanthus is a Poaceae family perennial crop of C4 bioenergy characterized by the multilateral use potential, including the production of biofuels. The paper aimed to study the opportunity to use the biomass generated by two Miscanthus genotypes: *Miscanthus* × *giganteus* and *Miscanthus sinensis* in the production of densified solid biofuels. We quantified the biomass generated by crops that were 5 years old, harvested from both genotypes after the vegetation period, the year 2020. Samples were taken from the experimental lots of the Alexandru Ciubotaru National Botanical Garden (Institute) from the Republic of Moldova in autumn, immediately after the initial onset of senescence and in spring of the following year, before the start of the growing season. The results showed that the above-ground biomass generated by both *Miscanthus* genotypes harvested in spring had had significantly higher quality characteristics compared to the biomass harvested in autumn. Virtually all qualitative indices of the *Miscanthus* × *giganteus* biomass harvested in spring comply with the requirements of the ENPlus international standards for densified solid biofuels. The *Miscanthus sinensis* biomass, both, had lower indices than the *Miscanthus* × *giganteus* biomass from both qualitative and quantitative points of view and the former can be used as a filler in various mixtures of raw material for the production of solid biofuels.

Keywords: *energy crops, Miscanthus x giganteus Titan, Miscanthus sinensis, biomass properties*

Rezumat. Miscanthus este o cultură perenă din familia Poaceae de bioenergie C4, caracterizată prin potențial de utilizare multilaterală, inclusiv în producția de biocombustibili. Lucrarea își propune să analizeze oportunitatea utilizării biomasei generate de două genotipuri de Miscanthus: *Miscanthus* × *giganteus* și *Miscanthus sinensis* în producția de biocombustibili solizi densificați. A fost cuantificată biomasa generată de culturi vechi de 5 ani, recoltate de la ambele genotipuri după perioada de vegetație, anul 2020. Au fost prelevate probe din loturile experimentale ale Grădinii Naționale Botanice (Institutul) Alexandru Ciubotaru din Republica Moldova toamna, imediat după debutul senescenței și în primăvara anului următor, înainte de începerea sezonului de vegetație. Rezultatele au arătat că biomasa supraterană generată de ambele genotipuri de Miscanthus recoltate primăvara a

avut caracteristici de calitate semnificativ mai mari în comparație cu biomasa recoltată toamna. Practic, toți indicii calitativi ai biomasei de *Miscanthus* × *giganteus* recoltați primăvara respectă cerințele standardelor internaționale ENPlus pentru biocombustibili solizi densificați. Biomasa *Miscanthus sinensis*, ambele variante, au avut indici mai mici decât biomasa *Miscanthus* × *giganteus* atât din punct de vedere calitativ cât și cantitativ, iar prima poate fi folosită ca umplutură în diverse amestecuri de materie primă pentru producerea de biocombustibili solizi.

Cuvinte cheie: *culturi energetice, Miscanthus x giganteus Titan, Miscanthus sinensis, proprietăți ale biomasei*.

Introduction

Biomass biofuels are currently considered as one of the main alternative energy sources. However, the use of plant lignocellulosic biomass as a raw material in the production of densified solid biofuels in the Republic of Moldova has only been flourishing for the last two decades. Particular attention in the biomass fuel production chain is focused on identifying certain types of biomass that can provide sufficient quantities to initiate the production of densified solid biofuels that can compete with traditional solid fuels [1]. Therefore, the biomass generated by some perennial energy plants has a special role in the process. The cultivation of perennials is argued by the fact that they present promising prospects for several sectors of the bioeconomy [2], ensuring the production of both a whole range of biomass industrial products and the production of renewable energy [3].

The main purpose of producing renewable energy from biomass is to replace fossil energy resources with biological ones [4]. It should be noted that the production of bioenergy is one of the nine objectives of the European Parliament's proposal on agricultural policy for 2021-2027 [5], which is particularly focused on the ongoing development of renewable energy sources.

This study emphasizes the qualitative estimation of the biomass generated by some perennials, which are suitable for cultivation under the conditions of the Republic of Moldova in terms of comparing their characteristics with those imposed by EN Plus 3 European standards.

Biomass quality is one of the most important factors that affect the performance of the final product and serves as an argument to start a business that would produce densified solid biofuels in the given geographical area [6,7]. The most important characteristics of the biomass used for energy purposes refer to the combustion power expressed by the calorific value, the content of moisture, ash and volatiles, the content of C, O, S, N and Cl.

It is also interesting to establish the content of the most important carbohydrate components of the biomass (lignin, hemicellulose and cellulose), the components that directly affect the quality of densified solid biofuels and the technological capacity to process and modify some properties by means of various thermochemical processes [1 pp. 26-28; 8]. The need for this study also derives from several researchers' statements about the dependence of the properties and productivity of energy crops on the region where they are grown, their genotype and agricultural management [9, 10-12].

The paper aims to consider and experimentally verify the opportunity to use the biomass generated by the *Miscanthus* × *giganteus (M.* x *giganteus)* and *Miscanthus sinensis* (*M. sinensis*) genotypes as a raw material for the production of densified solid biofuels in the form of pellets and briquettes.

The *Miscanthus* biomass samples taken from the experimental fields of the Alexandru Ciubotaru National Botanical Garden (Institute) from the Republic of Moldova in 2020 and 2021 served as the object of the research.

The study was conducted within the SAUM Solid Biofuels Laboratory using standard methods testing densified solid biofuels. As a result of the speciality literature review and experimental results on the use of the *Miscanthus biomass* as a raw material in the production of pellets and briquettes, it has been noted that this energy crop is a safe source of raw material for the production of densified solid biofuels, as well as has some other uses in bio-economy.

Materials and methods

Biomass selection, sampling and sample preparation. The biomass and densified solid biofuels in the form of pellets and briquettes from two *Miscanthus* genotypes: *M.* x *giganteus Titan* and *M. sinensis* were studied. Both types of biomass were taken from the experimental fields of the Alexandru Ciubotaru National Botanical Garden (Institute) of the Republic of Moldova. The samples were taken from the plantations, established in 2015.

The biomass for this study was taken from the harvest of 2020, i.e. in the fifth year of vegetation. Biomass samples were harvested from several randomly selected middle cuttings using manual cutters (see Figure 1). The surface of the cuts was set at 2 m^2, and the cutting height of approx. 5 cm. The samples were collected in two periods: in November, immediately after the initial onset of senescence and at the beginning of March of the following year (2021), before the start of the vegetation period.

The biomass harvested in autumn was dried by the forced conversion method in the SAUM Solid Biofuels Laboratory Dryer, and the spring harvest was naturally dried right in the field. The moisture at harvest was determined for both types of samples.

Figure 1. The process of harvesting the Miscanthus × giganteus biomass on the experimental field of the Alexandru Ciubotaru National Botanical Garden (Institute) from the Republic of Moldova in the spring of 2021.

Samples were taken at random from whole reeds, per about 200 kg during both harvest periods. Both the samples taken in autumn and those taken in spring were initially coarsely ground with the help of the ROJEK 517 50 branch shredder, produced in the Czech Republic. Chip sizes after shredding ranged from 50 to 100 mm.

Biomass sampling for testing was performed after manual biomass homogenization in accordance with the requirements of SM EN ISO 18135: 2017. The biomass samples and final products in the form of pellets and briquettes were prepared according to the requirements of EN ISO 14780: 2017. Thus, five samples were prepared for each sample group. The samples had been shredded beforehand in the SV 7 shredder with a 6 mm mesh screen.

Proximity analysis of the biomass. In order to be able to forecast the costs related to the biomass transportation and storage as well as to determine the biomass energy density, the bulk density of coarsely crushed biomass was determined immediately after harvest and estimated while the moisture content was 10% (reference moisture content for densified solid biofuels).

The bulk density was determined according to the SM EN ISO 17828: 2017 standard using the 50-litre container. The size of the biomass after shredding ranged from 35 to 100 mm.

The bulk density of the biomass at harvest was determined by means of the following relation:

$$BD_{ar} = \frac{m_2 - m_1}{V}, \quad (1)$$

where m_1 is the mass of the empty container, kg; m_2 is the mass of the container with the studied biomass sample, kg.

The bulk density of the dry base was determined by the relation:

$$BD_d = BD_{ar} \cdot \frac{100 - M_{ar}}{100}, \quad (2)$$

The bulk density for the given moisture content of the biomass was calculated as follows:

$$BD_{M\%} = BD_d \cdot \frac{100}{100 - M_{ar}} \quad (3)$$

where M is the moisture content at harvest,%

The moisture content was measured immediately after harvest by drying in accordance with the requirements of the standard SM EN ISO 18134-3: 2017. Drying was performed by keeping the temperature stable (105 ± 2) °C in the German oven Memmert UNB 100 until the dry samples obtained the same mass. Before drying, the samples were shredded in the SM 100 cutting mill, produced by the German company Retsch with a 1 mm mesh screen.

The ash content was determined by thermogravimetric testing in accordance with the requirements of the standard SM EN ISO 18122: 2017. The samples to be tested were previously ground in the SM 100 cutting mill with a 1 mm mesh screen. Next, the crushed mass with a grain size of up to 1 mm was dried in the Memmert heat-adjustable oven to zero humidity, according to the SM EN ISO 18134-3: 2017 standard. Calcination of the samples had been done in the oven with an LH 05/13 socket for 6 hours at the temperature of 550 °C.

The percentage of ash resulting from calcination was calculated using the following equations:

$$A_d = \frac{(m_3 - m_1)}{(m_2 - m_1)} \cdot 100, \quad (4)$$

$$A_M = A_d \cdot \left(\frac{100}{100 - W}\right), \quad (5)$$

where A_d is the dry ash content; A_M is the ash content with the moisture content of the biomass M %; m_1 is the mass of the empty crucible, g; m_2 the mass of the crucible plus the mass of the sample subjected to testing with 0% moisture, g; m_3 is the mass of the crucible plus the mass of ash, g; W is the moisture of the analyzed sample,%.

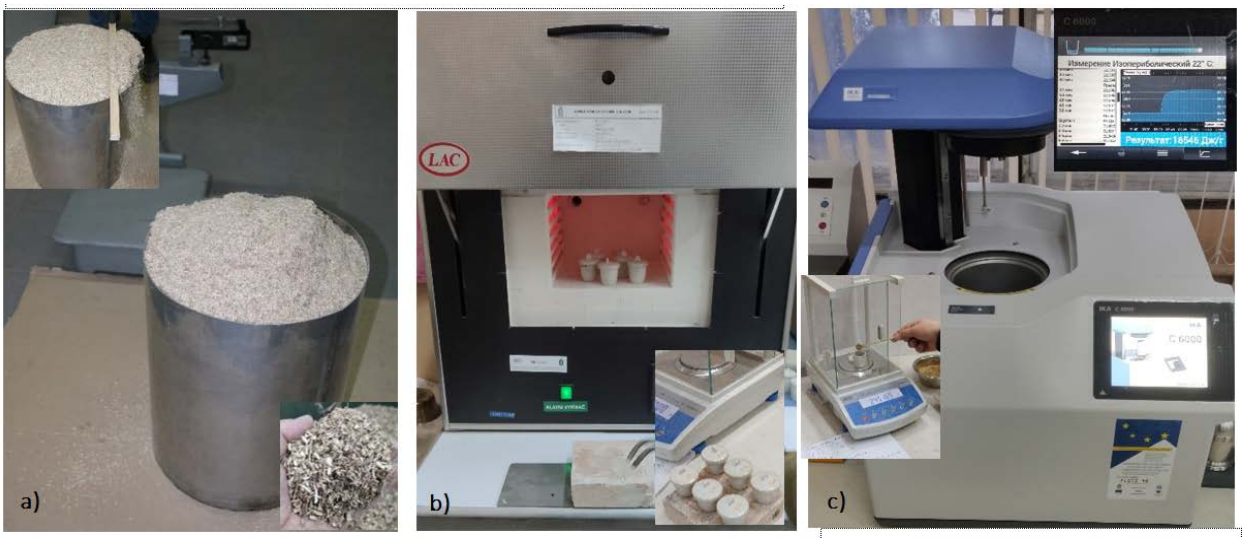

Figure 2. Sequences during miscanthus biomass analysis: *a) bulk density; b) ash content; c) calorific value.*

The content of volatiles for the studied samples V_d, expressed as a percentage, in relation to the mass in the dry base shall be calculated by the following formula:

$$V_d = \left[\frac{100(m_2-m_3)}{m_2-m_1} - M_{ad}\right] \cdot \left[\frac{100}{100-M_{ad}}\right] \quad (6)$$

where m_1 is the mass of the empty ampoule with a lid, g; m_2 is the mass of the ampoule with a lid and the tested sample before drying, g, m_3 is the mass of the ampoule with a lid and non-volatile residues after drying, g; M_{ad} is the moisture content of the analyzed sample in % determined in accordance with the standard SM EN ISO18134-3.

Biomass energy capacity. To determine the possible amount of heat that could be obtained from the burning of the studied biomass, its combustion power was determined by measuring the higher calorific value and calculating the net calorific value and energy density.

The highest calorific value was established in accordance with the requirements of the SM EN ISO 18125: 2017 standard by calcining the samples in the German isoperibolic calorimetric pump IKA C6000.

The net calorific value was calculated for the samples with the moisture of 0 and 10%, tested at constant pressure by means of the following formulas:

$$q_{p,net,d} = q_{v,gr,d} - 212.2 \cdot w(H)_d - 0.8 \cdot [w(O)_d + w(N)_d], \quad (7)$$

$$q_{p,net,M=10\%} = q_{v,gr,d} - (1-0.01M) - 24.43M, \quad (8)$$

where $q_{v,gr,d}$ is the highest calorific value at the constant volume, J/g; $q_{p,net,d}$ is the net calorific value measured for the samples with the moisture content of 0, J/g; $q_{p,net,M=10\%}$ is the net calorific value for the samples with the moisture of 10%, J/g; $w(H)_d$ is the mass participation of hydrogen determined in the dry basis, %; $w(O)_d$ is the mass participation of oxygen determined in the dry basis, %; $w(N)_d$ is the mass share of nitrogen determined in the dry basis, %.

Energy density was determined as the amount of energy stored per unit volume by means of the following relation:

$$Ed_{M=0} = BD_d \cdot q_{p,net,d}. \quad (9)$$

$$Ed_{M=10\%} = BD_{M=10\%} \cdot q_{p,net,M=10}. \quad (10)$$

where $Ed_{M=0}$ is the energy density of the dry base biomass; $Ed_{M=10\%}$ is the energy density of the biomass with the moisture content of 10%.

The proportions of C, H, N, S and Cl were analyzed using the elemental analyzer Vario Macro Cube CHNS & Cl, produced by the German company Elementary. The samples with the known mass are completely burned until the formation of gaseous combustion products, which separate on a chromatographic column.

The volatile matter content was determined for the *Miscanthus* samples, previously ground in the SM 100 cutting mill with a 1 mm mesh screen. The dimensions of the studied biomass particles did not exceed 1 mm and their mass was within (1 ± 0,1) g. The samples were kept for (7 ± 0,083) min in the oven with the LH 05/13 socket at the temperature of (900 ± 10) °C in accordance with the requirements of the standard SM EN ISO 18123: 2017.

Results and Discussions

Miscanthus is one of the perennial plants, which is among the most widespread energy crops, which can be potentially used as a raw material in the production of biofuels [13-15]. The energy potential of this crop is widely used in the United States and Europe, especially as a raw material for the production of biofuels [16]. *Miscanthus* is recognized due to its high socio-economic potential, perennial nature, high productivity and low cultivation requirements, since it can be cultivated extensively on soils, which are less suitable for other crops [17, 13]. The plant is resistant to diseases and pests [13; 4]. It is considered an effective plant for combating erosion; its cultivation can be carried out by means of agricultural techniques used in ordinary agrotechnical operations [18]. As it is a perennial crop, *Miscanthus* requires no circulation and can be cultivated for 15-20 years on soils less suitable for other crops [19].

Although *Miscanthus* seems to be a major candidate for the production of raw materials and continuous development of renewable energy sources from biomass, its production in the Republic of Moldova is at the initial stage, playing a minor role in national agriculture.

At the moment there are several registered varieties of *Miscanthus* thanks to the research carried out within the Alexandru Ciubotaru National Botanical Garden (Institute) from the Republic of Moldova. GIANT MISCANT, the Titan variety [20 p. 105] and four varieties of *Miscanthus* x *giganteus (JM Greef & Hodk & Renvoize*) - Aphrodite, Athena, Atropos and Titan (B) are among them [21 p. 92].

The *M.* × *giganteus* is an interspecies triploid hybrid from the natural cross of *M. sinensis* (2n = 2x) diploid and *Miscanthus sacchariflorus* (2n = 4 x) triploid, the Poaceae family, rhizome group C4 native to East Asia, which was introduced to Europe in the early 20th century as an ornamental plant [2, 22]. It has an erect stem, which is 2.5–3.5 m long (it can reach 5 m) with linear leaves that are 50–60 cm long and 2.8–3.3 cm wide, the ligule truncated with hairs, which 2–3 mm long. The inflorescence is a panicle, which is 30–55 cm long with branches of 15–21 cm, the harvest is 18-27 t/ha [23 pp. 36]. Its widespread use for the production of biofuels in Europe was registered at the end of the last century [24, 16].

The *M. sinensis* is a popular perennial herb, especially in warm areas, whose yields increase progressively in the first years of growth [25]. Generally speaking, the *M. sinensis* has characteristics, which are similar to those of the *M.* × *giganteus* genotype. However, it is an earlier species compared to the *M.* × *giganteus* and it is more tolerant to water stress. [26]. It has a lower yield than the *M.* × *giganteus*, with a lower aboveground biomass production [25], therefore the ability to use the *M. sinensis* genotype for energy purposes is less studied.

The following are the results of the biomass quantitative and qualitative study, resulting from the cultivation of the *M.* x *giganteus* genotypes, *Titan* and *M. sinensis* cultivated under the conditions of the Republic of Moldova. Energy capacity, proximal and final analysis are considered the most important parameters for the evaluation of the biomass used in the direct combustion process.

The main properties of the studied biomass are shown in Tables 1, 2 and 3. The values for the parameters presented in these tables represent the average calculated from five repetitions of each experiment and the confidence interval for each average value expressed as a standard deviation (σ) for the confidence level of 95% (α = 0.05) as $\overline{x} = \pm 1{,}96\frac{\sigma}{\sqrt{n}}$.

Moisture and ash content, volatiles and bulk density are considered as the elements of the proximal analysis. Carbon (C), hydrogen (H), oxygen (O), nitrogen (N), sulfur (S) and chlorine (Cl) are considered as final analyses.

Table 1

Proximity analysis of the *Miscanthus* x *giganteus* and *Miscanthus sinensis* biomass

Biomass	M_{rec}	A_d	$A_{r\,(M=10\%)}$	Vd	BD_{rec}	BD_d	$BD_{M=10\%}$
	%				kg/m^3		
M. x *giganteus titan (a.h.)*	43.2 ± 6	2.79 ± 0.03	3.1	81.49	182.6 ± 8	103.7	115.2
M.s x *giganteus titan (s.h.)*	18.4 ± 4	1.185 ± 0.1	1.32	83.65	142.4 ± 4	116.2	129.1
M. sinensis (a.h)	49 ± 7	4.07 ± 0.2	4.22	83.44	180.4 ± 7	92.0	102.2
M. sinensis (s.h.)	19 ± 3	2.21 ± 0.2	2.46	83.48	128.0 ± 3	103.6	115.2

Note: M_{rec} is the moisture content of the biomass at harvest; A_d is the dry ash content; $A_{r\,(M=10\%)}$ is the ash content calculated for the moisture content of the biomass equal to 10%; Vd is the volatile matter content; BD_{rec} is the bulk biomass density estimated immediately after harvest; BD_d and $BD_{M=10\%}$ is the bulk biomass density calculated in the dry base and for the moisture of 10% respectively; a.h. stands for „harvested in autumn"; s.h. stands for „harvested in spring".

Table 1 presents the results of the proximal biomass analysis generated by the two *Miscanthus* genotypes studied in this paper. Based on the analysis of the data from Table 1, it can be concluded that the moisture content of the biomass harvested in autumn, immediately after the initial onset of senescence, is significantly higher than that of the biomass harvested in spring, before the start of the growing season. Thus, the biomass harvested in autumn has a moisture content of approx. 2.5 times higher than the one harvested in spring (it is 45.2 ± 6 and 18.4 ± 4% respectively for the *M.* x *giganteus* and 49 ± 7% and 19 ± 3% respectively for *the M. sinensis*.

Having analyzed the data on the moisture content of the *Miscanthus biomass* studied in this paper, it can be concluded that the biomass harvested in spring can practically be processed directly into densified solid biofuels, without being further dried or by light drying under natural conditions.

It is important to note that the ash content of the biomass harvested in spring is significantly lower than that of the biomass harvested in autumn, with a decrease from 2.79%

to 1.32% for the *M.* x *giganteus* biomass and from 4.07% to 2,21% for the *M. sinensis*. This can be explained by the fact that the spring harvest had fewer leaves than the autumn one, as well as by the increased content of various mineral microparticles in the biomass harvested in autumn.

The volatile matter content is in the range of 81.49% in the *M.* x *giganteus titan (a.h.)* up to 83.65% in the *Ms* x *giganteus titan (s.h.)*. The biomass of the *M. sinensis* practically showed the same volatile matter content of 83.44% for the biomass harvested in autumn and 83.48% for the biomass harvested in spring.

The bulk density of both *M.* x *giganteus titanium* and *M. sinensis* biomass harvested in spring, recalculated in the dry base and at the average processing moisture in solid biofuels (10%) is higher than that of the one harvested in autumn. Thus, the dry bulk density of the *M.* x *giganteus* biomass harvested in spring (116.2 kg/m^3) is 16% higher compared to the biomass harvested in autumn (100.1 kg/m^3). As to the *M. sinensis* biomass, the ratio between the bulk density of the biomass harvested in spring and that harvested in autumn is even higher (approx. 26%), increasing from 82 kg/m^3 to 103.6 kg/m^3.

It should be noted that the bulk density of the *Miscanthus* biomass at harvest is inversely related to that previously established in the dry basis and for the moisture content of 10%. This is explained by the significantly higher moisture content at harvest of the biomass harvested in autumn compared to the biomass harvested in spring. This finding is an additional argument in favour of the autumn harvest of the *Miscanthus* biomass used in the production of densified solid biofuels. It should be also added that the biomass estimated directly after harvest, generated by the *M. x giganteus* has a bulk density of approx. 10% higher than that generated by the *M. sinensis*.

Table 2 shows the energy capacity of the biomass generated by the studied *Miscanthus* genotypes expressed by both the calorific value and energy density. The term calorific value refers to the amount of heat released by the complete and perfect combustion of a unit mass of particles and the cooling of the flue gas to 25 °C. [1 p. 56]. It is necessary to estimate the combustion power of the biomass by means of the highest and lowest calorific values.

Table 2

The calorific value and energy density of the biomass generated by the *M.* x *giganteus* and *M. sinensis* varieties

Biomass	$q_{V,gr,d}$	$q_{p,net,d}$	$q_{p,net,M=10\%}$	$Ed_{M=0}$	$Ed_{M=10\%}$
		J/g			MJ/m^3
M. x giganteus titan (a.h.)	18812.3 ± 245	17496.0 ± 252	15502.1 ± 124	1750.73	1723.57
M.s x giganteus titan (s.h.)	19688 ± 198	18409.1 ± 201	16578.3 ± 142	2139.1	2107.56
M. sinensis (a.h)	18685.2 ± 90.5	17552.8 ± 112	15553.2 ± 99	1615.11	1590.13
M. sinensis (s.h.)	19285.1 ± 175	18140.7 ± 176	16082.3 ± 156	1880.24	1852.10

Note: $q_{v,gr,d}$ is the highest calorific value at the constant volume; $q_{p,net,d}$ is the net calorific value in the dry base; $q_{p,net,M=10\%}$ is the net calorific value for the samples with the moisture of 10%; $Ed_{M=0}$ is the energy density of the biomass in the dry base; $Ed_{M=10\%}$ is the energy density of the biomass with the moisture content of 10%.

The highest calorific value is the total amount of heat that can be obtained from the combustion of a unit mass, including that from the condensation and transformation of vapours into water. However, under real combustion conditions, the water resulting from combustion is removed in the form of vapours together with the combustion products, without yielding the combustion heat hidden in the condensate. Therefore, our study presents the highest and lowest calorific values in the dry base, i.e. for the zero moisture, and the lowest value for the moisture of 10%, considering the average humidity at the reception of densified solid biofuels. [1 p. 46-53]. The calorific value of the biomass is closely related to the variation of the chemical composition and ash content, which can be traced by synchronizing the data in Table 1 with those in Table 2. Similarly, having analyzed the data in Table 2, we can state that the biomass harvested in spring had a slightly higher combustion power than that harvested in autumn and dried by means of the method of forced conversion. Thus, the biomass of the *Ms x giganteus titan (s.h.)* and *M. sinensis (s.h.)*, harvested in spring, showed higher calorific values of 19,688 ± 198 J/g and 19,285.1 ± 175 J/g respectively as compared to 18,812.3 ± 245 J/g and 18,685.2 ± 90.5 J/g for the biomass harvested in autumn.

Taking into account the difference in moisture content of the biomass harvested in spring compared to the one harvested in autumn, it can be deduced that harvesting biomass in spring is more advantageous for a number of economic reasons because in such a case the moisture conditioning of raw material before densification can be partially or completely excluded. Another important conclusion, which results from the analysis of the data in Table 2, is the possibility of obtaining densified solid biofuels with the combustion power at reception that corresponds to ENplus requirements, i.e. $q_r \geqslant 15.5$ MJ/kg - for briquettes and $q_r \geqslant 16$ Mj/kg - for pellets [27].

Table 3 summarizes the data obtained from the final analysis of the *Miscanthus* biomass. The final biomass analysis is extremely important as it has multiple effects, including the determination of the theoretical air-fuel ratio in thermal conversion systems in order to identify the thermal values and to know the level of environmental pollution.

This study has shown that the carbon content of the *M. x giganteus titan* biomass does not differ much from that of the *M. sinensis* biomass, though the difference is noticeable depending on the terms of harvest. Thus, the biomass harvested in spring has a carbon content of approx. 5 ... 6%. Correspondingly the situation with the oxygen content is opposite, i.e. the biomass harvested in autumn contains more oxygen than that harvested in spring (the difference of about 10%). The nitrogen content does not differ much depending on the harvest season, but the *M. x giganteus titan* biomass has a much higher nitrogen content than the *M. sinensis* biomass. It is necessary to mention that the studied biomass is in line with the ENPlus requirements in terms of this indicator. This moment is extremely important because the increased nitrogen content leads to the formation of nitrogen oxides (NO_x) which favours the formation of acid rain and smog [1 p. 75].

Table 3

Final biomass analysis (mass participation, %)

biomass	C	H	N	S	Cl	O (rest)
M. x giganteus titan (a.h.)	46.51	6.04	0.44	0.04	0.03	44.19
Ms x giganteus titan (s.h.)	49.07	5.86	0.47	0.04	0.04	43.38
M. sinensis (a.h.)	46.01	5.17	0.28	0.06	0.03	44.41
M. sinensis (s.h.)	49.01	5.23	0.27	0.05	0.03	43.02

A slightly increased sulphur content is noticeable for all biomass species. Although sulphur produces a large amount of heat when burned, its content in biofuels is limited to 0.05% because it is considered unfriendly to the environment and has increased corrosive activity. The chlorine content is within the limits of 0.03 ... 0.04%, practically within the limits required by the ENPlus standards.

Conclusions

Laboratory analysis of the biomass generated by two energy crops, the *M. x giganteus titan* and *M. sinensis*, show that the biomass harvested in spring before the beginning of the growing season has a moisture content (18.4 ± 4% and 19 ± 3% respectively), which is significantly lower than in the case of the biomass harvested in autumn immediately after the initial onset of senescence (45.2 ± 6% and 49 ± 7% respectively), which allows us to conclude that the biomass harvested in spring can be processed directly into densified solid biofuels without being further additionally dried forcefully or under natural conditions.

The biomass harvested in spring showed other high-quality parameters compared to those specific to the same type of biomass, harvested in autumn: respectively, the ash content for the *M. x giganteus titan* is 2.4 and it is 1.8 times lower for the *M. sinensis*; the calorific value at the moisture level of 10% was respectively 1.07 and 1.03 times higher; the energy density was respectively 1.22 and 1.11 times higher.

The chemical analysis of the studied biomass showed that the chemical composition of the *M. x giganteus titan* biomass does not differ much from that of the *M. sinensis* biomass, but the difference is noticeable depending on the terms of harvest.

The biomass used for the production of densified solid biofuels is recommended to be harvested in spring before the beginning of the growing season.

Virtually all qualitative indices of the *M. × giganteus* biomass harvested in spring comply with the international ENPlus standards on densified solid biofuels, so it can be used as a raw material in the production of pellets and briquettes.

The *M. sinensis* biomass has lower indices than the *M. × giganteus* biomass from both qualitative and quantitative points of view and can be used as a filler in the creation of various mixtures of raw material for the production of densified solid biofuels.

According to the development prospects of renewable energy sources, *Miscanthus* is likely to be one of the important contributors of biomass used as a raw material in the production of densified solid biofuels under the conditions of the Republic of Moldova.

The obtained results can be used by producers of densified solid biofuels as an argument for the use of the Miscanthus biomass as a raw material in the production of pellets and briquettes from plant biomass. Similarly, the results can serve as reference material for the argumentation of raw material mixtures based on Miscanthus.

Acknowledgements: This study was carried out thanks to the funding provided by the project 20.80009.5107.02 no. 42.2-PS within the State Program of the Republic of Moldova and fruitful cooperation with the team of the Alexandru Cebotaru Botanical Garden (Institute), particularly with Dr Victor Titei, the head of the Laboratory of Plant Resources. The authors thank Andrei Gudima, Boris Nazar and Alexandru Banari, the co-workers of the Laboratory of Solid Biofuels from the State Agrarian University of Moldova for their assistance in sampling and support in obtaining experimental data and statistical processing.

References

1. Marian Gr. Solid biofuels, production and properties. Ch: Bons Offices, 2016. pp. 172. ISBN 978-9975-87-1662.
2. Winkler B., et al. Implementing Miscanthus into farming systems: A review of agronomic practices, capital and labor demand. Renewable and Sustainable Energy Review. ELSEVIER, 2020, Vol. 132.
3. Țiței V. and Teleuță A. Perennial species and plant varieties for founding energy plantations in the Republic of Moldova. Intellect. 2014, Vol. 4, pp. 88-93.
4. Lewandowski I. Securing a sustainable biomass supply in a growing bio-economy. Global Food Security. ELSEVIER, 2015, Vol. 6, pp. 34-42.
5. PE. https://www.europarl.europa.eu/doceo/document/O-9-2020-000005_EN.html [accessed 18.02.2022]
6. Alakangas Eija. Biomass and agricultural residues for energy generation. In: Fuel Flexible Energy Generation. 2016, pp. 59-96.
7. Marian G., et al. Estimation of the heat capacity of lignocellulosic biomass from different areas of the Republic of Moldova in the concept of solid fuel production. In: Agricultural Science. UASM, 2013, Vol. 1, pp. 56-62.
8. Marian G., Gudîma A., Pavlenco A., Gorobeț V. *Torefierea* - a new direction to increase the quality of fire pellets produced from local biomass. Agricultural science. 2017, Vol. 1, pp. 74-81.
9. Dierking R.M., et al. Biomass and Bioenergy. ELSEVIER, 2016, Vol. 91, pp. 98-107.
10. Bilandžija N., et al. Energy Valorization Of *Miscanthus x Giganteom* Biomass: A Case Study In Croatia. Journal of Processing and Energy in Agriculture. 2017, Vol. 21, 1.
11. Bergs M., et al. *Miscanthus x giganteus* Stem Versus Leaf-Derived Lignins Differing in Monolignol Ratio and Linkage. Int. J. of Molecular Sciences. 2019, Vol.
12. Joachimiak K., Wojec R., and Wójciak A. Comparison of *Miscanthus x giganteus* and birch wood nssc pulping part i: the effects of technological conditions on certain pulp properties. WOOD RESEARCH. Copyright, 2019, Vol. 1, 64, pp. 45-58.
13. Smith, A.M., et al. The potential for production of high-quality bio-coal from early harvested Miscanthus by hydrothermal carbonization. Fuel. ELSEVIER, 2018, Vol 220, pp. 546-557.
14. Marian G., et al. Comparative analysis of biomass obtained from energy crops. Agricultural science ,. 2014, Vol. 2, pp. 70-76.
15. Țiței V., et al. Prospects for the utilization of the *Miscanthus giganteus* and *Polygonum sachalinense* for solid biofuel production in the Republic of Moldova. Scientific papers. Series A. Agronomy. 2016, Vol. V, LIX.
16. Lewandowski I., et al. The development and current status of perennial rhizomatous grasses as energy crops in the US and Europe. Biomass & Bioenergy. 2003, Vol. 25, pp. 335-361.
17. Sorică E. Analysis of profitability of implementing the miscanthus energetic crop technology for rhizomes capitalization. Agricultural Engineering. INMATEH, 2015, Vol. 2, 46, pp. 155-164.
18. Bajura T and Gandacova S. New bioenergetic sources for the national economy: Miscanthus. Annals of the National Institute of Economic Research. Economics, Finance, Social Policy, Demography, Statistics and Econometrics. INCE, 2020, Vol. X, pp. 16-21.
19. Sorică C., et al. Technology for promotion in Romania of energy crop Miscanthus, as renewable resource to increase energy competitiveness in independence purposes. scientific works (INMATEH). INMATEH, 2009, Vol. 29, 3, pp. 10-15.
20. CSTSP. Catalog of plant varieties for 2020. Chisinau: Lumina, 2020.
21. CSTSP. Catalog of plant varieties for 2020. Chisinau: Lumina, 2021.
22. Clifton - Brown J., et al. Breeding progress and preparedness for the mass - scale deployment of perennial lignocellulosic biomass crops switchgrass miscanthus, willow and poplar. GCB Bioenergy. John Wiley & Sons Ltd, 2019, Vol. 11, pp. 118-151.
23. Țiței V., and Roșca I. Good land use practices in the cultivation of crops with potential energy biomass: A practical guide for agricultural producers. "Bons Offices SRL" printing house. Chisinau: UCIP IFAD, 2021. p. 80. ISBN 978-9975-87-778-7.
24. Mountain I., et al. Biomass quality of some Poaceae species and possible use for renewable energy production in Moldova. Scientific Papers. Series A. Agronomy. 2018, Vol. LXI, 1, pp. 497-502.
25. Ouattara M.S., et al. Effects of several establishment modes of *Miscanthus* × *giganteus* and *Miscanthus sinensis* on yields and yield trends. GCB Bioenergy. John Wiley & Sons Ltd, 2020, Vol 12, pp. 524-538.
26. Clifton-Brown J.C and Lewandowski I. Overwintering problems of newly established Miscanthus plantations can be overcome by identifying genotypes with improved rhizome cold tolerance. New Phytologist. 2000, Vol 148, 2, pp. 287-294.
27. ST. SM EN ISO 17225: 2016.

Journal of Engineering Science *Vol. XXIX, no. 2 (2022), pp. 144 - 150*
Fascicle *Architecture, Civil and Environmental Engineering* *ISSN 2587-3474*
Topic *Environmental Engineering* *eISSN 2587-3482*

https://doi.org/10.52326/jes.utm.2022.29(2).14
UDC 662.767.2:628.33

SYNTHESIS AND IMPLEMENTATION OF BIOGAS PRODUCTION IN WASTEWATER TREATMENT PLANT

Artiom Moldovan*, 0000-0002-3399-6786

Technical University of Moldova, 168 Stefan cel Mare Blvd., Chisinau, Moldova
*Corresponding author: Artiom Moldovan, *artiom.moldovan@ie.utm.md*

Received: 02. 12. 2022
Accepted: 04. 28. 2022

Abstract. In this paper, the problem was to carry out a study on the process of mass production of biogas and to deduce the analysis of an example implemented in the wastewater treatment plant. The main problem is the correct processing of the activated sludge and the extraction of the biogas with its basic components. The method described in the paper is current as a technology in the biogas production industry by treating activated sludge from a wastewater treatment plant. For the extraction of biogas according to EU standards and the possibility to use it at each stage of extraction, methods and technologies specific to this process are used and explained.

Keywords: *biogas, desulphurization, gas flare, co-generation unit, PLC, SCADA, automatic control.*

Rezumat. În această lucrare problema analizată a fost studiul procesului de producere în masă a biogazului, inclusiv pe baza unui exemplu implementat în stația de epurare a apelor uzate. Problema principală este prelucrarea corectă a nămolului activ și extracția biogazului cu componentele sale de bază. Metoda descrisă în lucrare este actuală ca tehnologie în industria producției de biogaz prin tratarea nămolului activ dintr-o stație de epurare a apelor uzate. Pentru extracția biogazului conform standardelor UE și a posibilității de utilizare a acestuia în uz general, la fiecare etapă de extracție se folosesc metode și tehnologii specifice acestui proces, explicate în această lucrare.

Cuvinte cheie: *biogaz, desulfurare, ardere de gaz, unitate de cogenerare, PLC, SCADA, control automat.*

Introduction

Anaerobic digestion of sewage sludge is a well-known, efficient and environmentally friendly technology that allows the production of energy in the form of heat, electricity and fuel for vehicles, as well as the stabilization and reduction of sludge volume. The production of biogas in a wastewater treatment plant can be done in different ways, but the result depends on the correct operation of this system, with well-chosen equipment [1].

Original Biogas is the term used for the mixture of gases (methane, hydrogen and carbon dioxide, etc.) of biogenic origin that arise from the processes of fermentation or gasification of various organic substances. These gases are used by combustion as an energy

source (biogenic energy). The energy obtained from this chain, biomass → biogas → electricity and heat, is called renewable energy, for the following reason: carbon dioxide released into the atmosphere by burning biogas, is an amount at most equal to the amount assimilated by plants or feed consumed of animals, in their vegetal period. According to the Kyoto Protocol, this is a closed circuit of carbon dioxide, unlike fossil fuels (methane gas, coal, crude oil) which burn carbon dioxide which was assimilated many thousands of years ago. Typical sewage sludge comprises primary sludge separated from wastewater during pre-settling and excess biological sludge from the activated sludge system [2]. The characteristics of sewage sludge differ somewhat in different countries and areas, for example, due to water consumption and local industry. The total solids content (TS) is usually low and the volume of sludge is higher than if some of the water is removed before sludge treatment. Biological stabilization of sludge aims at the degradation of solid volatiles (VS), the organic content of the sludge, and the subsequent decrease of the sludge volume. Moreover, nitrogen and phosphorus content are important, especially when the stabilized sludge is reused as fertilizer or as a soil improver. Sewage sludge contains readily biodegradable materials and its typical methane production potential is approximately 300-400 m^3 / tVSadded [3]. The amount of wastewater collected through sewerage networks in Moldova is constantly increasing, so the amount of treated water increases, causing an increase in the amount of sludge processed and thus an increase in energy consumption specific to wastewater treatment and sewage sludge. In the coming years, the conditions for disposal and disposal of waste will be tightened in accordance with European regulations. Sludge resulting from the treatment process is classified as non-hazardous waste, which is allowed for storage. Improper treatment of sludge in landfills can lead to its disposal in authorized landfills. The use of renewable energy sources has a negligible impact on the environment, they emit greenhouse gases. Even if by burning, the biomass eliminates an amount of CO^2, this amount is absorbed by it during its growth, the balance being zero. At the same time, these technologies do not produce hazardous waste.

Biogas utilisation plant

Within this part of plant, the following plant components has to be controlled:

- Gas Desulphurization;
- Gas Holder;
- Gas Booster station;
- Gas Flare;
- CHP-units.

The produced gas is a product of the anaerobic sludge stabilization which has a specific energy content of about 6.4 kWh/m^3 because of its methane content. Due to this fact the gas can be used as fuel in combined heat and power stations after a pre-treatment. Therefore, the treated biogas is foreseen to be used for burning in a CHP unit which are providing the required heat for the dewatering pre-heating but also for heating the buildings. The combined heat and power unit generates additionally electrical energy which will be used in the wastewater treatment plant. If the produced gas is not required for heating purposes and the gas cannot be used for the CHP and also the storage capacity of the gas holder is exceeding, then the excess gas has to be burned by the gas flare without electrical and thermic usage. So consequently the gas flare plant is used as a security unit.

Gas desulphurization

The function of the biogas desulphurization system is removing H2S from biogas biologically. The control philosophy overview is:

a) The gas produced in each digestion tank will be collected on one biogas line and pass through the gravel filter located in Gas Room which is for coarse gas cleaning. The gravel filter also serves to separate and drain off condensation in the digestion gas. After the gravel filter, biogas passes through a desulphurization plant will be installed where the gas is undergone a desulphurization process. The biogas flowrate will be measured on the biogas line just before the desulphurization system. This flowmeter controls the operation of the aeration blower of the desulphurization system in order to prevent supplying excess air to the desulphurization unit.
b) Desulphurization system is the biological type and mainly consist of following components:

- Two centrifugal recirculation pumps;
- Two nutrient feeding pumps for biomass media;
- One blower for providing air to the biomass media;
- Hot water system including hot water pump;
- Ambient ex-sensors for controlling the leakage in control room.

c) The control of the whole plant will be carried out by an own local control panel is not part of the main PLC program. Status of operation and faults has to be transmitted to SCADA [4]. Biogas quality at the outlet of the desulphurization unit will be monitored with an inline biogas analyzer with following parameters:

- CH_4, H_2S, CO_2, O_2.

Biogas holder

The function of the biogas holder is an intermediate storage of biogas. After the desulphurization plant, the gas holder tank follows. The gas holder tank is directly integrated in the main gas pipe. There are two automatic condensate traps installed prior to and right after the gas tanks. These condensate traps are placed in a small chamber in front of gas holder. The removed and collected condensate flows into the drainage line which is transferring the drainage to condensate pumping shaft which also collects the drainage from desulphurization unit and gas room. Condensate collected from biogas utilization plant is pumped into the existing internal pipeline with the help of condensate pump. The control of the condensate pump takes place by two level switches placed in the shaft. The task of the gas holder is to store intermediately the peak gas production during the day so that the CHP can be fed with gas also in times when the gas production is low. The gas holder is equipped with level measurement transmitter. These are required for the control of the gas holder, gas flare and gas boiler as well as combined heat and power unit [5]. Biogas Holder is equipped with one blower which is functioning continuously in order to maintain the rigidity of the outside membrane of gas holder and maintain the necessary pressure in the biogas system over the interior membrane. Furthermore, the Biogas Holder is equipped with a mechanical excess pressure safety device for security reason.

This safety device compensates and balances every unusual pressure which is beyond the allowance. Several pre-set values have to be created and adjusted in the SCADA system, to ensure a proper operation of the gas utilization plant. So the level detector is quite important for the biogas management.

Biogas booster blowers

The function of the biogas booster blowers is delivering the biogas to CHP's with requested pressure. A ceramic filter will be provided on the biogas line after the biogas holder in gas room for further filtering of humidity in the biogas before sending it to the CHP's. Two gas blowers are installed in gas room in order to feed the biogas to two CHP-units. Capacity of the gas blowers are selected as to serve one CHP unit in his maximum capacity. These gas blowers are equipped with frequency converters in order to adjust the speed in accordance with the capacity signal (50-100%) receiving from CHP unit. A fine tuning related to the CHP capacity and blower speed will be done during commissioning phase. During operating with one CHP unit, an automatic exchange between duty and stand-by aggregate has to be provided to get even or similar operation times by a timer. In case of a failure at the duty aggregate, the stand-by aggregate takes over the job automatically. During operating with two CHP's, both of the blowers will function in accordance with the capacity signals (50-100%) receiving from two CHP units.

The following prerequisites have to be met for the operation of the biogas booster blowers in Automatic mode:

- The high temperature switches on the blower bearing are not activated and there is no other fault with the equipment;
- The low pressure switches on the suction side of the blowers are not activated;
- The high pressure switches on the discharge side of the blowers are not activated;
- The level in the biogas holder is not at or below Low level;
- Biogas quality (CH_4 and H_2S) is acceptable.

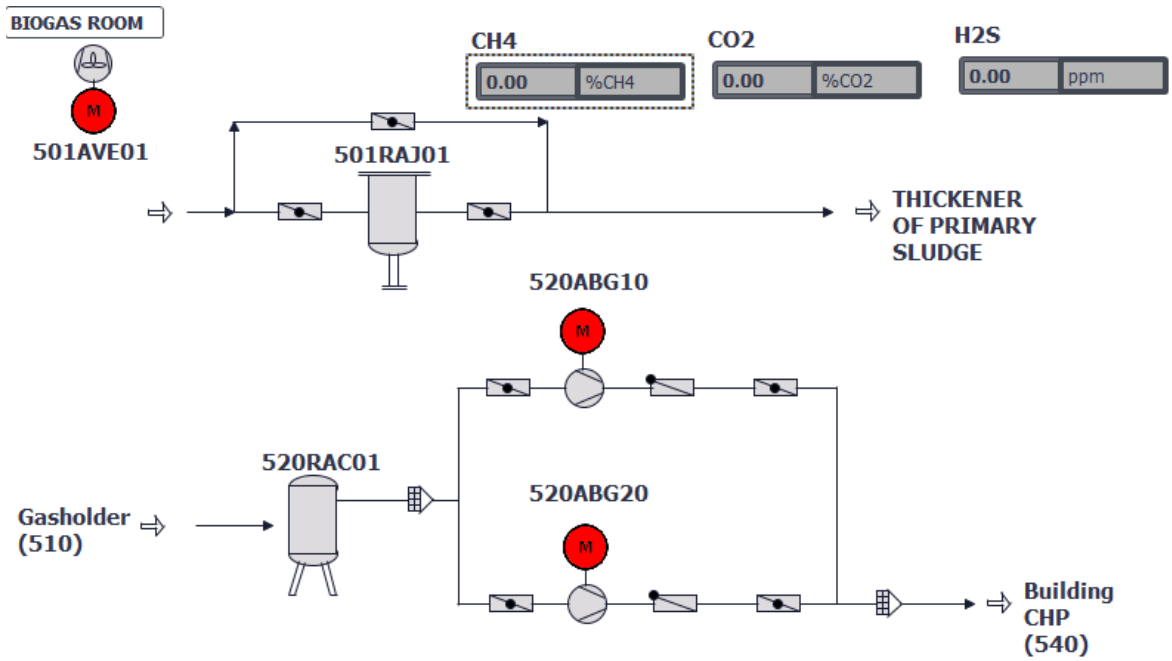

Figure 1. Biogas room [14].

Local control panel(s) for the biogas blowers shall be located in gas room, including an emergency stop button, automatic / manual switch and, for each device, safety separators, on / off buttons, motor speed control button, motor speed display, operation signals, fault / alarm shall be available [7]. The selector switches at the distribution board have to be in "AUTO" position in order to have the possibility of automatically operation. The demand for operation of the gas blower(s) in "AUTO"-mode will come from the CHP unit(s) when enough biogas is

stored within the gas holder for CHP operation (level is above low level). In case biogas blowers were in function (together with CHP's) when the level dropped below the Low level, biogas blowers will remain in function until the closing cycle of the CHP's are completed (switch off signal will come from CHP unit(s). Discharge of each blower is equipped with flow failure switch. In case of no flow is observed on the discharge line of the blower after a pre-set amount of time (e.g. 5 sec), blower will stop immediately and an alarm will be triggered on PLC/SCADA system for operator's check [11].

Biogas flare

The function of the biogas flare is burning excess biogas in case of an emergency. The combustion of biogas is carried out in the emergency flare, if the gas is not consumed by one of the gas consumers and the gas tank is filled up. The Gas Flares are switched on and off according to level in the biogas holder. Please refer to Biogas Holder chapter for conditions of switching on and off of the gas flare. When the starting signal is received from the biogas holder, the gas flare will first ignite the pilot light with opening pilot valve (Figure 2).

The flame detection is effected through a signal produced by the Thermocouple mounted inside the pilot and controls the burning process as follows:

- If the flame detector fails to recognize any flame the main gas valve closes and an alarm is generated;
- In case of successful ignition (thermocouple reaches 80 ˚C), system opens the main gas valve, switches on the biogas flare blower and ignites the main burner of the flame of the pilot burner.

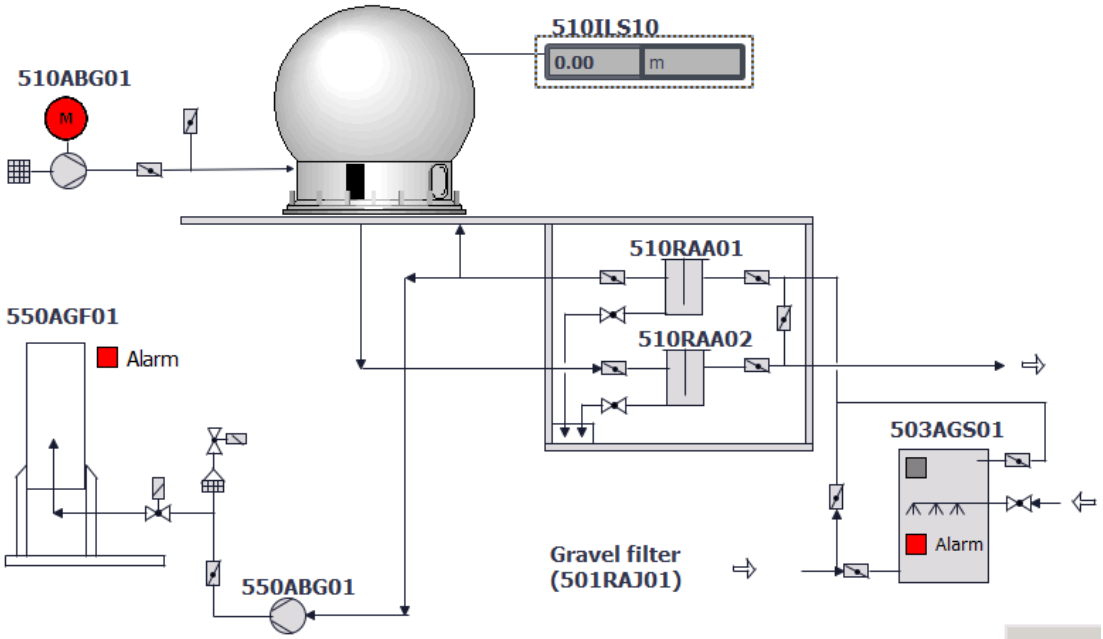

Figure 2. Desulphurization system, Biogas holder, Biogas flare [14].

The automatic control belongs to the local control panels of the gas flares and is not part of the main PLC program.

Cogeneration building

The function of the cogeneration building is utilization of the biogas for thermal and electrical energy production. The control philosophy overview is:

a) Control philosophy overview – CHP units

The operation of the CHP-units is carried out by their local control panel. Start and stop signals for CHP-units will be sent by the main PLC according to the filling degree of the gas holder supervised by the level measurement. Quality of the biogas measured after desulphurization unit will also have a control over the operation of CHP-units; if CH_4 or H_2S quality is not acceptable for a certain amount of time (e.g. 2 hours – time that may change the content in gas holder), CHP unit will not be allowed to function. After upgrading the existing control panels of the CHP Units with biogas operation, it will be also possible to adjust the capacity of each CHP-unit from PLC/SCADA system by sending 4-20 mA signals to the local control panel of each unit. Capacity of the CHP-Units will be used to control the frequency of the biogas blowers that will feed the "Active" CHP-Units. A fine tuning on the CHP-Unit capacity and biogas blower operation frequency will be done during commissioning and will be integrated into PLC system for coordinating the operation of both equipment which are placed in separate buildings. The generated power will be synchronized with the network and be fed via the step up transformer to the Medium voltage switchboard.

b) Heat recovery system of CHP units

Hot water circuit for dewatering pre-heating system consists of one twin hot water circulation pump, one automatic 3-way-control valve and one temperature sensor in the heating water return line. Twin hot water circulation pump for dewatering pre-heating delivers the water to the dewatering pre-heating heat exchanger. This twin pump is equipped with frequency converter. Operation of the twin hot water pumps for building heating is done manually by the operator. Twin hot water pump will function continuously with a frequency pre-set by the operator on PLC/SCADA when the switch of the twin pump is set as "Remote/Auto" on his local control panel. Operation signal from the twin hot water pump should start the aero term ventilations located in these buildings automatically.

c) Cogeneration building

A gas detector for CH4 and smoke is placed at the cogeneration building. Signals of this gas detector have to be transferred to PLC / SCADA for alarm, indication and recording purposes. In case that 20% limit value is detected in present gas concentration: start operation of the room ventilation until no gas (methane) is detected anymore in the cogeneration building and a warning will be triggered – high gas level is monitored and operated by the PLC program. In case that 40% limit value is detected in present gas concentration: close the motorized butterfly valve on the biogas feeding line to the CHP-Units and all drives within the corresponding places will be switched off immediately [15].

Conclusions

The energy recovery of the sludge from the municipal treatment plants must also constitute for the Moldavian operators, a technological priority beneficial for the environment and for the reduction of the final costs of wastewater and sludge treatment, presenting the following advantages:

- The risk of environmental pollution with organic pollutants, viruses and pathogens is completely eliminated due to high temperatures during the heat treatment process;
- The sludge from municipal wastewater treatment can be exploited energetically even for a low organic load of the influent, being able to obtain an energy gain of over 30% of the electricity consumption of the treatment plant, so a proportional increase in energy efficiency by 30%.

- In addition to the energy gain from final sludge treatment, the resulting amount of waste decreases significantly from dehydration to ash by more than 15 times, proportionally reducing transportation and storage costs.

References

1. Moldovan A., Nuca I. Automation of Wastewater Treatment Plant, SIELMEN 2019.Moldova, Chisinau.
2. 10th technical assessment on the Urban Waste Water Treatment Directive (UWWTD) implementation 2016 European review and national situation. https://op.europa.eu/en/publication-detail/-/publication/d90014c6-c578-11ea-b3a4-01aa75ed71a1/
3. Einola J.-K.M., Luostarinen S.A., Salminen E.A., Rintala J.A. Screening for an optimal combination of municipal and industrial wastes and sludges for anaerobic co-digestion. In: Proceedings of the 9th World Congress on Anaerobic Digestion, 2001, vol 1. Antwerpen, Belgium, pp. 357–362.
4. Milici L.D., Milici M.R. "Applications of monitoring and data transmission systems". Didactic and pedagogical publishing house, Bucharest, 2014, ISBN 978-973-30-3639-5, 202 page.
5. Walnut Elijah, Electric Drives, Course Guide. [RO]
6. Panaitescu Mariana, Wastewater treatment techniques. sew-age treatment plant design guide; Nautical Publishing House, 2011
7. Water purification processes and equipment; Romania, University "Petru Maior" TG. MUREȘ, 2011
8. Caraman S., Luca L. Advanced control strategies for biological wastewater treatment processes.
9. DECISION No. 950 din 25-11-2013 for the approval of the Regulation on the requirements for collection, treatment and discharge of wastewater in the sewerage system and / or in water bodies for urban and rural localities. [accessed 24.02.2022]. Available: https://www.legis.md/search/getResults?doc_id=120783&lang=en.
10. DECISION No. 833 of 10-11-2011 on the National Program for Energy Efficiency 2011-2020. [accessed 24.02.2022]. Available: https://www.legis.md/search/getResults?doc_id=110334&lang=en.
11. Virginia Ivanov Integrated monitoring and control systems for electrical equipment, Universitaria Publishing House, Craiova, 2008 [RO]
12. William Bolton, Programmable Logic Controllers. https://www.etf.ues.rs.ba/~slubura/Procesni%20racunari/Programmable%20Logic%20Controllers%204th%20Edition%20(W%20Bolton).pdf
13. Ciuru T. Modern Automation Equipment and Industrial Technological Equipment. Documentation, programming and practical application guide. Technical Publishing House - INFO, Chisinau 2009. [RO]
14. Personalized documentation within a company.
15. Production of biogas at wastewater treatment plants and its further application. [accessed 25.02.2022]. Available: https://www.researchgate.net/publication/322335429_Production_of_biogas_at_wastewater_treatment_plants_and_its_further_application

Journal of Engineering Science *Vol. XXIX, no. 2 (2022), pp. 151 - 160*
Fascicle *Food Engineering* *ISSN 2587-3474*
Topic *Food Industry and Management* *eISSN 2587-3482*

https://doi.org/10.52326/jes.utm.2022.29(2).15
UDC 621.798.147:339.37:004 (430)

TECHNOLOGICAL INNOVATIONS AS DRIVERS OF RETAIL 4.0 – HOW RFID COULD IMPROVE RETURNABLE BOTTLE LOGISTICS IN THE GERMAN BEVERAGE INDUSTRY

Stan Lukas Bührdel[1], ORCID: 0000-0003-3610-1877,
Patrick Siegfried[2*], ORCID: 0000-0001-6783-4518

[1]*Baden-Wuerttemberg Cooperative State University (DHBW), Coblitzallee 1-9, D-68163 Mannheim, Germany*
[2]*International School of Management GmbH, Mörfelder Landstraße 55, D-60598 Frankfurt/Main, Germany*
*Corresponding author: Prof. Dr. Dr. Patrick Siegfried, *patrick.siegfried@ism.de*

Received: 04. 03. 2022
Accepted: 05. 15. 2022

Abstract. This research paper discusses how RFID technology could improve current deposit bottle logistic processes in food retailing and which obstacles impede successful implementations. Research Methodology include desk research: Library, EBSCOhost, wiso.net, Google Scholar, Scientific Journals, Statista, SpringerLink. Implementation of RFID is potentially beneficial, but same obstacles remain outlook. To validate the conclusion further studying and practical proof of concept are necessary. Contributions: supply chain management, return logistics, food retail, beverage industry.

Keywords: *deposit bottle, food retailing, return logistics, reusable packaging, RFID.*

Rezumat. Această lucrare analizează modul în care tehnologia RFID ar putea îmbunătăți procesele logistice actuale ale sticlelor de depozit în comerțul cu amănuntul a alimentelor și obstacolele care împiedică implementările de succes. Metodologia cercetării include cercetare de birou: Library, EBSCOhost, wiso.net, Google Scholar, Scientific Journals, Statista, SpringerLink. Implementarea RFID este potențial benefică, dar rămân anumite obstacole. Pentru a valida concluzia, sunt necesare studii suplimentare și dovada practică a conceptului. Contribuții: managementul lanțului de aprovizionare, logistica returului, retail alimentar, industria băuturilor.

Cuvinte cheie: *sticla de depozit, vânzare cu amănuntul de alimente, logistică retur, ambalaje reutilizabile, RFID.*

Introduction

Logistics are currently undergoing a process of change, foremost due to technical innovations. Radio Frequency Identification (RFID), the main driver of the change, is a very promising technology that can be implemented to solve the challenges arising in the logistics sector. RFID systems have been used for several years and can now be considered a mature technology. Nowadays, they are being implemented in numerous different areas. The strong growing prevalence of RFID in Europe is illustrated in the figure below.

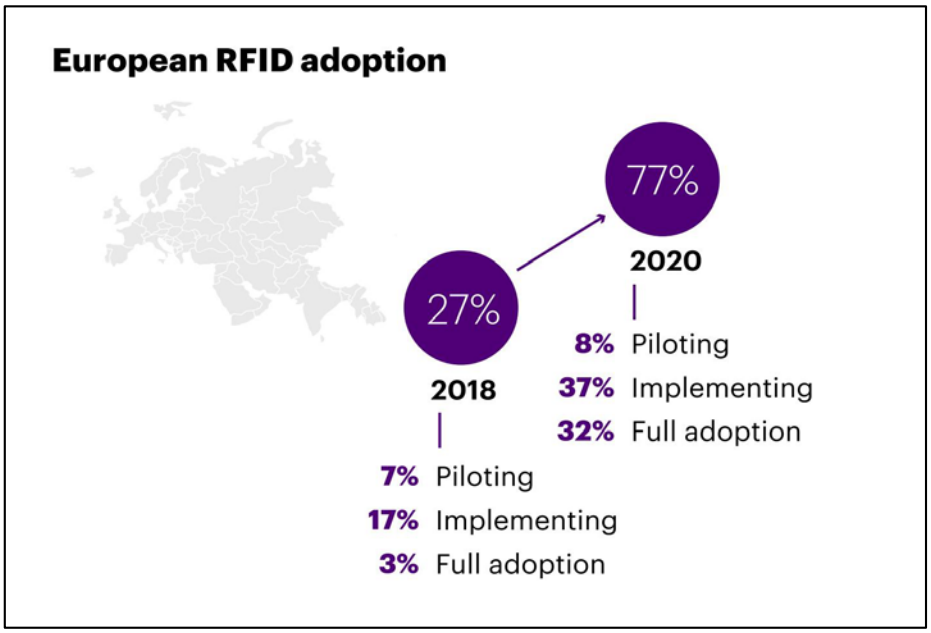

Figure 15. RFID adoption on the rise in Europe [1].

By nature, many logistics systems are very complex. A particularly sophisticated logistic system constitutes the reusable beverage container system in Germany. Therefore, not only good delivery logistics must be provided, but also complex return logistics [2]. Because of a growing diversification of the beverage containers' shapes and sizes, the logistical effort, e.g., in sorting, is strongly increasing. The sorting of the reusable containers is often carried out by hand and is thus labor and cost-intensive. Despite its complexity, the reusable beverage system is highly appreciated by politicians because it aligns with the environmental policy goals to decrease the use of packaging, allows to save resources, and has a positive impact on the environment [3]. Reusable systems are becoming more and more common in Germany. Consequently, the effort the retail sector must make is increasing noticeably. This is also the case for other stations of the comprehensive logistics system. Because of this need for improvement, the question arises to what extent RFID technology could help to optimize these sophisticated logistics systems and thus reduce the costs in local trade [4]. The focus lies on efficiency, that is to say on the optimization of the logistics system [5]. Relevant reference factors for this are time, space requirements, personnel requirements, and costs. In the following research paper, findings on this question are to be brought together, compared and weighed up to conclude on RFID systems in reusable bottle logistics.

1. Literature review and hypothesis development

RFID is a widely applied technology in logistics; therefore, many different publications can be found on issues surrounding the use of RFID systems in logistics processes, also with a focus on the use and implementation in the retail industry. A deeper examination of this topic reveals that most case studies and research papers only deal with the consideration of delivery logistics [6]. However, case studies that also examine the effects on return logistics are much rarer. In addition, the individual studies on RFID in return logistics often deal with cases of pool systems up to the retailer level, such as the Euro pallet system [7]. In countries like Germany, however, there are also pool systems that go down to the consumer level. The most prominent example of this is the returnable deposit system for beverage containers such as beer bottles or water bottles. These bottles, made of glass or PET, run in an even

more complex cycle than the before-mentioned Euro pallets. The reason why this system is even more complex is due to a large number of different types of containers, which are difficult to take back and to sort. Furthermore, there are often returned by customers in a shop that is different from the shop of original purchase [8].
Since such a logistics system has not yet been discussed in a research paper that I know of, this paper takes this as an opportunity to deal with the question of how useful it would be to implement RFID technology at the item level in a returnable bottle system. To answer this question, the existing literature on RFID in retail logistics is analysed. Potential opportunities and risks of such an implementation are highlighted and a conclusion is derived from this.
Before we take a closer view into the effects of RFID implementation in supply chains, the technology should be explained to ensure a solid ground of understanding.

1.1 Explanation of RFID Technology

A system using RFID which is the abbreviation for Radio Frequency Identification consists of two major components: a tag and a reader [9]. The electronic tag is affixed or embedded in an object and contains historical, transactional, or identifying data. This data can be wirelessly downloaded to a computer if an RFID reader is near the tag. After this point where the gathered information is loaded onto a computer, the data can travel anywhere on the internet [10].

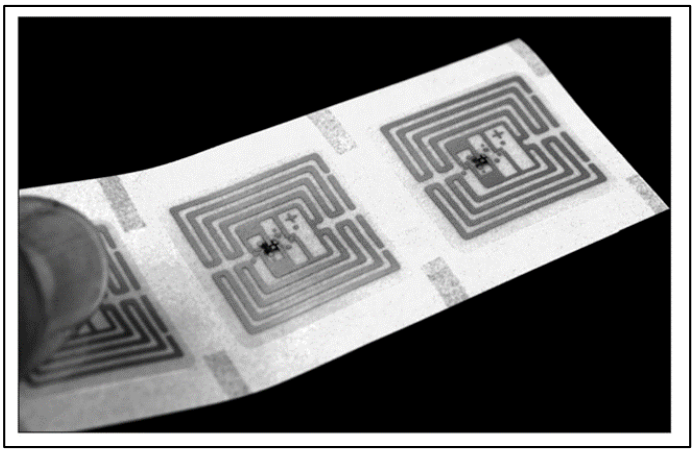

Figure 16. Picture of RFID tags [11].

There are two different types of tags. Active RFID tags are battery-powered. Passive tags have no power source. Therefore, they require electromagnetic power transmitted by the reading device to enable information exchange [12]. Each type of RFID tag has its advantages and disadvantages. The active tag provides a higher reading accuracy but has a costly price point due to increased complexity. Besides active tags are less robust and more difficult to be integrated with packages [12]. On the contrary passive tags have a simple structure, are more robust, last longer in storage, radiate less energy, and are cheaper [12].
Nowadays RFID tags can be complemented with RFID sensors. If these RFID using circuits are combined in a label this enables further functionality such as food quality monitoring. The following Figure 3 gives an overview of the different purposes and functionalities.
As you can see an RFID-based sensor system can combine identification with sensing purposes that can measure changes in physical parameters [12]. The enabling technology behind these additional functions is smart materials, which are responding to the physical change of environmental factors.

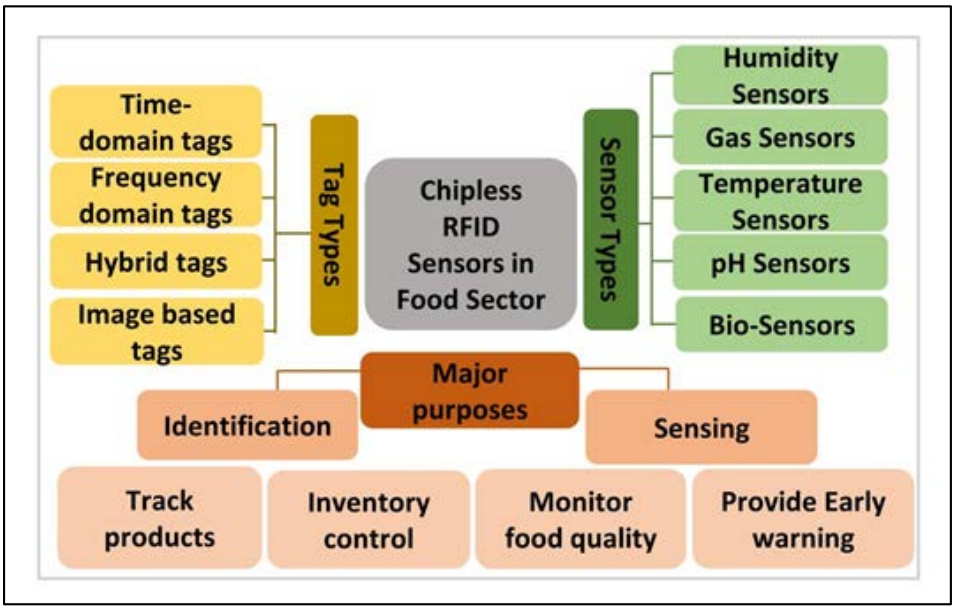

Figure 17. The framework of chipless RFID sensors in food packaging [12].

Smart materials are the fundamental elements of chipless RFID sensors. They react to changes in environmental factors such as humidity, temperature, the concentration of gases, pH, and light [12]. On the technical side, those functions are realized by changes in electrical properties [12]. While sensing purposes can be used to surveillance of freshness the identification part can be used to deliver sales, location, and demand structure information. [13]. These characteristics make combined RFID sensors with tracking and quality monitoring especially interesting for the food retailing industry.
Now that we have defined and explained RFID technology, I am going to review the different works of literature in this subject area.

1.2 Literature Review

Some of the earlier literature about RFID implementation focused on practical goals, such as reducing labor requirements and spoilage through efficient inventory management [14]. Despite uncertainties about costs and dispersion, the major retailers were very hopeful and expected to save billions of dollars if goods were equipped with RFID across the board, as this would make it easier to prevent theft [15]. Another issue that arose at the beginning of this millennium was the definition of common guidelines and standards. With the choice of EPCglobal in 2003, however, standardization was established [16].
A key challenge that acts as an inhibiting factor to widespread deployment is the price per RFID tag. Although the price of cheap, mass-produced RFID tags has fallen from €0.50 in 2007 to between €0.10 and €0.15 in 2010, RFID labels are still too expensive for item-level tagging despite the sharp drop in price over these three years [11]. This observation also serves as an explanation for the fact that retailers like Metro, which were initially very optimistic, do not have item-level tagging yet, as shown in the figure below.
Nevertheless, the prices per tag are currently still a degree too high, the RFID technology has come to stay, and the experience shows that the most innovative and adaptive retailers are discovering many new use cases besides typical inventory tracking [1]. New use cases could outline an overall positive effect on retailer's profitability.

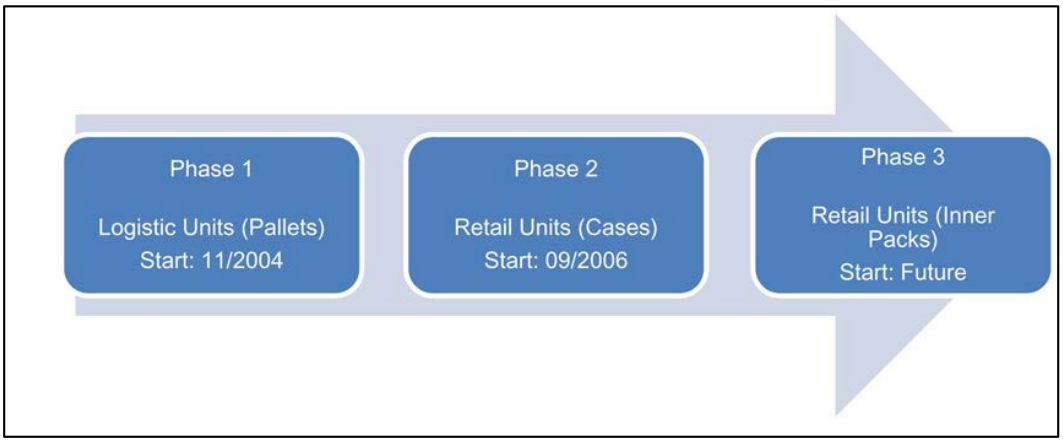

Figure 18. RFID roll-out phases at Metro [13].

In the case of multiple used returnable deposit bottles, there is a different view on the RFID tag price because the label costs can be allocated to the number of circulations. This means that slightly higher label costs are less of a problem.

1.3 Hypothesis development

If we take into consideration that the sorting process after the return of the bottles at the deposit vending machine is still very labor-intensive and requires manual work RFID-based automation appears as a suitable solution to optimize the handling with returnable bottles. Additionally, the results of other RFID implementation projects have proven a positive effect on efficiency and profitability several times.

This induces me to formulate the following hypothesis: An area-wide implementation of RFID for returnable beverage bottles would lead to a significant increase in efficiency and profitability of this pool system.

2. Research methodology

To fulfil the standards of proper research, it is essential to carry it out through appropriate data collection in terms of quality and quantity. The data used for this research paper consists of a collection of theoretical data. Theoretical data includes literature, journal articles, and internet documents.

The used literature and further resources were gathered through using different scientific search engines, for instance, the DHBW library, EBSCO, Google Scholar, Springer Link, and wiso.net. Subsequently, the main arguments were outlined and opposed. Advantages and disadvantages were weighed. In the conclusion, the personal view was brought in to draw an outlook.

There are two main ways to execute a research assignment, deductive or inductive. This research is deductive, which follows the approach of seeking truth by looking from different directions. Therefore, the deductive way of researching tests primarily existing theory [13].

3. Results and discussions

To be able to make a balanced statement about whether implementation of RFID would be beneficial, the following comparison of arguments for and against it is presented.

3.1 Challenges and Obstacles with RFID

- Besides the smart tags themselves, the other main cost components are the stationary readers and the corresponding IT infrastructure. The tag cost is variable, while the

installation of the readers and the adaptation of the IT infrastructure are primarily fixed costs [17].

- The collaboration leads to a continuously increasing complexity in handling information along supply chains due to a larger extent of data necessity and flow [13].
- Studies have identified cost-sharing as an obstacle; it is not symmetrically distributed. Looking at the supply chain as a whole, the dilemma becomes clear: item-level labeling seems to offer the greatest potential for the retailer but is the most expensive solution for the manufacturer who is best able to apply the labels [17].
- Cyber security risk: Attackers can read, misuse, falsify, destroy, or damage by mechanical means, remove or render unusable by shielding data exchanged between RFID tags and readers. Possible consequences would be a misuse of information, price manipulation, and product piracy [18].
- Technical problems, disturbances in the labeling of cans and other metal-containing products have not yet been solved [16].
- Rather than profitability, the central problem is sometimes that the critical mass of participating suppliers is not reached, as it happened to Rewe's RFID project "PERL" that was discontinued in 2007 for this reason [19].
- If there is a mix with items that are not RFID-tagged they will drag the efficiency of the store down by an amount that exceeds its 'share', so it should be considered to change all items from barcode to RFID at the same time [20].
- Further the following technical characteristics are implying the limitation of the RFID technology [12].
    - Reading accuracy is dependent on multiple factors and sometimes fail
    - Reading range is limited to very few meters
    - Conformability (Performance on flexible packaging) hasn't been widely tested
    - Fabrication/Production: Cost reduction and high-volume output is still challenging
    - Data capacity is technically limited
    - optimal tag placement on the item unclear [21]
- Especially with returnable bottles made of glass or PET the effect of RFID labels on their recyclability is likely to be negative [12]. It can be assumed that RFID labels have to be detached before recycling.
- Returnable bottles are thoroughly cleaned after a return. It is unclear whether adhesive RFID labels survive a cleaning cycle undamaged. If not, this would have a significant impact on the financial calculation of cost allocation in circulation.
- In implementing RFID there are five major struggles and roadblocks:
    (a) lack of technical expertise, [22]
    (b) the complexity of the technology, and [22]
    (c) uncertainty of the technology [22].
    (d) identifying the right suppliers and partners [1]
    (e) quantifying the value of RFID [1]

3.2 Potential and Benefits with RFID

- Retailers are seeing the benefits of RFID in generating massive amounts of data that fuels insights, facilitate greater accuracy of inventory, and it is a key enabler of omnichannel capabilities [1].

- Applying RFID technology additionally enables monitoring food quality inside the individual packages which helps retailers and consumers with the handling of fresh food [12].
- From the customer's perspective shopping becomes a more convenient experience, thanks to the wide range of RFID applications. It is conceivable that customers will be able to call up additional product information or even cooking recipes via the RFID chip [9].
- Advantages for the customer: In a matter of seconds, the scanner at the checkout reads all the codes without having to unload the goods from the shopping cart and place them on a belt [23].
- For retailers: many inventory-relevant work steps can be enormously simplified and accelerated, thus liberating personnel capacities. At goods receipt, it is no longer necessary to scan individual pallets or products; instead, by passing through an RFID-powered receipt gate, a complete delivery can be booked into the inventory - virtually without any time delay [24].
- Case studies show that by implementing RFID systems the quota of container losses is reduced [25].
- RFID-enabled processes are more efficient due to the elimination of errors caused by manual verification [10].
- RFID in logistics systems reduces shrinkage and improves cash flow by quicker billing because quantities can be easily compared and reconciled instantaneously [10].
- The very notable potential to reduce the out-of-stock rate of suppliers' products which implies a large savings potential, as the average stock-out rate vary between 7-10 percent [14].
- A study using the regression analysis with Cobb–Douglas production function shows that RFID retailers have higher labor to gross income elasticity than their non-RFID counterparts, indicating that RFID retailers have higher labor productivity [26].
- Consequently, because of the higher labor productivity a lower number of workers is required, which is viewed positively due to the increasing shortage of skilled workers [27].
- New research by Accenture states retailers that have fully adopted RFID are reporting more than 10% return on investment [1]
- Further they found that retailers that have engaged with suppliers on source tagging are seeing a higher return on investment (16% higher) than those who have not [1].
- With reusable and recyclable RFID transport containers a great cost-efficiency can be achieved because the same transponder can be utilized several times [14].

The following Figure shows the development of the potential cost for RFID labels if they can be reused on circulating deposit bottles.

Figure 5 implicates that the price of one RFID label becomes less relevant in a reusable container system. As a result, the mentioned benefits overweigh the disadvantages on the pricey side. Therefore, an implementation of RFID seems to be more attractive than first assumed. The prerequisite is that the RFID labels are not damaged when the containers are cleaned. This is unclear for adhesive labels. Molded-in RFID tags, on the other hand, do not pose any problems when it comes to cleaning. Besides variable costs, there are additional launch costs for computer software and RFID reader hardware, which are about 1000 € per reading device [12].

RFID type/circulations	1	15	20	25	35	50
adhesive label	0,10 €	0,007 €	0,005 €	0,004 €	0,0029 €	0,002 €
in-mould label	0,15 €	0,01 €	0,0075 €	0,006 €	0,0043 €	0,003

Figure 19. *Cost development of RFID labels used on circulation reusable bottles. (own graphic)*

Because of these pertinent set-up costs, the recommendation is to run a proof of concept first. If the first initiative shows successful outcomes a wider adoption process should be started.

Conclusion

After taking a closer look at the RFID-based supply chain process, various challenges and opportunities were illuminated. The reviewed literature stated consistently that the implementation of RFID in supply chains increases the efficiency of related logistic processes. [28] Despite increased efficiency, a positive effect on the profitability of the companies using RFID was unclear for quite some time.[29] The latest data shows a positive double-digit return on investment when RFID has been implemented. [1]

In the case of the specific system of reusable deposit bottles there lies an interesting opportunity for further optimization in retail logistics. Even though there are some obstacles and unanswered questions, the considered case is attractive in the sense that the advantages on the item level take effect in interaction with slighter cost disadvantages, due to reusability. Furthermore, in the current operating process, there is a substantial amount of labor tied to the manual sorting of bottles. Due to automatization, this labor could be liberated, and costs reduced. As a conclusion, I recommend setting up an empirical proof of concept to discover if the theoretical approach is also practically correct.

Limitation

This research paper only provides a narrow scope of how RFID works and where chances and opportunities lie and propose an idea of an interesting case for further analysis. Because reverse logistics are complicated and I do not have sufficient knowledge in this area of logistics, I can't predict barriers that arise in the practical implementation. Therefore, I propose to use this provided idea to turn it into a limited proof of concept to validate if it's also empirical sensible to implement RFID in reusable bottles

References

1. Accenture. *Retail RFID Study 2020: A new era for RFID in retail*. https://www.accenture.com/_acnmedia/PDF-155/Accenture-RFID-In-Retail.pdf#zoom=40
2. Sann M., Siegfried P. The opportunities and threats of the omnichannel in terms of the logistical challenges of the furniture industry, Bulletin of Taras Shevchenko National University of Kyiv. Economics. 2021; 2(215). pp. 47-55, https://doi.org/10.17721/1728-2667.2021/215-2/6
3. Martínez-Sala A. S., Egea-López E., García-Sánchez F., & García-Haro J. Tracking of Returnable Packaging and Transport Units with active RFID in the grocery supply chain. *Computers in Industry*. 2009; *60*(3). 161–171. https://doi.org/10.1016/j.compind.2008.12.003
4. Michel V., Siegfried P. Digitale Speditionen in der Lebensmittellogistik Digital freight forwarders in food logistics. logistics Journal. 2021; pp. 1-15, DOI: 10.2195/lj_NotRev_michel_de_202102_01, ISSN 1860-5923

5. Siegfried P., Zhang J. Developing a sustainable concept for the urban lastmile delivery. Open Journal of Business and Management (OJBM). 2021; Volume 9. Issue 1. pp. 268-287. DOI: 10.4236/ojbm.2021.91015
6. Siegfried P. Handel 4.0 Die Digitalisierung des Handels - Strategien und Konzepte 1. Book on Demand. Norderstedt. 2021; ISBN-13: 9783754345030
7. Siegfried P. Lebensmittelhandel-Business Cases Arbeitsfragen and Lösungen. Book on Demand. Norderstedt. 2020; ISBN: 978-3-75197-990-0
8. Siegfried P. Handel 4.0 - Erfolgreiche Unternehmenskonzepte mit Arbeitsfragen and Lösungen. Book on Demand. Norderstedt. 2021; ISBN: 978-3-75197-975-7
9. Pezoldt K., & Gebert R. *RFID im Handel - Vor- und Nachteile aus Unternehmens- und Kundensicht. Ilmenauer Schriften zur Betriebswirtschaftslehre:* 2011; *Volume 8*. Verl. proWiWi; Univ.-Bibliothek. http://nbn-resolving.de/urn:nbn:de:gbv:ilm1-2011200484
10. Boeck, H., & Wamba, S. F. RFID and buyer-seller relationships in the retail supply chain. *International Journal of Retail & Distribution Management*. 2008
11. Vaih-Baur C., & Kastner S. *Verpackungsmarketing: Fallbeispiele - Trends - Technologien. Edition HORIZONT*. Deutscher Fachverlag GmbH. 2010; https://www.wiso-net.de/document/DFVE__9783866412132207
12. Fathi P., Karmakar N. C., Bhattacharya, M., & Bhattacharya, S. Potential Chipless RFID Sensors for Food Packaging Applications: A Review. *IEEE Sensors Journal*. 2020; *20*(17). 9618–9636. https://doi.org/10.1109/JSEN.2020.2991751
13. Drauz R., & Handel D. *Impacts of RFID on the Information Exchange in a Retail Supply Chain*. Växjö universitet, Ekonomihögskolan, EHV. 2007; https://login.ezproxy-dhma.redi-bw.de/login?url=https://search.ebscohost.com/login.aspx?direct=true&db=edsbas&AN=edsbas.CBBB39C7&lang=de&site=eds-live
14. Kärkkäinen M. Increasing efficiency in the supply chain for short shelf life goods using RFID tagging. *International Journal of Retail & Distribution Management*. 2003
15. Rees J., Brück M., & Böhmer R. Funkchips: Funkchips. Die Welt in 96 Ziffern. Dieser Chip wird Ihr Leben verändern. 2005; *WW NR. 003 VOM 13.01.2005 SEITE 036*(003). 36. https://www.wiso-net.de/document/WW__0000160108
16. Liening B. RFID im Wareneingang. *Lebensmittel-Praxis*(008). 2006; 65. https://www.wiso-net.de/document/LP__0000105475
17. Gaukler G. M., Seifert R. W., & Hausman W. H. Item-Level RFID in the Retail Supply Chain. *Production and Operations Management*. 2007; *16*(1). 65–76. https://doi.org/10.1111/j.1937-5956.2007.tb00166.x
18. Özel H. *Bedeutung und Anwendungsgebiete des RFID-Systems: Werden Verbraucher zunehmend zu gläsernen Menschen und wie können sie sich vor Datenmissbrauch schützen?* Diplomica Verlag. 2008; https://www.wiso-net.de/document/DIPL__9783836612463107
19. Hunold M. *Die Wirtschaftlichkeit von RFID-Systemen in der Intralogistik eines Handelsunternehmens : Anwenderbeispiel zur Implementierung und Bewertung RFID-induzierter Prozesse*. 2014; https://login.ezproxy-dhma.redi-bw.de/login?url=https://search.ebscohost.com/login.aspx?direct=true&db=edsbas&AN=edsbas.15041005&lang=de&site=eds-live
20. Piramuthu S., Wochner S., & Grunow M. Should retail stores also RFID-tag 'cheap' items? *European Journal of Operational Research*. 2014; *233*(1). 281–291. https://doi.org/10.1016/j.ejor.2013.08.051
21. Lutz T., Hering N., & Kropp S. Smart.NRW: Grundlagenentwicklung für RFID-Einsatz auf Umverpackungsebene. Mit RFID auf Umverpackungsebene zur echtzeitfähigen Supply-Chain im Handel. *UdZ - Unternehmen Der Zukunft. FIR-Zeitschrift Für Betriebsorganisation Und Unternehmensentwicklung*(2). 2011; 48. https://login.ezproxy-dhma.redi-bw.de/login?url=https://search.ebscohost.com/login.aspx?direct=true&db=edstem&AN=edstem.TEMA20111000469&lang=de&site=eds-live
22. Koh C. E., Kim H. J., & Kim E. Y. The impact of RFID in retail industry: issues and critical success factors. *Journal of Shopping Center Research*. 2006; *13*(1). 101–117.
23. Wirtschaftswoche. RFID: Aktives Etikett. *WirtschaftsWoche Online*. 2003; Vom 2003-12-19. https://www.wiso-net.de/document/WWON__396738
24. Salditt T. C. *Netzwerkmanagement im Handel: Prozessinnovationen im Handel am Beispiel der RFID-Technologie. SpringerLink Bücher*. Gabler. 2008; https://doi.org/10.1007/978-3-8349-9700-5

25. Kim T., & Glock C. H. On the use of RFID in the management of reusable containers in closed-loop supply chains under stochastic container return quantities. *Transportation Research Part E: Logistics and Transportation Review*. 2014; *64*. 12–27. https://doi.org/10.1016/j.tre.2014.01.011
26. Shin, S., & Eksioglu, B. An empirical study of RFID productivity in the U.S. retail supply chain. *International Journal of Production Economics*. 2015; *163*. 89–96. https://doi.org/10.1016/j.ijpe.2015.02.016
27. Kempcke T. Retail 4.0 prägt die Handelslogistik. *Retail Technology Journal*. 2018; (01). 80. https://www.wiso-net.de/document/RTJ__65C6DC754DF464E16E7AB7A1647D56E7
28. Siegfried, P./Michel, A./Tänzler, J./Zhang, J. Analysing sustainability issues in urban logistics in the context of growth of e-commerce. Journal of Social Sciences. 2021; Volume IV. Issue 1. pp. 6 – 11. DOI: https://doi.org/10.52326/jss.utm.2021.4(1).01
29. Shin S., & Eksioglu B. Effects Of RFID Technology On Efficiency And Profitability In Retail Supply Chains. *Journal of Applied Business Research (JABR)*. 2014; *30*(3). 633. https://doi.org/10.19030/jabr.v30i3.8582
30. Chwallek A. Die Revolution hat begonnen. *Der Handel*. 2016; (3). 10–15. https://www.wiso-net.de/document/HAND__20160307350557
31. Fan X., Xu X., Zou B., & Bai Q. Returnable containers management in a single-vendor multi-buyer supply chain with investment in reducing the loss fraction. *Measurement*. 2019; *143*. 93–102. https://doi.org/10.1016/j.measurement.2018.12.003
32. Ilic A., Ng J. W. P., Bowman P., & Staake T. The value of RFID for RTI management. *Electronic Markets*. 2009; *19*(2). 125–135.
33. Thoroe L., Melski A., & Schumann M. The impact of RFID on management of returnable containers. *Electronic Markets*. 2009; *19*(2-3). 115–124.

Journal of Engineering Science *Vol. XXIX, no. 2 (2022), pp. 161 - 171*
Fascicle *Food Engineering* *ISSN 2587-3474*
Topic *Biotechnologies, Food Chemistry and Food Safety* *eISSN 2587-3482*

https://doi.org/10.52326/jes.utm.2022.29(2).16
UDC 663.4:573.4

THE INFLUENCE OF MICROORGANISMS ON BEER QUALITY

Aliona Sclifos* ORCID: 0000-0002-6070-0936,
Iurie Scutaru, ORCID: 0000-0002-9199-5183

Technical University of Moldova, 168 Stefan cel Mare Blvd., Chișinău, Republic of Moldova
Corresponding author: Aliona Sclifos, aliona.sclifos@enl.utm.md*

Received: 03. 24. 2022
Accepted: 05. 15. 2022

Abstract. The paper investigated the influence of microorganisms on the quality of Oettinger and Timișoreana beer, in the context of improving the manufacturing methodology of the finished product. Two types of yeast were used for fermentation: Oettinger and SAB-5. At the end of the fermentation process, the microbiological sample was selected to determine the anaerobic bacteria harmful to the beer. Various methods of seeding and sampling were analyzed, such as seeding on several types of media: Wort, Endo and NBB-A, media used to determine the types of microorganisms present at each stage of production. As the level of free amino acids (FAN) is a significant indicator of the completion of the fermentation process, the influence of FAN on the dissociation of yeast and diacetyl content was also analyzed. Subsequently, at the end of the fermentation process, microbiological growths were determined.

Keywords: *OT-Oettinger and TM-Timișoreana beer, microorganisms, yeast, culture media, bacteria Pectinatus, FAN - free amino acids.*

Rezumat. Lucrarea a investigat influența microorganismelor asupra calității berii Oettinger și Timișoreana, în contextul îmbunătățirii metodologiei de fabricație a produsului finit. Pentru fermentare au fost folosite două tipuri de drojdie: Oettinger și SAB-5. La sfârșitul procesului de fermentație, proba microbiologică a fost selectată pentru a determina bacteriile anaerobe dăunătoare berii. Au fost analizate diferite metode de însămânțare și prelevare, precum însămânțarea pe mai multe tipuri de medii: Must, Endo și NBB-A, medii utilizate pentru determinarea tipurilor de microorganisme prezente în fiecare etapă de producție. Deoarece nivelul de aminoacizi liberi (FAN) este un indicator semnificativ al finalizării procesului de fermentație, a fost analizată și influența FAN asupra disocierii conținutului de drojdie și diacetil. Ulterior, la sfârşitul procesului de fermentație, au fost determinate creşteri microbiologice.

Cuvinte cheie: *bere OT-Oettinger și TM-Timișoreana, microorganisme, drojdie, medii de cultură, bacterii Pectinatus, FAN - aminoacizi liberi.*

Introduction

Beer is a finished product obtained by a biotechnological process in which yeast is used to convert fermentable carbohydrates from the wort into ethyl alcohol, carbon dioxide and other secondary compounds. Beer yeast belongs to the Ascosporogene group, the Saccharomycetaceae family, the genus Saccharomyces cerevisiae [1]. In 1970 Lodder describes Saccharomyces cerevisiae cells as being spheroidal, sublimed, ovoid, ellipsoidal or cylindrical to elongation, which appear alone in pairs, occasionally in short chains or groups. Cells can be grouped into three classes by size. A large type, 4,5-10,5 x 7,0-21,0 μm (microns); a small cell type ranging from 2,5-7,0 x 4,5-11 μm and an intermediate cell group measuring 3,5- 8,0 × 5,0-11,0 μm. Some yeast may form filaments which can be up to 30 mm long. The yeast cells of beer fall into either of these categories; however, they tend to be quite large cells, a consequence of polyploidy. A critical parameter in brewing is the correct management of yeast between fermentation, as the characteristic flavour of any beer is largely determined by the yeast strain used and the composition of the wort [2].

The most commonly used beer yeast belongs to the genus Saccharomyces cerevisiae due to some essential characteristics for the brewing process, such as high efficiency ethanol production, the metabolism of sugars using the preferential fermentation path based on the presence of Crabtree (glucose breathing suppression) and its ability to tolerate many environmental stress (primarily the presence of ethanol). The quality of any beer is mostly determined by the used yeast strain and, as a result, currently are being analyzed new yeast strains in order to obtain innovative beers.

Beer yeasts are classified in two categories Ale and Large yeasts also known as high fermentation and low fermentation yeasts [3]. In the production of "ale", the yeasts of which belong to the species Saccharomyces cerevisiae traditionally lead to "peak fermentation", where the yeasts accumulate on the surface of the fermentation wort and the temperature at which they ferments is 14 to 25 °C [4,5].

The fermentation process of beer is influenced by yeasts whose objective is to metabolize sugars in ethanol, carbon dioxide and a variety of secondary metabolites that greatly influence chemical composition, colour and sensory quality. Minor metabolites, which are produced by the yeast of beer and which influence the quality of the beer are: esters, higher alcohols and acids which contribute positively to the flavour. These myriads of minor components characterize a brand of beer and make it identifiable for a drinker. The chosen yeast must also control the removal of undesirable aromatic components from raw materials or from fermentation. Much of this aroma improvement is taking place at maturation [5,6].

In brewing, the most commonly used input products are Saccharomyces cerevisiae (ale beer) and Saccharomyces pastorianus (lager beer). Their widespread use is primarily due to the repression of glucose respiration (Crabtree-positive) and the preference for the fermentative pathway, the efficient production and tolerance of large amounts of ethanol, the production of desired flavours, and the absence of toxin production [6,7]. In Figure 1. is shown the metabolic activity of Saccharomyces that influences the quality of beer. This simplified scheme summarizes the main metabolic pathways related to the modulation of beer flavour by Saccharomyces [8].

The aroma profiles of beer can be attributed mainly to biochemical activities during fermentation in the yeast cell, in which the sugars in the must are converted into ethanol and volatile compounds, such as alcohols and higher esters, which are intermediates and secondary products of yeast metabolism. These volatile compounds are different from the

aromatic compounds present in malt and hops and have a significant impact on the aroma and taste of beer. Ethanol and CO_2 are the primary by-products formed during fermentation, other yeast-derived active aromatic compounds are carbonyls (aldehydes / ketones), higher / fusible alcohols, esters, fatty acids, organic acids and sulphur compounds. The two main classes of nutrients that influence the performance of brewer's yeast are carbohydrates and nitrogen compounds [5,9].

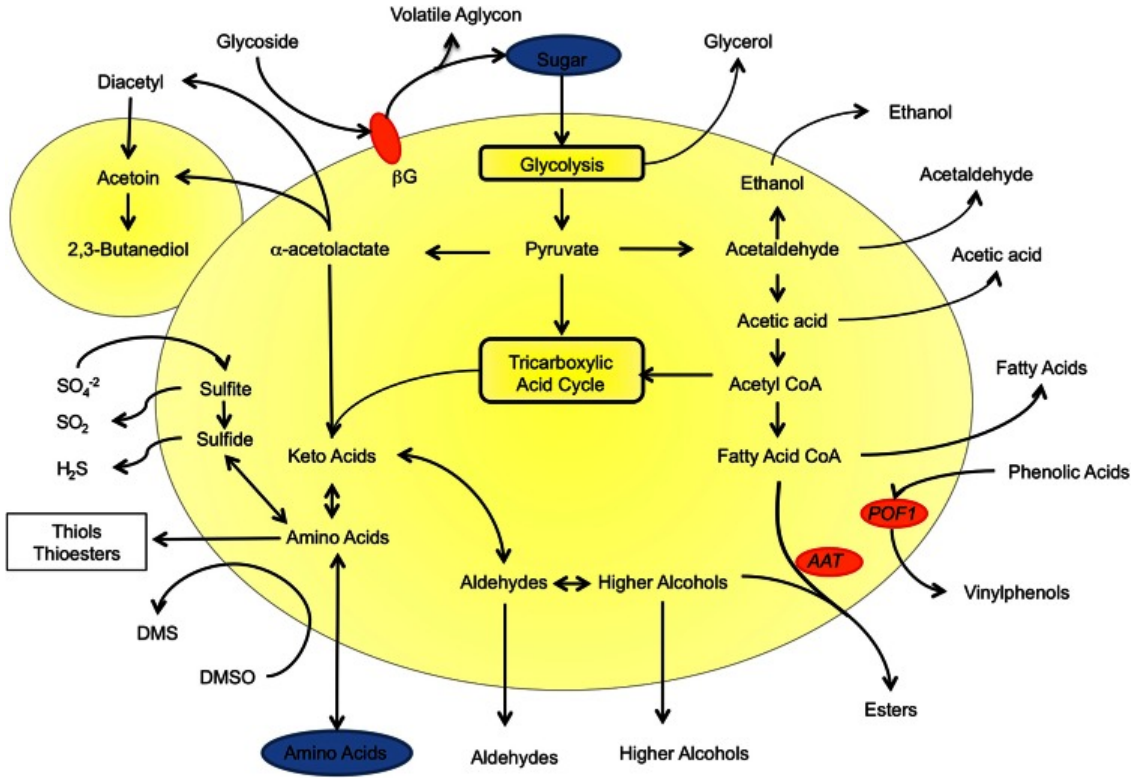

Figure 1. Overview of Saccharomyces metabolic activities that influence beer quality [8].

Yeast strains and many carbohydrates during brewing process (glucose, sucrose, fructose, maltose, galactose, refiner, and maltotriosis) can be used and the main characteristic which distinguishes "ale" and "lager" yeasts is the capacity of "lager" yeast for fermentation of melibiose. The generalized pattern of sugar absorption begins with the absorption of the simplest sugars (glucose and fructose), followed in the increasing order of complexity of disaccharides (maltose) and trizaccharides. As regards nitrogen compounds, the main function of malt is to provide yeast-like nitrogen sources, which are amino acids, ammonium ion, and some di- and tri-peptides [5]. The majority of the must-free amino nitrogen (FAN) is used by the yeast to form the proteins needed to increase yeast. However, the level and composition of FAN in the must has a significant influence on higher alcohol, ester, vicinal dictation and H_2S formation due to the function of amino acid metabolism in the formation of these aromatic compounds [10].

Fermentation conditions are ideal for bacteria to grow, and contamination can delay or extend fermentation and cause various flavours and odours. Typically, specific gravity, pH and flavour are checked during preparation, and microbiological analysis is performed only if problems occur during fermentation [9].

Methodology

In this paper, beer production schemes and micro-organisms that may develop in some technological processes were analysed. Micro-organisms may be beneficial to production in

some cases, and in others may cause damage to the finished product or performance which will pose a risk to human health, which would run counter to the quality requirements of all producers and required by consumers.

The analyses have been carried out on the basis of two types of beer Oettinger and Timişoreana. Their basic parameters are: alcohol, pH, quantity of CO_2 and quantity of O_2, antibacterial compounds resulting from the addition of boiling hops. Beer wort is a by-product that can be used by microorganisms as a substrate for development. Beer on the other hand is less beneficial for the development of microorganisms. Because of the high alcohol content, the low oxygen content, the high content of CO_2, the izo-α-acid and β-acid content, which are antiseptic substances. All microbiological analyzes was carried out under the "Olympus" type of microscope.

Thus, the latest generation equipment from the economic entity was used in the research process, which allows to analyse and research of all aspects of the finished product in detail, the experimental results obtained being subject to further analysis.

Results and discussions

Initial parameters were determined at the beginning of the experiments on the determination of micro-organisms in beer to ascertain whether conditions were favourable for the development of certain micro-organisms. The tables below show the general parameters of the beers examined, the fermentation process that was carried out at the first boiled must (Table 1) and further after the second must (Table 2).

Table 1

General parameters of bottled Oettinger and Timisoreana beer

Physico - chemical indices	***Timişoreana***	***Oettinger***	***Permissible limits after MEBAK and SM 143:2001 Beer. National assortments [11 - 15]***
Ethyl alcohol, % vol, la 20 °C,	4.90 ± 0,42	5.24 ± 0.13	5.1 ÷ 5.7
Bitter, IUB	21 ± 0.78	17 ± 0.59	18 ÷ 22
pH-logH^+	4.39 ± 0.18	4.41 ± 0.17	4.0 ÷ 4.6
Ca^+,mg/l	29 ± 0.59	28 ± 0.59	40 ÷ 80
Density,	1.00907 ± 0.006	1.00751± 0.006	-
Extract, P P	11.4 ± 0.42	12.23 ± 0.17	12.0 ÷ 12.4
Concentration of CO_2, w/w	0.53 ± 0.13	0.56 ± 0.13	0.49 ÷ 0.57
Concentration of O_2	0.084 ± 0.051	0.054 ± 0.042	-

The general parameters obtained are within the permissible norms according to the MEBAK standard and SM 143:2001 Beer. National assortments [11 - 15].

In this paper the values of FAN (FAN- free amino nitrogen) and diacetyl were determined. The sum of the nitrogen compounds bioavailable in must is represented by free amine nitrogen. Excessive FAN content can lead to problems with taste and microbiological stability of beer.

Table 2

General parameters of bottled Oettinger and Timisoreana beer

Physico - chemical indices	***Timişoreana***	***Oettinger***	***Permissible limits after MEBAK and SM 143:2001 Beer. National assortments [11 - 15]***
Ethyl alcohol, % vol, la 20 °C,	4.95 ± 0,17	5.19 ± 0.16	4.7 ÷ 5.3
Bitter, IUB	20 ± 0.59	19 ± 0.68	16 ÷ 24
pH-logH^+	4.39 ± 0.17	4.45 ± 0.15	3.9 ÷ 4.6
Ca^+,mg/l	29 ± 0.59	30 ± 0.59	35 ÷ 50
Density,	1.00527 ± 0.004	1.00823± 0.006	-
Extract, P P	11.19 ± 0.17	12.31 ± 0.17	10.85 ÷ 11.35
Concentration of CO_2, w/w	0.56 ± 0.13	0.57 ± 0.14	0.51 ÷ 0.59
Concentration of O_2	0.089 ± 0.042	0.077 ± 0.069	-

Brewer's yeast and wild yeast ferment excess amino acids in long-chain alcohols (propanol, iso-butanol). FAN levels are also a good indication of the completion of fermentation. FAN monitoring with the DR6000 will help to overturn tanks more quickly once FAN levels are sufficiently low. The typical FAN content is 200 - 250 mg / L in must and 10 - 120 mg / L in beer.

The concentration of FAN (Table 3 and 4) also directly influences the dissociability of diacetyl. Thus to analyse this interdependency, the determination of FAN in the must was carried out and how the dissociation of diacetyl from the yeasts took place in the fermentation process.

Table 3

Values of FAN at first fermented wort at temperature of 17 °C.

Date of the experience	**Value of FAN**		**The admissible value of FAN in wort after *MEBAK* [11].**	**Measure-ment unit**
	Oettinger wort	**Timişoreana wort**		
19.10.2021	217± 0,5		200 ÷ 250	mg/L

Table 4

Values of FAN second fermented wort at temperature of 17˚C.

Date of the experience	**Value of FAN**		**The admissible value of FAN in wort after *MEBAK* [11].**	**Measure-ment unit**
	Oettinger wort	**Timişoreana wort**		
19.10.2021	224± 0,5		200 ÷ 250	mg/L

The general parameters obtained are within the permissible norms according to the MEBAK standard [11].

Concentration of diacetyl is important to be determined because during the fermentation of the yeast, 2-acetolactate and 2-acetohydroxybutylate appear during fermentation. By oxidation, they are transformed into vice, diacetyl and 2,3-pentanedione dicetones. However, diacetyl may also appear as a characteristic metabolic product of microorganisms. The beer produces an altered flavour when content of vicious dicetone is too high. This often results in a candy flavour of burned sugar and butter or an oily sensation in the mouth that is unpleasant for the consumer. The target value for blond beer is less than 0.05 mg / kg.

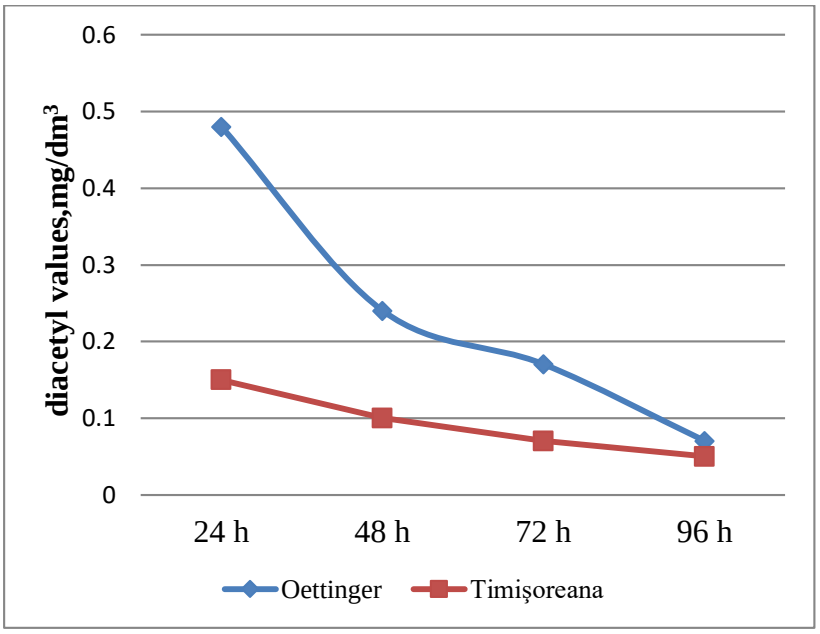

Figure 2. The quantity of diacetyl formed during fermentation of the first wort, at which the FAN value is 217 mg/dm^3.

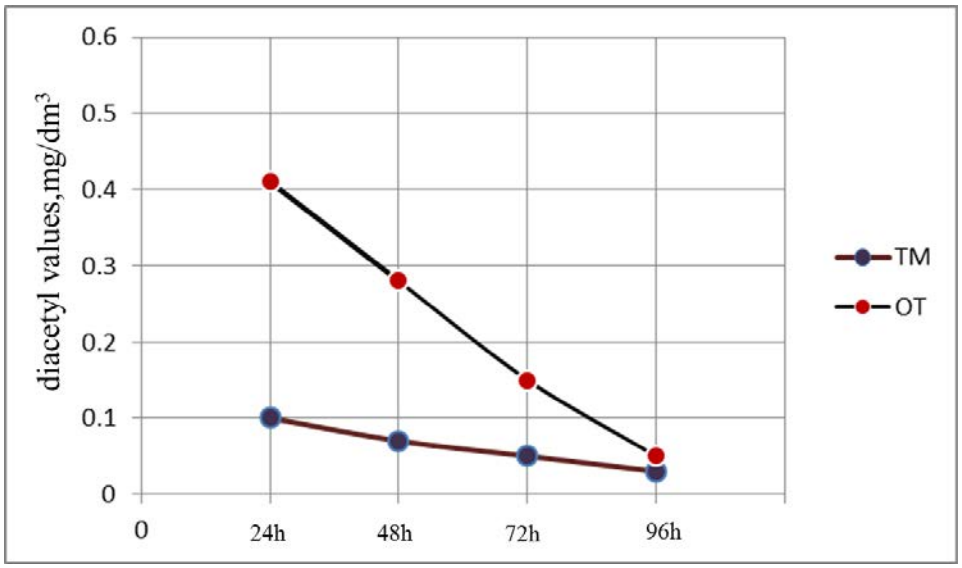

Figure 3. The quantity of diacetyl formed during fermentation of the second wort, at which the FAN value is 224 mg/dm^3.

Figure 2 and 3 represent the decrease amount of diacetyl according to the FAN concentration in the beer wort. The value of diacetyl is an indicator of the finishing fermentation process. At the end of fermentation, the yeast enters what is known as the stationary phase. This phase takes place when the beer goes through a maturation process to develop the right balance of flavours. One of the key elements of maturation is the reduction of di-acetyl. Not only does yeast produce the di-acetyl precursor, it also consumes the produced di-acetyl and reduces it enzymatically. The yeast reabsorbs di-acetyl from the medium and converts it into acetoin and later into 2,3-butane-diol, both with high flavour thresholds (difficult to detect), so as a result neither contributes much in terms of flavour [16,17]. But the amount of diacetyl is influenced by several parameters such as: Ca^{2+} ions, of Zn^{2+}, sulphur ions and the initial amount of free amino nitrogen of the must. Also the level of di-acetyl is influenced by: the temperature at which the fermentation takes place, by the bacterial contamination, by the yeast strain, by the level of aeration [18,19].

To control the aroma and quality of beer, breweries rely on several tests to prove and maintain consistency. Brewers' associations and government agencies have established guidelines for testing specific parameters that are important for determining and controlling beer quality. We emphasize a key parameter for brewing - Free Amino Nitrogen (FAN). FAN testing is part of the quality control analysis of standard brewing, because they allow the estimation of protein content and serve as an indicator of beer quality [20,21].

The general FAN content of the wort may affect the absorption rate of the valine and thus the production of diacetyl. The larger is initial FAN content both the maximum concentration of diacetyl during fermentation will decrease [11].

Experience has shown that a small decrease in the quantity of FAN will lead to a reduction in the amount of diacetyl initial during fermentation, as faster absorption of preferred amino acids of yeasts takes place, resulting in higher demand for valine and its increased absorption due to lower competition for interactions. Figures 4 and 5 show the type of yeast used for the fermentation of the wort for the beers analysed.

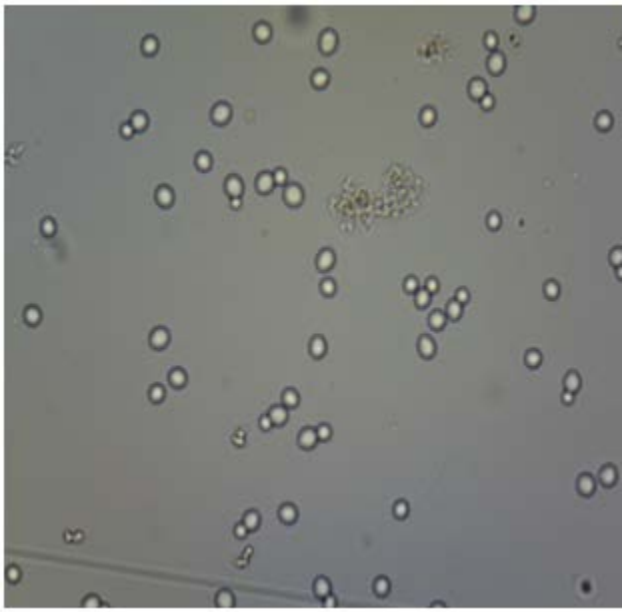

Figure 4. Oettinger yeast used for the fermentation of Oettinger beer.

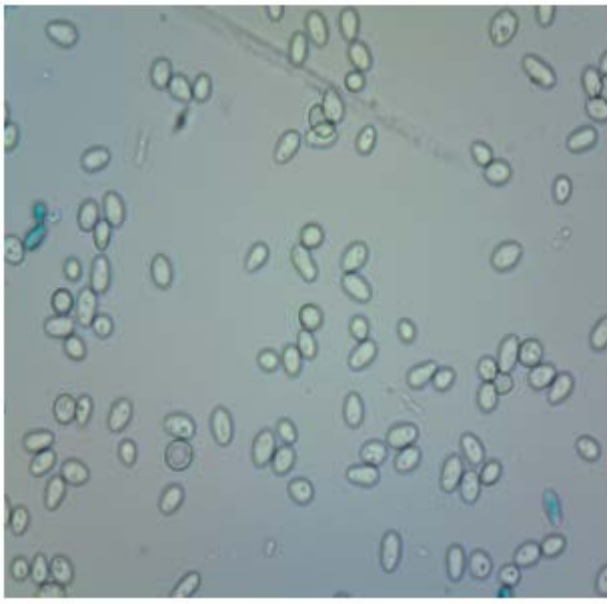

Figure 5. SABB-5 yeast used for the fermentation of Timișoreana beer.

Determination of microbiological increases at the end of the fermentation process.

The possibility of infecting beer with microorganisms is possible at any stage of production. Thus, to ensure that a quality finished product is produced, it is necessary to keep all production processes under control.

Two types of high fermentation yeasts (Oettinger and SAB-5) were used in the fermentation process, which at the end of the fermentation process with the help of cooling jackets fitted to the cubic-tapered tanks were subjected to cooling and sedimentation at the bottom of the tanks to collect them. After the yeast collection has taken place, the microbiological sample for the determination of bacteria and the presence of yeasts has been selected. The results of the seeding are represented in figure 6. Here we can see the presence of yeast colonies [19, 22].

Microscopic findings have shown that the colonies of yeast obtained from the sowing of the fermented must are of culture. Visual analysis of this conclusion can be sufficient, because the yeast colonies were white, consistent and glossy. Wild yeast colonies are usually small in diameter and have a white to transparent colour, appear to be aqueous [23, 24].

In Figure 6 (b) is microscopically represented a colony of yeast raised on the Wort medium. In this picture we can see large and medium diameter yeast cells, their cell wall is smooth and cell organs are not seen inside the cells. Thus, we can see that the yeasts presented are pure culture yeast and that they are young yeasts. Old yeasts are yeasts whose cell wall is rough, cells are large and cell organs are observed inside the cell. These yeasts look like they would crack soon. The expression of young yeasts takes into account that yeasts are used in the first stages, and are the first generations of yeasts used in the manufacturing process [25, 26].

a) b)

Figure 6. Wort sowing results after fermentation process: a) cultural characteristics; b) morphological characteristics.

Microbiological inoculations were also performed to determine the anaerobic bacteria harmful to beer. The determination of anaerobic bacteria harmful to beer is performed on NBB-A medium (Figure 7, 8) and the use of Anaerolult to achieve an anaerobic environment, by the absorption of oxygen by Anaerocult and the elimination of carbon dioxide, the ideal environment for the development of Pectinatus bacteria.

Today most breweries are trying to trace Pectinatus bacteria, because beer as a finished product is not favorable for the development of many other micro organizations such as L. Patentis, L. lindneri, Ped. Damnosus and others. The ideal growth environment for Pectinatus bacteria is in the filling unit and on the filling unit. Oxygen is not needed for the development

of these micro-organisms, on the contrary, it requires a CO_2. Pectinatus are relatively acidic and tolerant to ethanol [22 - 24].

Figure 7. Bacterial growth on the anaerobic environment of the OT beer.

Figure 8. Results of increases on the NBB-A anaerobically environment of TM beer.

From the results obtained after inoculation on NBB-A medium under anaerobic conditions for TM beer, no increase was registered, that indicates that the beer is not infected with microorganisms harmful to beer. Thus the product obtained will not present any risk of damage to the appearance and gustatory qualities.

Figure 9. Microscopic results of colonies raised under anaerobic conditions.

The second seed was Oettinger beer. Several colonies have been grown after seeding and thermostats of the samples for 10 days. Thus, for the identification of the types of microorganisms that have developed, it was necessary to perform staining according to Gram. Following the test, it was identified that the grown microorganisms are Gram-negative (Fig.9). Following the study, we determined that Pectinatus bacteria are Gram negative bacteria but also that they appear individually, in pairs or in short chains.

Conclusion

The concentration of diacetyl in the fermentation process must reach values lower than 0.1 mg/l, otherwise the beer will have a buttery taste and an oily consistency. Following the determinations of the diacetyl concentration, the values were lower than 0.1, so the fermentation process was finished.

The FAN values were analysed and identified in the first and second fermentation must, where the determined values must be within the permissible limit of 200-250 mg/l, which was demonstrated by obtaining values of 217 and 224 mg./l for the first must of fermentation and respectively for the second must.

The importance of determining the FAN indicator lies in the fact that this index is perceived as a good parameter for anticipating the healthy development of yeast, viability, vitality and fermentation efficiency, which results in a higher quality of beer.

In order to determine the microorganisms, general parameters were determined in the Oettinger and Timişoreana beers, which fall within the admissible values according to the MEBAK standard.

Following the microbiological control, the presence of culture yeasts in the fermentation process was determined, which is not a problem, because the beer filtration process is planned in such way as to retain the tube as well as microorganisms such as yeasts. The amount of yeast added has to provide 12-15mil cells / ml must. The yeast we add has to ensure the start of the fermentation of the whole mass after 12-16 hours at 6ºC. In some cases the amount of yeast must be higher (in the case of higher density musts), and in that environment a higher number of cells is required to be added.

Moreover, the presence of Pectinatus bacteria in the finished product was also analysed. Following the anaerobic incubations in Oettinger, there was ascertained that the number of colonies increased, but in Timişoreana they were not observed. Due to the fact that there was no acidification or disturbance in the storage of Oettinger beer for a long period of time, we can conclude that the grown colonies were not Pectinatus bacteria.

Acknowledgment: The research was funded by State Project 20.80009.5107.09 *"Improving of food quality and safety through biotechnology and food engineering"*, running at Technical University of Moldova.

Bibliography

1. Khorunina S.I. Biochemical and physicochemical fundamentals of malt and beer technology. Moscow „Kolos'' 1999. [in Russian]
2. Hornsey I. *Brewing* 2nd *Edition*. RCS Publishing, 2013.
3. Annie E. Hill. Brewing Microbiology, *Managing Microbes, Ensuring Quality and Valorising Waste*. Woodhead Publishing, 2015.
4. Graeme M. Walker and Graham G. Stewart. *Saccharomyces cerevisiae in the production of fermented beverages.* 2004. https://www.mdpi.com/2306-5710/2/4/30
5. Capece A., Romaniello R., Siesto G., and Romano P. *Conventional and Non-Conventional Yeasts in Beer Production*. 2018. https://www.mdpi.com/2311-5637/4/2/38.
6. Nuno Bourbon-Melo, Margarida Palma, Miguel Pinto Rocha etc. *Use of Hanseniaspora guilliermondii and Hanseniaspora opuntiae to enhance the aromatic profile of beer in mixed-culture fermentation with Saccharomyces cerevisiae.* 2019. https://pubmed.ncbi.nlm.nih.gov/33397613/.
7. Dennis E. Briggs, Chris A. Boulton, Peter A. Brookes, Roger Stevens, *Brewing. Science and practice*. CRC Press, Cambridge England, 2004.
8. Nicholas A. Bokulich, Charles W. Bamforth, *The Microbiology of Malting and Brewing,* 2013. https://journals.asm.org/doi/full/10.1128/MMBR.00060-12.

9. Carl A. Batt and Mary Lou Tortorello, *Encyclopedia of Food Microbiology*. Elsevier Science, 2014. https://azdoc.tips/documents/encyclopedia-of-food-microbiology-2014.
10. Krogerus K., and Brian R. Gibson, *125th Anniversary Review: Diacetyl and its control during brewery fermentation.* 2013. https://onlinelibrary.wiley.com.
11. Standard analysis parameters according MEBAK of lactic acid-fermented cereal-based beverages produced from differently. https://cz.hach.com/asset-get.download.jsa?id=50904526659
12. SM 143: 2001 Bere. National assortments.
13. GOST 12790-87 Beer. Methods for determining carbon dioxide and stability.
14. GOST 12787-81 Bere. Methods for determining alcohol, actual extract and calculation of dry matter in malt wort.
15. How to measure dissolved oxygen in the brewery. https://my.hach.com/ cms/documents/IN-Beverage/LIT2149-how-to-measure-DO-in-a-brewery.pdf.
16. How to control the level of diacetyl in beer? https://www.malt.ro/drojdii-fermentatie/di-acetil-bere.
17. Alexander Tyakht, Anna Kopeliovich, Daria Effimova etc. Characteristics of bacterial and yeast microbiomes in spontaneous and mixed-fermentation beer and cider.2020. https://www.researchgate.net/publication/346193239
18. FAN monitoring in brewery applications. https://ro.hach.com › asset-get.download.jsa
19. Pure Brewer's Yeast Crops | PDF – Scribd. https://ru.scribd.com/document/435276697/ Culturi-Pure-de-Drojdii-de-Obtinere-a-Berii
20. Krogerus K., and Brian R., Gibson. *125th Anniversary Review:* Diacetyl and its control during brewery fermentation. 2013. https://onlinelibrary.wiley. com/doi/full/10.1002/jib.84.
21. https://www.creeaza.com/familie/alimentatie-nutritie.Procese-microbiologice-la-fabr723.php.
22. PG-08-01 Sampling of foodstuffs http://www.ansa.gov.md ›files› Procedures for microbiological criteria for foodstuffs ... for methods of sampling and analysis of samples for official control [in Romanian].
23. 23. SM EN ISO 9308-1:2017 Water quality - iTeh Standards https://standards.iteh.ai › cen
24. SM EN ISO 6222:2014. 7.2. Determination of coliform bacteria. Determination of escherichia coli. Drinking water. Groundwater. SM SR ISO 9308-1: 2016, PS no. 3
25. Graeme M. Walker, Graham G. Stewart. *Saccharomyces cerevisiae* in the production of fermented beverages. https://rke.abertay.ac.uk/en/publications/saccharomyces-cerevisiae-in-the-production-of-fermented-beverages
26. Encyclopedia of Food Microbiology. Reference Work • Second Edition • 2014. https://www.sciencedirect.com/referencework/9780123847331/encyclopedia-of-food-microbiology.